Université de Lille

Ecole Doctorale

Sciences de la Matière, du Rayonnement et de l'Environnement

THESE

Pour obtenir le grade de

Docteur de l'Université de Lille

en Molécules et Matière Condensée

Agathe MAZAUD

Document confidentiel

Aqueous plant extraction using glycerol and sugar-based hydrotropes: physicochemical approach and application to rosemary

Extraction végétale en phase aqueuse à l'aide d'hydrotropes à base de glycérol ou de sucres : approche physico-chimique et application au romarin

Thèse dirigée par :

Pr. Véronique Nardello-Rataj

Soutenance le 3 décembre 2020

Membres du jury

Pr Bruno ANDRIOLETTI	Université Claude Bernard Lyon 1	**Rapporteur**
Dr. HDR Pierre BAUDUIN	ICSM - CEA Marcoule	**Rapporteur**
Pr Sophie THIEBAUD-ROUX	Toulouse INP – ENSIACET	**Examinateur, Présidente**
Dr. HDR Anne-Sylvie FABIANO-TIXIER	Avignon Université	**Examinateur**
Dr. Raphaël LEBEUF	Centrale Lille Institut	**Co-encadrant**
Pr Véronique NARDELLO-RATAJ	Centrale Lille Institut	**Directrice de thèse**
Dr. Mickaël LAGUERRE	Givaudan	**Invité**

Remerciements

Acknowledgments/Remerciements

Bien que cette thèse soit rédigée entièrement en anglais, j'ai souhaité rédiger cette partie « Remerciements » en français, étant donné qu'elle s'adresse principalement à des francophones.

Ce sujet de thèse a été pour moi passionnant et très enrichissant. Ainsi, je souhaite remercier toutes les personnes ayant contribué à l'accomplissement ce travail. Tout d'abord, à Lille, je souhaite adresser mes sincères remerciements à ma directrice de thèse Pr Véronique Nardello-Rataj, qui m'a donné la chance de travailler sur ce sujet à la fin de mon master. Grâce à sa rigueur, ses idées toujours innovantes et sa bienveillance, elle a largement contribué à l'accomplissement de ce projet. Je souhaite également remercier chaleureusement mon co-encadrant Dr. Raphaël Lebeuf pour sa disponibilité, son soutien et pour ses nombreux conseils en chimie organique entre autres, toujours très pédagogiques.

Je souhaite aussi adresser mes remerciements à l'entreprise Naturex (maintenant Givaudan) pour avoir financé cette thèse CIFRE. Plus particulièrement, je tiens à exprimer ma sincère reconnaissance au Dr. Mickaël Laguerre, mon encadrant industriel pendant ces trois années, qui m'a apporté de nombreux conseils pertinents lors d'échanges bien souvent téléphoniques mais toujours très enrichissants. Je souhaite remercier aussi toutes les personnes que j'ai pu côtoyer au sein de Naturex pour leur accueil et leur sympathie, en particulier au Dr. Antoine Bily, qui a apporté son expertise dans le domaine de l'extraction en participant à quelques réunions en début de thèse, et à Céline Gérin, qui m'a accueillie avec bonne humeur dans le laboratoire de Naturex.

Je souhaite également remercier l'équipe GREEN de l'Université d'Avignon, qui m'ont accueillie chaleureusement pendant quelques mois afin d'effectuer les mesures de turbidité sur le Crystal Eyes. En particulier, je tiens à remercier le Pr Farid Chemat et Dr. Anne-Sylvie Fabiano-Tixier pour leur contribution à ce travail, et pour les échanges scientifiques que nous avons pu avoir. Je souhaite remercier également les doctorants et post-doctorants de l'équipe pour leur accueil sympathique lors de mon court séjour à Avignon.

Enfin je souhaite remercier toutes les personnes avec qui j'ai eu la chance de travailler à Lille, au sein de l'équipe CISCO de l'UCCS, et en particulier au Dr. Christel Pierlot pour son aide à l'établissement et la réalisation des plans d'expériences, à Adeline Delaporte, Romane Boisard et Melissa Schoelchery pour leur aide précieuse pour les images prises au microscope, et à Céline Delabre, toujours disponible en cas de problème avec l'HPLC. Je remercie aussi le Pr Jean-Marie Aubry pour m'avoir donné goût à la chimie de formulation et la physico-chimie lors de mes années à l'ENSCL. Plus généralement, je souhaite remercier l'ensemble de l'équipe pour leur bonne humeur et leur humour quotidien. Tout d'abord, les permanents : Fermin, Jeff, Loïc, Benjamin J. et Mike, toujours présent pour répondre à toutes mes questions, et les anciens, actuels et futurs doctorants : Valentin G (Val), le plus grand passionné de culture Ch'ti que je connaisse, Florian (Broux, on se serre les coudes entre bretons !), Greg, la joie de vivre incarnée, Tristan (à quand la prochaine soirée Jaja ?), mon grand Charles, que j'ai été si contente de revoir

à Lille à trois bureaux de moi après tant de souvenirs à l'école, Alex, le roi des Ti-punchs, Guillaume et son rire légendaire, Valentin B, le danseur du labo, Lucie, Adrien, Jordan et Yaoyao, la relève des doctorants, à qui je souhaite bon courage ! Bien plus que des collègues, vous êtes tous bien évidemment devenus des amis.

Finalement, je souhaite exprimer ma reconnaissance à ceux qui m'ont soutenu, à mes amis d'école d'ingénieur dont ceux habitant à Lille, les deux Julien, Arthur et Louise, et évidemment Lénaik et Julia, qui a aussi contribué à la découverte d'une activité nouvelle et inattendue pour moi, le triathlon ! Et puis ceux qui sont repartis de Lille mais qui ont toujours été là même de loin : Cédrine, Floria, Charlène, Toni, Guillaume, Anne, Manon B, Fanny, Natalia, Manon L, Louise en particulier. Merci aussi à Maxime pour m'avoir soutenue dans cette thèse et surtout pendant la rédaction, qui n'a pas été de tout repos.

Enfin, je souhaite remercier ma famille élargie, mes grands-parents pour leur soutien et intérêt pour mon domaine d'activité, Manu, France et Anouk pour leur humour et les soirées passées en leur compagnie, et bien sûr mes parents pour leur amour et leur immense soutien depuis toujours.

Résumé

Les préoccupations grandissantes concernant la santé et l'environnement rendent la demande en ingrédients naturels toujours plus forte. Parallèlement, les fournisseurs d'ingrédients naturels tentent de rendre les procédés d'extraction plus performants, plus sûrs, moins consommateurs en énergie et en ressources non-renouvelables. Les hydrotropes, capables de solubiliser des composés hydrophobes dans l'eau, constituent une alternative prometteuse aux solvants organiques, souvent dérivés du pétrole, potentiellement explosifs et émetteurs de composés organiques volatiles. Afin de développer un nouveau procédé d'extraction hydrotropique efficace à base d'amphiphiles biosourcés, nous nous sommes intéressés à la compréhension des cinétiques et des phénomènes physico-chimiques impliqués dans l'extraction de l'acide carnosique (AC), un puissant antioxydant phénolique présent dans le romarin et la sauge officinale. L'extraction de l'AC par des hydrotropes modèles de type éthers de polyéthylène glycol a permis de démontrer l'efficacité et la compétitivité de l'extraction hydrotropique par rapport à une extraction conventionnelle utilisant un solvant. Des relations structure/propriétés physico-chimiques/efficacité ont été établies, puis généralisées aux hydrotropes biosourcés à base de glycérol (éthers de butyle, pentyle, et isopentyle) ou de sucres comme le xyloside d'amyle qui a été sélectionné par la suite pour son efficacité, sa biodégradabilité et sa disponibilité. L'optimisation des conditions d'extraction à l'aide de plans d'expériences a permis de doubler la quantité d'AC récupéré dans l'extrait sec. Pour finir, différentes techniques de précipitation de l'AC contenu dans des solutions hydrotropiques ont été comparées afin de faciliter sa récupération. Parmi elles, l'addition d'eau comme anti-solvant s'est révélée la plus efficace pour précipiter l'AC extrait du romarin. Sur la base de la composition et de l'aspect du précipité obtenu selon différentes conditions de précipitation, nous avons finalement pu établir un mécanisme visant à expliquer les différentes étapes de la précipitation hydrotropique.

Mots-clés : Extraction, Romarin, Hydrotrope, Acide carnosique, Physicochimie, Xyloside d'amyle

Abstract:

The growing concerns for health and environment makes the demand for natural ingredients ever higher. At the same time, natural ingredients manufacturers are trying to design effective, safer and less energy-costly extraction processes while avoiding the use of non-renewable resources. Hydrotropes are able to solubilize hydrophobic compounds in water, and constitute a promising alternative to organic solvents, which are often derived from petroleum, potentially explosives and producers of volatile organic compounds. To design a new effective hydrotropic extraction process using biobased amphiphiles, we investigated the physical chemical and kinetic phenomena governing the extraction of carnosic acid (CA), a powerful phenolic antioxidant that occurs in rosemary and sage. The CA extraction using alkyl polyethylene glycols ethers as model hydrotropes demonstrated the efficiency and the competitiveness of hydrotropic extractions compared to conventional solvent extractions. Quantitative Structure/properties relationship (QSPR) studies were established and generalized to biobased hydrotropes including butyl or pentyl glycerol ethers, and sugar-based hydrotropes such as amyl xyloside, which was further selected for its efficiency, biodegradability and commercial availability. The optimization of the extraction conditions led to double the CA recovered in the dry extract. Finally, different techniques have been investigated to precipitate CA from a hydrotropic solution. Among them, the addition of water as an anti-solvent appears as the more effective for precipitating CA from rosemary extract. Finally, the comparison of the precipitate composition and aspect obtained using various precipitation conditions led us to establish a mechanism explaining the different steps of the hydrotropic precipitation.

Key words: Extraction, Rosemary, Hydrotrope, Carnosic acid, Physicochemistry, Amyl xyloside

Table of contents

Table of abbreviations

AO: Antioxidant

BA: benzoic acid

BHA: Butylated Hydroxyanisole

BHT: Butylated Hydroxytoluene

BP: Boiling Point

CA: Carnosic acid

CAC: Critical Aggregation Concentration

CAR: Carnosol

C_iE_j: Alkyl polyethylene glycol ethers with *i* is the number of the carbon atoms of the alkyl chain and *j* the number of ethylene oxide units in the polar headgroup

C_iGly: 1-monoalkyl glycerol

C_iGlyco: alkyl polyglycosides including:

- C_iGlu: alkyl polyglucosides
- C_iXyl: alkyl polyxylosides

C_iP_j: Alkyl polypropylene glycol ethers with *i* is the number of the carbon atoms of the alkyl chain and *j* the number of propylene oxide units in the polar headgroup

C_{max}: Hydrotrope concentration at which the S_{max} is reached

CMC: Critical Micellar Concentration

COSMO-RS: COnductor like Screening MOdel for Real **S**olvents

CP: Cloud Point

CPE: Cloud Point extraction

DES: Deep eutectic solvents

DP: Degree of polymerisation

DR-13: Disperse Red 13

EO: Essential oils

EF: Enhancement factor

GC-FID: Gas Chromatography – flame ionization detector

HCPE: Hydrotropic Cloud Point Extraction

HLB: Hydrophilic Lipophilic Balance

HPLC: High Performance Liquid Chromatography

HVED: High Voltage Electric Discharge

IL: Ionic liquids

LA : Lauric acid

LC: Liquid crystals

log *P*: Partition coefficient octanol-water

MW/MAE: Microwave/Microwave Assisted Extraction

MCA: 12-*o*-methyl carnosic acid

MHC: Minimum Hydrotropic Concentration

NaBMGS: Sodium butylmonoglycol sulfate

NaB: Sodium benzoate

NaCIN: Sodium cinnamate

NaCS: Sodium cumene sulfonate

NaNBBS: Sodium *n*-butylbenzene sulfonate

NaPTS/PTSA: Sodium *p*-toluene sulfonate/*p*-toluene sulfonic acid

NaS: Sodium salicylate

OA: Oleanolic acid

PEF: Pulsed-Electric Field

RA: Rosmarinic acid

TGA: Thermogravimetric Analysis

TFA: trifluoroacetic acid

UA: Ursolic acid

US/UAE: Ultrasound/Ultrasound Assisted Extraction

VG: veratrylglycerol-b-guaiacyl ether

V_m: Molecular volume

VOC: Volatile Organic Compound

SDS: Sodium docecyl sulfate

SXS: Sodium xylene sulfonate

S_{max}: maximum solubility of solute in a hydrotropic solution

S_w: solubility in water

^{1}H NMR: Proton Nuclear Magnetic Resonance

General introduction

In food and cosmetics industries, since most of the products are not consumed immediately upon manufacture, an important challenge is to ensure consumers no loss of quality or safety during storage and transport. However, many products contain high amounts of lipids such as unsaturated fatty acids which are prone to oxidation.[1,2] This is a natural reaction with oxygen from air induced by light, heat or the presence of metal. The formation of free radicals and then peroxides is responsible for the rancidity of fats and oils and can be harmful to health (**Figure 1**).[2] When antioxidants (AO) are present, they react with peroxy radicals to form radical AO (AO•). For example, a catechol moiety forms a free radical semiquinone, which can be stabilized to a certain extent by resonance as shown in **Figure 1**.[3] Thanks to the partial stabilization of AO• by resonance, the reaction of the peroxy radical is energetically more favorable with AO than with another fatty acid. Then, the highly reactive AO• reacts in turn with another peroxy radical and gives a stable oxidized form of the AO, an *o*-quinone in the case of catechol.[1] Through this reaction, two free radicals are eliminated, so the presence of AO induces the termination of the radical propagation and at the same time, limits the formation of peroxides.

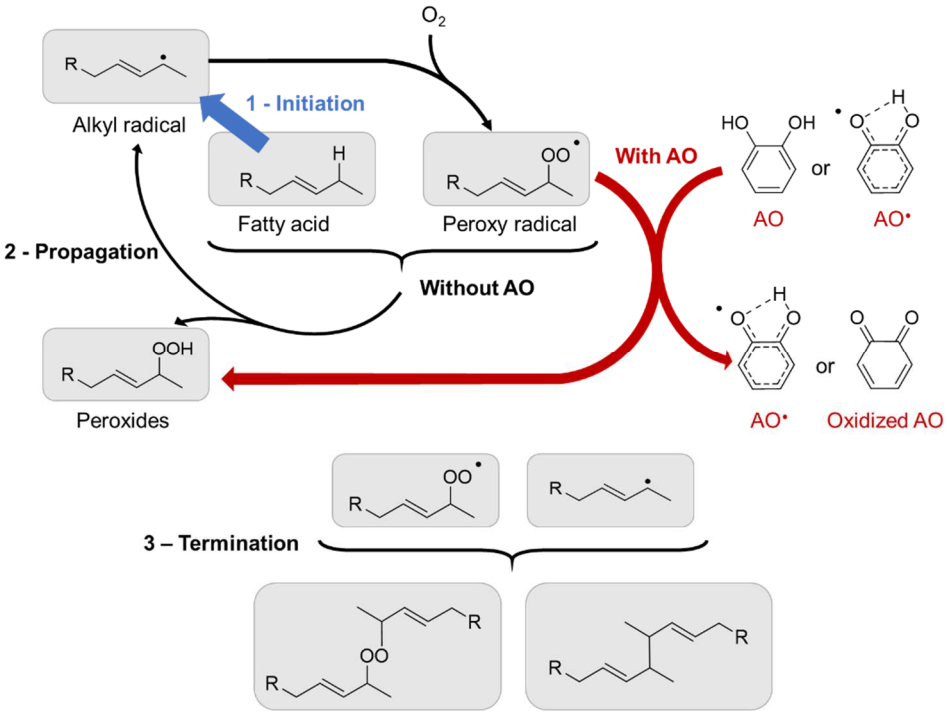

Figure 1. Schematic representation of the initiation (blue), propagation and termination steps of the radical oxidative degradation of unsaturated fatty acids, and its prevention through the action of a catechol antioxidant (AO, red)

Spices and herbs have been unknowingly used as natural AO to prevent food from degradation for thousands of years. However, since the XXth century, synthetic AOs such as Butylated Hydroxyanisole (BHA) or Butylated Hydroxytoluene (BHT) have been promoted in the industry for their cheapness, availability and efficiency. In recent years, the interest for natural

food preservatives has grown based on consumer requirements and because they are considered to be healthier and more eco-responsible than synthetic petro-sourced ones.[4,5]

Typically, rosemary and sage leaves have been used since Antiquity[6] for culinary purposes as flavoring or food preservatives, and their antioxidant properties were highlighted by Chipault et al. in the middle XXth century.[7] The authors compared the antioxidant index of 32 ground spices including thyme, paprika, cloves or turmeric on frozen lard and found rosemary and sage to have the highest effects. More than 50 years later, in 2010, rosemary extract was registered by the European Commission as food additives in the AO category and received the number E392.[8] Since then, it is employed as natural AO in food preparations such as vegetable fats, meats, or dairy products. Noteworthy, several studies have reported that rosemary extract has a higher antioxidant activity compared to BHA and BHT.[9,10]

This remarkably high antioxidant power has been attributed to **carnosic acid** (CA), a phenolic diterpene identified by Linde in 1964 and Wenkert in 1965 in sage and rosemary respectively (**Figure 2**).[10–12] It could account for 90 % of the antioxidant capacity of rosemary extract, according to Aruoma et al.[13] Like many other AO, CA contains a catechol group in its structure, a moiety known to exhibit high radical scavenging capacity.[14] During the initial oxidation the catechol group is converted to an *o*-quinone (**Figures 1, 2**), but interestingly, CA quinone is able to isomerize into carnosol (CAR) and regenerate the catechol group, according to the reaction mechanism illustrated in **Figure 3**.[12] Thus, CA participates in two successive oxidation reactions and doubles its antioxidant power compared to similar molecules, which makes it a particularly interesting and efficient natural AO.

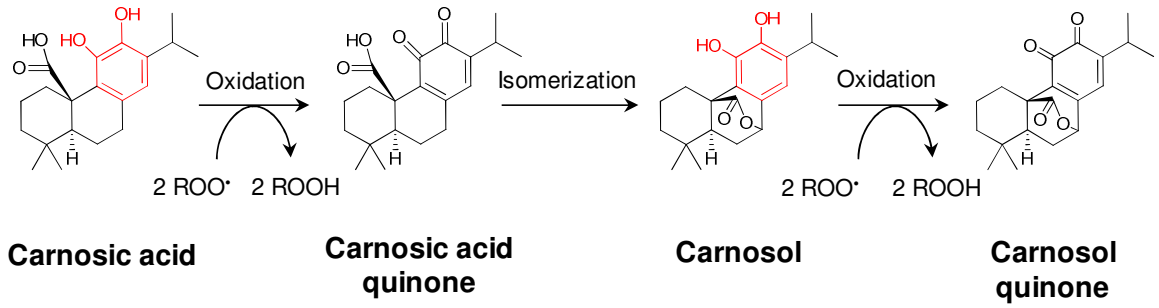

Figure 2. Two successive reactions of oxidation from CA to carnosol quinone. The catechol moiety is colored in red.

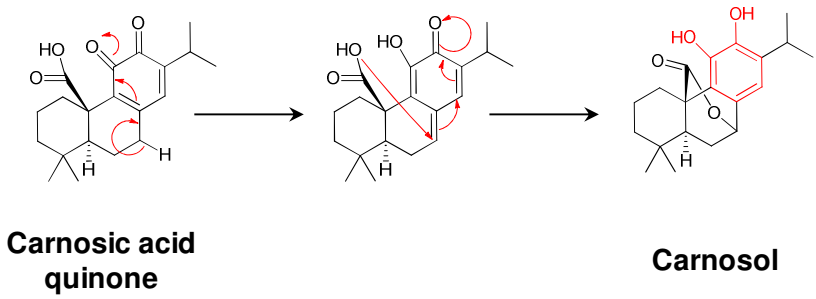

Figure 3. Isomerization mechanism leading to the regeneration of the catechol group (in red) in CAR.[12]

In order to improve the production of natural CA, its presence *in planta* has been widely studied. CA is a rare secondary metabolite as it has only been found in nine species of plants, all from the Lamiaceae family, which includes most aromatic herbs (*e.g.* mint, thyme, sage, oregano). Among these plants, rosemary has the highest concentrations, between 0.3 to 5 wt.% in dried leaves, followed by sage, which can reach up to 2-3 wt.% in dried leaves.[8] Unsurprisingly, this finding coincides with the previous results showing that rosemary and sage had the most important antioxidant index and with the attribution of the antioxidant power to CA. This bioactive has only been found in leaves and flowers, and is at least 10 times less concentrated in stems, roots and seeds than leaves.[15,16] It should be noted that the concentration in leaves strongly depends on the age of the plant, its geographical origin, the time of harvest, the storage and drying processes.[17]

Rosemary is a shrub reaching up to 2 m height, native to the Mediteranean basin, as suggested by its Latin name *ros-marinus* meaning "dew of the sea".[6] Its leaves have the margins folded inwards and have the particularity of being covered on their underside with an important number of trichomes, which are outgrowths of the epidermis, typically glandular or hair-like, with a secretory or protection against light, heat or dryness function (**Figure 4**). Sage leaves have the same particularity, they are covered by trichomes on their under and upper sides (**Figure 5**).

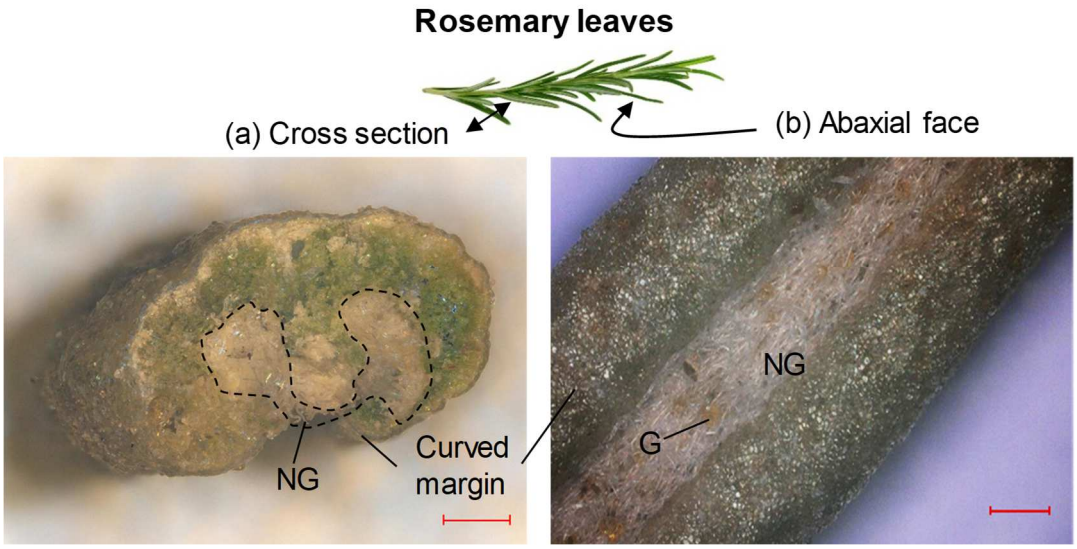

Figure 4. Microscopic images of rosemary leaves (a) cross section and (b) underside face captured on a digital microscope. Scale bars: 200 µm. G: glandular trichomes, NG: Non-glandular trichomes.

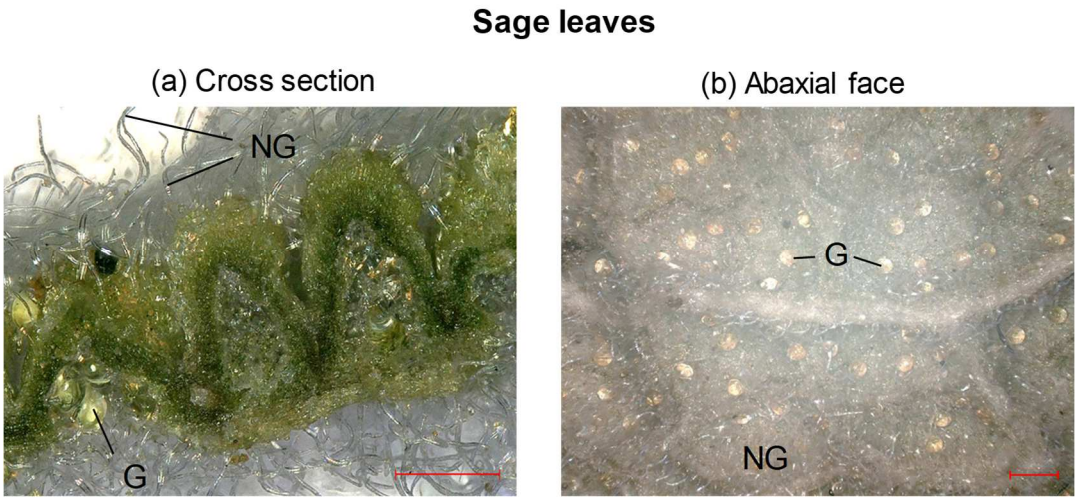

Figure 5. Microscopic images of sage leaves (a) cross section and (b) underside face captured on a digital microscope. Scale bars: 200 µm. G: glandular trichomes, NG: Non-glandular trichomes.

Brückner et al. have shown that CA accumulates in trichomes, especially in young trichomes. Since CAR was not found in the trichomes but was present in the rest of the leaf, they suggested that CA was biosynthesized in the trichomes and then transferred to the whole leaf to protect cells from oxidative stress.[18] Other derivatives of CA such as 12-*o*-methyl carnosic acid, isorosmanol, rosmanol occur in the leaves in smaller amounts (6 to 600 times less concentrated than CA).[15]

Trichomes are also the storage place of essential oils (EO)[19] which are generally composed of 30 to 50 molecules with a predominance of monoterpenes: 1,8-cineole, α-pinene, camphor, and depending on the region of origin, borneol, *p*-cymene (Cuba, Turkey), verbonone (Corsica, Sardinia) can be among the major constituants.[20] With a concentration of 1 to 2.5 wt.% of EO in its leaves, the extraction of volatiles from rosemary by hydrodistillation has been performed for centuries.[21–23] EO have been used for medicinal purposes and as fragrances in the perfume industry.

In rosemary, 10 to 15 wt.% of the compounds can be extracted.[22,24] Besides CA, its derivatives and EO, rosemary leaves contain many other extractable phenols including hydroxycinnamic acids (*e.g.* coumaric, rosmarinic acids), flavonoids and glycosidic derivatives of flavonoids, di- and triterpenes (**Figure 6**).[25–29] In addition to those specific secondary metabolites, rosemary leaves are made up of fibers (17.7 – 42.6 wt.%) such as cellulose, the main component of the cell walls, proteins (5 wt.%), lipids (15 wt.%), minerals (mostly Ca and K, 2 – 4 wt.%), some vitamins (mostly vitamin A, < 0.01 wt.%), water (depending on the drying method) and free sugars. The leaves are covered with a layer of waxes called cuticle, which can be 2 to 6 µm wide on the trichomes.[30] It consists of a mixture of fatty acids and waxes composed of very long alkanes, with abundant presence of C_{29} to C_{35} alkyl chains.[31,32]

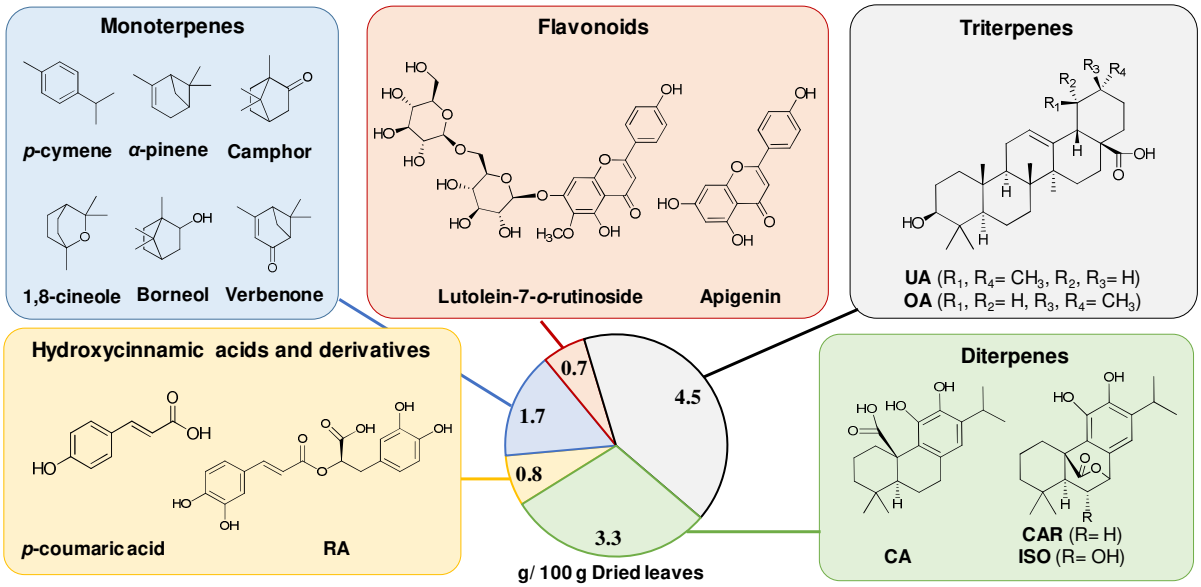

Figure 6. Most represented extractable compounds of rosemary classified in five chemical groups and a mean concentrations in rosemary leaves calculated from refs[21–23] for essential oils and refs[6,26–29] for the other bioactive compounds. RA: rosmarinic acid, UA: ursolic acid, OA: oleanolic acid, CA: carnosic acid, CAR: carnosol, ISO: isorosmanol.

Finally, it is noteworthy that three pigments have been found in rosemary: chlorophyll a, xanthones and carotenes with a maximum total mass of 0.4 wt.% (calculated from the reported mass yield and content).[33] Knowing the composition is important to perform extractions because *(i)* some products are undesirable during extraction since they may lower the CA purity of the extract, or even make the extract colored and odorous in the case of pigments and monoterpenes respectively and *(ii)* other components of rosemary like fatty acids and alkanes of the cuticle can lower the mass transfer of the solute to the solvent by forming a barrier between CA, inside the cells and the solvent.

To isolate CA from other rosemary compounds, maceration and Soxhlet extractions with conventional solvents like acetone, chloroform, hexane and ethanol have been used since CA was discovered.[8,24,34–36] However, the use of such organic solvents must be avoided to limit flammability and explosive risks, and reduce the dangers to human health and environment, since most of those molecules are generally considered as harmful. One interesting way to solubilize and extract hydrophobic compounds like CA by avoiding such risks is the use of amphiphiles in aqueous solutions.

In this context, extractions of CA from rosemary using hydrotropic and surfactant solutions were carried out in order to find which physicochemical parameters of the amphiphile govern the extraction and which conditions would optimize the extraction. This work has been performed in a CIFRE project, with the society Naturex (part of Givaudan) which is an international leader in the natural ingredients fields. Since 1992, they have developed and produced plant extracts with flavoring, coloring and antioxidant properties for the food, cosmetics, and nutraceutical industries.

The manuscript is divided into four main parts. The **first chapter** is a literature review addressing the plant extraction processes and focusing on the hydrotropic extraction. The physicochemical mechanisms of each technique are detailed and their relative drawbacks/advantages are pointed out. As it is the core of this thesis work, extractions of CA from rosemary and sage are taken as examples whenever possible. A part has also been dedicated to the techniques usable for the recovery of a dry extract. Finally, current trends to design more eco-responsible extractions are also presented with a discussion about the use of bio-based hydrotropes. This chapter highlights the enthusiasm for the search for alternative extraction methods to solvent-based ones and clearly demonstrates the interest of hydrotropic extraction.

Modes of action of hydrotropes during an extraction process are not clearly detailed in the literature and no guide can be found to select the best hydrotope. To try to answer this question, we have first conducted a systematic study of a well-defined series of hydrotopes in order to identify the chemical and physicochemical key parameters and to define a mathematical model for the hydrotropic extraction. This is the subject of **chapter II**. For this purpose, fourteen amphiphiles including hydrotropes and surfactants from a homogenous series of alkyl polyethylene glycol ethers (abbreviated as C_iE_j where *i* is the number of the carbon atoms of the alkyl chain and *j* the number of ethylene oxide units in the polar headgroup) were investigated for the extraction of CA from rosemary. First, their ability to solubilize CA in water was assessed and correlated to their physicochemical properties. Then, their capacity to extract efficiently CA from rosemary was investigated under different conditions and the kinetics of extraction were studied in more details. The influence of phytochemicals on the Cloud Point (CP) of hydrotropes was also investigated, as well as the effect of hydrotropes on the plant material at the microscopic scale. Finally, the recovery of CA as a solid extract was first attempted by an innovative method using the CP, and then a more classical method using the Minimum Hydrotropic Concentration (MHC) of the hydrotrope, showing the viability of the process.

By taking advantage of the results obtained previously with the C_iE_j model hydrotropes, the investigations could be extended to bio-based hydrotropes in order to develop a fully "green" extraction system, meeting the specifications of our industrial partner, Naturex. Thus, in **chapter III**, we report on an in-depth study of two families of bio-based hydrotropes. The first one uses commercially available sugar-based molecules such as *iso*-amyl xyloside and heptyl glucoside and the other one consists in synthetic monoalkyl glycerol derivatives. In this section, the physicochemical properties of amphiphiles were studied and used to validate the model established for alkyl polyethylene glycol ethers in the previous chapter. After studying the wettability of the plant by the best amphiphiles, they were used to extract CA from rosemary and sage. Finally, the extraction conditions have been optimized for the most promising amphiphile, *iso*-amyl xyloside, to provide an efficient extraction.

Chapter IV specifically deals with the recovery of a CA-rich rosemary dry extract for further use. To find the easiest and most effective way to recover CA after it was extracted from rosemary, two methods were compared. First, the method of crystallization of the extract was investigated. For that purpose, turbidity measurements of hydrotropic solutions containing pure CA were performed at different temperatures. Then, the efficiency of this method was studied in an extraction process. The second pathway to recover CA was to dilute the hydrotropic solution under its MHC. This method reveals to be very efficient and was optimized to provide a dry extract with a good yield and high purity.

Chapter I. General concept of the hydrotropic extraction of natural compounds

I.1. Introduction to green extraction processes

I.1.1. How to get a dry extract from the plant?

Bioactive compounds are molecules which are biosynthesized in plants and having one or more properties of interest in medicine, as an additive in cosmetic or agro-food products, or for other various applications. Their industrial production involves successive steps with a general objective: to provide the maximum amount of extract with maximum enrichment in the target molecule. Nowadays, environmental and safety concerns are increasingly taken into account. New processes tend to limit the use of solvents posing risks to humans (toxicity) or environment (VOC emissions) and are designed to limit energy by reducing the time and number of unit operations, their temperature and the use of other conditions requiring energy.[37,38]

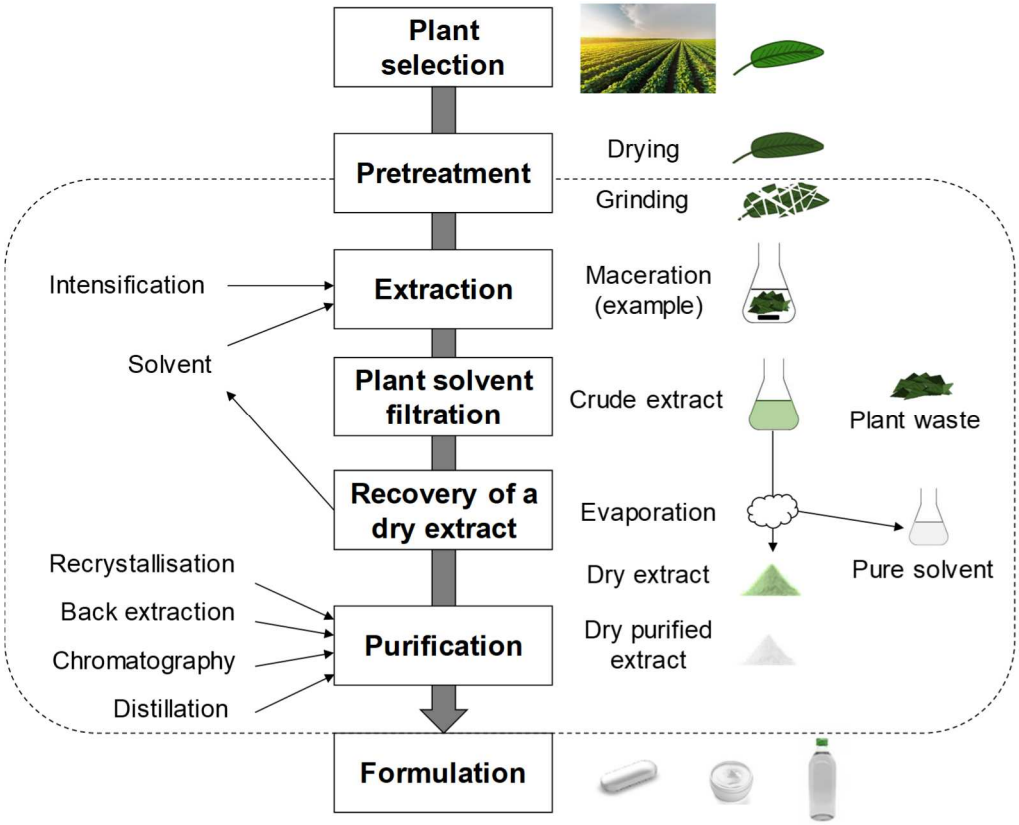

Figure I.1. Schematic representation of the natural compounds production, from plant to formulated products. The different steps in the dotted box will be addressed and studied in this thesis work

The first step to produce natural compounds is the **plant selection** (**Figure I.1**). It includes the selection of the species, culture and harvest conditions in order to obtain the highest amount of target molecule and to ensure its renewability.[39,40]

The **extraction** step (**Figure I.1**), which is generally preceded by the **pre-treatment** of the plant (drying, grinding), consists in the separation of the target compounds from the plant by solubilization in a solvent. Traditionally, organic solvents are used to extract hydrophobic bioactives, and water to extract essential oils (EO) by hydrodistillation.[41] The solvent is chosen according to the polarity of the target molecules, for example fats can be extracted with hexane, petroleum ether, terpenes and terpenoids with acetone, chloroform, ethanol, sugars with ethanol, methanol, water.[37] This step can be optimized by the choice of the method (*e.g.* Soxhlet, maceration, percolation), conditions (*e.g.* stirring, heating) and use of intensification technique (*e.g.* ultrasounds, microwaves). For example, a patent describes extractions of CA from rosemary and sage using acetone, petroleum ether, toluene, dichloromethane or ethanol and using either Soxhlet or maceration techniques.[36]

Then, the plant must be separated from the solvent to recover a liquid crude extract. This operation is generally performed by **filtration**. This step can be eliminated by choosing suitable extraction methods such as Soxhlet extraction or percolation. Thanks to the low boiling points of organic solvents, the concentration and recovery of bioactive compounds is generally achieved by **evaporation** of the solvent (**Figure I.1**). This way, the pure solvent is recovered and can be used for another extraction.[42]

The powder obtained is then purified to remove the extracted by-products (**Figure I.1**). This step requires at least one unit operations which can be a solid-liquid extraction, a selective recrystallization with temperature, a liquid chromatography or a distillation depending on the target molecule and the by-products to remove. In the case of CA, two patents described purification methods: the first consisted of two recrystallizations from cyclohexane in the presence of activated carbon, with a final purity of 73 %,[36] and the second used a pH differential precipitation. Indeed, by adding water and adjusting the pH of the plant extract between 7 and 10, impurities such as UA were precipitated while CA was solubilized and precipitated by acidification below its pKa only after the removal of impurities by filtration.[43]

Optimizing the extraction step is important to reduce the environmental impact of purification because the fewer compounds co-extracted, the easier the purification step and the less energy consumed. Finally, the pure extract is formulated either in a liquid or solid form depending on its specific application (**Figure I.1**).[42]

The plant/solvent extraction is a key step in the production of the natural ingredient and must therefore apply the principles of green chemistry. Following them, the solvent should be reusable, non-toxic, non-flammable, non-VOC and biodegradable, the method (*e.g.* maceration, Soxhlet, percolation), the intensification, the pre-treatment, the pressure and temperature conditions should be chosen to reduce the energy consumed of both this step and the following ones.[37,38]

I.1.2. Mechanisms of plant extraction

In plants, secondary metabolites have a specific biological function or can be intermediates for the synthesis of other molecules such as polymers. Under natural conditions, secondary metabolites are located inside the cells from where they have to be extracted to be recovered in the solvent. This process, like solid-liquid extractions, is usually described in four steps, presented in **Figure I.2**.[40]

First, the solvent diffuses inside the plant through intercellular spaces, capillaries or pores of the plant, and then, through the cell wall and the plasmic membrane to enter the cell. The grinding of the plant material can reduce the diffusion path and increase the exchange surface area, thus facilitating the access of the solvent to the cells. Without grinding, in the case of leaves, another barrier must be crossed because leaves are covered with a cuticle, a very hydrophobic layer composed of long alkanes, primary alcohols, fatty acids, aldehydes (C_{12} - C_{40}) and esters (C_{30} – C_{60}), polymers of fatty acids and triterpenes. The second step is the solubilization of the solute(s) by the solvent in the cell. This is usually a quick or instantaneous operation, provided that an adequate solvent is used.

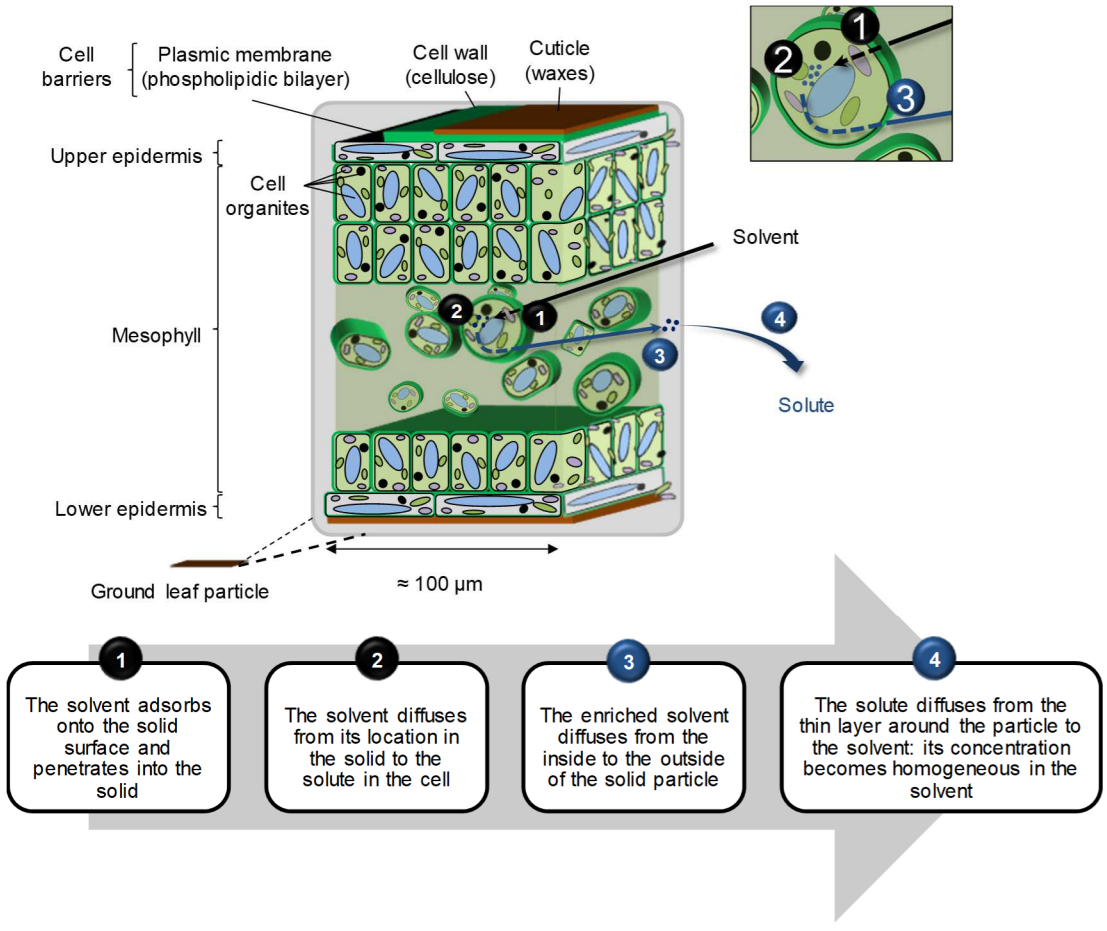

Figure I.2. 3D Representation of a ground leaf particle (0.1 mm), its internal structure and the path of the solvent (black) and solutes (blue) during extraction.

The third step is the mass transfer of the solutes from the cell to the surface of the plant particle, following the reverse path of the solvent described in the first step (cell wall and internal spaces of the plant). Finally, the solute generally diffuses from the plant particle to the bulk solution by convection. With an adequate stirring, the mass transfer should be negligible and it should not be a limiting step.

Among the four steps, the extraction rate is generally limited by the diffusion of the solutes through the cell barriers. The plasmic membrane is a phopholipidic bilayer and the cell wall is mostly composed of cellulose. The diffusion through these structures may be enhanced both by a chemical affinity between the transferred molecule and the layer, by the small volume of the molecule or by a higher porosity of the cell wall.[38]

I.1.3. Intensification techniques to increase mass transfer

In order to increase the mass transfer of the solutes and since grinding as pre-treatment provides particles too large to allow the solvent to access all the cells, several intensification techniques have been developed with the aim of breaking down the cell barriers during extractions and release the plant material in the medium.

Ultrasound and microwave-assisted extractions (UAE and MAE respectively) are the most reported processes using intensification techniques. Indeed, they have been studied for more than 50 years, they require relatively inexpensive equipment (< 200 k€), they are very effective in mechanical cell disruption and therefore in the reduction of extraction time (< 1 h).[44,45] **Ultrasound** (US, 18 – 1000 kHz) produces microbubbles which repeatedly grow and collapse. This phenomenon, called cavitation, creates shock waves and water microjets which are implied in the enlargement of the pores and the cell disruption.[46] However, ultrasounds also produce free radicals which can degrade the target molecules.[47] On the other hand, **microwaves** (MW) heat the solvents or samples with a high dielectric constant. Cells generally contain a high amount of water, which is highly dielectric. The increase in internal temperature induces first the increase in internal pressure and then, due to this phenomenon, the disruption of the cells. In the case of a highly dielectric solvent, the plant material is heated both from the inside and from the heated solvent, so the process is quicker. This technique is not suitable for the extraction of thermo-degradable molecules.

As far as CA is concerned, the efficiency of MAE and UAE has already been compared to conventional extractions.[29,35,48] Compared to extractions performed in ethanol at 40 °C during 4 h, the concentration of extracted CA slightly increased from 2.11 to 2.46 and 2.21 g/L using MAE and UAE on de-oiled ground rosemary leaves respectively, but decreased from 0.36 to 0.32 and 0.11 g/L when MAE and UAE were applied on fresh leaves. The yield of these extractions performed in ethanol increased in both cases, when microwaves and ultrasounds were applied discontinuously, leading to lower purity. However, the time of extraction could be reduced to 7 min.[48] While extractions were tested in ethanol in the same time (30 min) and temperatures (40 °C), it was found that the use of US probe was more efficient compared to

reactions in US reactor or US bath; it increased the amount of CA extracted but the purity was slightly lowered from 8.41 to 8.21 %. Microwaves had quite the same effect, but when microwaves were used under vapor pressure to keep temperature to 125 and 150 °C, the mass yield highly increased from 10 to 25 % and the amount of CA extracted decreased, leading to extracts with small purities of 2.1 – 2.5 %. The decrease in the CA amount extracted can be due to its thermo-degradability. However, although CA is highly reactive to free radicals, US in smooth conditions did not seem to degrade it.[35] In general, the CA content in the extract decreases when US and MW are used. Combined with an increase in mass yield, it means that other co-products are more efficiently extracted under the effect of intensification, but that the effect on CA is less important, meaning that CA is more accessible than other co-products. This may be related to the location of CA in the trichomes, which are outgrowths and therefore always in contact with the solvent, while other compounds located inside the leaves are likely to be more easily extracted under the effect of US or MW.

Other cell disruption techniques are currently being developed and are thus still more expensive and less optimized. Electrically assisted extractions using a **pulsed electric field** (PEF) or **high voltage electrical discharges** (HVED) induce electroporation through the application of high voltage pulses during a short time (2 µs – 0.01 s) to plants placed between two electrodes.[40] In addition, the negative pressure cavitation extraction and the instant controlled pressure drop technique are novel techniques using a controlled pressure in the extraction to induce cell disruption.[37]

Finally, the polysaccharides of the cell wall can be digested using **enzymes** (carbohydrases such as cellulases) before or during extraction. The hydrolysis of the structural polysaccharides releases some compounds which were bounded in the polymer network and facilitates the access of the solvent to the cells.[49] The extraction of EO from rosemary and thyme has already been improved by using cellulases and hemi-cellulases enzymes. Cellulase was more efficient than hemi-cellulase and they were more efficient when combined.[50]

Thanks to intensification, extraction times and thus, energy consumed are reduced. However, the energy required for the intensification technique must be taken into account. For example, enzymatic hydrolysis needs 60 to 100 kJ/kg while pulsed-electric field extraction (electrically assisted) only needs 1 – 15 kJ/kg and mechanical grinding requires 20 – 40 kJ/kg.[40]

Interestingly, some intensification techniques have already been used in solvent-free processes. For example, solvent-free microwave extractions have been performed to recover EO from rosemary, mint and polyphenols from sea buckthorn and onions. They consist of the application of microwaves on the plant which induces the cell disruption, the mass transfer of solutes to the outside of the plant material and the recovery of the liquid extract by gravity or by application of vacuum.[51]

I.1.4. Alternative extraction methods to conventional organic solvents

In addition to intensification techniques and pretreatments, the choice of the extraction medium is determinant for the extraction procedure. In order to reduce the environmental footprint of the solvent production, some extractions were designed with **agro-solvents** rather than petro-solvents. Ethanol, which is conventionally used in extractions of pigments, antioxidants or other polyphenols can be produced from biomass. Methyl tetrahydrofurane and terpenes (*d*-limonene, *p*-cymene) have already been used for the extraction of fats and oils,[52] and aqueous solutions of glycerol for the extraction of polyphenols.[53]

However, although the low boiling points of organic solvents allow convenient evaporation and recovery of both the solid extract and the pure solvent which can be recycled, this property and the supposed toxicity of some organic solvents raise serious concerns related to storage, flammability, VOC emissions and worker exposure. To avoid the use of solvents with low boiling points, the whole process must be redesigned to fit with the characteristics of the chosen extraction medium.

Considerable work has been done to develop inventive methods using pressurized gas or non-toxic liquids such as water or ethanol. **Supercritical CO_2** has already replaced organic solvents in extraction processes because it is able to solubilize compounds of various hydrophobicities such as volatile oils, flavonoids, terpenes, fatty acids, antioxidant compounds or pigments.[54] In fact, the solubilization of molecules can be adjusted by changing the pressure and temperature conditions, or by adding ethanol as co-solvent. In its supercritical state, CO_2 has a very low viscosity and high diffusivity so it can easily penetrate the plant material. Moreover, since its critical point is reached at quite low temperature and low pressure (T = 31.06 °C, P = 7.38 MPa), supercritical state can be achieved without spending a lot of energy. When the reactor is depressurized, CO_2 automatically turns into gas and separates from the extract which is therefore a solvent-free extract.[55] This method has already been performed for extracting CA several times and resulted in CA-enriched extracts, with purities from 2 to 3 times higher.[56–58] The addition of 7 % of ethanol was found important to increase the amount of extracted CA.

Likewise, **subcritical water** (T = 100-374 °C, P = 1.5-22 MPa, liquid state) and supercritical water (T > 374 °C, P > 22 MPa) are used as green extraction solvents since under such pressures and temperatures, the solubilization of less polar molecules is made possible. Indeed, due to the disorganization of water structure induced by the breaking of intermolecular H-bonds under these conditions, its dielectric constant considerably drops from about 80 at ambient temperature and pressure to 5 at the critical point, giving water similar properties as organic solvents such as ethanol (ε = 24) or chloroform (ε = 5).[59] It is thus able to dissolve EO, flavonoids, and polyphenols or phenols such as CA, which have been extracted in subcritical water at 200 °C, 60 bar by Ibañez et al.[60] Depressurization causes the loss of these properties to water, so the extracted organic compounds become insoluble and can be recovered by filtration.[37]

Subcritical water or supercritical CO_2 may replace organic solvents and avoid the risks associated with low boiling points of solvents but they require equipment which may be expensive and not suitable for large-scale extractions. Moreover, according to Giacometti et al., it is necessary to develop technologies that use low temperatures and consumes little energy in order to provide environmentally friendly extractions of bioactive compounds from aromatic plants.[61] However, to solubilize CA or other hydrophobic solutes in water at low temperature, a solubilizer must be added.

Only few CA extractions solubilized by a third molecule in aqueous solutions have been reported and used **ionic liquids** (IL) and **deep-eutectic solvents** (DES) as solubilizers (**Figure 7**). First, aqueous solution of 1-octyl-3-methylimidazolium bromide (IL, 1 M) has been reported for RA and CA extractions (UAE) from rosemary leaves at room temperature.[62] More recently, an aqueous solution of DES (15 wt.% of tetrapropyl ammonium chloride, 55 wt.% of 2-propanediol and 30 wt.% of water) was found more efficient than ethanol (70 %) and acetone to extract CA and CAR from rosemary.[63]

The separation of the solute from the IL solution was performed for other extractions than rosemary and most of the times it is performed by back-extraction with an organic solvent (*e.g.* ethyl acetate, chloroform, dichloromethane, *n*-butane) as reported after extractions of norstictic acid, a phenolic compound, from lichen or caffeine from guaraná seeds.[64,65] However, such methods do not avoid the use of organic solvents, so other techniques have been reported using water, as reviewed by Bogdanov.[65] After the extraction of the volatile oils from the fruits of *Forsythia suspensa* by $[C_2C_1im][C_1CO_2]$ (1-Ethyl-3-methylimidazolium acetate), they were recovered by hydrodistillation of the crude extract. In addition, the pH-dependance of the aloe vera anthraquinones solubility in water and $[C_4mim]Cl$ (1-butyl-3-methylimidazolium chloride) was used in a biphasic aqueous solution of IL to transfer anthraquinones from the IL phase to the aqueous phase by changing pH from 4 to 14. Finally, shikimic acid, a cyclohexene from star anise, was recovered by precipitation using water as an anti-solvent.[40]

IL are excellent extractants and furthermore, they can be used in aqueous medium (0.05 – 2.5 M) to act as solubility agents.[65] However, despite they are promoted for their low flammability compared to most of the organic solvents, most of IL still contain toxic products with low biodegradability such as imidazolium derivatives, and because of their ionic character, IL are generally corrosive.[66] Moreover, although some bio-based IL have already been developed at the laboratory scale from sugar derivatives for example, they are not commercially available yet.[67] On the contrary, DES are easy to prepare from bio-based compounds, by a simple mixture of the components, which are often low toxic and cheap, and constitute an interesting alternative to organic solvents, as already pointed out by Naturex.[68] However, both IL and DES are, by definition, mixtures, meaning that more compounds will have to be separated from the extract in the recovery step.

The use of amphiphiles such as hydrotropes or surfactants as solubility enhancers would avoid the use of expensive equipments, flammable and/or toxic organic solvents while performing the extraction in water (**Figure I.3**).

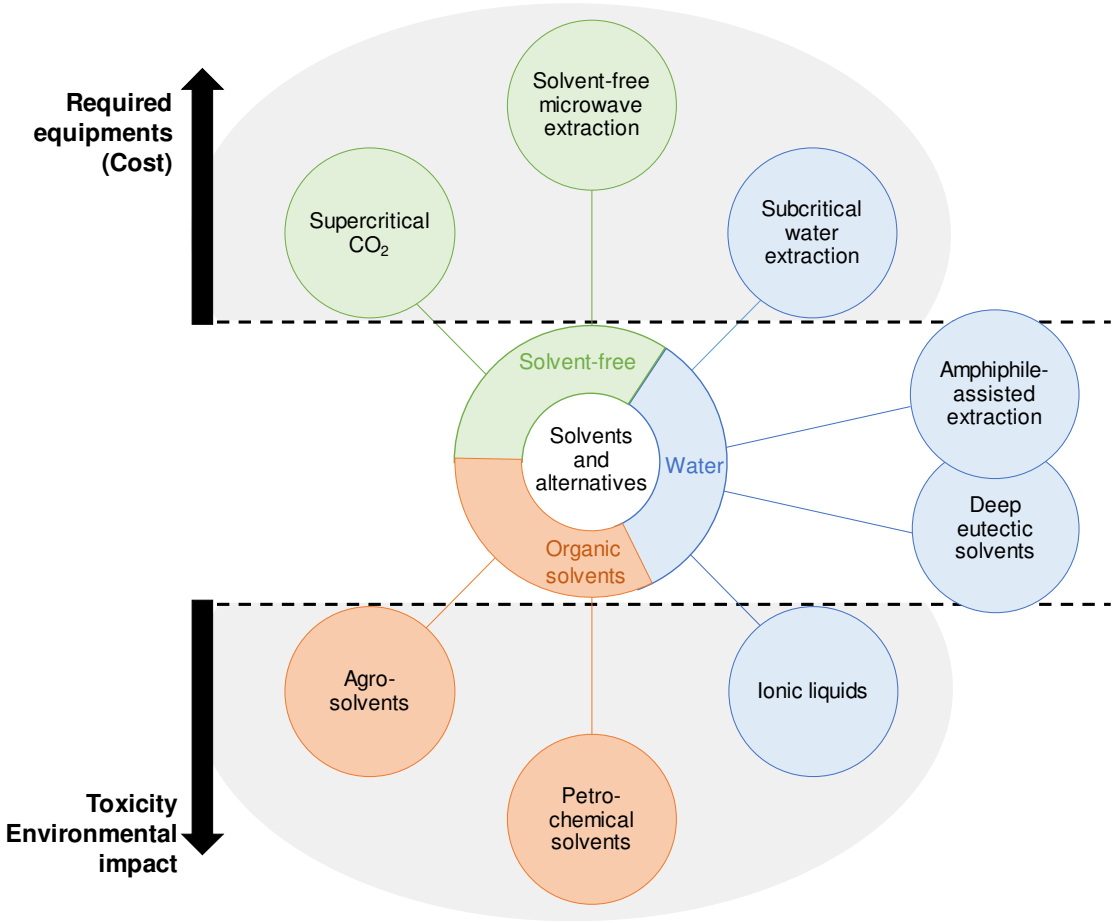

Figure I.3. Solvents, alternative solvents and techniques and their drawbacks. The scales are inspired from the classification of the alternatives solvents by Chemat et al.[53]

I.1.5. Aqueous micellar extraction: advantages and drawbacks

a. Surface and interfacial tensions: wettability of the plant surface

A surfactant, *i.e.* surface-active agent is an amphiphilic molecule (with both a hydrophobic and a hydrophilic moiety) with the property to lower the tension (or energy) at the liquid/liquid, liquid/solid or liquid/gas interface by accumulating there. Current micellar extraction procedures include liquid-liquid (*e.g.* extraction of antioxidants from olive mill wastewater, phenols from red flesh orange juice)[69] and solid-liquid extractions (*e.g.* tanshinones from sage[70], anthraquinones from *Morinda citrifolia* roots[71], chlorophylls from spinach[72]). For solid-liquid extractions, a low surface tension of the solvent is particularly important to increase the wettability of the plant. Since the plant surface is generally covered with pores, cavities and/or outgrowths, the solvent must have a low surface tension to cover all the cavities, increase the exchange surface with the plant and enter the pores[39] (**Figure I.4**).

b. Micellization and solubilization

In the case of a water-air system, when the water surface comes to a point where it is saturated of surfactants, their concentration in the water phase increases rapidly and they start to self-assemble into micelles to minimize the energy of the system. This phenomenon occurs at the Critical Micellar Concentration (CMC ≈ 10^{-4} – 10^{-2} M). The formation of the micelles creates hydrophobic microenvironments, which can solubilize poorly-water soluble molecules (**Figure I.4**).[49]

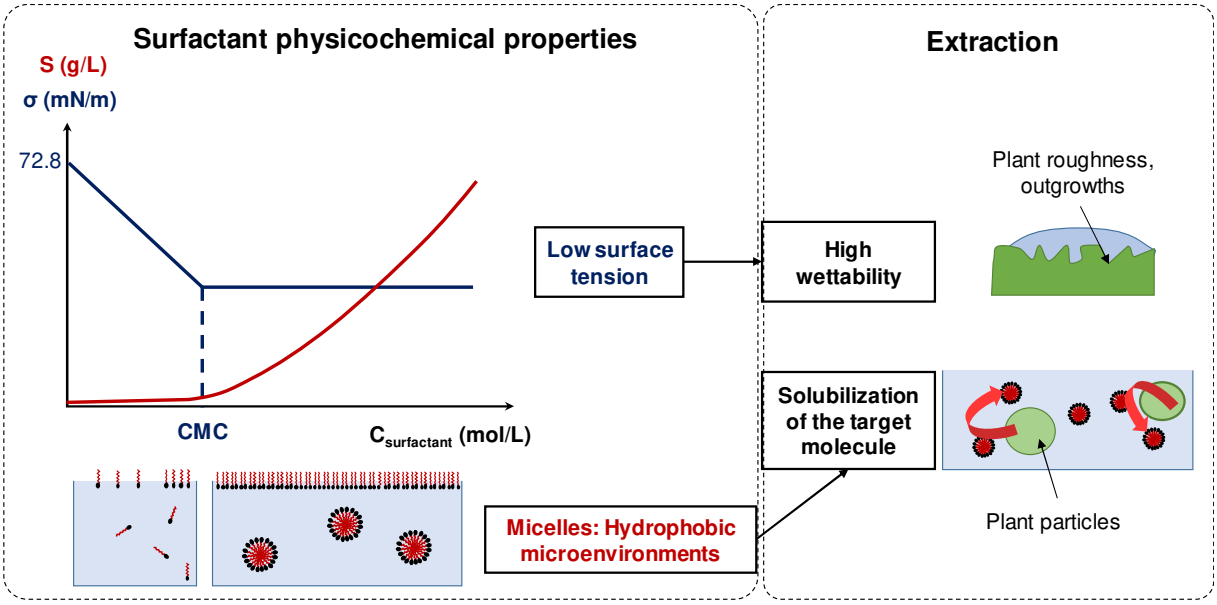

Figure I.4. Application of the physicochemical properties of surfactants to the micellar extraction mechanism.

c. Cloud point: concentration of the extract in a smaller phase

Interestingly, aqueous solutions of some nonionic surfactants and especially many poly(ethylene oxide) surfactants such as Triton X-100 or Genapol X-080 phase separate above a temperature called “cloud point” (CP). Indeed, the surfactant micelles stabilized in water by interactions can be destabilized by the breaking of the H-bonds due to heating which induces a phase separation, hence the formation of a surfactant-rich phase and a surfactant-poor phase between which the extracted molecules partition.[73]

This property has mainly been reported for concentrating a liquid extract and three processes can be pointed out (**Figure I.5**):

- **Cloud Point Extraction (CPE)**: This method can be considered as a purification technique. A liquid extract is recovered by a surfactant-free extraction from plant, which may be performed by organic solvent and surfactants are added to the liquid extract to concentrate the target compounds in a smaller phase. The solution is heated until phase separation and electrolytes such as NaCl are often added to the mixture to help the

phenomenon. For example, Katsoyannos at al. reported phenols and carotenoids extraction from olive mill wastewater and fresh-red orange juice which were obtained from a milling and a pressing process respectively. For this purpose, a mixture of Tween® 80 and NaCl, at pH 2.5 – 3.5 were used.[69] Furthermore, Zhou et al. reported ethanolic extractions of flavonoids from *Apocynum venetum* leaves followed by the liquid-liquid CPE of the crude extract using a mixture Genapol X-080/NaCl/CTAB.[74]

- **Micelle-mediated extraction and CPE**: the plant material is first extracted by the surfactant solution and then, a CPE is applied on the micellar crude extract, as presented above. For example, coumarin derivatives of *Cortex fraxini* were extracted using aqueous solutions of Genapol X-080 (5 %) and then concentrated by addition of salt (20 %) or heating (55 °C).[75]

- **Aqueous two-phase extraction:** the micellar extraction and the concentration of the extract can also be performed in a one-step process. For example, triterpenes of sage (ursolic and oleanolic acids) were extracted with aqueous solutions of Brij® 56, Genapol® X-080 or Tween® 65 (7 wt.% in water) above their CP at 105, 50 and 65 ° C respectively, with rigorous stirring. Due to strirring, small droplets of the surfactant-rich phase are dispersed in the medium, hence the solution becomes cloudy. The chromatograms of the crude extracts obtained with Genapol X-080 and the ethanol/water mixture (70/30) were compared and the surfactant solution showed higher selectivity compared to organic solvents, since many compounds are detected on the chromatogram of ethanolic extract but not on the chromatogram of the micellar extract.[76]

Interestingly, the concentrated micellar extracts can be directly used in cosmetic formulations. For example, bromelain which are proteolytic enzymes have been extracted from pineapple by enzymatic-assisted extraction, concentrated using a solution of Triton X-100 and directly formulated in cosmetic creams and gels.[77]

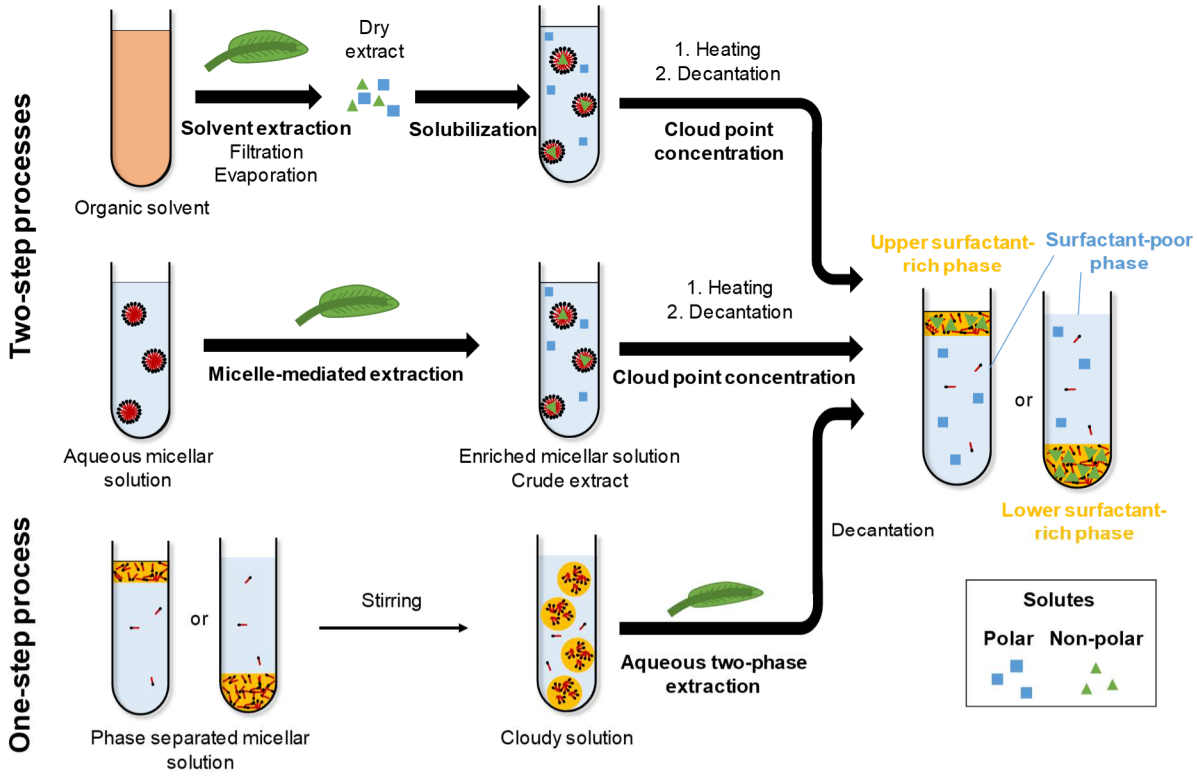

Figure I.5. Role of nonionic surfactants in the extraction and concentration process of an extract.

d. Extraction process with ionic surfactants

Similarly, solutions of ionic surfactants can be used to extract and/or concentrate the extract in a smaller phase. Indeed, the extraction of cryptotanshinones from *Salvia miltiorrhiza* Bunge was more efficient with Sodium dodecyl sulfate (SDS) than water or conventional solvents (methanol, ethanol, ethyl acetate, dichloromethane).[70] SDS was also found better than cetrimonium bromide (CTAB) to extract piperine from black pepper. In this study, piperine solubilized in the surfactant solutions was recovered by crystallization with temperature.[78]

For the concentration step, ionic surfactants do not present any CP, but they can be destabilized by addition of electrolytes ("salting-out" effect), organic solvents or pH change instead of heating.[73] However, non-ionic surfactants are generally preferred for performing a coacervative extraction.[79,80]

e. Liquid crystals: undesirable viscous phases

The particularity of surfactants is their propensity to form liquid crystals (LC) at a certain concentration (lyotropic LC) or a certain temperature (thermotropic LC) leading to very viscous phases. However, during the extraction step, the viscosity of a solvent can limit its penetration inside the plant material and the mass transfer of the solute.[69] In addition, in the last step of the CPE, when surfactants (with alkyl chain lengths longer than 10 – 12 carbon atoms) concentrate to 50 - 90 % in a surfactant-rich phase, LCs can be formed, which is not convenient for the

recovery of an extract. To overcome this phenomenon, methanol can be added to lower the viscosity.[75]

I.1.6. Hydrotropes as alternative to surfactants for aqueous extraction

a. Definition, chemical structure and main properties

The concept of hydrotropy has been introduced by Neuberg in 1916[81] defining hydrotropes as molecules able to improve the solubilization of organic substances in water. Therefore, the concept of hydrotrope was a general term for a molecule which, in aqueous solution, solubilizes other molecules which would otherwise not be dissolved. Since then, this concept has evolved and the physicochemical phenomenon underlying the formation of a hydrotropic phase has been the subject of many researches.

Currently, hydrotropes are defined as short amphiphiles which *(i)* forms weak aggregates, unorganized structures, *(ii)* solubilizes important amounts of hydrophobic compounds at high concentration, and *(iii)* breaks surfactant LC.[82,83] These characteristics are presented here in more detail.

Formation of weak aggregates

For a part of the scientific community that relies on osmometric studies and molecular dynamics simulations of solubilization, hydrotropic aggregation is a stepwise phenomenon which involves the successive formation of dimers, trimers, tetramers successively,[84] or bigger aggregates at higher concentration. For example, the aggregation number of sodium *n*-butyl benzene sulfonate (NaNBBS) turned out to be 36 – 40.[83] They consider hydrotropic aggregation to be a **non-cooperative phenomenon** which occurs above the Critical Aggregation Concentration (CAC), defined as the CMC counterpart of surfactants, which cannot be used for hydrotropes since they do not form real micelles.

This phenomenon has also been viewed as a prerequisite for solubilization, which occurs above another concentration called **Minimum Hydrotopic Concentration (MHC).**[85] This theory is corroborated by the fact that the MHC is currently considered to be **constant** for a given hydrotrope regardless the hydrophoby/polarity of the solute. To our knowledge, Balasubramanian at al. were the first in 1989 to draw that conclusion,[86] *i.e.* MHC does not vary when changing the solubilized molecule. They tested the solubilization of three hydrophobic probes (fluoresceine diacetate, perylene and ethyl p-nitrobenzoate) in aqueous solutions of five anionic hydrotropes: sodium salicylate (NaS), sodium p-toluene sulfonate (NaPTS), sodium xylenesulfonate (SXS), sodium cumenesulfonate (NaCS), and sodium butylmonoglycol sulfate (NaBMGS). The MHC determined for these three probes (NaBMGS: 0.8 mol/L) corresponds approximately, but is slightly higher, to the CAC (NaBMGS: 0.7 mol/L), strongly suggesting that the aggregation is a necessary condition to solubilization.[86]

On the other hand, thermodynamicists have noticed that urea molecules form a near-ideal mixture with water (they do not form aggregates) but have similar properties compared to other hydrotropes which are prone to aggregate. On the basis of the solubilization curves of butyl acetate and benzyl benzoate in sodium benzoate (NaB), NaS and urea, they identified the presence of a solute as the main driving force for hydrotropic aggregation, hence the aggregation comes a **cooperative phenomenon**.[87]

In both cases, despite the lack of consensus on the phenomenon origin, researchers agree that hydrotropes form weak aggregates. This property is useful for differentiating hydrotropes from surfactants, which aggregate strongly and form organized micelles and from co-solvents, which do not structure.[88]

Solubilization of important amounts of hydrophobic compounds at high concentration

According to the first definition of hydrotropy, surfactants and co-solvents which can dissolve hydrophobic compounds would have been considered as hydrotropes. However, the concentration of amphiphiles required for such solubilization (MHC for hydrotropes) is different for surfactants (10^{-2} – 10^{-3} M), hydrotropes (≈ 1 M) and co-solvents (2 – 3 M).[89]

Moreover, at high concentration, hydrotropes are much more efficient to solubilize hydrophobic compounds compared to surfactants which form liquid crystalline phases, thus limiting the solubility due to high viscosity. This was first demonstrated for the solubilization of octanoic acid in solutions of SXS compared to solutions of sodium octanoate.[86] In **Figure I.6**, this phenomenon is illustrated for the solubility curves of CA in aqueous solutions of Tween® 80, a commercial surfactant derived from a polyethoxylated sorbitan and oleic acid, and C_4E_2, a short-chain alkyl polyethylene glycol ethers (C_iE_j, with *i* the numbers of carbon atoms in the alkyl chain and *j* the number of ethylene oxide units) generally considered as hydrotrope.[90]

Noteworthy, solubility curves were performed at pH 2, to avoid deprotonation of CA. Indeed, despite its deprotonation would increase the water-solubility of CA, it has also been noticed in a previous study that it would increase its reactivity and its degradation.[91] This may be related with a higher reactivity of catechols in alkaline solutions, as shown by Maier et al.[92] As a result, Tween® 80 solubilizes CA above 0.5 wt.% whereas the MHC occurs at 15 wt.% for C_4E_2, but this latter can solubilize 40 g/L of CA, so 2.5 times more than the maximum solubility reached with Tween® 80 at 10 – 15 wt.%.

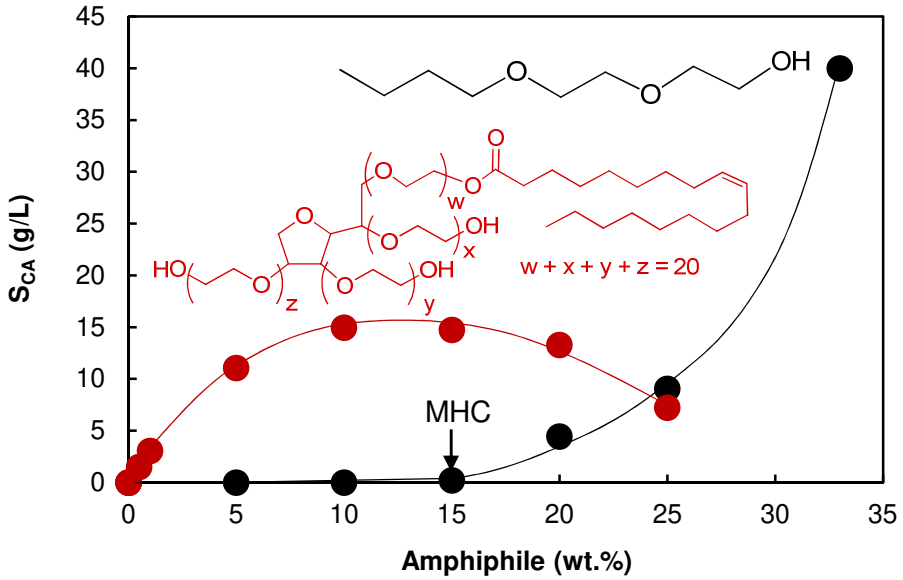

Figure I.6. Saturation concentration of CA in aqueous solutions of Tween® 80 and C_4E_2 after 24 h of stirring, at pH 2, 25 °C (experimental method precised in section II.6.2)

Destabilization of liquid crystals

To explain the breaking of LC, Guo et al. used a model of pentanol molecules inserted between SDS surfactants to tune the SDS packing parameter in such a way that they form lamellae in water instead of the standard spherical micelles (**Figure I.7**, a). In the presence of an ionic hydrotrope, SXS, the system evolves with the hydrotrope inserted between SDS molecules, in the "palisade layer", near their sulphate groups, establishing dipole/dipole and/or ion/dipole interactions (**Figure I.7**, b). Pentanol molecules which have a low polarity migrate to the space between two SDS layers, as far as possible from the hydrophilic moiety (**Figure I.7**, a). The intercalation of pentanol in the palisade layer *i.e.* between SDS molecules and below SXS ones strongly destabilizes the lamellar structure by inducing a modification of the oil/water interface curvature (**Figure I.7**, c) [93]. Indeed, a lamellar structure is normally characterized by its zero-value curvature.

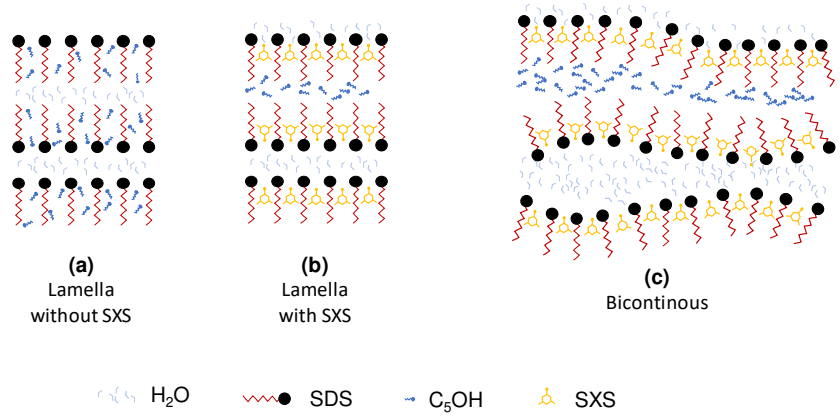

Figure I.7. Structure transition from lamella to bicontinous induced by SXS [93]

b. Hydrotropic extraction: a promising process

Regarding extraction, hydrotropes meet almost all the requirements since they exhibit the same useful properties as surfactants without forming LC. Indeed, like surfactants, hydrotropes are surface-active and they solubilize even more hydrophobic compounds than surfactants. In addition, the ability of surfactants to phase separate above their CP, a convenient property for extraction processes (section I.1.5), has also been reported for some non-ionic hydrotropes. Indeed, alkyl ethers of polyethylene glycols (C_iE_j), propylene glycols (C_iP_j), glycerol, isosorbide and tetraols also have a CP (< 100 °C),[90,94–96] and this property has also been used in a process called "Hydrotropic cloud point extraction" (HCPE) for the extraction of piperine from black pepper with alkyl glycerol ethers as hydrotropes.[94]

Despite all their convenient properties, hydrotropes have not been widely reported in extraction processes. In particular, no hydrotropic extraction of CA has ever been reported, according to SciFinder® (**Figure I.8**) The key word "carnosic acid" was refined for "rosemary OR sage" and then "extraction" to get only the papers of interest. Then, the number of journal article for each category of interest was noted by refining with the corresponding key words. The category "organic solvents" include all the articles which use at least one of the following solvent: acetone, hexane, chloroform, petroleum ether, methanol, ethanol, diethyl ether, ethyl acetate and tetrahydrofurane.

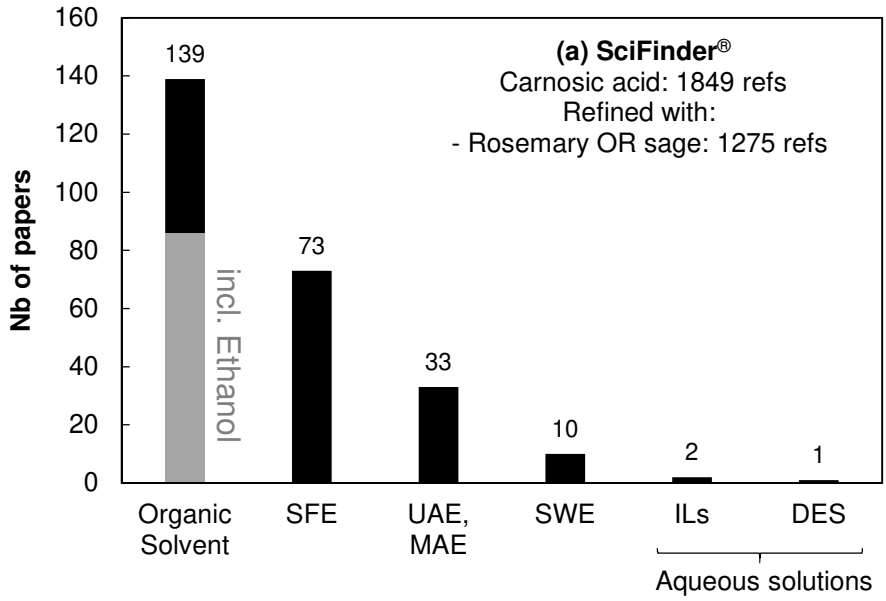

Figure I.8. Number of journal articles found on SciFinder® (07/29/2020) about CA extraction from rosemary or sage classified by extraction techniques. Among the journal articles of the search "carnosic acid" refined with "rosemary OR sage", the key word "extraction" was combined with the key words relative to the extraction techniques (in italic): SFE: *Supercritical* fluid extraction, UAE: *Ultrasounds*-assisted extraction, MAE: *Microwave*-assisted extraction, SWE: *Subcritical water* extraction, ILs: *ionic liquid*, DES: *deep-eutectic solvents.* The other techniques non reported had no result when searched.

Apart from CA, the number of papers containing the key words “extraction” and “hydrotrope” (159 references) are very few compared to those containing “extraction” and “supercritical fluid” or “cloud point” or “micelle” or “subcritical water”, which relates to other green extraction techniques or those containing “extraction” and “ultrasounds” or “microwaves” or “pulsed electric field” or “high voltage electric discharge” or “enzyme” relating to intensification techniques (**Figure I.9**).

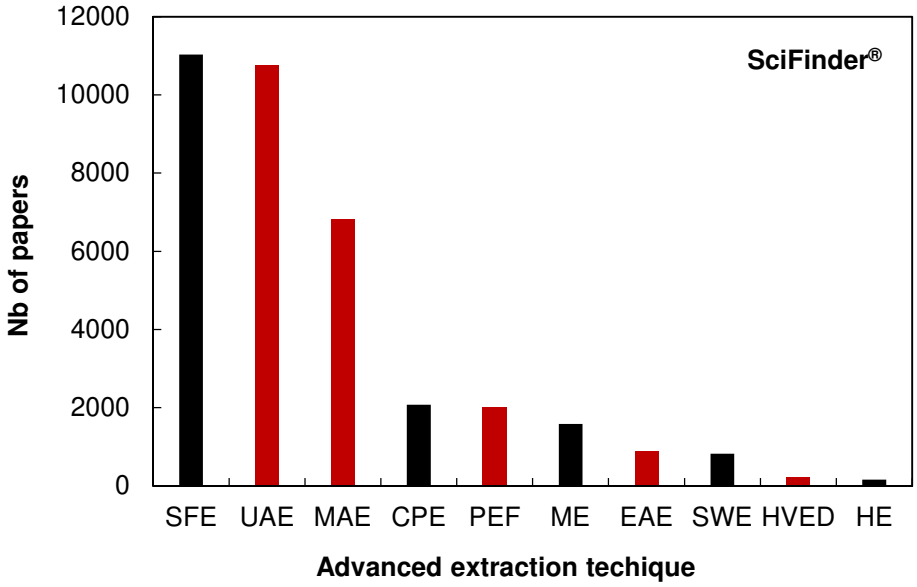

Figure I.9. Number of journal articles found on SciFinder® (07/27/2020) about different extraction techniques using intensification (in red) or alternative solvents (in black). The key word “extraction” was combined with the key words relative to the extraction techniques (in italic): SFE: *Supercritical* fluid extraction, UAE: *Ultrasounds*-assisted extraction, MAE: *Microwave*-assisted extraction, CPE: C*loud point* extraction, PEF: *Pulsed electric field*, ME: Micellar extraction (key word: *micelle*), EAE: *Enzyme*-assisted extraction, SWE: *Subcritical water* extraction, HVED: *High voltage electric discharge*, HE: Hydrotropic extraction (key word: *hydrotrope*)

Subsequently, the literature on hydrotropic extraction is reviewed with an emphasis on the role of hydrotropes during extraction, the existing techniques to recover a dry extract and the evolution of the chemicals and techniques used to make the whole process more eco-compatible.

I.2. Roles of hydrotropes in the extraction process

Hydrotropes have been used in extraction processes since the 1950's, for both liquid/liquid and solid/liquid extractions. A conceptual map based on the data concerning "hydrotropes" and "extraction" from SciFinder® gave a global visualization of the research themes studied in the same time than hydrotropic extraction (**Figure I.10**). In blue and purple are shown the articles relative to the cosmetic and pharmaceutical application of hydrotropes. Conventional techniques studied with extraction such as solubilization, purification, biomass, and mass transfer are depicted in red and green. Noteworthy, by highlighting the word "solubilization", the conceptual map points out that hydrotropes are generally used for their solubilization properties in extraction processes. Interestingly, a yellow group composed of "paper pulp" or "pulping", "wood" and "sodium xylene sulfonate" stand out on the left. Indeed, more than half reported extraction processes since 1950 relate to the extraction of lignin from wood or other lignocellulosic materials with alkyl benzene sulfonates and generally with sodium xylene sulfonate (SXS).

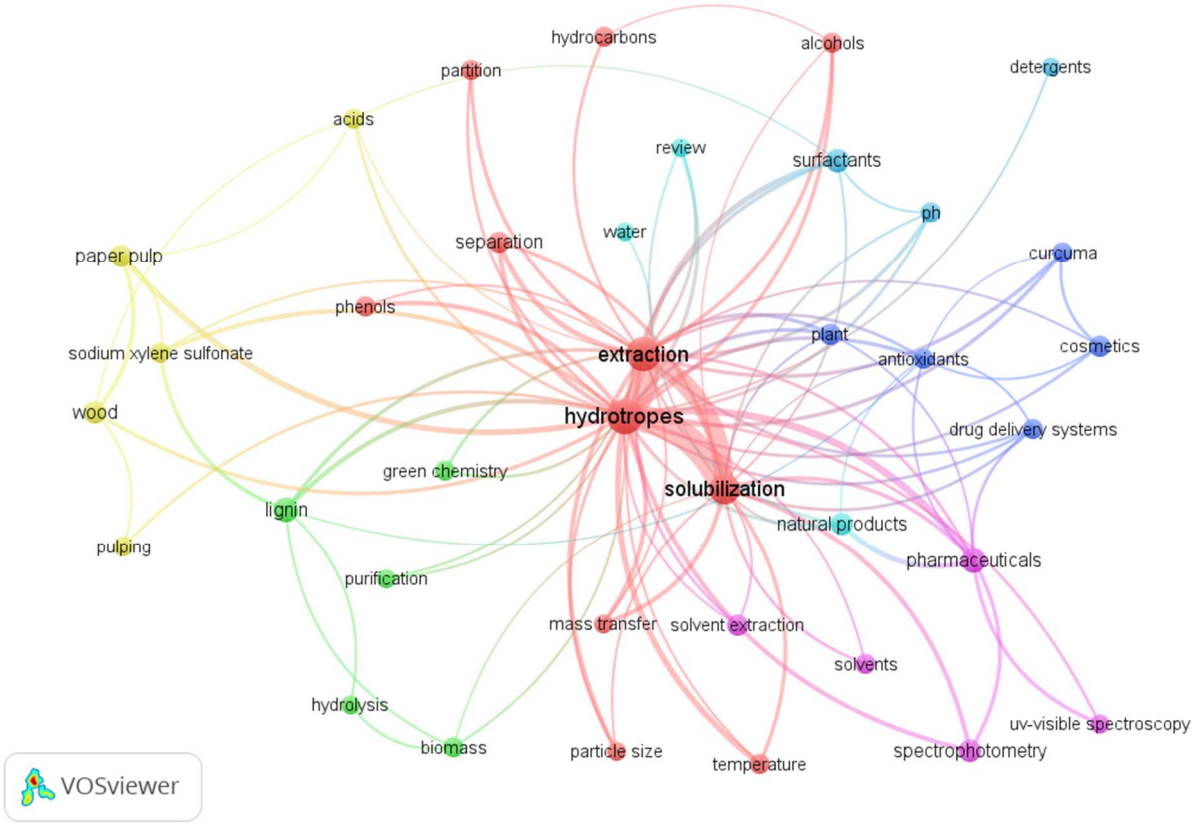

Figure I.10. Conceptual map performed on VosViewer of the references containing the key words "hydrotrope" and "extraction" on SciFinder®

I.2.1. Effect of hydrotropes on lignocellulosic materials

Lignin is a biopolymer of phenolic compounds such as *p*-coumaryl alcohol, found in most plants, particularly in wood and stems and in fewer quantity in leaves.[97,98] Along with cellulose and hemi-cellulose, it is a major component of cell walls and gives it rigidity. Its presence in wood is undesirable for paper production because it is responsible for yellowing of paper, so its extraction has started to interest industrials. Moreover, since cellulose, hemi-cellulose and lignin are very abundant molecules, and given the fact that they can be precursors of many bio-based molecules, their isolation from each other has been widely studied.[99]

In 1938, McKee was the first to use sodium, calcium and ammonium salts of benzoic, salicylic, xylene sulfonic, cymene sulfonic, benzene sulfonic, phenol sulfonic, and toluene sulfonic acids as hydrotropes in an extraction process, as stated in its patent. SXS (30 wt.%) has been found to be the most efficient solubilizer and extractant of lignin from woods (*e.g.* poplar wood).[100]

A mechanism of lignin solubilization by *p*-toluene sulfonic acid (PTSA) has recently been proposed by Ji et al.[98] They found that PTSA was highly effective in removing lignin and hemicellulose (86 and 77 % resp.) compared to IL ([Amim][Cl], removal < 15 %) and choline chloride-lactic acid, a DES (ChCl-Lac, removal < 20 %). According to molecular dynamics simulations and quantum chemistry calculations using veratrylglycerol-b-guaiacyl ether (noted VG) as a model compound of lignin, they proposed that both C–H – π interactions and strong H-bonds between PTSA and VG helped to solubilize lignin. Moreover, they noticed that the amount of phenolic alcohols in solution increased after the hydrotropic process, suggesting the depolymerisation of lignin (**Figure I.11**).

According to Chen et al., the hydrolysis of glycosidic bonds in carbohydrates and lignin-carbohydrate complexes and ether bonds in lignins is enabled by the deprotonation of PTSA (pKa = - 2.8 at 20°C), as shown in **Figure I.11**. Thus, a near-complete dissolution of lignin was performed in 20 min at 60 - 80 °C.[101] The structure of hemi-cellulose is less organized than the structure of cellulose making hemi-cellulose more prone to hydrolysis but sulfonic acid derivatives also seem to destructure cellulose fibers under specific conditions. Indeed, Novy et al. observed the ultrastructure of cellulose by confocal laser scanning microscopy using fluorescence carbohydrate-binding modules to reveal crystalline and paracrystalline cellulose. They found that the action of SXS (40 wt.%) at 190 °C during 4 h on hardwood chips modified the cellulose ultrastructure and produced fragmented cellulose fibers (**Figure I.11**).[102]

Therefore, a sulfonic acid derivative is able to destructure cellulose, the main component of the cell wall, to hydrolyse lignin and hemi-cellulose and to dissolve the produced monomers or oligomers in aggregates for non-water soluble compounds or directly in water for sugars, as summarized in **Figure I.11**. It is likely that such action on the cell wall increases its porosity and improves a putative mass transfer through the cell wall, and therefore the extraction of bioactives located inside the cells.

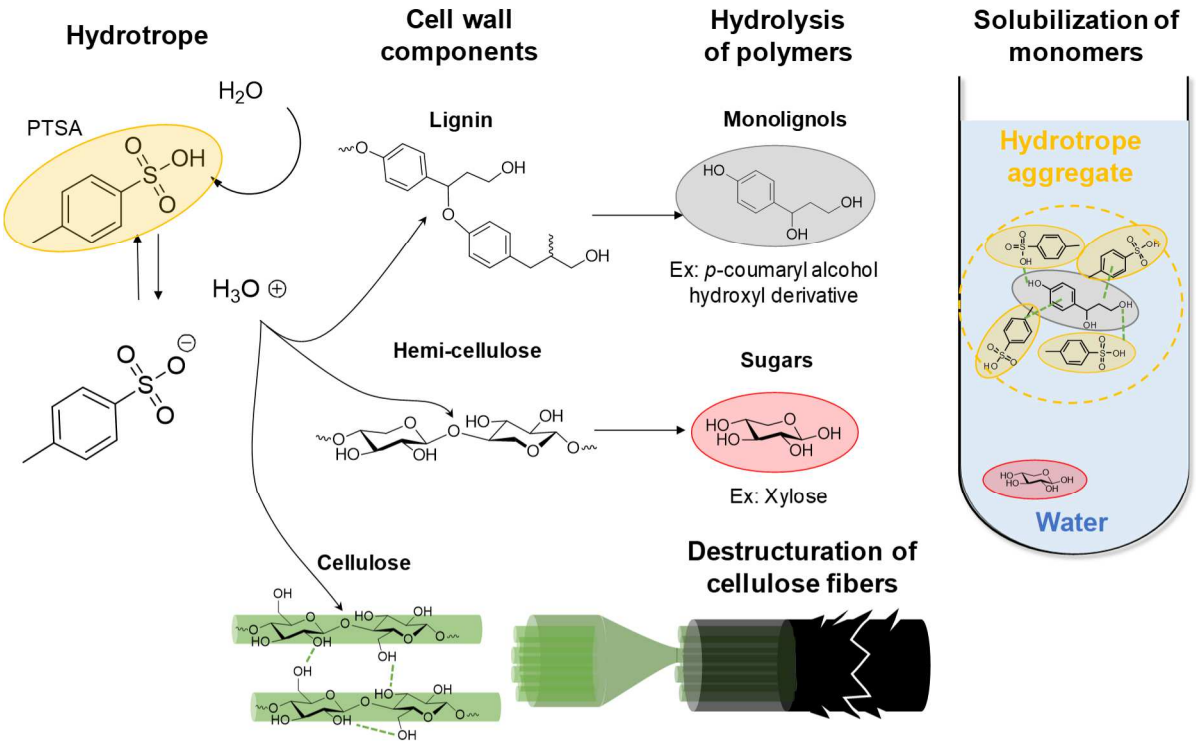

Figure I.11. Overview of the roles of PTSA as an hydrotrope on the molecules of the cell wall according to mechanisms proposed by Ji et Lv.[98], Chen et al.[101] and Novy et al.[102]

I.2.2. Cell membrane crossing

Besides lignin and hemi-cellulose, the extraction of other bioactives has also been reported several times over the past 20 years, since Gaikar and co-workers reported the extraction of curcuminoids and piperine from turmeric rhizomes and black pepper respectively, using mainly alkali (sodium or potassium) salts of benzoic, salicylic and aromatic sulfonic acids.[103,104] Since then, only a few plant extractions using hydrotropy have been reported in the literature. One can cite the extraction of embelin from embelia ribes[105], that of forskolin from *Coleus Forskohlii* roots[106] or andrographolide from *Andrographis paniculata* Leaves[107].

In their study of hydrotropic extraction of piperine from *Piper Nigrum* (black pepper), Raman and Gaikar have proposed a mechanism of mass transfer through cell walls and membranes.[103] They used five anionic hydrotropes (NaNBBS, NaCS, NaPTS, NaBMGS, SXS) and analyzed the liquid extract composition after the extractions. They detected the presence of inorganic phosphorus, reducing sugars and amino acids, from what they deduced that hydrotropes had probably destabilized the phospholipid bilayer and dissolved some structural proteins and carbohydrate polymers such as extensins, hemi-cellulose or cellulose from the cell wall. This phenomenon is not surprising since it has been demonstrated that hydrotropes can break polymers of the cell wall and destructure cellulose (section I.2.1). They suggested a process in which hydrotropes cross the wall, which has just been dissolved, then the phospholipid bilayer membrane, which has also been disorganised (**Figure I.12**). Such a dizorganisation is in

agreement with the previous results of Guo[93] established on SDS/pentanol lamellar phases (section I.1.6), since the phospholipid bilayer is structured like surfactant lamellar phases. Interestingly, this suggests that the penetration of the hydrotrope in plants through the cell membrane and the inhibition of the surfactant LC both result from the ability of the hydrotropes to intercalate between mono- or bicatenary surfactants. In other words, macro- and mesoscopic scale behaviors of hydrotropes can be inferred from the many intermolecular interactions taking place at the nanoscale.

When the physical chemical barrier is broken enough, piperine can be solubilized by hydrotropes and transferred to the solution. As mentioned previously, hydrophobic compounds are solubilized by hydrotropes through aggregation, a phenomenon which occurs above the MHC. Therefore, MHC is the minimum concentration required to extract organic compounds. The steps for the hydrotropic extraction mechanism are showed in **Figure I.12**, on the basis of the schematic representation proposed by Gaikar et al.[103]

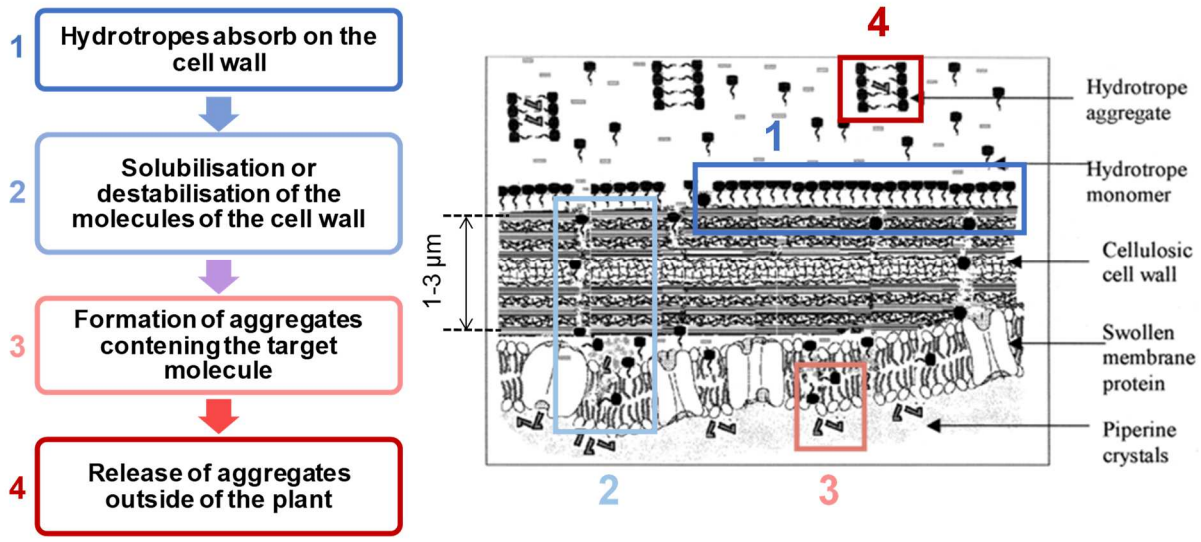

Figure I.12. Schematic representation of the mass transfer during extraction of piperine from *Piper Nigrum* (black pepper).[103]

I.2.3. Selective extractions of actives

The efficiency of hydrotropic solubilization may differ between active compounds, therefore hydrotropes selectively solubilize one active rather than others. This is one of the major strengths of hydrotropes, as selective extraction facilitates the next step of purification. For example, it has been shown that embelin from embelia ribes can be extracted and recovered with a purity of 90 and 92% using NaCS and NaNBBS respectively, compared to pure embelin obtained with a conventional multistep extraction and purification process.[105]

Interestingly, urea, citric acid, nicotinamide, NaS were very efficient to separate solutes with close chemical structures and close boiling points such as phenol/*o*-chlorophenol[108] and NaBMGS in the separation of *o*- and *p*-chlorobenzoic and nitroaniline isomers.[109] In this last

study, *o*-isomers are more soluble in hydrotropic solutions than *p*-isomers, and thus, when the hydrotropic solution with an adequate concentration is added to the mixture, all the *o*-isomers are solubilized and the recovered solid is only composed of *p*-isomers. This selectivity supposes a non-negligible effect of the chemical structure of the solute on its interaction with the hydrotrope, and on its aggregation.

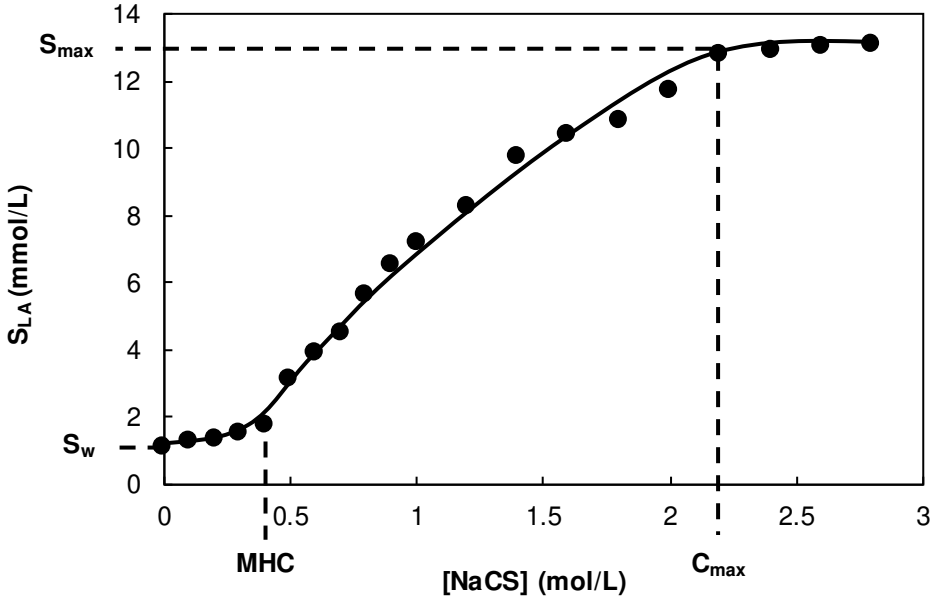

Figure I.13. Solubility curve of lauric acid (LA) in aqueous solutions of sodium cumene sulfonate according to values from ref[110]

To better compare the extractability of the solutes and the effect of hydrotrope, researchers have introduced the enhancement factor (EF), as the ratio between the quantity of solute that is solubilized by hydrotropes at any hydrotrope concentration and the quantity solubilized in pure water, noted S_w.[111] Usually, authors report the maximum EF, *i.e.* using the solubility at the plateau, or at the C_{max} (noted S_{max}, **Figure I.13**). It depends both on the hydrotrope and the solute and is increased with temperature, as shown for lauric and benzoic acids (LA and BA resp.) in **Table I.1**. The comparison of the maximum EF and solubilities of BA and LA highlights the fact that sodium benzoate (NaB) is the best hydrotrope for solubilizing LA whereas sodium salicylate (NaS) is a better solubilizer for BA. The EF is convenient to compare the action of different hydrotropes on the same solute.

However, a smaller EF can mean both a lower hydrotropic solubility or higher water solubility, so this is not sufficient to compare the behaviors of two solutes in aqueous solutions of the same hydrotrope. Taking NaB as example, EF(LA) > EF(BA) but $S(LA)_{max} < S(BA)_{max}$. Consequently, in an extraction process, BA would preferentially be solubilized and extracted compared to LA, but the action of the hydrotrope on its solubility is less important.

Since solubilization is hydrotrope-solute dependant, Herbig et al. wondered which physicochemical parameter of the solute had an effect on the EF in solutions of urea (40 wt.%).[112] Among the 12 solutes tested, several ionisable molecules (*e.g.* salicylic acid, diclofenac) were tested under acidic and basic conditions (pH 4 and 8) to modify their solubility in water and their interactions with their environment in hydrotropic solutions. They found that solutes with log *D* (log *P* corrected with pH) comprised between 2 and 4.5 had the highest EF. Indeed, molecules with log *D* below 2 are more soluble in water, and the increase in solubility is not as important when hydrotrope is added, whereas molecules with log $D > 4.5$ have a lower solubility in the hydrotropic phase. Therefore, the selectivity of hydrotropic processes can be shaped by the choice of hydrotrope and its concentration, with an accurate study of the solubility curves of the target compounds and the undesirable ones.

Table I.1. Maximum solubilities (mmol/L) and enhancement factors EF of BA and LA at 30 and 40 °C for several hydrotropes (NaB: sodium benzoate, NaS: sodium salicylate)

Solute	**LA**[113]				**BA**[111]	
Temperature (° C)	**30**		**40**		**30**	
	$\mathbf{EF_{max}}$	$\mathbf{S_{max}}$	$\mathbf{EF_{max}}$	$\mathbf{S_{max}}$	$\mathbf{EF_{max}}$	$\mathbf{S_{max}}$
NaB	23.3	13.9	26.0	19.3	6.63	21.3
NaS	12.5	9.0	15.1	14.0	9.43	30.3
Nicotinamide	4.7	3.2	10.1	7.8	3.34	10.7

To sum up, hydrotropes have two major roles in plant extractions: *(i)* they transfer through the cell wall and can destructure it, especially if it contains a high amount of lignin and hemi-cellulose, they also transfer through the cell membrane, which is similar to a lamellar LC, *(ii)* they solubilize organic compounds through aggregation, a highly hydrotrope-solute dependant phenomenon.

I.3. Recovery of a dry extract

Plant extractions are generally performed using an organic solvent and followed by the recovery of the target compounds which induces the removal the solvent.[114] The solute crystallization (or precipitation if amorphous particles are produced) is a two-step process composed of crystal nucleation and growth, and induced by the **supersaturation** (ΔS) of the solution, that is the difference between the actual concentration of a solute and its solubility in the solution.[115] If the supersaturation is not important enough, the solute may not precipitate due to metastability. In solvent extraction processes, three main methods are used to achieve supersaturation: *(i)* the evaporation or distillation of the solvent, which is a convenient method considering their low boiling point, *(ii)* the cooling of solution when the solubility of the solute depends on the temperature, *(iii)* the addition of an antisolvent.[116] The two latter methods can be used to purify

the extract at the same time by selectively crystallizing the target compound or the "impurities" using their different solubilities upon cooling or addition of the antisolvent.[115] Those methods have been adapted to hydrotropic solutions, as reported below.

I.3.1. Addition of water as anti-solvent: selective recovery

The easiest way to get supersaturation in a hydrotropic solution is the dilution with water to the MHC (**Figure I.14**), which can be analogous to the addition of an anti-solvent without using organic solvent. It has been used in many processes and studied in detail for the recovery of a curcuma extract, in comparison with pure curcuminoids.[117] The use of pure compounds was efficient in modelling the crystallization of the extract because in both cases, fine crystals were obtained due to higher nucleation rates than growth rates.

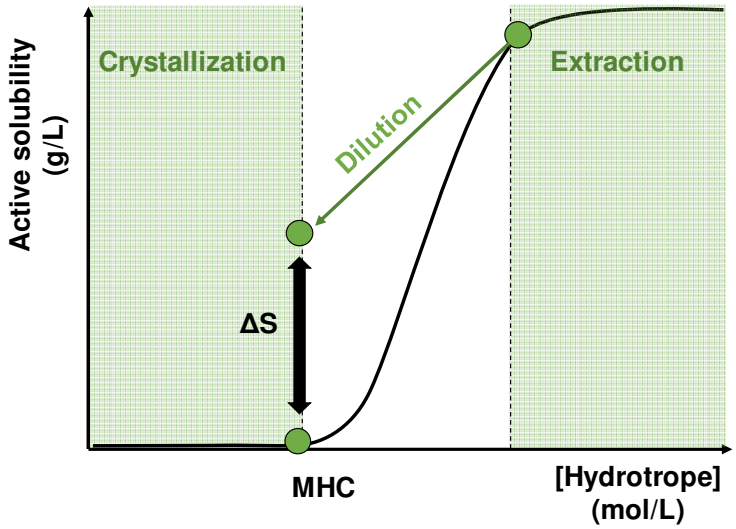

Figure I.14. Characteristic active solubility curve in hydrotropic solution and schematic representation of the precipitation step. ΔS = supersaturation

Interestingly, as shown in **Figure I.14**, the concentration of both solute and hydrotrope decrease and therefore, it is clear that the highest value of supersaturation is always reached at the MHC. The superstation is lower above MHC due to the increase in solubility of the solute, and is also lower below the MHC due to a decrease in the solute concentration.

I.3.2. Evaporation of hydrotropes: case of solvo-solfactants

"Solvo-surfactants" is the name given to a new class of hydrotropes described by Lunkenheimer in 2004.[118] Like hydrotropes and surfactants, they can form aggregates, and consequently, they are able to solubilize hydrophobic molecules. On the other hand, like solvents, they have low boiling points. Among the reported solvo-surfactants, one can cite alkyl glycerol ethers, alkyl polyethylene or polypropylene glycol ethers (C_iE_j or C_iP_j, with *i* the alkyl chain length and *j* the number of ethylene or propylene oxide units) which present low boiling points (BP = 170 – 270 °C at 1 bar) and can be recovered by evaporation under vacuum (BP = -1 – 70 °C at 1 mbar).

An innovative process of the extraction of piperine using solvo-sufactants C_4E_1, monopentyl glycerol (C_5Gly) and 1-butyl-3-methyl glycerol ether ([4.0.1], 40 %) has been reported. Regarding the recovery of the extract, the solute was first concentrated by a temperature-induced liquid-liquid phase separation, which occurs above the CP of the hydrotropes in a similar process compared to surfactants. In this study, a temperature of 60 °C was applied to induce the phase separation. Studying the extraction of piperine with mono and di-alkyl glycerols used as hydrotropes, it has been shown that the solute (piperine) could preferentially migrate to the hydrotrope-enriched phase without significant degradation. Then, the phases were manually separated and the dry extract was recovered by heating the hydrotrope-enriched phase at 60 °C under vacuum to evaporate the hydrotrope.[94]

I.3.3. Crystallization of an extract by cooling: case of sodium cumene sulfonate

The standard cooling process to selectively crystallize solutes from a solvent has also been adapted to phytochemicals extracted in hydrotropic solutions. It has been studied, for instance, for the precipitation of piperine extracted from black pepper. By cooling an aqueous hydrotropic solution of NaCS from 80 °C to 30 °C, the authors showed, as expected, that the solubility of piperine decreased with decreasing temperature.[119] Thus, it is necessary to increase temperature using this hydrotrope for extraction and to cool the system down to cause the precipitation. The precipitation from the aqueous hydrotrope solutions showed higher nucleation rates than crystal growth rates, leading to smaller crystals than those obtained by dilution with water.

I.4. Recent advances and future of the hydrotropic extraction processes

Most hydrotropic plant extractions have been performed with sodium alkyl benzene sulfonates, sodium benzoate or salicylate. When hydrotropes were compared, NaCS (2 M) was found to be

the most efficient hydrotrope in many cases such as for the extraction of andrographolide from *Andrographis paniculata* leaves (30 min, 30 °C)[107], forskolin from *Coleus Forskohlii* roots (3 h, 30 °C)[106]. NaNBBS (2 M) was also described as the best hydrotrope for the extraction of piperine from black pepper (2 h, 27 °C)[103] and nicotinamide (2 M) for the extraction of vanillin from vanilla beans (2 h, 50 °C).[120] However, in the latter case, only resorcinol, nicotinamide, citric acid and NaS were tested.

Although the extraction of actives (apart from lignin) from biomass is a recent process, it has evolved over the past 20 years to better fit the principles of green chemistry. Thus, hydrotropic extractions have been increasingly designed to increase yields, reduce time of extraction and energy consumption and to use renewable, bio-based hydrotropes. The evolutions of the hydrotropes used and the conditions of extraction are reported below.

I.4.1. Intensification of the hydrotropic extraction

For less than 10 years, certain hydrotropic extractions using intensification techniques have been attempted. The extraction of EO from different species of lemongrass (*Cymbopogon*) using hydrotropes is a good example of the practice changes (**Table I.2**). Indeed, Desai et al. reported for the first time in 2012 the extraction of citral from *Cymbopogon flexuosus* (Steud.) Wats. with NaS and NaCS. They found that the maximum yield (15.8 mg/g of dried leaves) was reached with NaS at 1.75 M, with 5 wt.% of plant loaded at 63 °C during 4.5 h.[121] Then, six years later, geraniol was extracted from another lemongrass (*Cymbopogon martini*) using ultrasounds and NaCS was a better extractant compared to NaPTS, NaS and resorcinol. The time of extraction was reduced to 16 min and the hydrotrope concentration to 1 M thanks to the action of ultrasounds.[122]

Finally, in a recent study about the extraction of EO from *Cymbopogon winterianus*, by hydrodistillation compared the effect of resorcinol, NaCS, NaPTS and NaS (0.2 M) in the aqueous medium. During such process, the plant permeability is increased by the presence of hydrotropes, thus liberating the EO in water. Then, due to heating, oil and water are removed by evaporation, whereas other bioactives and hydrotropes remain in the solution. The highest EO yield was obtained with resorcinol and the authors found a 56 % increase in EO yield using ultrasounds but no effect of microwaves. Both microwaves and ultrasounds reduced the time of extraction and utility consumption by 56 % and the carbon emissions by 29 and 36 % respectively.[123]

Table I.2. Hydrotropic extractions of EO from lemongrass

Target molecule	Technique	Intensification	Tested hydrotropes	Optimal solution	Optimal conditions
Citral[121]	Maceration	No	NaS NaCS	NaS 1.75 M	Plant:solution ratio = 5:95 T = 63 °C t = 4.5 h
Geraniol[122]	Maceration	US	NaS NaCS NaPTS NaS	NaCS 1 M	t = 16 min
All volatiles[123]	Hydro-distillation	US MW	NaCS Resorcinol NaPTS	Resorcinol 0.2 M	Use of US

In another study, Mishra et al. extracted andrographolide in conventional hydrotropic extraction with an optimum amount reached within 20 min using NaCS at 2 M and 30 °C. After dilution with water, 96 % of the target molecules were recovered with a purity of 94 %.[107] In 2014, Hartarti et al. reported a hydrotropic extraction of andrographolide using microwaves: with a power of 119.7 W, in 15 min, solutions of NaB and urea (3 M) gave yields of 10.9 and 1.0 % respectively.[124] However, Mishra et al. had estimated the andrographolide content at 2.3 %, so the maximum yield to reach 94 % of purity in the extract is 2.45 %, corresponding to 100 % of available andrographolide extracted, and 6 % of the dry extract composed of by-products. Hartarti et al. do not report the purities obtained, but if plants of the two articles present the same content of andrographolides, then the purity of the NaS extract cannot exceed 21 % (if 100 % of andrographolides are extracted).

In this case, the optimization of the conventional hydrotropic extraction was sufficient to maximize the yield and the purity of the extract. The optimization of a microwave hydrotropic extraction did not manage to lower consequently the time of extraction, and has only increased the yield with a necessarily negative impact on the purity.

I.4.2. Towards eco-friendly hydrotropes and hydrotropic extractions

a. Extractions using ionic aromatic hydrotropes

Processes with anionic hydrotropes such as alkyl benzene sulfonates have increasingly been designed to be more eco-responsible. For example, extraction of citral with NaCS and NaS, reported in **Table I.2**, was followed by the recovery of an extract through hydrotropic dilution, and then, by evaporation of water in order to recover a hydrotropic solution at 1.75 M. No loss of yield was observed between the use of the new and the recycled solution.[121]

Another study reported sodium cinnamate (NaCIN) as extractant of forskolin and curcumin from *Coleus Forskholii* and *Curcuma Longa*, respectively.[125] This study investigated the particularity of NaCIN to be a photo-switchable hydrotrope, and found that this hydrotrope *(i)* was efficient to recover 75 % of forskolin and 71 % of curcumin, *(ii)* was isomerized within 6 h from *trans*-NaCIN to *cis*-isomer (**Figure I.15**), destabilizing the aggregate structure, and inducing the precipitation of organic solutes. In the precipitate, 3 % of the dissolved forskolin and 17 % of the dissolved curcumin, with purities of 30 and 49 % respectively were recovered. However, the authors pointed out that isomerization must be reversible so that the hydrotropic solutions can be recycled.

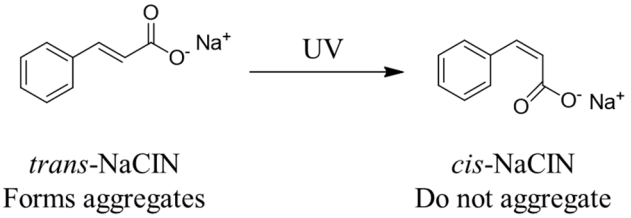

Figure I.15. Isomerization of sodium cinnamate under UV irradiation

b. Short-chain bio-based amphiphiles as new eco-compatible hydrotropes

The definition of hydrotropes has evolved over the years. For a long time, anionic surfactants composed of an aromatic ring substituted by a sulfonate, or carboxylate group were the only reported hydrotopes. Typically, SXS, NaCS and NaB were used.[83] Then, non-ionic hydrotropes such as resorcinol and the natural nicotinamide (a vitamin B) and urea were studied.[126] Noteworthy, the hydrotropic properties of adenosine tri-phosphate (ATP) have recently been reported and it is now not only considered for its energetic role, but also as a biological hydrotrope with a role of solubilizer in the cells.[127] It is likely that other natural hydrotropes may be discovered in the future.

Over the past 20 years, the hydrotropic behavior of short non-ionic amphiphiles similar to small surfactants was investigated. Short-chain C_iE_j and C_iP_j have been assimilated to hydrotropes since they do not form well-defined structures in water such as micelles.[89] Since then, 1-mono and di-alkyl ethers of glycerol[90,94], alkyl polyglycosides (C_iGlyco),[128] mono alkyl ethers of isosorbide (C_i-Iso),[95,129] erythritol and pentaerythrytol[96] with alkyl chain lengths "*i*" comprised

between 4 and 6 have been proposed as bio-based hydrotropes. The chemical structures of the main chemical families of hydrotropes with their most reprensentative examples are presented in **Figure I.16**.

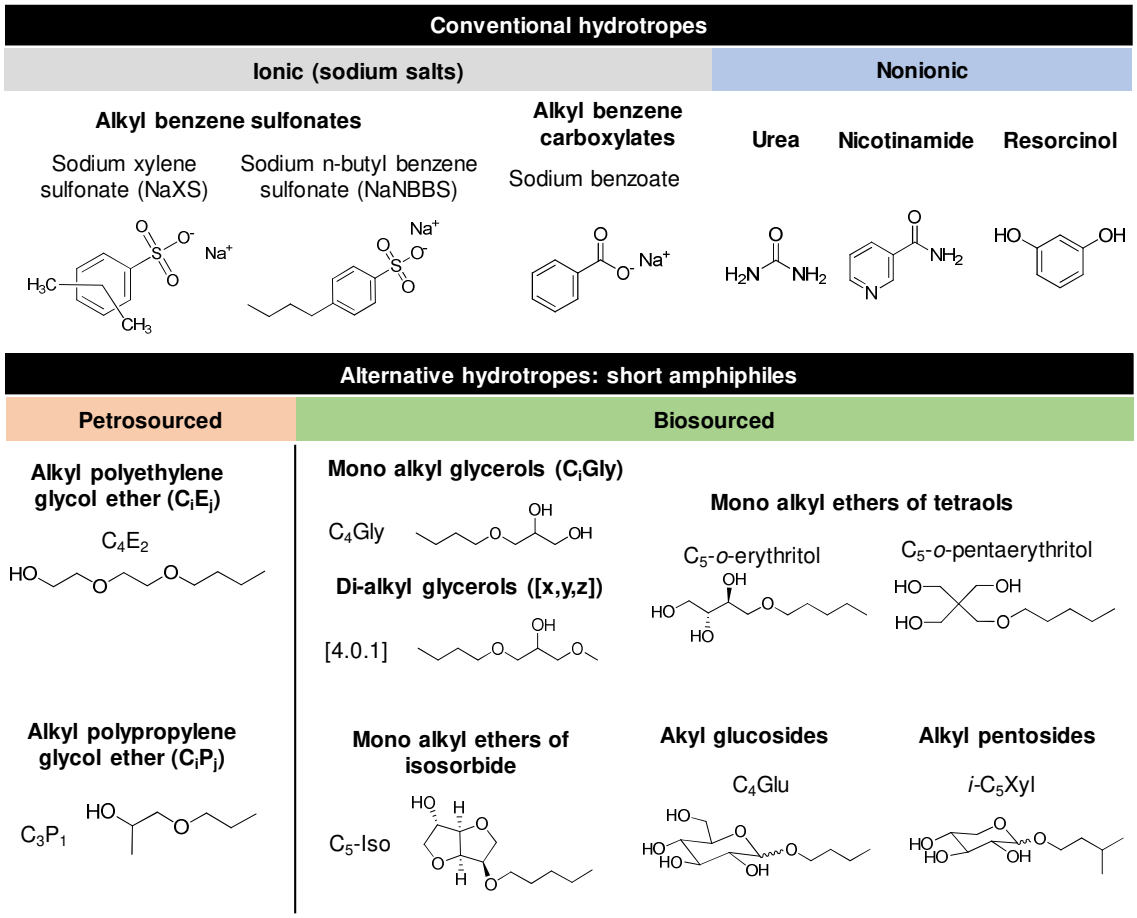

Figure I.16. Main chemical families of hydrotropes

Bio-based hydrotropes are synthesized with precursors recovered or derived from biomass. Several alcohols can derive from biomass (**Figure I.17**) and are used as alkyl chain precursors, directly in the hydrotrope synthesis (C_iGlyco),[130] or after bromation to get bromoalkanes to synthesize C_i-Iso[95], or oxidation to get aldehydes to synthesize C_iGly in a one-step catalyzed process[94] and alkyl ethers of tetraols in a two-step (acetalisation and hydrogenolysis) catalyzed process.[96] The polar head must also be issued of carbohydrates from wheat bran starch, food waste or other renewable feedstock (**Figure I.17**). Noteworthy, some polar heads are more interesting than others to limit the number of steps for their synthesis: sugars (glucose and pentoses) and glycerol are common products which can be easily obtained in large amounts from biomolecules. Erythritol and isosorbide may also be biobased, but their production requires more steps, which is less recommended in green chemistry.[95,131] Among these hydrotropes, only several alkyl polypentosides (*i*-C_5Xyl) and alkyl polyglucosides (C_4, C_7Glu) have been commercialized in large scale.

Regarding the environmental impact, the short amphiphiles cited above are non-VOC (unless C_iE_j with $i \leq 4$),[132] and can be biodegraded in aerobic conditions in 5 days such as C_iGlyco and C_iE_j.[133] Particularly, *i*-C_5Xyl and C_7Glu passed the OECD 301F test which consists of the measurement of consumed oxygen by manometric respiratory within 28 days with results of 86 and 82 %, far exceeding the 60 % pass level.[134–136] Other experiments assessed of low dermatologic and ocular irritation, low health toxicity and low eco-toxicity for aquatic organisms.[130,137,138]

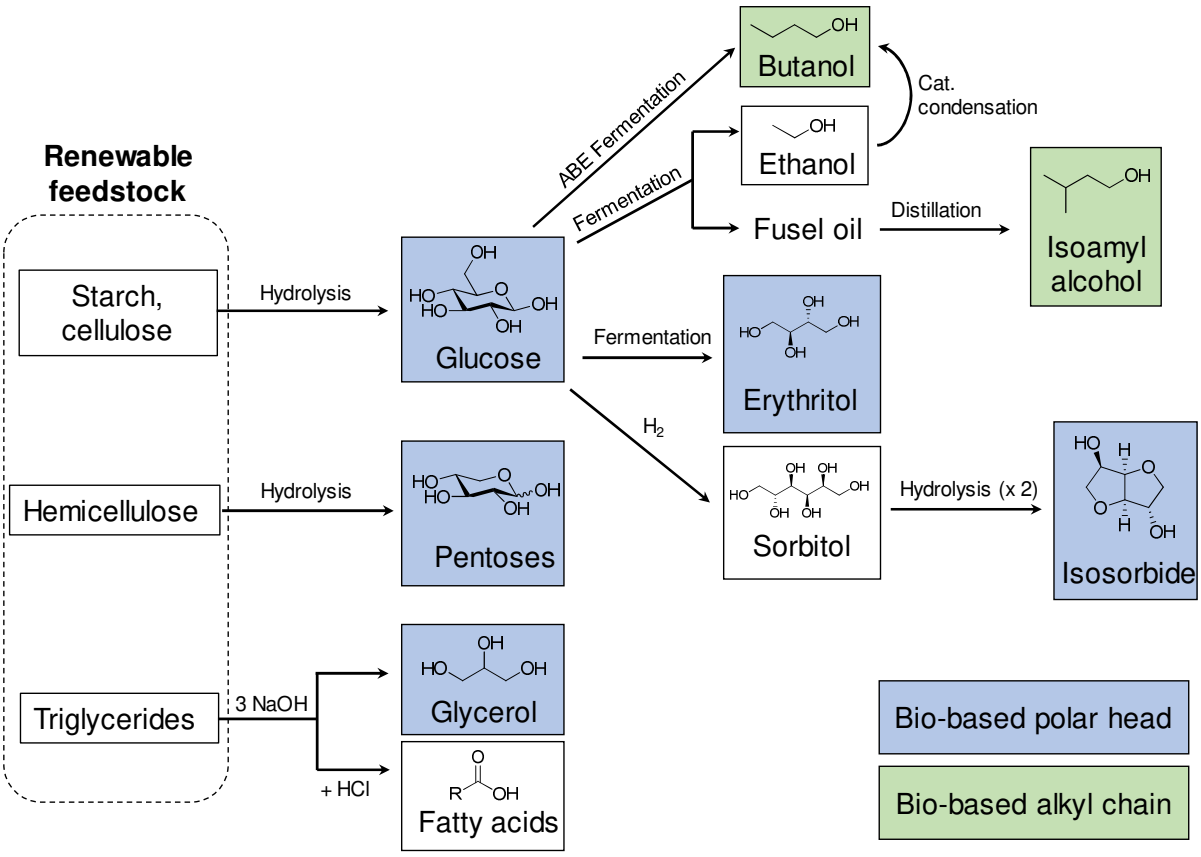

Figure I.17. Synthesis pathways of hydrotropes precursors from biomass. ABE = Acetone, butanol, ethanol process

So far, only two alkyl glycerol ethers ([4.0.1] and C_5Gly) and C_4E_1 have been reported in a hydrotropic extraction process, for the extraction of piperine.[94] Confirming the growing interest in short amphiphiles as hydrotropes and for bio-based hydrotropes, short alkyl ethers of glycerol (C_iGly with *i* comprised between 1 and 6) have also been recently reported as solubilizers of syringic acid and gallic acid and the recovery of the precipitated solutes by dilution with water was studied.[139] Two patent applications also described the concept of hydrotropic extraction using C_iGlyco for the extraction of argan leaves, vanilla, mangosteen, and olive pomace.[140,141]

I.5. Conclusions of chapter I

The plant/solvent extraction mechanism is generally limited by the mass transfer of the target molecule across cell barriers (cell membrane, cell wall, cuticle). To break the cell barriers and improve the mass transfer, intensification techniques such as ultrasounds and microwaves are generally used. Moreover, a high solubilization of the target molecule is required. To solubilize hydrophobic target compounds, organic solvents are generally used, but due to high flammability and explosive risks, their use may be avoided.

Thanks to their ability to aggregate, surfactants and hydrotropes have been used as solubilizers for target molecules, and have also showed particular advantages, such as the concentration through CP. Interestingly, hydrotropes are better solubilizers compared to surfactants which have a solubilizing power limited by the formation of LC. Moreover, it has been reported that their use on plant material induces a destabilization of the cell wall by solubilization of hemi-cellulose and lignin, destructuration of cellulose and destabilization of the phospholipidic barrier. Thus, the use of hydrotropes is likely to avoid, or reduce the use of intensification techniques since cell wall has already been destabilized. Hydrotropic extractions of lemongrass EO have been reported to be improved by ultrasounds,[123] but the use of microwaves for the extraction of andrographolide has not been found more efficient or quicker, but lowered the purity of the extract.[107,124]

Hydrotropic extractions would make it possible to avoid the use of flammable and VOC solvents by performing extractions in aqueous medium (hydrotropes may be used at 10 – 40 %). A general process for hydrotropic extraction, with the three existing recovery ways for recovering a solid extract is presented in **Figure I.18**, to sum up this chapter.

In an environmentally friendly approach, bio-based hydrotropes may be used instead of conventional benzene sulfonates. Among them, we will further interest in mono-alkyl glycerol ethers abbreviated as C_iGly and alkyl polyglycosides (C_iGlyco), which can be produced by bio-based precursors. C_iGlyco are particularly relevant for industrial applications thanks to their large-scale commercial availability whereas the hydrotropes derived from glycerol have proven to be of interest for their ability to be removed by evaporation under vacuum, like solvents and their ability to concentrate the extract by heating above the CP.[94]

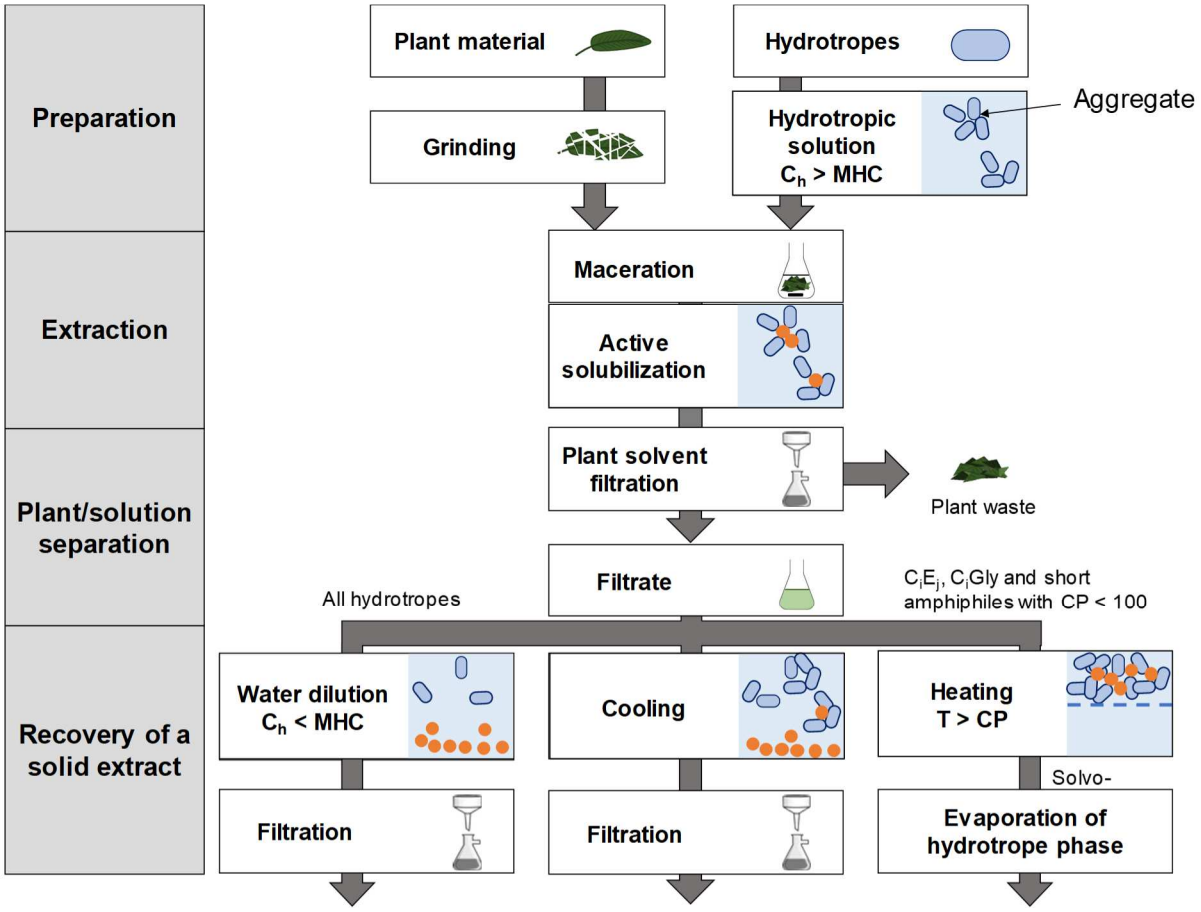

Figure I.18. Hydrotropic extraction process with illustrations of the macro or mesoscopic scales. C_h: hydrotrope concentration

General experimental part

A. Plant material and chemicals

A.1. Plant material

Rosemary leaves (*Rosmarinus officinalis* L.) and sage leaves (*Salvia Officinalis. L.*) were provided by Naturex. They were harvested and dried in Morocco. The dried rosemary leaves contain 2.72 wt.% of CA, whereas the dried sage leaves contain 1.85 wt.% CA according to Soxhlet extractions (24 h, acetone, HPLC quantification).

Hydrotropic extractions could be performed with whole leaves or ground leaves. In the latter case, for the grinding, 20 g of dried leaves were milled in a blender (Philips HR2056/90) for 1 min providing a powder with an average particle size of about 0.5 mm.

A.2. Amphiphiles

a. Commercially available amphiphiles

Molecule	Notation	Purity (%)	Origin	Chapter
Tween 80		> 99	Sigma Aldrich	I
1-butoxy ethanol	C_4E_1	> 99	Sigma Aldrich	II
ethylene glycol mono*iso*-butyl ether	*i*-C_4E_1	> 99	TCI	II
diethylene glycol monobutyl ether	C_4E_2	> 99	TCI	I, II
triethylene glycol monobutyl ether	C_4E_3	> 99	TCI.	II
diethylene glycol monohexyl ether	C_6E_2	95	Sigma-Aldrich	II
Sodium xylene sulfonate	SXS	> 90	Fluka	II
Ethanol	EtOH	96	VWR	II
Propanol	PrOH	> 99	Alfa Aesar	II
Butanol	BuOH	> 99	TCI	II
Simulsol® SL4 butyl glucoside	C_4Glu	62.7[a]	Seppic	III
Appyclean® 6505 *iso*-amyl polyxyloside	*i*-C_5Xyl	65.8 [a]	Wheatoleo	III, IV
Sepiclear® G7 heptyl polyglucoside	C_7Glu	78.9 [a]	Seppic	III
Simulsol® AS48 ethylhexyl polyglucoside	$C_{6,-2}$Glu	67.2 [a]	Seppic	III
Appyclean® 6781 caprylyl-capryl polyglycoside	$C_{8/10}$Glyco	66.9 [a]	Wheatoleo	III

[a] Checked by thermogravimetric analysis (section III.1.1)

b. Synthetic amphiphiles

Molecule	Notation	Chapter
Pentyl diethylene glycol ether	C_5E_2	II
***Iso*-amyl diethylene glycol ether**	*i*-C_5E_2	II
Pentyl triethylene glycol ether	C_5E_3	II
Hexyl triethylene glycol ether	C_6E_3	II
Hexyl tetraethylene glycol ether	C_6E_4	II
Octyl triethylene glycol ether	C_8E_3	II
Octyl tetraethylene glycol ether	C_8E_4	II
Decyl tetraethylene glycol ether	$C_{10}E_4$	II
Dodecyl tetraethylene glycol ether	$C_{12}E_4$	II
Butyl glycerol ether	C_4Gly	III
Pentyl glycerol ether	C_5Gly	III
***Iso*-amyl glycerol ether**	*i*-C_5Gly	III

These alkyl polyethylene glycol ethers were synthesized in the laboratory according to a method described elsewhere.[142–144] Their purity was assessed by ^{1}H NMR (≥ 97 wt.%) and by comparing their CP with the reference values.

Butyl and pentyl glycerol ether C_4Gly and C_5Gly were prepared from their corresponding glycidyl ethers in a one-step-process by condensation with water at 115 °C over 48 h.[94]

Iso-amyl glycerol ether *i*-C_5Gly was prepared from 3-methylbutan-1-ol (98%, Aldrich), epichlorydrin (99%, Aldrich), $ZnCl_2$ (98%, Aldrich) and NaOH (VWR) in a two-step process.[94,145] First, 3-methylbutan-1-ol (176 g, 2 mol) and $ZnCl_2$ (13.7 g, 0.1 mol) were heated to 100 °C under stirring. Epichlorydrin (200.6 g, 2.17 mol) was added dropwise over 1 h while the solution was kept at 100 °C, then heated to 115 °C for 5 h. Then, the epoxide was formed using a NaOH solution (55 wt.%, 200 mL) at 50 °C and stirred over 65 h. The product was extracted with diethyl ether. The organic phases were washed with water, dilute HCl and water once again, dried over $MgSO_4$. The solvent was filtered and evaporated. The epoxide was purified by distillation under vacuum ($3x10^{-2}$ mbar, 40 – 60 °C, 180 g). Finally, it was heated to 110 °C in excess of water (260 mL) during 48h. Water was evaporated and the product directly distilled under vacuum ($3x10^{-2}$ mbar, 80 – 90 °C) to give a colorless liquid (110 g, 0.68 mol, 34 %).

^{1}H NMR (300 MHz, $CDCl_3$): 3.86 (m, 1H), 3.76-3.61 (m, 2H), 3.56-3.46 (m, 4H), 2.79 (bs, 1H, OH), 2.41 (bs, 1H, OH), 1.68 (non *a*, J = 6.8 Hz, 1H), 1.48 (q *a*, J = 6.8 Hz, 2H), 0.90 (d, J = 6.8 Hz, 6H).

A.3. Standards

Molecule	Purity (%)	Origin	Chapter
Phosphoric acid	85	Sigma-Aldrich	I, II, III, IV
Carnosic acid	>98	Chengdu Biopurify Phytochemicals Ltd	I, II, III, IV
Ursolic acid	>98	Chengdu Biopurify Phytochemicals Ltd	II, III
Camphor	>98	Sigma-Aldrich	II, III
Rosmarinic acid	>96	Sigma-Aldrich	II, III
Myristic acid	>99	Sigma-Aldrich	III
Stearic acid	>98	TCI	II, III
Behenic acid	>99	TCI	III
Propyl gallate	>98	TCI	III
Octyl gallate	>98	TCI	III
Dodecyl gallate	>98	TCI	III
Hexadecyl gallate	>95	TCI	III

B. Quantification of carnosic acid concentration by HPLC

For HPLC analyses, methanol (HPLC grade) was purchased from VWR and trifluoroacetic acid (TFA, 99 %) was from Alfa Aesar. Ultrapure water was obtained from a ThermoFisher apparatus (18.2 MΩ.cm).

Samples to be analyzed were previously diluted by 10 in methanol (HPLC grade) containing 0.1 % (v/v) of TFA and filtered with 0.2 µm PTFE syringe filters. Analyses were performed using an HPLC apparatus LC 20AD from Shimadzu equipped with an autosampler (injection = 10 µL), a C_{18} column (Interchim, 5 µm particle, 3.0 x 150 mm) maintained at 30 °C, and a UV detector (SPD 20A) set at 210 and 230 nm. The mobile phase was a mixture of methanol/water in a 80:20 v/v ratio with 0.1 % (v/v) TFA in methanol, in isocratic mode, with a flow rate at 0.5 mL/min releasing CA after 12 min of retention time.

Chapter II. Model hydrotropic extraction of carnosic acid from rosemary with alkyl polyethylene glycol ethers (C_iE_j)

As mentioned in the previous chapter, so far, the hydrotropic extraction mechanisms have only been reported for ionic amphiphiles such as alkyl benzene sulfonates. However, non-ionic amphiphiles present a promising alternative to ionic hydrotropes since many non-ionic surfactants and hydrotropes such as alkyl glycerol ethers (C_iGly) or alkyl glycosides (C_iGlyco) can be derived from biomass. Many non-ionic hydrotropes are also fully miscible with water and known for their high solubilization capacity, as shown for butyl diethylene glycol ether (C_4E_2) in **chapter I**. Also, due to their nature, different interactions with the biological membranes of the plant can be expected. In this chapter, we investigated the **mechanism of extraction with non-ionic hydrotropes** and the influence of the **amphiphile structure on the extraction efficiency**.

II.1. Alkyl polyethylene glycol ethers (C_iE_j) as nonionic hydrotropes of choice for a comprehensive study

Well-defined alkyl polyethylene glycol ethers, abbreviated as C_iE_j – where *i* represents the number of carbon atoms of the alkyl chain length and *j* the number of ethylene oxides – can serve as convenient amphiphilic models for structure-activity relationship studies since their properties can be readily tuned depending on *i* and *j*.[146,147] For the sake of convenience and based on immediate availability on the market, petro-sourced C_iE_j have been used. However, in the longer term, it is entirely feasible, and even preferable, to prepare these hydrotropes from bio-based synthons.[148–150] Indeed, it has been shown that ethylene oxide could be synthesized from bio-ethanol and that the alkyl chain could be a fatty alcohol derived from biomass.[151,152]

Within the large family of C_iE_j, a subclass can be considered for short alkyl chain lengths, *i.e.* $i \leq 8$ carbon atoms. They are categorized as hydrotropes[81] because of their capacity to self-assemble in water like surfactants, but at higher concentration and without forming well-defined aggregates such as micelles.[88,153] In addition, aqueous solutions of C_iE_j phase separate at their cloud point (CP), which is reached when heating induces the breaking of H-bonds which naturally stabilizes aggregates in water. This property constitutes another advantage for extraction. Indeed, micellar extraction generally consists of a CP phase separation to concentrate the bioactives in a smaller phase, as reported for the extraction of antioxidants from olive mill wastewater or phenols from red flesh orange juice.[69] As far as hydrotropes are concerned, a promising similar type of process has also been described for the extraction of black pepper. Short chain mono and di-glycerol alkyl ethers and butyl monoethylene glycol (C_4E_1) were used for the hydrotropic extraction and then, piperine was recovered after *(i)* a CP phase separation, and *(ii)* evaporation of hydrotropes under vacuum.[94]

In this study, extractions were performed with a homologous series of twelve C_iE_j with *i* ranging from 4 to 12 and *j* from 1 to 4, including two surfactants ($C_{10}E_4$ and $C_{12}E_4$) for comparison, which were chosen for their miscibility with water (CP > 0 °C). Two other were chosen with branched alkyl chains to be compared to their linear isomers (**Figure II.1**).

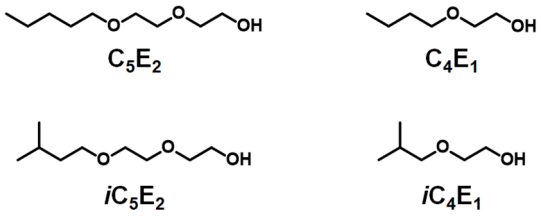

Figure II.1. Branched hydrotropes *i*-C_4E_1 and *i*-C_5E_2 and their linear isomers

For most extractions, plants are prepared by grinding (extraction of sage[70], piperine from black pepper[94] or chlorophylls from spinach[72]). In this first experimental chapter, we chose to perform extractions at room temperature without intensification nor pretreatment, to focus on the influence of the physicochemical properties of C_iE_j. Indeed, conditions leading to medium extraction efficiency will allow a better discrimination of the candidates. Therefore, whole rosemary leaves were used and the effects of the chemical structure, CP, log *P*, hydrophilic-lipophilic balance (HLB) of the hydrotropes were studied in regards to CA solubilization and extraction efficiency. Extraction kinetics were also investigated, and microscopic changes of leaves structure due to extraction were noticed in order to determine the mechanism of hydrotropic extraction with C_iE_j in comparison with conventional extraction with alcohols such as ethanol and butanol. Finally, the recovery of CA was undertaken using the HCPE process reported for piperine,[94] and by dilution of the extraction solution with water, leading to the precipitation of the extract.

II.2. Solubilization of carnosic acid in aqueous solutions of alkyl polyethylene glycol ethers (C_iE_j)

CA has a poor solubility in pure water at room temperature (< 0.1 g/L). In its protonated form, CA is considered as a hydrophobic compound with a log *P* equal to 5.4 (at pH 2, SciFinder® data).[154] Additionally, the fact that CA is apolar has been recently substantiated by comparing the sigma-profiles of CA and water using COSMO-RS (COnductor like Screening MOdel for Real **S**olvents) calculations.[63] This method which combine statistical thermodynamics and quantum chemical theories screens the charge density on the surface of molecules to predict thermodynamic properties such as their chemical potential, their activity coefficient. Thanks to those predictions, it is able to estimate the strength of interactions between two molecules, and thus, physicochemical descriptors such as log *P*. Amazingly, CAR, which is the main CA

oxidized derivative, has shown to be slightly more polar than CA despite the acidic function is lactonized. The CA water-insolubility can however be overcome by adding a cosolvent such as ethanol above 40 % (v/v)[155] or commercially available alkyl polyethylene glycol ethers surfactants.[156,157]

II.2.1. Investigation of commercial C_iE_j hydrotropes: C_4E_1 and C_4E_2

a. Influence of carnosic acid on the Cloud Point of C_4E_1

C_4E_1 is certainly the most studied ethoxylated hydrotrope and the only one that has proven its efficiency in the hydrotropic extraction process.[94] Therefore, the solubilization of CA in C_4E_1 aqueous solutions was investigated. Since phase separation occurs before saturation, the phase diagram (temperature-hydrotrope concentration) of the C_4E_1-CA-water ternary system was determined at different CA concentrations. Indeed, the evolution of the CP with the C_4E_1 concentration has already been reported for binary systems containing only C_4E_1 and pure water. The lower critical solution temperature (LCST), which is the lowest temperature at which a liquid-liquid phase separation is observed[146,158] was found to be 48.7 °C at about 30 wt.% C_4E_1 (**Figure II.2**). Noteworthy, the CP stabilizes at a plateau between 20 and 45 wt.% C_4E_1.

The CA-hydrotrope solubilization was studied at pH 2 (H_3PO_4 1 % v/v) to make sure that CA remains in its protonated form, which is less likely to oxidize into quinone (which can further isomerize into CAR).[92,159,160] **Figure II.2** shows the evolution of the CP with the C_4E_1 concentration for solutions containing 0, 5 and 20 g/L of CA. In presence of phosphoric acid only, the CP of C_4E_1 remained stable from 20 to 50 wt.%, at about 3.5 °C below the plateau observed in its absence. It demonstrates the salting out effect of H_3PO_4, like for electrolytes such as NaCl or NaBr.[161,162]

CA also decreases the CP with its concentration. The depression of CP induced by the presence of CA was expected since this effect has already been reported for organic compounds, even the polar ones such as alkyl parabens or alkanols, in $C_{12}E_6$ solutions and Triton X-100.[163–165] That can be explained by preferential solubilization of the hydrophobic compound into the surfactant aggregates, leading to a micellar growth and change of shape and, as a consequence, to a CP decrease.[163] Noteworthy, the effect on the CP seems to be more important at low concentrations of C_4E_1 than at high concentrations. Increasing the C_iE_j concentration induces the formation of aggregates that are less concentrated in CA, resulting in a less important effect on aggregates.

This is problematic for measuring the solubility limits of a compound in C_4E_1 solution because no saturation (when there is remaining solid) can be observed before the CP occurs. Indeed, as depicted by the pictures which show the solutions of 0, 10, 20, 30, 40 and 50 wt.% C_4E_1 containing 20 g/L of CA at 20 °C, CA (in yellow) remains solid only when no hydrotrope is present in solution, otherwise it is solubilized in a liquid phase containing the hydrotrope, either separated from an aqueous phase (10, 20, 30 wt.%) or homogeneous (40, 50 wt.%).

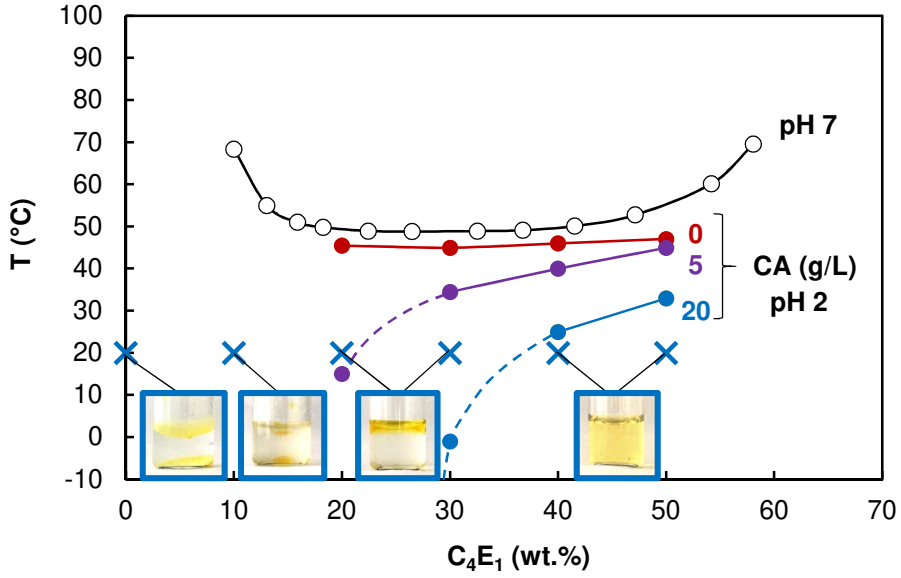

Figure II.2. Temperature of liquid-liquid phase separation (CP) of C_4E_1 aqueous solutions at pH 7 (empty points) from ref[94] and pH 2 (full points) containing no CA (red), 5 g/L CA (purple) and 20 g/L CA (blue). Pictures show solutions containing 20 g/L CA at 20 °C at 0, 10, 20, 30, 40 and 50 wt.% C_4E_1.

The effect of the ratio between CA/C_4E_1 on the CP decrease can be surprising since an increasing salt concentration generally gives parallel CP curves as showed for NaCl in C_8E_5 solutions. To quantify this phenomenon, we found an interesting correlation between the CP decrease (ΔCP) and the molar concentrations [CA] and [C_4E_1], as indicated in **Figure II.3** and **Eq.II.1** with 'CP_0' the CP with no solute at pH 2 and 'CP' the CP at pH 2 at [CA] and [C_4E_1].

$$CP_0 - CP = 7134 \times \frac{[CA]}{[C_4E_1]^{2.5}} \qquad (II.1)$$

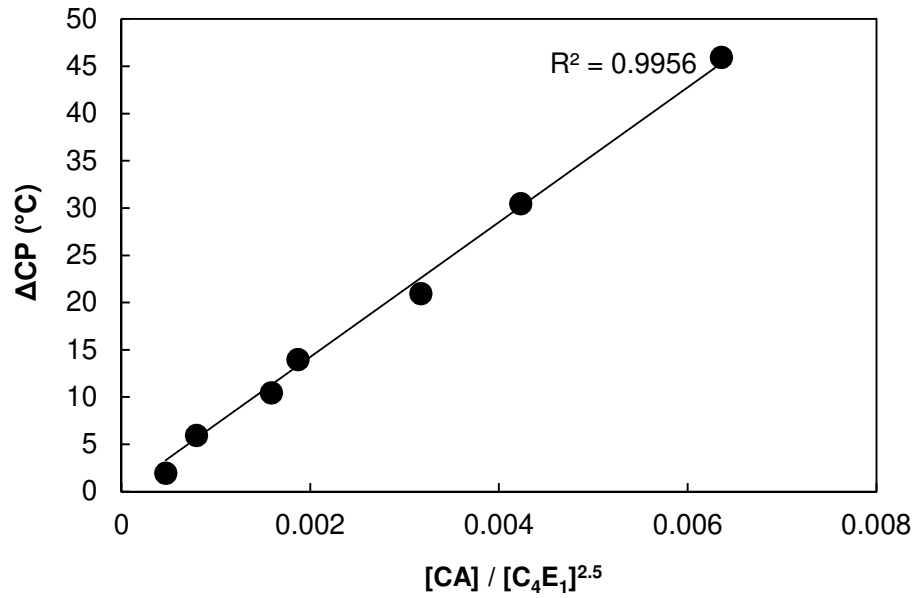

Figure II.3. Correlation between the salting out effect measured by the CP decrease (ΔCP), [CA] and [C_4E_1].

b. High solubilizing power of C_4E_2 solutions

As the CP of the commercially available C_4E_2 is very high (> 100 °C even in the presence of CA), the solubility of CA in this hydrotropic solution was determined as a function of the hydrotrope concentration and compared to that obtained with sodium xylene sulfonate (SXS) (**Figure II.4**).[86]

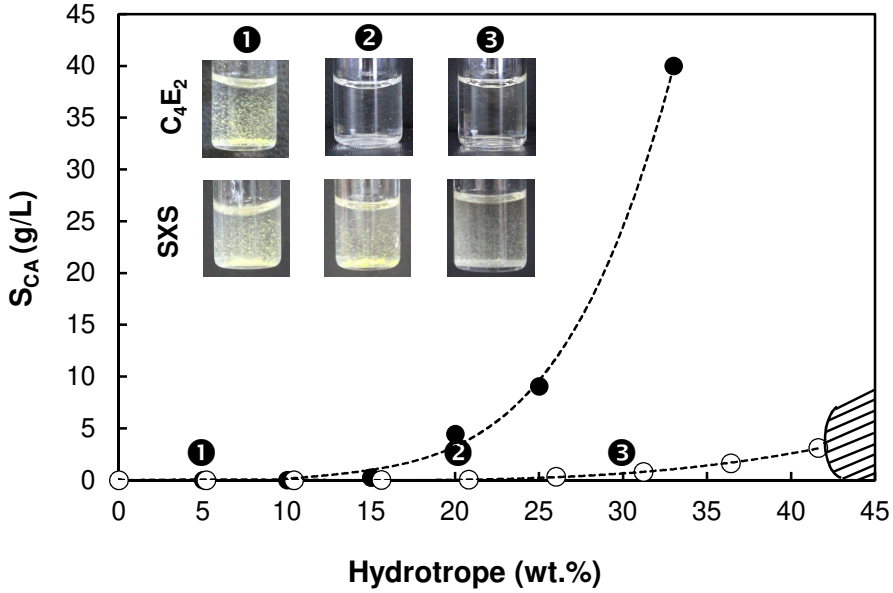

Figure II.4. Solubility (S) of CA in aqueous solutions of C_4E_2 (●) and SXS (○) at pH 2 after 24 h under stirring. Pictures show solutions at 2.5 g/L CA with 5 (❶), 20 (❷) or 30 (❸) wt.% of C_4E_2 and SXS at pH 2.

The MHC of C_4E_2 is 10 wt.% and a solution of 30 wt.% C_4E_2 can solubilize more than 25 g/L of CA, which is more than ten times the maximal amount of CA that can be extracted from rosemary at ratio 1:10 (w/v). The MHC of SXS, which is an archetypical hydrotrope, is 20-25 wt.%, twice the MHC of C_4E_2. Due to a SXS saturation level in water nearing 42 wt.% in our conditions (pH = 2, T = 25 °C), the maximal CA content that can be solubilized in those solutions (S_{max}) is 3 g/L. By comparison, C_4E_2 shows an excellent solubilizing capacity. Indeed, the pictures of the solutions containing 2.5 g/L of CA (the targeted concentration) show a good solubility in C_4E_2 as soon as 20 wt.% is reached, contrary to SXS, even up to 30 wt.%.

II.2.2. Physicochemical properties of the alkyl polyethylene glycol ethers (C_iE_j with *i* = 4-12 and *j* = 1-4)

Depending on their chemical structure, C_iE_j have different Critical Aggregation Concentration (CAC), surface tension (σ_{CAC}), HLB, octanol-water partition coefficient (log *P*), molecular volume (V_m) and CP. Those main physicochemical properties and descriptors are summarized in **Table II.1** for the well-defined C_iE_j with *i* ranging from 4 to 12 and *j* from 1 to 4 as well as for SXS. The CAC and surface tensions at CAC (σ_{CAC}) were compiled from the literature[166–169] and measured when missing (for *i*-C_4E_1, *i*-C_5E_2 and C_5E_2, curves presented in **Appendix 1**). Noteworthy, C_4E_j and C_5E_j remarkably lower the surface tension of water to 25-35 mN/m compared to SXS which only reaches 52 mN/m, despite their CAC are of the same order of magnitude (0.25-0.89 mol/L for C_iE_j with *i* = 4-5 and 0.48 mol/L for SXS). Overall, CAC values are divided by 10 when two carbon atoms are added whereas no clear evolution is observed with *j*, the number of ethylene oxides. The surface tension of C_iE_j always remains between 27.2 and 35.2 mN/m.

To have comparable values of log *P* and molecular volumes (V_m) for all C_iE_j, they were calculated with the Cosmo-*Quick* software (COSMO-RS method), which uses the prediction of the thermodynamic properties such as the activity coefficient to calculate the solubility of molecules in solvents or their partition between two solvents, *i.e.* the log *P* for octanol/water partition.[154] As far as SXS is concerned, the V_m was calculated for xylene sulfonic acid, giving an approximate value of the V_m of the SXS anionic part, but this prediction could not give a precise enough value of log *P* (COSMO: 2.0 *vs* literature: -1.86).[170] As a result, its V_m was found to be close to those of C_4E_1 and C_4E_2. HLB were calculated according to Griffin's equation (**Eq.II.2**), where M_H and M_T correspond to the molecular mass of the hydrophilic part and the molecular mass of the whole molecule respectively.[171] This equation has been introduced for non-ionic surfactants, and more precisely for C_iE_j, so it could not be used for SXS, but should be well suited for the other hydrotropes.

$$HLB = \frac{M_H}{M_T} \times 20 \qquad \text{(II.2)}$$

As expected, log *P* values increase with increasing *i*, reflecting an increase of lipophilicity, as well as V_m, which reflects an increasing size while HLB values decrease. Similarly, HLB and V_m increased with increasing *j* while log *P* generally decreased, as a result of an increasing hydrophilicity.

Finally, the LCST were reported for each C_iE_j from the literature.[168,172,173] Unsurprisingly, when the hydrophilicity of the amphiphile is increased by increasing *j* or decreasing *i*, the LCST increases. However, as a preamble of the extraction study, it is more interesting to have the CP values at the hydrotrope concentration used for the extraction. The concentration of each C_iE_j was fixed at 30 wt.%, which is well above their CAC (see **Table II.1**), and the CP of amphiphiles at this concentration were also reported.

Table II.1. Physicochemical properties of alkyl polyethylene glycol ethers (C_iE_j) with i = 4 to 12 and j = 1 to 4.

i	j	CAC[a]		σ_{CAC}	HLB[b]	log P[c]	V_m[c,d]	LCST[e]	$CP_{30\%}$[f]	$CP_{30\%+CA}$[g]
		mmol/L	g/L	(mN/m)			(Å^3)	(°C)	(°C)	(°C)
iso-4	1	890	105	25.8	10.3	0.89	166.7	24.5[172]	25.8	21.4
4	1	830[168]	97.9	27.2[168]	10.3	0.68	165.6	48.7[168]	49.5	45.8
4	2	880[168]	143	28 [168]	13.0	0.72	220.0	>100[168]	>100	>100
4	3	550[174]	113	35.2	14.5	-0.04	275.9	>100	>100	>100
iso-5	2	370	65.1	27.7	11.9	0.96	240.1	n.d.	42.6	40.6
5	2	290	51.0	29.2	11.9	1.11	241.1	39[168]	41.5	39.8
5	3	257[168]	56.5	30.3[168]	13.5	0.33	297.0	62.8[168]	69.0	67.0
6	2	n.d.[h]	n.d.[h]	n.d.[h]	11.1	1.69	260.8	7.2[168]	11.0	9.2
6	3	81[168]	19.0	31[168]	12.7	0.69	316.7	45.1[168]	47.8	45.1
6	4	84[168]	23.3	31.7[168]	13.9	0.68	371.4	66.1[168]	66.5	65.5
8	3	7.5[166]	1.97	n.d.[h]	11.4	1.77	360.0	10.9[168]	19.3	17.3
8	4	8.5[167]	2.60	30[167]	12.6	1.33	414.8	38.3[168]	43.9	42.1
10	4	0.86[169]	0.287	29.4[169]	11.6	2.12	455.7	20.5[173]	33.6	31.4
12	4	0.05[169]	0.018	27.6[169]	10.7	2.77	497.9	6.6[173]	LC above 19 °C[175,176]	
SXS		479[86]	100.7	52[86]	-	n.d.	204.6	-	-	-

[a] Critical Aggregation Concentration ; [b] Calculated according to Griffin's relation ; [c] From CosmoQuick®, with a calculation based on the COSMO-RS method and refined with real values of similar molecules ; [d] Molecular volume ; [e] Lower Concentration Solution Temperature, [f] CP at 30 wt.% C_iE_j, [g] CP at 30 wt.% C_iE_j and 2.5 g/L CA ; [h] Not determined because CP < 25 °C.

Because following extractions were performed at a plant:solvent (P:S) ratio of 1:10 (w:v) and the CA content in rosemary dried leaves is typically around 2.5 wt.%,[8] an average concentration of 2.5 g/L of CA can be expected in the liquid extract if all CA available in rosemary is extracted from the raw material. CA is readily soluble in almost all hydrotropic systems leading to homogeneous single-phase solutions at 25 °C, except for *i*-C_4E_1, C_6E_2 and C_8E_3 solutions, for which a two-phase system has already been obtained at 25°C due to a lower CP (**Figure II.5**). In these cases, CA is solubilized in the upper C_iE_j-rich phase. Nevertheless, at 5 °C, all C_iE_j form a single phase.

In accordance with the previous results (**Figure II.2**), the presence of 2.5 g/L of CA systematically leads to a decrease of the CP of C_iE_j solutions from 1 to 4 °C (**Table II.1**) with a larger reduction (≈ 4 °C) for C_4E_1 and *i*-C_4E_1. No CP has been observed for C_4E_2 and C_4E_3 up to 100 °C. In the case of $C_{12}E_4$, its aqueous solution at 25 °C is very viscous due to the formation of liquid crystals (LC). Indeed, at such temperature and high concentration, this surfactant is known to form a lamellar phase.[175] For $C_{10}E_4$, no LC were formed at room temperature but a lamellar phase appeared just above the CP (> 34 °C), in accordance with previously reported

data,[177] whereas the short alkyl chain C_iE_j hydrotropes ($i \leq 8$) do not form LC at 30 wt.% whatever the temperature.

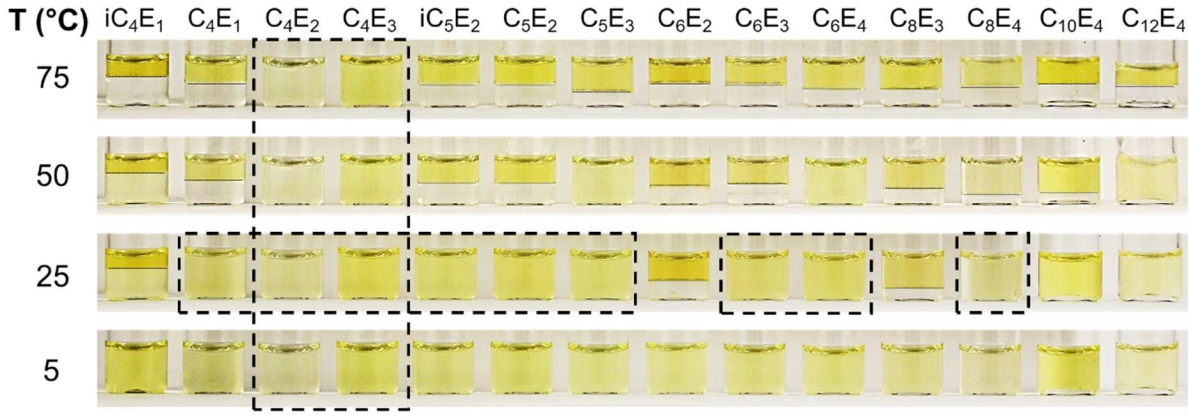

Figure II.5. Thermal behavior at 5, 25, 50 and 75 °C of aqueous solutions containing 30 wt.% of C_iE_j (i = 4 to 12 and j = 1 to 4) and 2.5 g/L of CA. In biphasic systems, CA is solubilized in the yellow amphiphile-rich upper phase.

In a previous study, a correlation had been found between the ratio i/j and the LCST for 25 hydrotropes and surfactants, excluding C_4E_1.[168] Thus, we examined the evolution of the CP at 30 wt.% of C_iE_j solutions containing CA (empty points) or not (full points) in **Figure II.6**. As previously reported for LCST, the CP decreased with i/j, excepted for C_4E_1 and i-C_4E_1. Noteworthy, despite C_4E_2 is not represented in **Figure II.6**, it does not fit the correlation either. Indeed, with a i/j = 2, its CP at 30 wt.% should be about 45 °C whereas it is actually above 100 °C.

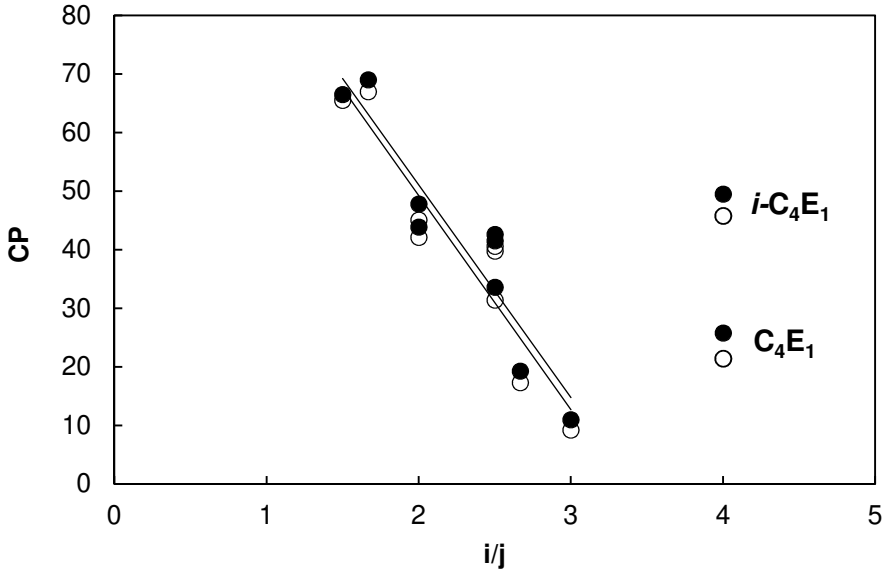

Figure II.6. Evolution of the CP with the ratio i/j of aqueous solutions of 30 wt.% C_iE_j at pH 2 with no CA (○) and 2.5 g/L CA (•)

II.3. Hydrotropic extraction of carnosic acid with aqueous solutions of alkyl polyethylene glycol ethers (C_iE_j with *i* = 4-12 and *j* = 1-4)

II.3.1. Influence of alkyl chain length (*i*) and ethylene oxide number (*j*) on the hydrotropic extractions

As explained above, extractions were performed at 30 wt.% for each amphiphile, well above their CAC (**Figure II.7**). Moreover, the aqueous solutions were acidified with 1 % (v/v) of phosphoric acid (*i.e.* pH ≈ 2) to limit the oxidative degradation of CA into carnosol (CAR).[159] Hydrotropes have already been reported to enhance the transfer of piperine from the plant to the solvent through the cell wall barriers.[103] On the other hand, some C_iE_j have been shown to improve the foliar uptake of pesticides in bitter orange, barley and *Chenopodium album*, which is a mass transfer in the opposite direction.[178–180] However, to our knowledge, they have never been used for rosemary extraction.

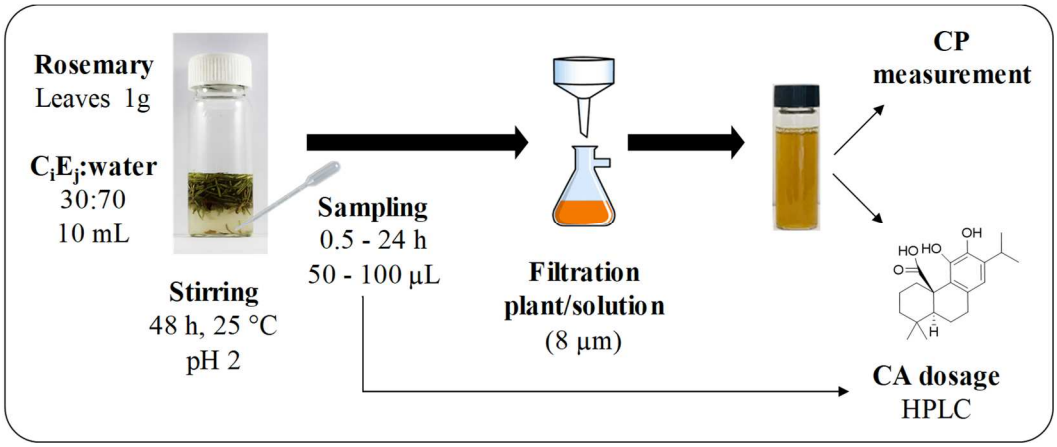

Figure II.7. Schematic representation of the different steps for extraction of CA from rosemary leaves with aqueous solutions of C_iE_j

Here, the efficiency of rosemary extraction was studied with fourteen C_iE_j and compared to ethanol (EtOH), propanol (PrOH), 1-butanol (BuOH) and SXS. **Figure II.8** shows the concentration of CA (quantified by HPLC) in the filtrate obtained after 24 and 48 h of extraction for the different systems (**Figure II.7**). All extractions were performed at least two times and the mean values were used to limit errors due to the plant variability and the measurements.

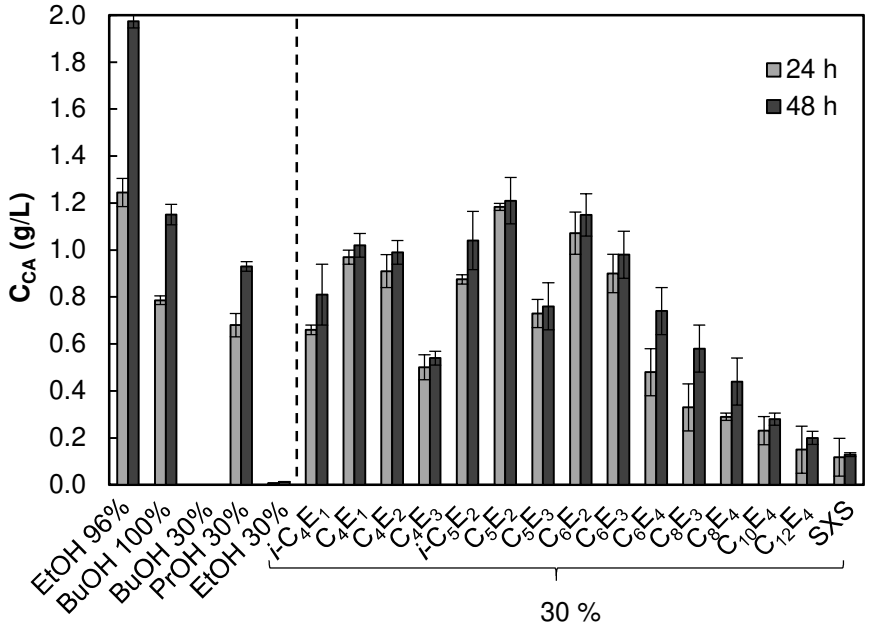

Figure II.8. Concentration of CA in the filtrate after 24 and 48 h of extraction from 1 g of whole leaves of rosemary in contact with 10 mL of solutions at 25 °C, at pH 2.

First, all the hydrotropic C_iE_j-based solutions are efficient towards the extraction of CA from rosemary. C_4E_1, C_5E_2 and C_6E_2 give the best results which are of same order of magnitude as neat BuOH. As expected since it is the most common solvent used in CA extraction (see **Chapter I**), EtOH at 96 wt.% extracts the highest amount of CA after 48 h. However, its efficiency after 24 h is similar to that of C_5E_2 for example. In comparison with the hydrotropic solutions, 30 wt.% aqueous solution of ethanol does not extract CA at room temperature. That is not surprising since CA is not soluble at this temperature in such a mixture, but can however be partially overcome by heating to reflux as reported by Jacotet-Navarro et al.[155] Similarly, no CA was found in the filtrate obtained after extraction using 30 wt.% BuOH solutions because liquid-liquid phase separation occurred providing a small organic phase, which was lost during filtration by remaining on the glass walls and the plant. Conversely, as PrOH is miscible with water at 30 wt.% and more hydrophobic than EtOH, it significantly solubilizes CA. A concentration of 0.93 ± 0.02 g/L was extracted from rosemary after 48 h, which is about 25 % less than the best hydrotrope (1.21 g/L for C_5E_2). SXS, which is one of the first hydrotropes used for plant extractions,[103] is not efficient at this concentration and pH compared to short C_iE_j. This can be related to the low solubility of CA (< to 0.8 g/L) in the SXS solutions, compared to C_4E_2 solution (**Figure II.4**).

Comparing C_iE_j between them, we can see that for a same alkyl chain length *i*, a decrease in the amount of extracted CA is observed when the ethylene oxide number *j* increases, *e.g.* C_4E_1 > C_4E_2 > C_4E_3; C_5E_2 > C_5E_3; C_6E_2 > C_6E_3 > C_6E_4, and C_8E_3 > C_8E_4. Interestingly, when *j* is kept constant, a non-linear trend with the extraction efficiency is observed when increasing the alkyl chain length for the C_iE_2 and C_iE_3 series. Indeed, they reach a maximum of efficiency for C_5 and C_6 respectively. More precisely, for the C_iE_3 series, there is a parabolic-like influence of the alkyl chain length *i* on the extraction efficiency with an optimal point at *i* = 6, beyond which

increasing *i* leads to a collapse of the efficiency. For the C_iE_4 series, the effect is linear with a negative correlation between *i* and the extraction efficiency. At least for some series, this shows that an optimal structure can be attained to maximize the extraction performances. Overall, a good hydrotropic C_iE_j extractant should have a few ethylene oxide number in its polar head while keeping an appropriate "hydrophilic-lipophilic balance". Short-chain hydrotopes C_iE_j are globally better extractants of CA than longer-chain hydrotropes/surfactants C_iE_j.

II.3.2. Rationalization of the amphiphile efficiency

a. Relationship between concentration of extracted carnosic acid and structural properties (*i*, *j*) of alkyl polyethylene glycol ethers

The efficiency of the C_iE_j, which strongly depends on both *i* and *j*, is in the following order: $C_5E_2 > C_6E_2 > C_4E_1 > C_4E_2 > C_6E_3 > C_5E_3 > C_6E_4 > C_8E_3 > C_4E_3 > C_8E_4 > C_{10}E_4 > C_{12}E_4$. Thus, we first tried to predict the amount of extracted CA from their chemical structure using only *i* and *j*. The coefficients of the equation (**Eq.II.3**) were calculated by multiple linear regression between C_{CA} *i*, *j*, i^2, j^2 and *i*/*j* for all C_iE_j with a correlation coefficient of 0.82 (**Figure II.9**). From the comparison of the factors of the equation, we can say that *i* is more influent than *j*. Therefore, an amphiphile must have a small alkyl chain to be efficient. However, this correlation must be improved because the difference between *i*-C_4E_1 and C_4E_1 or *i*-C_5E_2 and C_5E_2 cannot be taken into account since they have the same *i* and *j*. Moreover, *i* and *j* characterize only alkyl polyethylene glycols, so they could not be transposed to other amphiphiles.

$$C_{CA} = 2.5 + 0.42\,j - 1.15\,i - 0.02\,i^2 + 0.09\,j^2 - 0.47\frac{i}{j} \qquad \text{(II.3)}$$

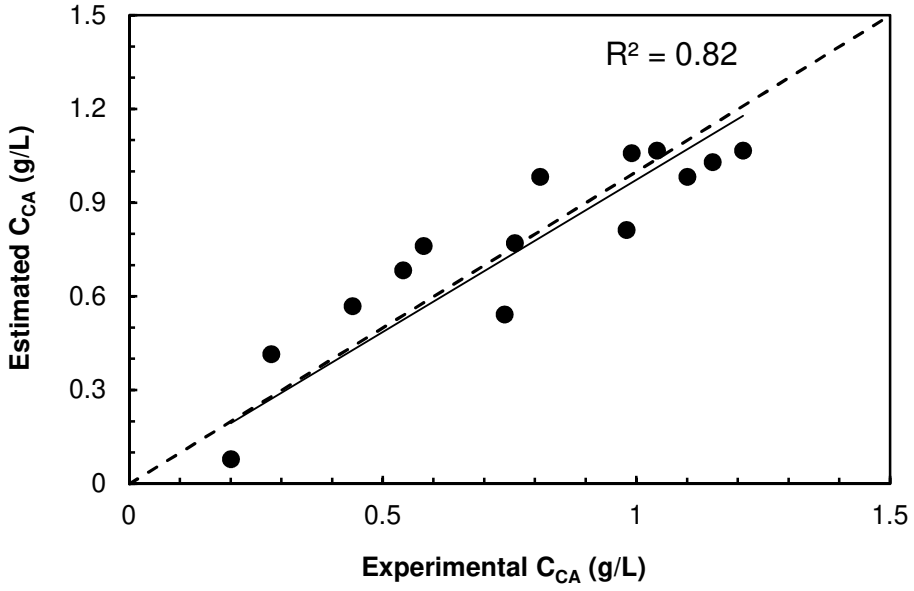

Figure II.9. Correlation between experimental and estimated concentration of extracted CA based on the Eq.II.3

b. Relationship between concentration of extracted carnosic acid and physicochemical descriptors (HLB, log *P*, V_m) of alkyl polyethylene glycol ethers

The diffusion of a molecule inside the plant requires both lipophilicity and mobility, the latter being directly related to the size of the molecule.[181] This can be related to the structure and chemical composition of the cell barriers which are crossed during the diffusion. Indeed, during the diffusion across the phospholipid bilayer, the molecule crosses two types of environments: one mainly composed of the hydrophilic glycerol and phosphate functions and the other one composed of the hydrophobic alkyl chains of the phospholipids. Thus, very polar and apolar molecules require a lot of energy to cross the hydrophobic core and the hydrophilic layers respectively. A medium hydrophobicity and polarity is better suited to reduce the energy of the diffusion.[182,183] In addition, the molecule needs to diffuse across the cell wall (≈ 200 nm), mainly composed of polar cellulose fibers. This layer is known to allow the diffusion of water, ions and water-soluble molecules such as plant hormones, but not proteins, hydrophobic molecules or particles with a diameter greater than 4 nm, which corresponds to the porosity of the matrix.[184]

Based on these considerations, the molecular volume (V_m) was plotted as a function of HLB and log *P* (**Figure II.10,** a and b) for each linear C_iE_j.[171] Contour lines representing the concentration of extracted CA at 48 h were calculated with Origin®. Each line is a set of points corresponding to theoretical amphiphiles with the same efficiency for an extraction in the same conditions. According to the calculation, there is an optimum of efficiency for hydrotropes with a log *P* above 1 or a HLB below 12.5 and with a V_m below 250 Å^3. Indeed, C_5E_2, which is the best hydrotrope has a log *P* of 1.11, a HLB of 11.9 and a V_m of 241 Å^3.

These diagrams suggest the existence of equations to estimate the concentration of extracted CA. Indeed, "isoconcentration" curves can be represented as concentric circles with a center corresponding to the theoretical properties to maximize the efficiency of an hydrotrope, and the radius corresponding to a function of the concentration of extracted CA (**Figure II.10,** c, d).

The coefficients of the equation (**Eq.II.4**) of the circles, with r, the radius and the equation (**Eq.II.5**) connecting r to C_{CA} were calculated by multiple linear regression between ln(C_{CA}) and V_m/100, (V_m/100)^2, log *P*, log *P*^{2} for all C_iE_j with a rather good correlation coefficient of 0.9 (**Figure II.10,** e). Similarly, **Eq.II.6** connects r' to HLB and V_m and **Eq.II.7** shows the relation between r' and C_{CA}. The same methodology was used than that used with log *P* but V_m/55, (V_m/55)^2, HLB and HLB^2 were used instead of the previous factors. **Eq.II.4** suggests that the best hydrotrope should have a log *P* = 1.37 and a V_m = 240 Å^3 and **Eq.II.6** suggests that it should have a HLB = 11.9 and a V_m = 218 Å^3.

$$r^2 = \left(\frac{V_m - 240}{100}\right)^2 + (\log P - 1.37)^2 \qquad \text{(II. 4)}$$

$$C_{CA} = 1.2 \times \exp\left(-0.3r^2\right) \qquad \text{(II. 5)}$$

$$r'^2 = \left(\frac{V_m - 218}{55}\right)^2 + (HLB - 11.9)^2 \quad \text{(II. 6)}$$

$$C_{CA} = 1.15 \times \exp\left(-0.066\, r'^2\right) \quad \text{(II. 7)}$$

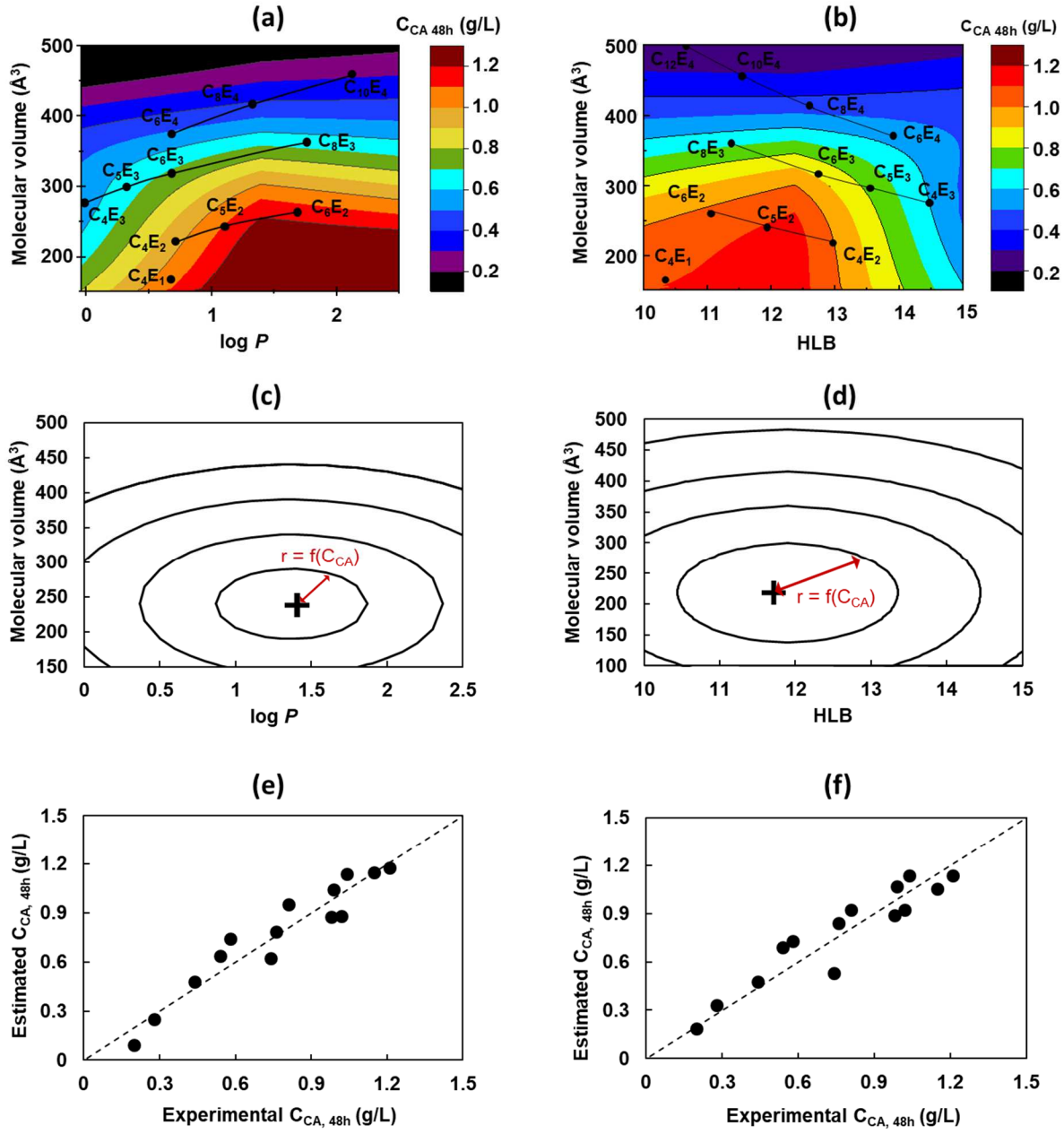

Figure II.10. (up) Color-coded contour plot of the concentration of extracted CA after 48 h versus molecular volume and log *P* (a) or HLB (b) of the amphiphiles. Each contour line is calculated with the Origin® software, (middle) Contour plots calculated by Eq.II.4 and 5 (c) and Eq.II.6 and 7 (d). The maximum of efficiency is supposed to be at the center of the circles (log *P* = 1.37, V_m = 240 Å^3), and (HLB = 11.9, V_m = 28 Å^3). The radius is function of the concentration. (down) Correlation between experimental and estimated concentration of extracted CA. Estimation based on the Eq.II.4 and 5 (e) and Eq.II.6 and 7 (f).

The comparison of branched hydrotropes *i*-C_5E_2 and *i*-C_4E_1 with their isomers C_5E_2 and C_4E_1 (**Figure II.8**) shows that the ramification induces a significant decrease of the amount of CA extracted. This can be related to the volume of the alkyl chain because for the same number of carbons, a branched chain is shorter but larger. Therefore, the decrease of efficiency can be related to a decrease of the mobility and a weaker diffusion through plant barriers.

II.3.3. Cloud point variation during extraction

Noteworthy, most of the extractions were performed in homogeneous solutions except for C_6E_2 and C_8E_3 because of their CP below 25 °C. In the case of *i*-C_4E_1, the extraction started in homogenous solution but as the CP decreased with the enrichment of the solution by phytochemicals such as CA, a biphasic mixture was obtained at the end. In each case, the CP was reduced after extraction. In the case of C_6E_2, the CP is not observable after extraction because the mixture is still biphasic at 0 °C. Post-extraction CPs were compared to the CPs of the hydrotropic solutions containing 2.5 g/L of CA, which is close to the maximum concentration that can be reached after extraction (**Figure II.11**). Indeed, the rosemary dried leaves used for these extractions contain 2.7 wt.% CA.

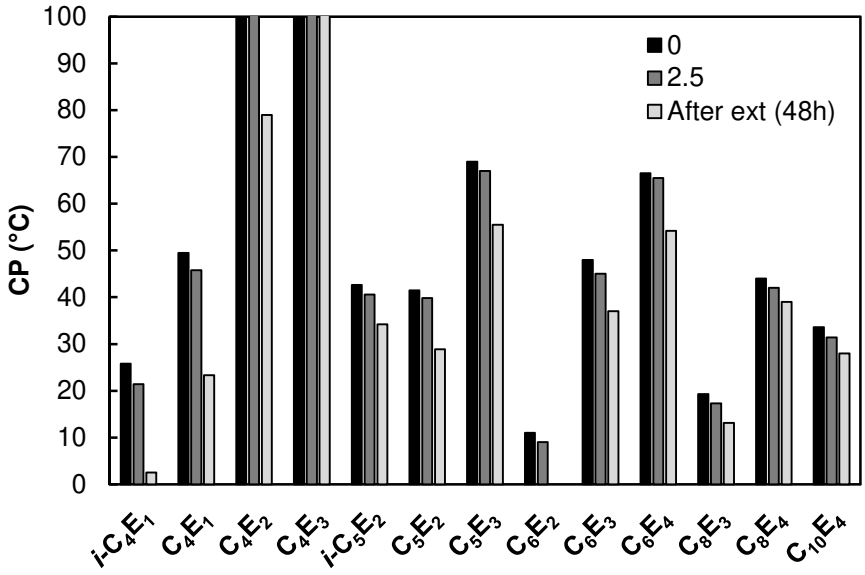

Figure II.11. Thermal behavior of the solutions of amphiphiles without any solute (black bars) or in the presence of 2.5 g/L (dark grey) and after extraction, *i.e.* with CA and many other phytochemicals solubilized (light grey).

CP can inherently limit the range of usable temperature during the extraction procedure. For the purification step, on the contrary, reaching the CP post-extraction can advantageously concentrate CA in a smaller phase. Noteworthy, the lower the CP, the less consumed energy. In **Figure II.11,** since the reduction of the CP is higher in amphiphile solutions after extraction than with only 2.5 g/L CA, other extracted compounds than CA induce a depression of the CP. One can assume at first sight that the more the CP is reduced, the more phytochemicals are

extracted, but all the phytochemicals do not reduce the CP in the same way. This was verified by investigating the thermal behavior of solutions of C_4E_1 (30 wt.%) containing 1 to 25 g/L of CA, rosemarinic acid (RA) and pure camphor (C) which are constitutive of rosemary (**Figure II.12**). Solutions of 1 to 25 g/L of ursolic acid (UA) in C_4E_1 (30 wt.%) were not possible to prepare due to its low solubility. Stearic acid (SA) was soluble at 1 g/L at room temperature and while heating at 5 and 10 g/L. However, when SA was concentrated at higher concentrations (15, 20 and 25 g/L), the CP occurred while SA was not completely solubilized. Therefore, the CP was not reported in the results. For CA, RA and camphor, CP linearly decreased with the amount of solubilized solute.

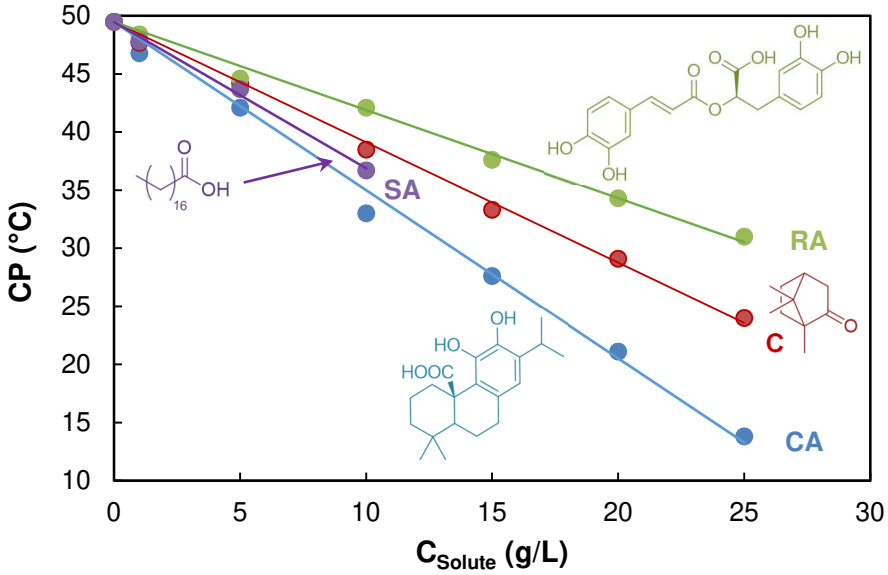

Figure II.12. Evolution of the cloud point (CP) of an aqueous solution of 30 wt.% C_4E_1 at pH 2 containing increasing amounts of camphor (C), carnosic acid (CA), rosmarinic acid (RA) and stearic acid (SA; not soluble above 10 g/L).

Normalizing the concentration of added solutes, the CP-depression effect of phytochemicals is in the following order: CA > SA > RA > C. It is known that the reduction of CP is a consequence of an increase of the micelle volume due to the incorporation of the hydrophobic compounds into the micelle core.[164,185] This CP-depression effect seems to be partly determined by the phytochemical polarity (*i.e.* log *P*); a trend already reported with homologous series of phenols and phthalates.[163] In **Figure II.12**, the same behavior is indeed observed for RA (log *P* = 0.8), camphor (log *P* = 2.1) and CA (log *P* = 5.4, SciFinder® data), but the CP depression effect of SA (log *P* = 8.7) is between CA and camphor, although it should be more important based on log *P* only. This can be explained by the more amphiphilic and less rigid character of SA compared to the other molecules.

As the significant decrease of CP post-extraction cannot be assigned to CA only, this effect can be considered as an indicator of the selectivity of the extraction. For example, *i*-C_4E_1 extracts 0.81 g/L of CA, which should theoretically correspond to a CP of 24.4 °C. However, the solution after extraction has a CP of only 2.5 °C. In other words, while the CP should be reduced

by 1.4 °C, it is reduced by 23.3 °C, 16 times more than expected. In the case of *i*-C_5E_2, 1.04 g/L CA was extracted and the CP was reduced only 10 times more than expected. One could conclude that *i*-C_4E_1 probably extracts more hydrophobic compounds, besides CA, than *i*-C_5E_2. Obviously, this cannot be applied to hydrotropes with CP > 100 °C (*e.g.* C_4E_2) or CP < 0 °C after extraction (*e.g.* C_6E_2).

II.3.4. Kinetics of the extractions

To optimize the time of extraction, the kinetics were studied over 48 h to ensure completion. **Figure II.13** reports the amount of extracted CA as a function of time for C_4E_1, C_4E_2 and C_4E_3 and clearly shows that the slope of the extraction curve decreases when the number of ethylene oxide units increases. The kinetics of the other amphiphiles are shown in **Figures II.13 and II.14** for C_iE_j with i < 8, and in **Appendixes 2-5** for C_iE_j with i > 8, SXS and alcohols.

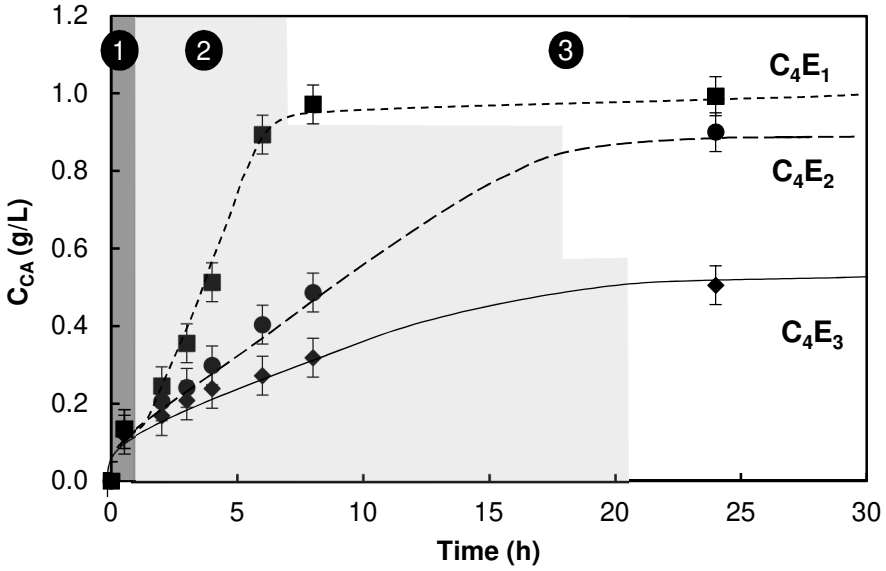

Figure II.13. Kinetics of the extractions performed with aqueous solutions containing 30 wt.% of C_4E_1 (■), C_4E_2 (●) and C_4E_3 (◆) at 25 °C, pH 2 focused between 0 and 30 h. The different steps are indicated as follows: ❶ (dark grey) washing step, ❷ (light grey) diffusion step and ❸ (white) plateau corresponding to completion of extraction.

The extraction process can be divided into three steps as reported by Pinelo et al. for the extraction of phenols from apple skin.[186] First, a washing step ❶ takes place in the first minutes of extraction and corresponds to the solubilization of the *easily accessible CA* located in some broken cells in rosemary leaves.[40] The nature of the C_iE_j has no influence during this step and about 0.12 g/L of CA is extracted in 30 min. Then, during the several hours of the diffusion step ❷, there is a mass transfer of CA from the inside of the plant to the solution, helped by the amphiphile which diffused into the plant and solubilizes CA. Finally, until completion of extraction, the amount of extracted CA increases very slowly until reaching a plateau. The times at which the plateau is reached are reported in **Table II.2** for the different C_iE_j.

The kinetics of extraction were found to be linear for all the C_iE_j at the beginning of the diffusion step (**Figure II.15**). Interestingly, for some C_iE_j, such as C_4E_1, C_5E_3, C_6E_2 or C_6E_3, the diffusion step is completely linear until the plateau occurs (**Figures II.13 and II.14**). To take into account the real efficiency during the diffusion step (step ❷ in **Figure II.13**), we determined a constant rate *k* which corresponds to the slope of the kinetic curve at the beginning of the extraction, considering the linear part as modelled by an apparent zero-order kinetic.[187] Values of *k* are given in **Table II.2** for the different C_iE_j and diffusion steps of the kinetics are shown in the **Figure II.15** for all C_iE_j, SXS, EtOH 96 wt.% and BuOH 100 wt.%.

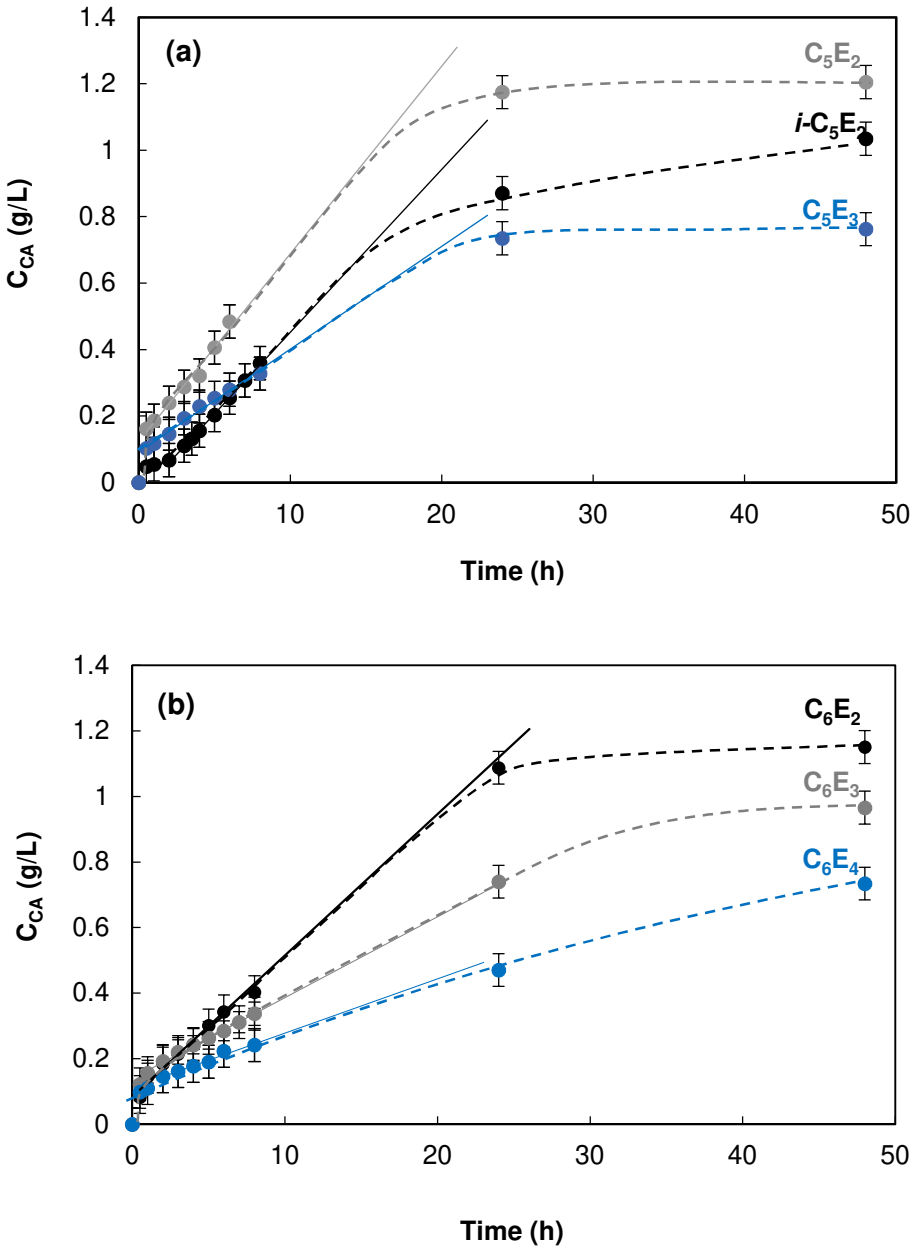

Figure II.14. Kinetics of the extractions performed with aqueous solutions containing 30 wt.% of (a) C_5E_2 (grey), *i*-C_5E_2 (black), C_5E_3 (blue), (b) C_6E_2 (black), C_6E_3 (grey), C_6E_4 (blue) at 25 °C, pH 2 between 0 and 48 h.

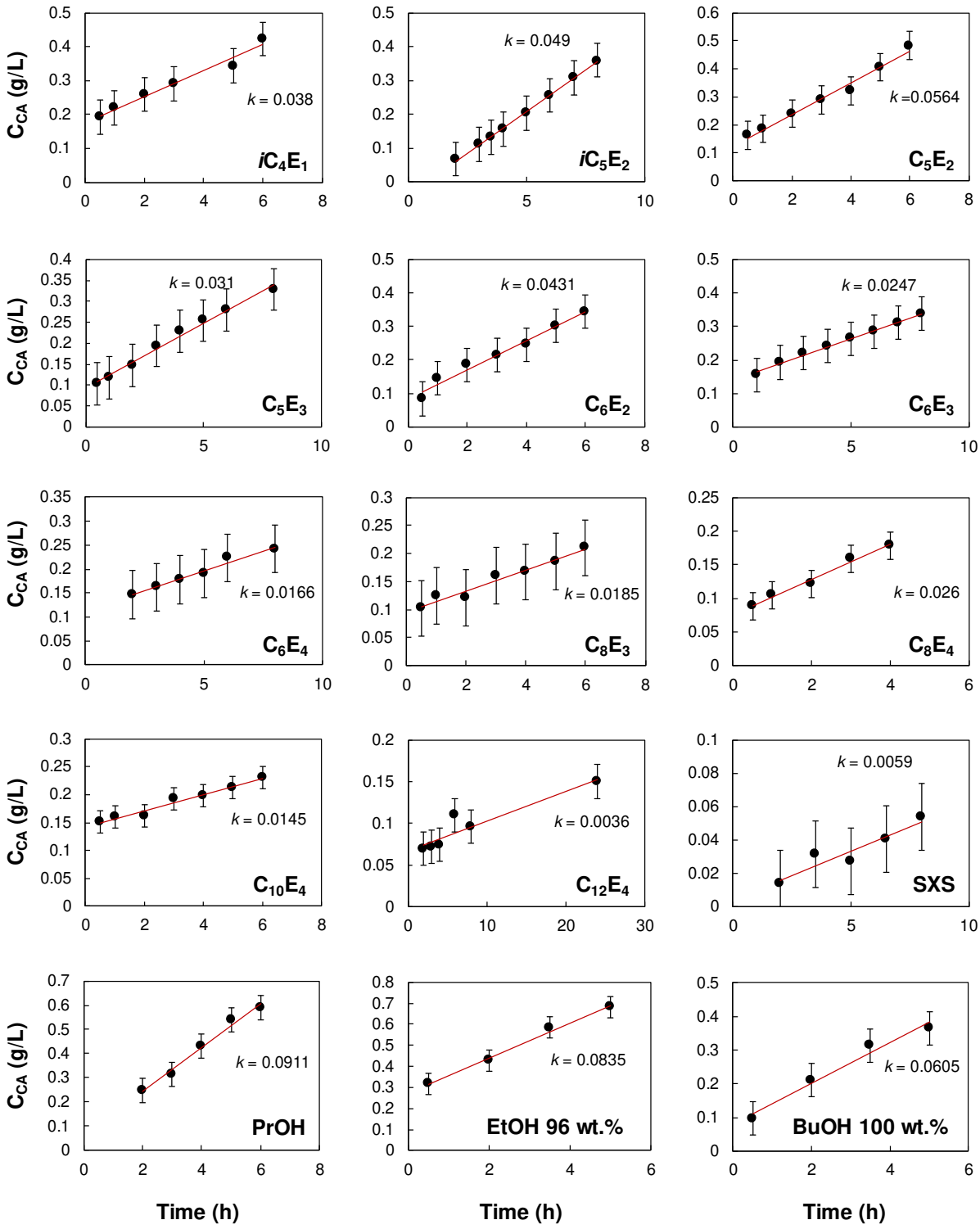

Figure II.15. Linear evolution of the concentration of extracted CA during the diffusion step for each amphiphile.

For the C_4E_j series, the extraction is faster when *j* is lower (**Figure II.13, Table II.2**). The same trend occurs for the other series C_5E_j and C_6E_j (**Figure II.14, Table II.2**). Moreover, for the C_iE_2, C_iE_3 and C_iE_4 series, a parabolic-like trend is observed with the highest extraction rate for the hydrotrope with a C_5, C_5 and C_8 alkyl chain respectively. The linear alkyl chains C_4E_1 and C_5E_2 also show higher constant rates than their branched isomers.

Table II.2. Concentration of CA at the end of extraction, transfer coefficients *k* obtained by linear regression between C_{CA} and t, and times of extraction completion ($t_{plateau}$).

	$C_{CA\ 48H}$ (g/L)	*k* (g/L/h)	$t_{plateau}$ (h)
PrOH 30 %	0.93	0.091	15
BuOH 100 %	1.15	0.061	> 24
EtOH 96 %	1.97	0.084	> 24
***i*-C_4E_1**	0.81	0.038	> 24
C_4E_1	1.02	0.154	8
C_4E_2	0.99	0.048	17
C_4E_3	0.54	0.022	21
***i*-C_5E_2**	1.04	0.049	> 24
C_5E_2	1.21	0.056	21
C_5E_3	0.76	0.031	24
C_6E_2	1.15	0.043	24
C_6E_3	0.98	0.025	> 24
C_6E_4	0.74	0.017	> 24
C_8E_3	0.58	0.018	> 24
C_8E_4	0.44	0.026	> 24
$C_{10}E_4$	0.28	0.015	15
$C_{12}E_4$	0.20	0.004	> 24
SXS	0.12	0.006	24

II.3.5. Physicochemical key parameters for an "ideal" hydrotrope

For selecting the best hydrotropes, which should be able to extract the highest amount of CA as fast as possible, the constant rates *k* were plotted as a function of the amount of CA extracted at 48 h (**Figure II.16**).

In terms of kinetics, we have the following order: C_4E_1 >> C_5E_2 > C_4E_2 = *i*-C_5E_2 > C_6E_2 > *i*-C_4E_1 > C_5E_3 > C_8E_4 > C_6E_3 > C_4E_3 > C_8E_3 > C_6E_4 > $C_{10}E_4$ > SXS > $C_{12}E_4$. While there is a relatively good correlation between the extraction rate *k* and the amount of CA extracted for the different C_iE_j, C_4E_1 seems to have a different behavior as its extraction is much faster compared to other amphiphiles. Noteworthy, C_4E_1 had already been reported with a different behavior when the CP was correlated with *i*/*j* (**Figure II.6**). The extraction with C_4E_1 can be stopped after only 8 h because all CA that can be extracted by C_4E_1 (1.02 g/L) has already been

recovered. However, if the extraction was fast with C_4E_1, the final CA concentration obtained in the extract after 48 h of extraction was not the highest one (**Figure II.16**). On the contrary, EtOH 96 wt.% is the most efficient extractant after 48 h but its kinetics is much longer: the extraction rate raised smoothly between 24 and 48 h to reach a high concentration of CA in the final extract. Extractions with C_iE_j at 30 wt.% cannot be compared neither with BuOH 30 wt.%, which is immiscible with water, nor with EtOH 30 %, which cannot solubilize CA, but were compared with PrOH 30 %. Indeed, 0.93 g/L of CA were recovered with an extraction with PrOH 30 %, which is slightly lesser than with C_4E_1 or C_4E_2 (**Figure II.8**), and its *k* is comprised between those of C_4E_1 and C_4E_2.

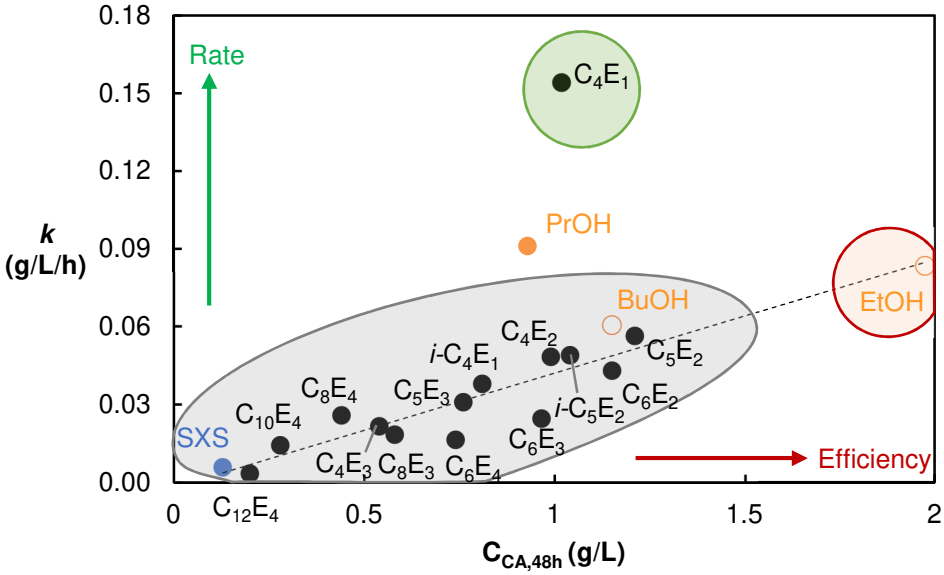

Figure II.16. Constant rates *k* for the linear part of the extraction curves as a function of the concentration of CA extracted after 48 h, at 25 °C, pH 2 with 30 wt.% C_iE_j, SXS or PrOH (full points), 96 wt.% EtOH and 100 wt.% BuOH (empty points).

II.3.6. Optimization of the hydrotropic extraction with C_4E_1

a. The case of sage

From a practical point of view, C_4E_1 is the most interesting hydrotrope because it gives one of the highest amount of CA and its extraction can be stopped after few hours whereas it takes generally more than 20 h with the other hydrotropes. Therefore, we used hydrotropic solutions of C_4E_1 at 30 wt.% to compare the extractions of CA from rosemary and sage (**Figure II.17**). Since sage and rosemary do not contain the same CA content with 2.7 and 1.85 wt.% CA respectively, the percentage of extracted CA from leaves was used instead of the concentration in the filtrate to compare the efficiencies of the extractions. Therefore, the concentration of CA in the filtrate with C_4E_1 after 24 h of extraction, 0.99 g/L (**Figure II.8**), represents 36.5 % of extracted CA from the available part in rosemary. This value could be increased to 44 % by performing the extraction at 40 °C. Extractions from sage gave similar results, slightly lower at

34.5 % and 42 % at 20°C and 40°C respectively, suggesting that similar extraction mechanisms occur for the both plants (**Figure II.17**).

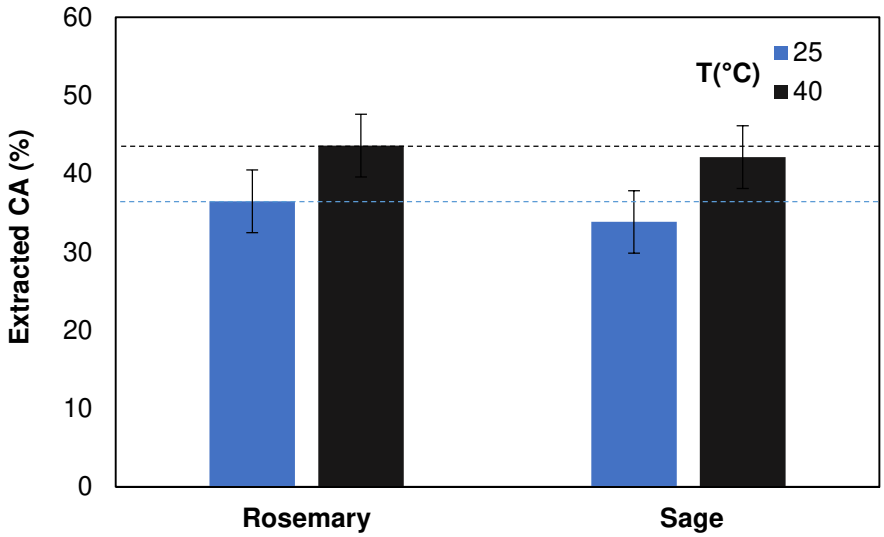

Figure II.17. Percentage of extracted CA in the 30 wt.% C_4E_1 solution after 24 h of extraction from 1 g of whole leaves of rosemary and sage in contact with 10 mL of solutions at 25 and 40 °C, at pH 2.

b. Identification of the key conditions for the hydrotropic extraction with C_4E_1

The effect of the P:S ratio and the C_4E_1 concentration were also investigated on extractions performed on whole leaves of rosemary at 25 and 40 °C, as shown in **Figure II.18**. With a P:S ratio of 1:10, which has been used for all the previous extractions, the amount of extracted CA at 25 °C increases by a factor 2.5 (from 15 to 37 %) while increasing the C_4E_1 concentration from 20 to 30 wt.%. However, it remains stable at 37 % from 30 to 40 wt.% C_4E_1. The same behavior is observed when extractions are performed at 40 °C because the amount of extracted CA increases by a factor 3.6 to reach 44 % from 20 to 30 wt.% C_4E_1 and remains stable at higher C_4E_1 concentration.

Interestingly, when the amount of rosemary leaves is divided by 4, *i.e.* at a P:S ratio of 1:40, the same relative amount of CA is extracted in the 40 wt.% C_4E_1 solution at 25 °C (34 *vs* 36 %) and at 40 °C (43 *vs* 44 %). At this P:S ratio, the solution at 20 wt.% C_4E_1 is as efficient as the one containing 40 wt.% to extract CA at 25 and 40 °C with respectively 33 and 46 % of extracted CA. Therefore, with a too high P:S ratio, the amount of extracted CA falls down, meaning that the extraction is limited by the hydrotrope/available CA ratio, *i.e.* the hydrotrope/rosemary ratio. However, once a sufficient hydrotrope/rosemary ratio is reached, it can be considered that the amount of CA extracted from whole leaves of rosemary will only depend on the temperature, whatever the P:S ratio and the hydrotrope concentration.

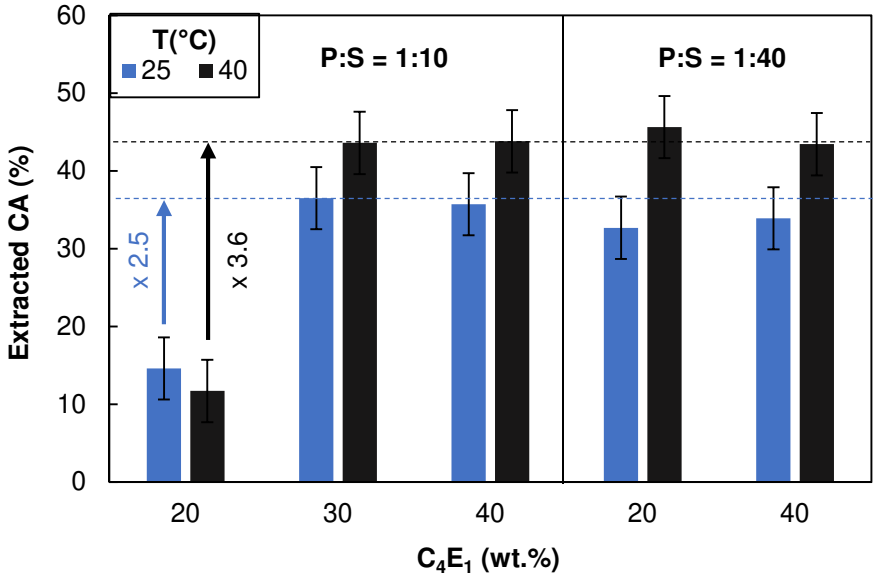

Figure II.18. Amount of extracted CA solution after 24 h of extraction in 20, 30 and 40 wt.% C_4E_1 aqueous solutions from 500 mg and 125 mg of whole leaves of rosemary (ratio P:S = 1:10 and 1:40 respectively) in contact with 5 mL of solutions at 25 °C, at pH 2.

II.4. Microscopic observations of rosemary leaves after extraction with aqueous solutions of alkyl polyethylene glycol ethers and short alcohols

II.4.1. Structural characteristics of rosemary leaves

Leaves are the site of photosynthesis, that is, the place where the carbon dioxide is converted into dioxygen and sugar through redox reactions under the action of light.[184] For that purpose, leaves are composed of many chlorophyll cells, called "mesophyll cells" which can be of two types: *(i)* a continuous layer of palisade mesophyll cells and *(ii)* spongy mesophyll cells between which gases can flow. Noteworthy, thanks to its strong antioxidant power, CA may have a role of protection of the photosynthetic electron transport chain since they are only found in chloroplasts, which are mostly present in these chlorophyll cells.[15] Mesophyll cells are comprised between the upper and the lower epidermis, as shown in **Figure II.19**. The upper epidermis is covered by a very hydrophobic layer of about 10 µm width composed of long alkanes, fatty acids and triterpenes to protect the leaves from water and to limit evapotranspiration.[31] Cuticle also covers the trichomes with a 2–6 µm width.[19,30] As well, each tissue has his own function: the collenchyma provides structural support and the vascular tissues transport nutrients and fluids internally.[23,184] The lower epidermis is covered by numerous hair-like and glandular trichomes, where CA is biosynthesized and essential oils are stored, which constitute a particularity of rosemary and other Lamiaceae plants.[18,19] The fact that the margins are folded inward is also a particularity of rosemary and certainly an adaptation to its warm and dry natural environment.

Considering that trichomes contain a high amount of CA whereas the other part of the leaves contains lower CA amount and higher CAR, 12-*o*-methyl carnosic acid (MCA) and other CA derivatives amounts,[18] it should be interesting to extract only trichomes, which are in direct contact with the medium of extraction, to reach a higher CA purity in the final extract.

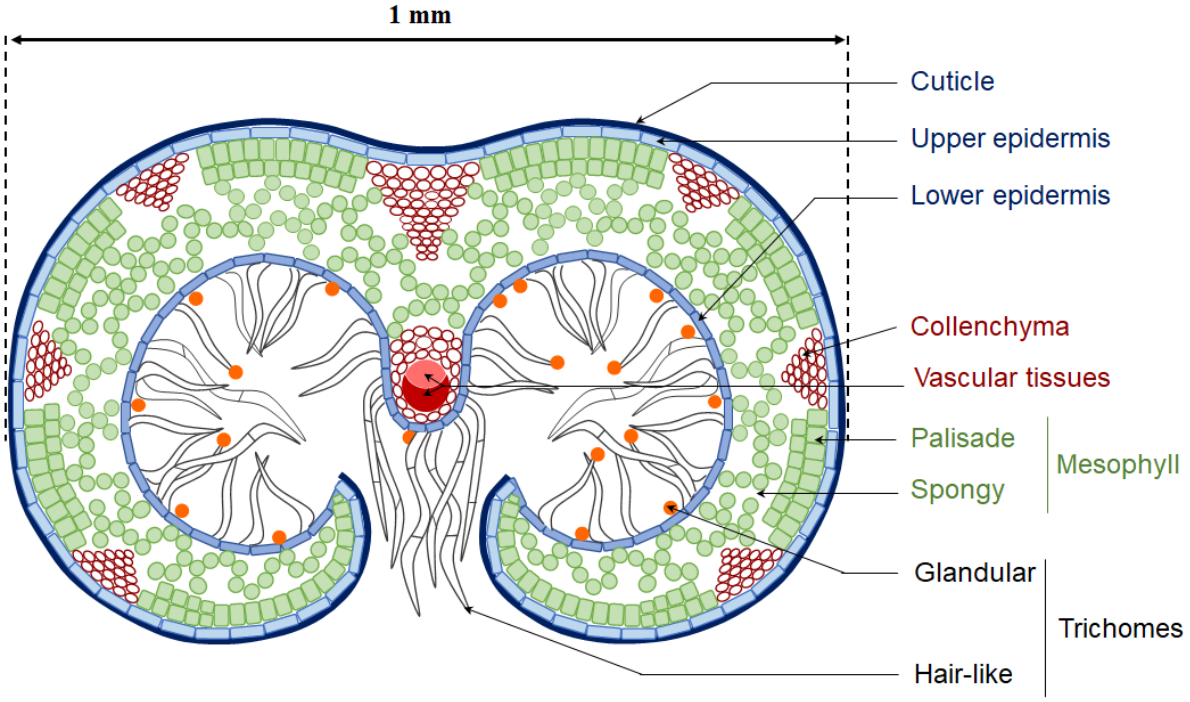

Figure II.19. Scheme of the internal structure of a rosemary leaf observed in cross section

II.4.2. Impact of treatment on the plant material

Cross sections of rosemary after 48 h of extractions with C_iE_j were observed by optical microscopy and compared to leaves before extractions (**Figure II.20**). Trichomes seem to be cut/degraded after the extractions performed with C_6E_2 and the spacing between margins seems to be increased. For example, a leaf before extraction (untreated) has its margins spaced 229 µm apart whereas a C_6E_2-treated leaf has its margins spaced 715 µm apart. To appreciate the effect of C_iE_j on the leaf structure, trichomes were counted by observing the opening (as presented as an example by the red crosses in **Figure II.20**) and the width opening has been measured on leaves after 48 h in contact with different C_iE_j, BuOH, EtOH and water. The results are shown in **Figure II.21**.

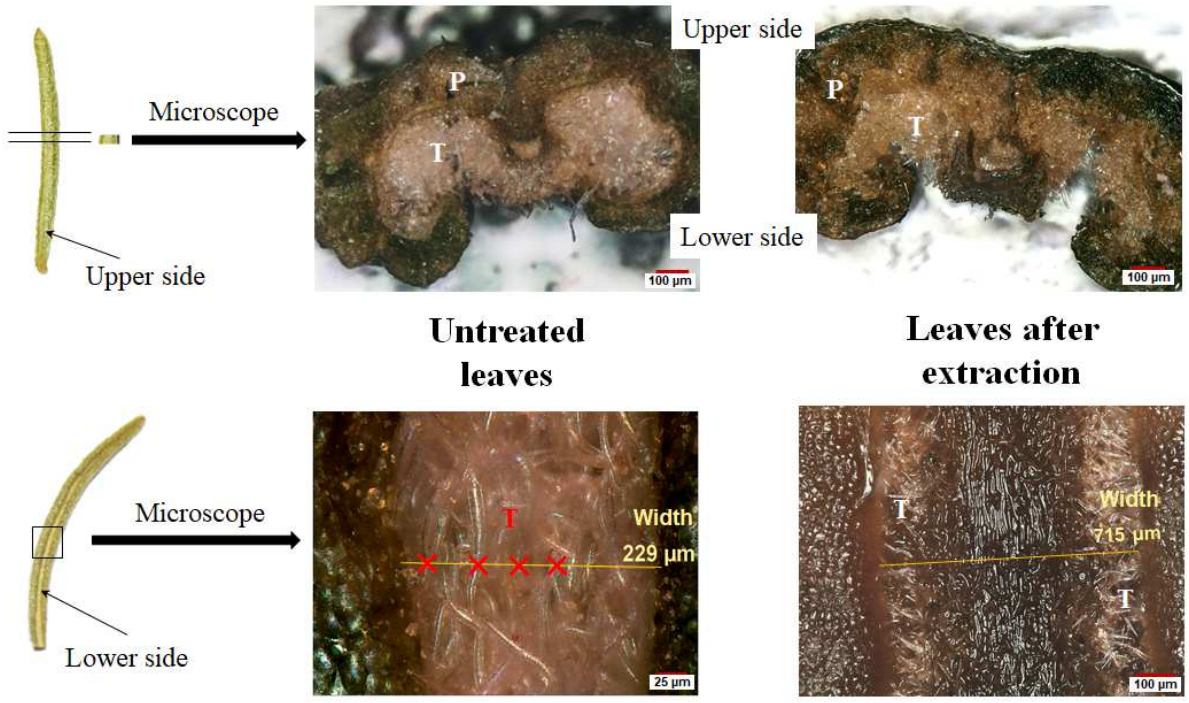

Figure II.20. (left) Top-view (up) and bottom view (down) of a whole rosemary leaf, microscopic observations of cross sections (up) and bottom view (down) of rosemary leaves before extraction (middle) and after 48 h in contact with a 30 wt.% C_6E_2 aqueous solution at pH 2 and 25 °C (right). P: parenchyma, T: trichomes

The width of the opening on the lower side of leaves was found larger after treatment with water and aqueous solutions of C_iE_j and EtOH, but unchanged with pure solvents EtOH 96 wt.% and BuOH 100 wt.%. This result can be related with the fact that untreated rosemary leaves are as rigid as leaves after treatment with pure EtOH and BuOH, whereas they are softer after treatment with the aqueous solutions. The presence of water induces a swelling of the material that may participate to extraction by providing to hydrotropes an easier access to trichomes. More importantly, the density of trichomes decreases after a treatment with C_iE_j, whereas it looks unchanged after a treatment with water, EtOH 30 and 96 wt.% and BuOH 100 wt.% at ambient temperature, showing the clivage/degradation of the trichomes. As a consequence, we can assume that CA should be more delivered into the hydrotropic solution. This suggests that C_iE_j penetrate inside the leaves and interact with the structural molecules of the cells, *i.e.* molecules of the cell wall or the cell membrane. On the contrary, pure EtOH can extract CA but does not destruct the leaves, so it is able to diffuse through the cell barriers without destabilizing them.

The kinetic performance of small amphiphiles like C_4E_1, may be explained by a hybrid behavior combining the extraction mechanisms of alcohols with that of other C_iE_j. For instance, C_4E_1 degrades trichomes as the other C_iE_j but may also penetrate inside the plant matrix to extract CA as EtOH does.

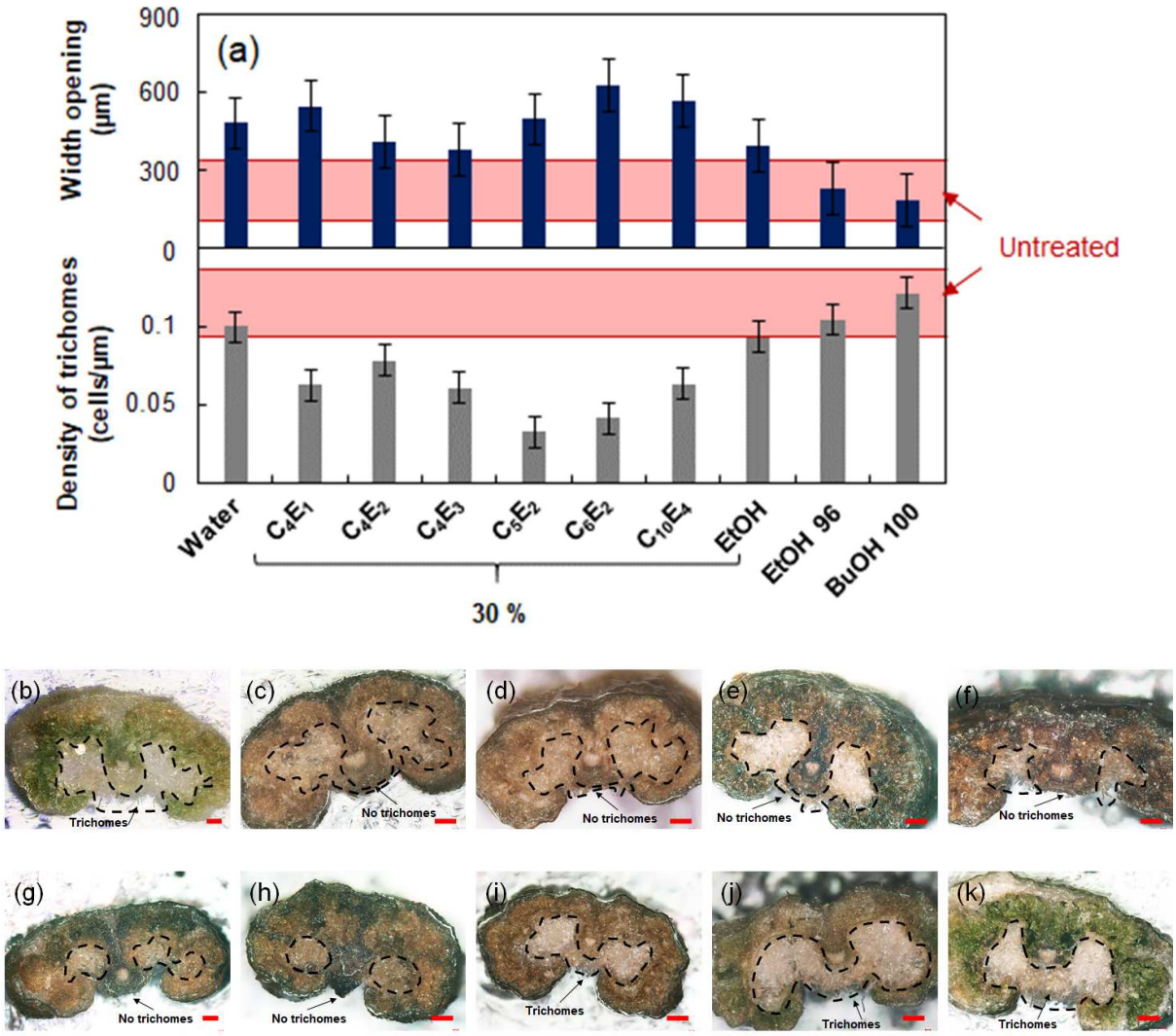

Figure II.21. Analysis of the structure of rosemary leaves before extraction (red background) and after 48 h in contact with water, aqueous solutions of C_iE_j or solvents (a), and cross sections of rosemary leaves after 48h in contact with water (b), aqueous solutions of C_4E_1 (c), C_4E_2 (d), C_4E_3 (e), C_5E_2 (f), C_6E_2 (g), $C_{10}E_4$ (h), EtOH (i) at 30 wt.%, EtOH at 96 wt.% (j), and BuOH at 100 wt.% (k). Trichomes are located inside the dotted lines. The width of the opening and the number of trichomes present in the opening have been measured by numeric microscopy on nine different leaves for each experiment.

II.5. Recovery of a solid extract

As mentioned in section I.1.1, the plant/solution extraction is generally followed by the recovery of a solid extract from the liquid extract, previously separated from the plant. Contrary to solvents, which are easily separated from the extracted molecules by evaporation, the recovery of a solid extract from a hydrotropic solution may be challenging. Indeed, water and hydrotropes are generally less easily evaporated because of their higher boiling points. However, two options can be investigated: the HCPE process including CP phase separation and evaporation of the hydrotrope from the resulting smaller phase containing the extract,[94] and

the dilution to a hydrotrope concentration below its MHC, which induces the precipitation of the extract.[119] C_4E_1, which presented the best compromise between CA extraction yield and kinetic rate, has also a CP which can be used to concentrate the extract and a low boiling point to be evaporated under vacuum, making it suitable for HCPE process. Therefore, both processes, *i.e.* HCPE process and hydrotropic dilution, were compared to recover a rosemary extract from 40 wt.% solutions of C_4E_1.

II.5.1. Hydrotropic Cloud Point Extraction (HCPE) of rosemary leaves

To ensure that the extraction of CA is not limited by C_4E_1 amount, it was performed with a high hydrotrope/rosemary ratio. Whole rosemary leaves were extracted with an aqueous solution of 40 wt.% C_4E_1 at room temperature (25 °C) and 40 °C during 24 h with a P:S ratio of 1:40, with a total volume of 25 mL, as shown in **Figure II.22**.

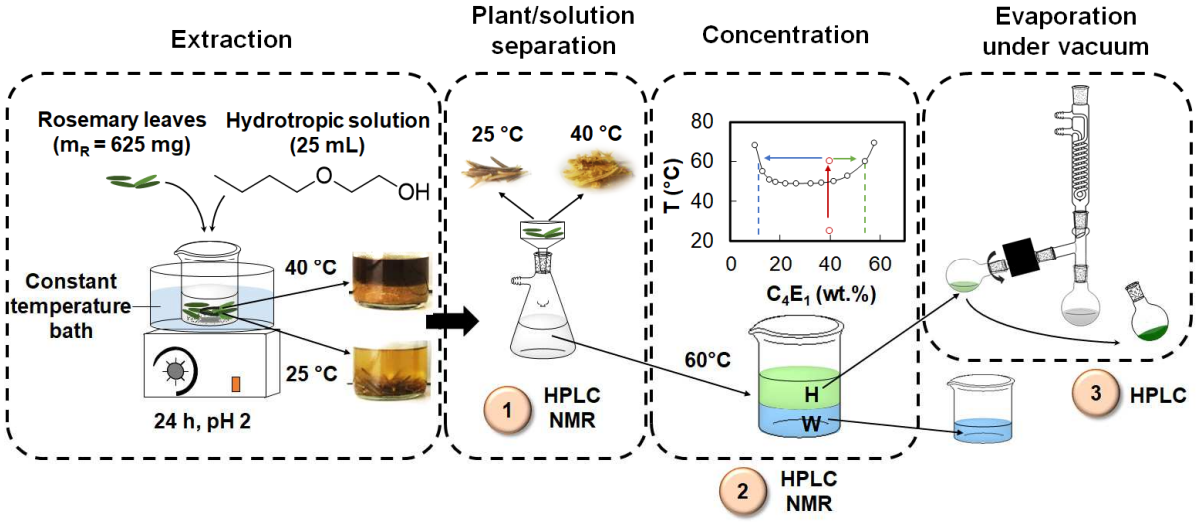

Figure II.22. Schematic procedure of the HCPE process performed on rosemary whole leaves with a 40 wt.% C_4E_1 aqueous solution at pH 2, pictures of the crude extract and leaves after extractions at 25 and 40 °C and phase diagram of C_4E_1 aqueous solutions at pH 7 from ref[94] explaining the phase separation in a hydrotrope-enriched phase (H, green) and a water-enriched phase (W, blue). The CA concentration or content is quantified by HPLC at three different stages noted 1, 2 and 3 whereas the C_4E_1 concentration is quantified by ^{1}H NMR only in the liquid phases at the stages 1 and 2.

A solution containing 40 wt.% C_4E_1 at pH 2 exhibits a CP at 46 °C according to **Figure II.2**, and this CP is lowered after extraction according to section II.3.3. Noteworthy, at the end of the extraction performed at 40 °C, two phases were recovered, showing once again the effect of the solutes on the CP. The solution was cooled below its CP and thus homogenized before the separation of the rosemary leaves from the hydrotropic solutions by Büchner filtration. The CA and C_4E_1 concentrations in the filtrates were quantified respectively by HPLC and by ^{1}H NMR (**Table II.3**). The extractions performed at 40 °C were more efficient compared to extractions

at 25 °C, as expected from the results of section II.3.6. Interestingly, the leaves that had been treated at 40 °C turned brown-yellow with a destroyed aspect, whereas those extracted at 25 °C kept their original aspect (**Figure II.22**). This can be related to the denaturation induced by hydrotropes as previously reported (section II.4.2), which can be more important at 40 °C.

The resulting filtrates were heated to 60 °C in an oven to induce their phase separation in two phases: a hydrotrope-enriched phase with CA at the top, noted "H" and a water-enriched phase at the bottom of the vessel, noted "W". This partition can be well understood by the study of the phase diagram (**Figure II.22**). Indeed, if the 40 wt.% C_4E_1 solution contained only C_4E_1 and water, the heating from 25 to 60 °C would provide two phases with 12 and 55 wt.% C_4E_1 in relative proportions that equilibrate with the global amount. Here, the two phases are separated by Pasteur pipette and the ^{1}H NMR quantification of C_4E_1 showed that extraction at 25 °C was separated in two phases of 8 and 57 wt.% of C_4E_1 and 9 and 55 wt.% of C_4E_1 for the extraction at 40°C, as reported in **Table II.3**. As expected, the hydrotrope-enriched phase contained all the CA in both experiments (HPLC quantification). However, the CA concentrations were not improved compared to the mother filtrates while they were contained in smaller phases, meaning that the global amount of recovered CA has been lowered. Nevertheless, the isolation of the CA-enriched phase from the hydrophilic phase already consisted in a first purification step because some very polar extractives are eliminated by remaining in the water phase. This residual hydrophilic phase was thrown away but may be recycled for another hydrotropic extraction by adjusting the hydrotrope concentration.

Finally, the organic phase was evaporated under vacuum in a 50 °C bath since C_4E_1 has a relatively low boiling point (171 °C at 1 bar and 8 °C at 1 mbar[94]). Whether the extractions were performed at 25 or 40 °C, 166 mg of pasty and dark extracts were collected, corresponding to a mass yield of 27 %, as calculated by **Eq.II.8**. This extract was solubilized in methanol, and analyzed by HPLC to evaluate the final CA content in the extract, as calculated by **Eq.II.9** and reported in **Table II.3**.

$$\text{Mass yield} = \frac{\text{mass of the dry extract}}{\text{initial mass of rosemary}} \times 100 \qquad \text{(II. 8)}$$

$$\text{CA content} = \frac{\text{CA mass recovered in the dry extract}}{\text{mass of the dry extract}} \times 100 \qquad \text{(II. 9)}$$

Table II.3. Quantitative results regarding the CA and C_4E_1 concentrations in the filtrate after plant/hydrotropic solution separation (stage 1), in hydrotropic phase (H) and water-enriched phase (W) after CP phase separation (stage 2), CA content and yield of the solid extract (stage 3) after extractions performed at pH 2.

Stage	$T_{extraction}$ (°C)	20		40	
1	C_4E_1 (wt.%)	40		40	
	C_{CA} (g/L)	0.25		0.35	
		H	W	H	W
2	C_4E_1 (wt.%)	57	8	55	9
	C_{CA} (g/L)	0.22	0	0.35	0
3	Mass yield (%)	27		27	
	CA content (wt.%)	1.12		1.45	

To evaluate the CA loss during the HCPE process, carnosol (CAR), the oxidized product of CA was also quantified by HPLC and the CA recovery rate (RR_{CA}) was calculated for each stage from **Eq.II.10**. The CA/CAR ratio and RR_{CA} are reported in **Figure II.23**.

$$RR_{CA} = \frac{\text{CA mass in the precipitate}}{\text{CA available in rosemary}} \times 100 \qquad (II.10)$$

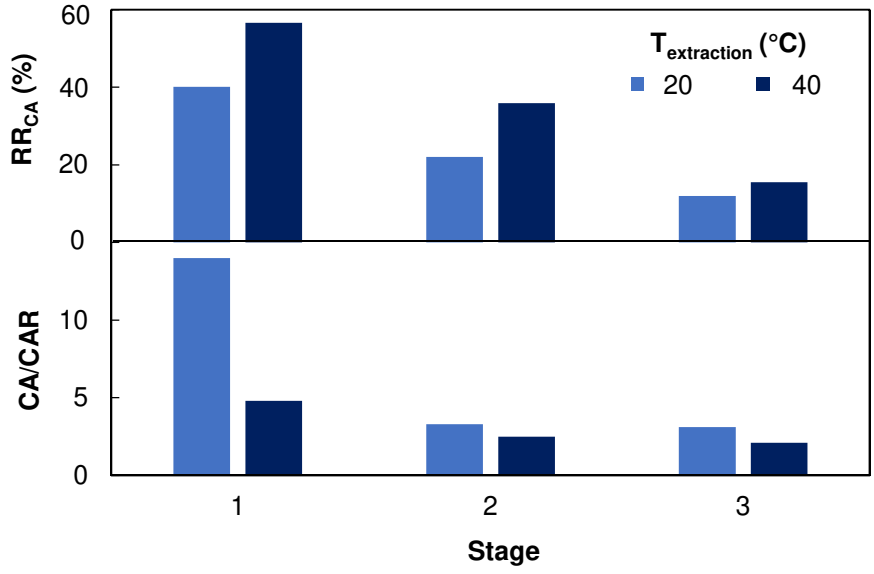

Figure II.23. CA/CAR ratio and CA recovery rate (RR_{CA}) in the filtrate after plant/hydrotropic solution separation (stage 1), in hydrotropic phase after CP phase separation (stage 2), and in the solid extract (stage 3)

In normal conditions, the CA/CAR ratio is usually comprised between 10 and 15.[6,8] As such, the CA/CAR ratio after the extraction at 25 °C (stage 1) was equal to 14, suggesting that no CA had been oxidized in CAR. However, the CA/CAR ratio after the extraction at 40 °C was

lowered to 4.8, indicating that CA was thermodegraded into CAR. Interestingly and contrarily to the CA/CAR ratio, the RR_{CA} after an extraction at 40 °C is always higher than that after an extraction at 25 °C. Temperature has a dual opposite effect: it facilitates the CA recovery all the while facilitating CA degradation.

At the second step (after the phase separation), the RR_{CA} was calculated from CA concentration in the hydrotrope-enriched phase and the volume of this latter. As it was already suggested by the C_{CA} (**Table II.3**), the recovery rate and the CA/CAR ratio were lowered compared to their values at the first stage. This result strengthens our previous hypothesis according to which CA is thermodegraded, although in this case, the thermodegradation occurs during the heating step (at 60 °C) used to pass above the CP.

The solid extracts contain only 1.12 and 1.45 wt.% of CA (**Table II.3**) after extractions at 25 and 40 °C, associated with a CA/CAR ratio of 3.1 and 2.1 respectively. The recovery rate has decreased again and is not satisfying since only 12 and 15.5 % of the available CA are recovered.

To sum up, the HCPE process is a rather long and constraining method which is not well suited to CA because of its thermosensitivity. Indeed, more than 70 % of the extracted CA in the first stage is lost during the concentration process, and the CA content in the final extract is close to 1 wt.%, which is not acceptable from an industrial standpoint.

II.5.2. Hydrotropic dilution with water

For this study, whole rosemary leaves were extracted with 40 wt.% C_4E_1 during 5 h, at room temperature (25 °C) in a P:S ratio of 1:10, at pH 2. Then, the solution was filtered under vacuum on Büchner. The filtrate was analyzed by HPLC and it was found that 24 % of the available CA had been extracted, corresponding to a concentration of 0.59 g/L in the filtrate. Although it is a poor recovery rate, experiments have been performed on this solution which contained enough CA to test the dilution process. The filtrate was divided in five samples of 2 mL which were diluted to 5, 7.5, 10, 12.5, and 15 wt.% C_4E_1 by addition of respectively 14, 8.66, 6, 4.2, and 3.32 mL of acidic water. According to the literature, the CAC of C_4E_1 is 0.83 mol/L[90], *i.e.* about 10 wt.%. Therefore, CA should be theoretically insoluble in the hydrotropic solution if there is less than 10 wt.% of hydrotropes, inducing its precipitation.

The aim of this experiment is to confirm the precipitation of CA and to evaluate the possibility to precipitate it selectively compared to the other co-products of extraction in order to increase the CA content. After each dilution, the solutions were filtered through 0.2 µm PTFE filters. The precipitates were diluted in 10 mL of ethanol and were analyzed by HPLC, as well as the filtrates.

As desired, when diluted to 5, 7.5 and 10 wt.% of hydrotrope, the major part of CA is recovered in the precipitate since only 2, 1 and 12 % of the total CA remain in the filtrate (**Figure II.24**). The maximum CA content in the precipitate (10 wt.%) is reached when the solution is diluted

to 7.5 wt.% (**Figure II.25**). On the contrary, when diluted at 12.5 and 15 wt.% C_4E_1, CA mostly remains in the filtrate because only 37 and 7 % of CA are recovered in the precipitate respectively (**Figure II.24**).

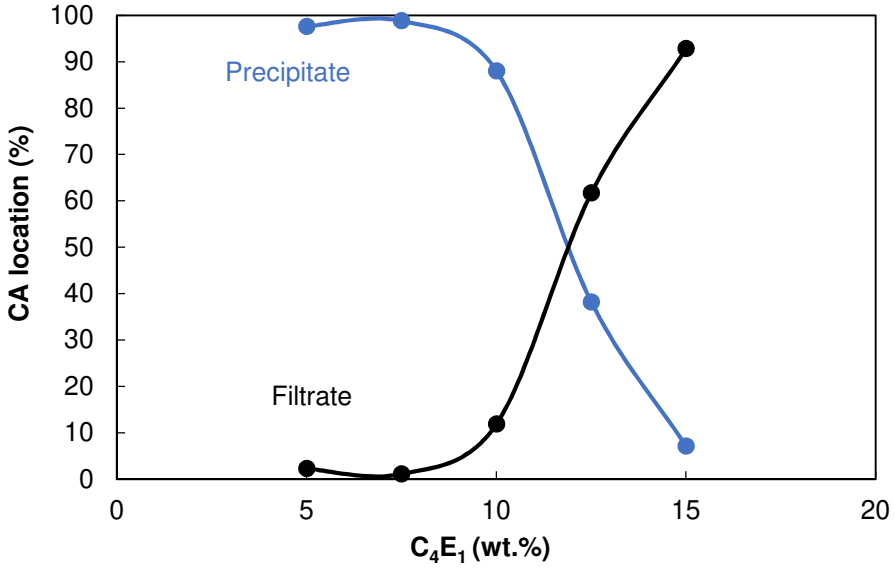

Figure II.24. Influence of the dilution factor on the distribution of CA between precipitate and filtrate after hydrotropic dilution with acidic water, represented by the final hydrotrope concentration.

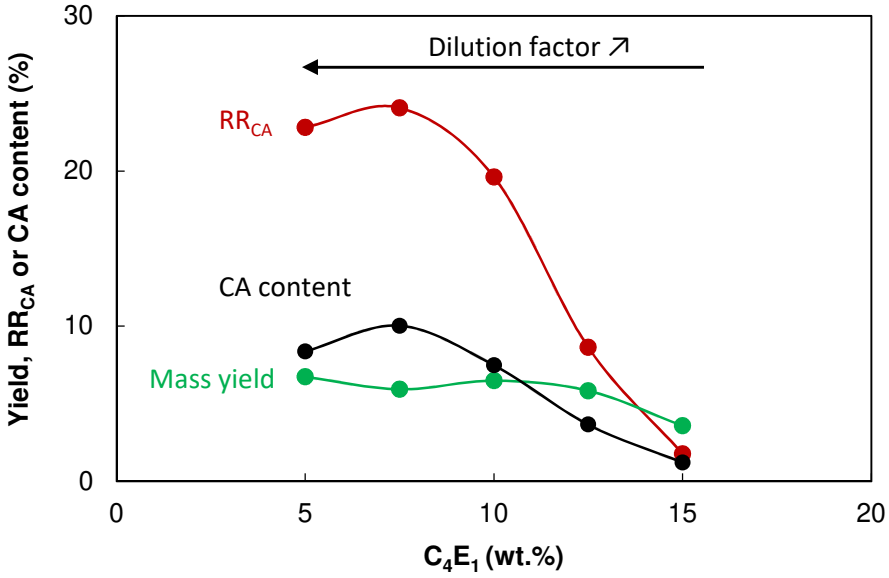

Figure II.25. Influence of the dilution factor during hydrotropic dilution with acidic water, represented by the final hydrotrope concentration, on the mass yield (green), CA recovery rate (red) and content (black) in the dry extract obtained after an extraction of rosemary using 40 wt.% C_4E_1 for 5 h.

While the dilution factor increases, the mass yield increases from 3.5 to 6.7 %, the CA recovery rate from 1.2 to 24 % and the CA content from 1.2 to 10 wt.%. Noteworthy, when diluted to 7.5 wt.%, all the CA extracted (24 % of the available CA in rosemary) is recovered in the precipitate. Moreover, no CA was oxidized or lost in the filtrate. This dilution process looks thus very efficient and attractive due to its easiness, with a practicable dilution (the total volume increased from 2 to 10.66 mL).

In addition, the fact that the low dilution (15 wt.% final C_4E_1) provided a precipitate with a mass yield of 3.5 % and only 1.2 wt.% CA, a purification of the extract through stepwise dilution and filtration may be possible, as presented in **Figure II.26**. Indeed, considering 100 g of hydrotropic extract concentrated at 40 wt.% C_4E_1, a dilution by a factor 2.66 would lead to a 15 wt.% concentrated solution (266 g) and the precipitation of 3.5 g of extract with 1 wt.% CA (35 mg CA). The residual filtrate would weight 263 g. A second dilution by a factor 2 would lead to 526 g of a 7.5 wt.% C_4E_1 solution, including a solid extract containing CA and co-products that can only precipitate at 7.5 wt.% but not at 15 wt.% C_4E_1. Among the 6.75 g which should precipitate in a one-step dilution, 3.5 have already been discarded, so only 3.25 g should precipitate. Since the 6.75 g should have been composed of 10 wt.% CA (675 mg), and 35 mg CA have already been lost in the first dilution step, then 640 mg CA should be recovered in the 3.25 g extract, corresponding to a CA content of about 20 wt.%, twice the amount that would be obtained by a direct one-step dilution to 7.5 wt.%. The initial amount of CA would thus be distributed as follows: 7 % in the first precipitate, 1 % in the second filtrate and 92 % in the second precipitate. This "thought" purification experiment may be transposable to other hydrotropic systems. We thus tried next to optimize the extraction step with other bio-based hydrotropes.

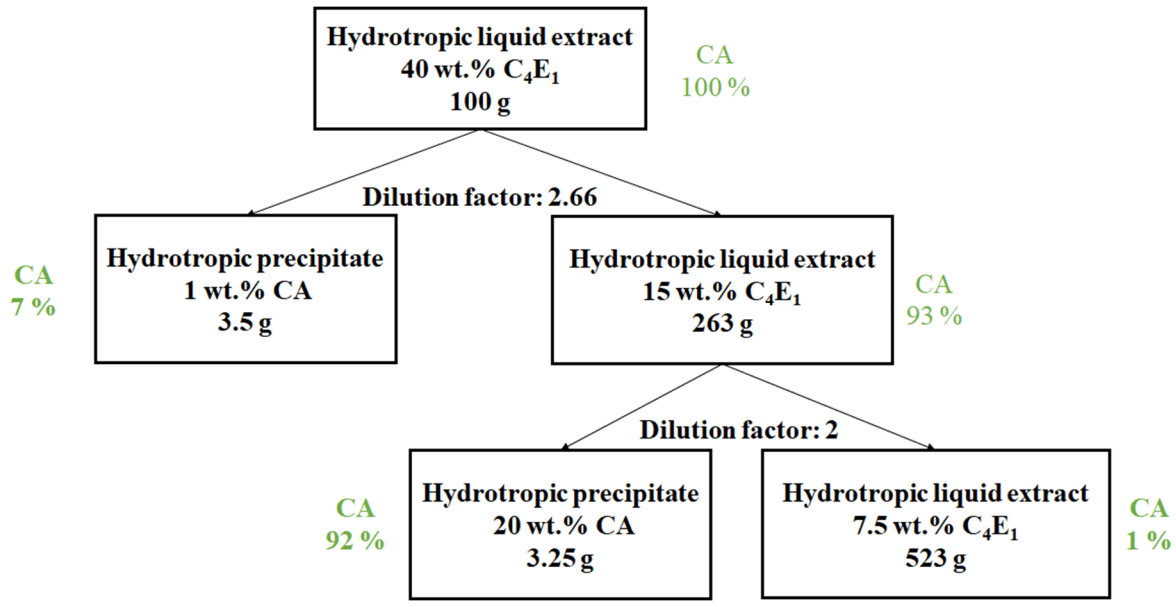

Figure II.26. Theoretical sequential dilution to 15 and 7.5 wt.% of a 40 wt.% C_4E_1 rosemary extract containing CA to increase the CA content in the extract.

II.6. Experimental part

II.6.1. Determination of the cloud point of C_iE_j aqueous solutions

Aqueous amphiphilic solutions were prepared with adequate concentration of CA and C_iE_j and 1 % (v/v) of phosphoric acid. In most cases, solutions were homogeneous at room temperature and were heated until clouding. Otherwise, solutions were cooled in an ice bath before this procedure. Same experiments were carried out with solutions containing additionally 2.5 g/L of CA. All the CP measurements were triplicated and reproducible within 0.2 °C.

II.6.2. Solubility curve of carnosic acid in C_4E_2 and SXS aqueous solutions.

Hydrotropic solutions of C_4E_2 and SXS were prepared at different concentrations and acidified with 1 % (v/v) of phosphoric acid (85 %) to avoid CA oxidation in water.[159] Solutions were added with 20-25 g/L of CA and continuously stirred for 24 h at room temperature. If not saturated, the solution was added with more solute to reach the saturation. The solution was then filtered using a syringe equipped with a PTFE filter (Φ = 0.2 µm). The amount of solubilized CA was determined by HPLC quantification.

II.6.3. Critical Aggregation Concentration (CAC) determination by tensiometry

Hydrotropic solutions of *i*-C_4E_1, C_4E_3, C_5E_2 and *i*-C_5E_2 were prepared at different concentrations in ultrapure water (ThermoFisher, 18.2 MΩ.cm). Their surface tensions were measured by a tensiometer K100 (Kruss) using a Wilhelmy plate at 25 °C. Triplicated measurements gave a standard deviation below 0.2 mN/m.

II.6.4. COSMO-RS calculations of the log *P* and V_m values

For all C_iE_j, molecular geometries were drawn on COSMO *Quick* (COSMOlogic) which was used to calculate the molecular volumes as well as the octanol-water partition coefficient (log *P*). This latter is predicted with a COSMO-RS method combined with a non-linear correction term using a Random Forest QSPR, and is valid only at 25 °C.

II.6.5. Hydrotropic extractions

a. Typical extractions with whole rosemary leaves

All the extractions were performed by macerating 1 g of rosemary leaves in 10 mL of an aqueous solution containing 30 wt.% of amphiphile and acidified with 1 % (v/v) of phosphoric acid (pH 2). The solutions were stirred at room temperature for 48 h with an Intelli-Mixer RM-2L rotator. For the kinetic study, 100 µL of solution were sampled at 30 min then every hour for 8 h and finally at 24 h. After 48 h, the solutions were separated from the plant by Büchner filtration under vacuum (cellulose filters, Φ = 8 µm). CA amount was quantified by HPLC and all experiments were performed twice.

b. Optimization of the hydrotropic extraction with C_4E_1

Extractions were performed by macerating 1 g or 250 mg of rosemary or sage leaves in 10 mL of an aqueous solution containing an adapted concentration of C_4E_1 and acidified with 1 % (v/v) of phosphoric acid (pH 2). The solutions were magnetically stirred in a thermostated bath at 25 or 40 °C for 24 h at 250 rpm. After 24 h, the solutions were separated from the plant by Büchner filtration under vacuum (cellulose filters, Φ = 8 µm). CA amount was quantified by HPLC and all experiments were performed twice.

c. Hydrotropic Cloud Point Extraction (HCPE) process

Extractions were performed by macerating 625 mg of rosemary leaves in 25 mL of an aqueous solution containing 40 wt.% C_4E_1 and acidified with 1 % (v/v) of phosphoric acid (pH 2). The solutions were magnetically stirred in a thermostated bath at 25 or 40 °C for 24 h at 200 rpm. After 24 h, the solutions were separated from the plant by Büchner filtration under vacuum (cellulose filters, Φ = 8 µm). Then, they were heated to 60 °C until complete phase separation (20 min) and the two phases were separated by Pasteur pipette. CA concentrations were quantified by HPLC before phase separation and in both phases after separation. The amount of C_4E_1 was quantified by ^{1}H NMR by comparison with the signal of residual water in the hydrotrope-rich phase. Finally, the hydrotrope-rich phase was evaporated under vacuum. The resulting extract was solubilized in methanol to quantify the CA and CAR contents by HPLC.

d. Recovery by dilution with water

Extractions were performed by macerating 2 g of rosemary leaves in 20 mL of an aqueous solution containing 40 wt.% C_4E_1 and acidified with 1 % (v/v) of phosphoric acid (pH 2). The solutions were magnetically stirred in a thermostated bath at 25 or 40 °C for 5 h at 400 rpm. Then, the solutions were separated from the plant by Büchner filtration under vacuum (cellulose filters, Φ = 8 µm) and the filtrate was separated in 5 samples of 2 mL. Those samples were diluted with the required amount of water acidified 1 % (v/v) of phosphoric acid (pH 2) and

then filtered through syringe filters (PTFE, Φ = 0.2 µm). The filters were freeze-dried and 10 mL of ethanol was passed through the filters, thus solubilizing CA. The amount of CA in ethanol was quantified by HPLC.

II.6.6. Microscopic observation of the plant material

To observe the cross section of the leaves, small slices of leaves had to be prepared by two close and cautious straight cuts perpendicular to the leaves using a razor blade. Then, to avoid the leaf to move, the small section was stuck on a microscope slide using a double-sided adhesive. Then, the cross section could be observed by a numeric microscope Keyence VHX-6000. The bottom side of the leaves could also be observed to see the trichomes of leaves and pictured by the microscope software.

II.7. Conclusions of Chapter II

In the past years, increasing attention has been focused on green extraction. Among different processes, aqueous hydrotropic extraction has the advantage of being safer than the use of flammable solvents, generating negligible atmospheric pollution, and requiring non-ATEX industrial equipment. In this chapter, we investigated the extraction of CA from rosemary using a series of alkyl polyethylene glycol ethers at ambient temperature. In a first time, the analysis of the solubility curve of CA in C_4E_2 aqueous solutions showed that C_4E_2 was able to provide an efficient solubilization of CA. Furthermore, the solubilization of CA, like other lipophilic molecules, lowered the CP of the C_iE_j. This effect seems to be more important with more lipophilic molecules and at lower C_iE_j concentrations, as reported for C_4E_1.

Moreover, the analysis of the extraction kinetics highlighted their evolution in three steps: washing, diffusion and a plateau. Considering both the kinetics and the amount of extracted CA by the different hydrotropes, we have shown that the C_iE_j should have preferentially *(i)* a small molecular volume (< 250 $Å^3$), *(ii)* a log *P* above 1, and *(iii)* a linear alkyl chain rather than a branched one to pass through the plant material. Among all the C_iE_j, C_5E_2 and C_4E_1 look the best ones as they provide 1.21 g/L of CA over 21 h and 1.02 g/L over 8 h respectively. They are more efficient than SXS, a conventional ionic hydrotrope, and than aqueous solutions of EtOH and PrOH at a same concentration. As far as aqueous solutions (at 30 wt.%) of SXS and EtOH are concerned, their low efficiency can be explained by the low solubility of CA, which can be a limiting factor of the extraction. Otherwise, the difference of efficiency must be explained by the diffusion of the amphiphiles and the mechanism of extraction. As far as the diffusion through the plant material is concerned, it is likely to be related to the structural and physicochemical characteristics of the amphiphiles.

On the basis of miscroscopic observations, a mechanism of the hydrotropic extraction can be proposed as follows: (1) Water penetrates into the dried leaves inducing their swelling and softening, (2) thanks to the softening, which provides a better accessibility of amphiphiles to the trichomes, hydrotropes diffuse into the trichomes area, (3) trichomes are degraded or cut through the action of hydrotropes, which certainly liberate the molecules, including CA, which are contained inside (**Figure II.27**). Since no structural changes were observed with pure solvents, it should be noted that this mechanism is particular to hydrotropic extraction, and that pure alcohols only use their ability to diffuse into the plant, which may be related to their small size. It is likely that some hydrotropes such as C_4E_1 extract CA by both phenomena, explaining the higher kinetics compared to pure solvent.

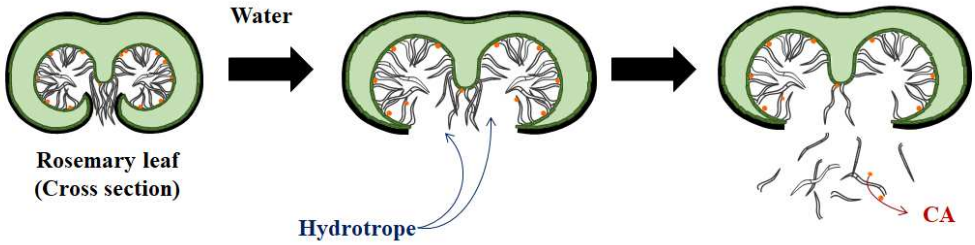

Figure II.27. Proposed mechanism of hydrotropic extraction of rosemary leaves in three steps: softening, diffusion of the hydrotropes into the plant, liberation of CA and other rosemary components with trichome clivage

Finally, concerning the recovery of CA, it can be performed by dilution below the MHC with water inducing its precipitation, as shown with C_4E_1.[103] A sequential dilution could also potentially provide a purer solid extract. Using this method, the hydrotropic solution can then be recycled by removing a part of water to adjust the hydrotrope concentration, or playing with the CP temperature to separate the hydrotrope.[121] Another way to recover CA and recycle the hydrotrope in the same time would be to take advantage of the CP by separating the phase constituted of the hydrotrope and the solute formed after gentle heating, then distilling the hydrotrope (or the solute) under vacuum if volatile enough. That consists in the HCPE process.[94] However, this method was not suited for CA since it was thermodegraded into CAR.

Alkyl polyethylene glycol ethers are currently mostly petro-sourced molecules, but could be, in a longer term, produced by bio-based precursors. However, in the following chapters, we will take advantage of these first results to study non-ionic hydrotropes such as alkyl monoglycerols or alkyl polyglycosides, which are currently or could be, in the near future, commercialized as bio-sourced molecules, and may be more biocompatible.

Chapter III. Hydrotropic extraction with sugar and glycerol-based hydrotropes

In **chapter II**, we have shown that short-chain alkyl polyethylene glycol ethers (C_iE_j) are particularly efficient for the extraction of CA from rosemary providing a competitive aqueous hydrotropic extraction compared to alcoholic or micellar ones.[188] Noteworthy, nonionic hydrotropes have demonstrated a better efficiency in that case compared to ionic hydrotropes such as sodium xylene sulfonate, despite these latter are used in most of the reported hydrotropic extractions.[37,83,189]

This chapter focuses on CA extraction using sugar and glycerol-based hydrotropes. Indeed, as shown in **chapter I**, those hydrotropes can be derived from biomass, they do not emit VOC, and sugar-based hydrotropes are highly biodegradable which make them interesting as an alternative to solvents, or, among hydrotropes, to C_iE_j. For that purpose, five commercial alkyl polyglycosides (C_iGlyco) and three synthetic alkyl glycerols were used: **butyl glucoside (C_4Glu)**, ***iso*-amyl polyxyloside (*i*-C_5Xyl)**, **heptyl (C_7Glu)** and **ethylhexyl ($C_{6,2}Glu$) polyglucosides**, **caprylyl-capryl polyglycoside ($C_{8/10}Glyco$)**, **butyl (C_4Gly)**, ***iso*-amyl (*i*-C_5Gly)** and **pentyl (C_5Gly) glycerol ethers**. Their ability to solubilize and extract CA from rosemary and sage leaves is discussed.

First, special attention was given to physicochemical properties of those amphiphiles and their solubilizing power. Then, the molecular model established for C_iE_j was tested and validated for these bio-sourced hydrotropes. Finally, the extraction was optimized through an experimental design approach aimed at finding the extraction conditions that maximize the concentration of extracted CA, the extraction yield, and the final CA content in the dry extract. In particular, the influence of temperature, hydrotropic concentration, stirring speed and time of extraction were evaluated, providing an efficient process to extract CA with *i*-C_5Xyl hydrotrope.

III.1. Structure and properties of sugar and glycerol-based amphiphiles

III.1.1. Physicochemical characterizations of alkyl monoglycerol and polyglycosides

a. Short-chain alkyl polyglycosides as commercial complex mixtures

Alkyl glycosides are commercially available bio-sourced amphiphiles, which makes them very interesting for industrial applications. Indeed, their production from wheat bran or poplar has already been developed at a large scale.[130] However, unlike C_iE_j, which have allowed to establish a relationship between the efficiency of the hydrotrope and some key parameters, thanks to their well-defined structure, commercial C_iGlyco are complex mixtures. Therefore,

in order to transpose the model established for C_iE_j on C_iGlyco, their composition has been investigated.

First, to prepare C_iGlyco solutions at a precise concentration, the amount of active ingredient in the commercial solutions has to be quantified. Indeed, for convenience, industrials commercialize C_iGlyco in liquid aqueous solutions containing 30-40 wt.% water. The precise amount of water was determined by thermogravimetric analysis (TGA), as presented in **Figure III.1**, and the precise amphiphile content was calculated assuming that the solutions only consist of water and C_iGlyco. During the experiments, the commercial mixtures were heated under nitrogen at 10 °C/min from 30 to 500 °C. At 140 °C, all the water is evaporated but the hydrotrope is still in its original form. The following contents were thus measured: 62.7, 65.8, 78.9, 67.2, 66.9 wt.% for C_4Glu, *i*-C_5Xyl, C_7Glu, $C_{6,-2}Glu$ and $C_{8/10}Glyco$ respectively.

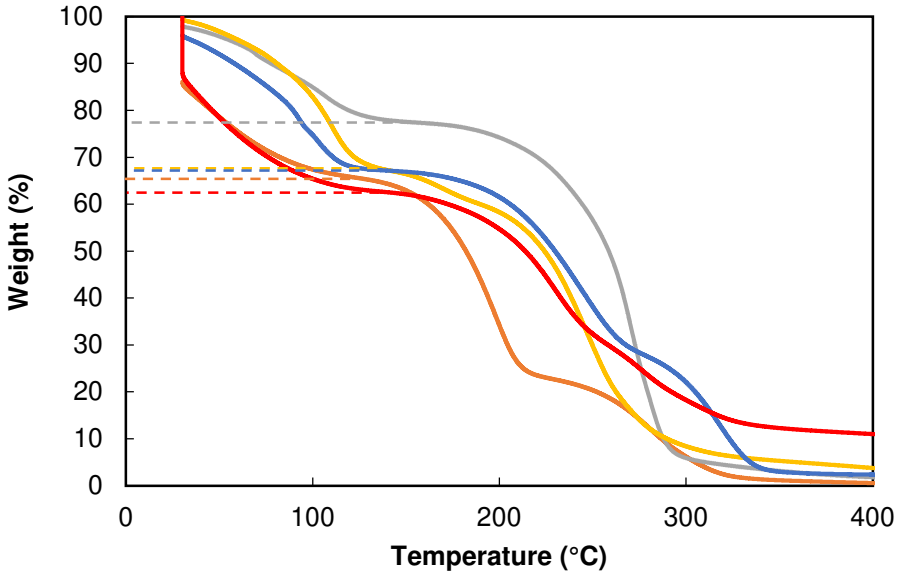

Figure III.1. Thermogravimetric analysis (TGA) of C_4Glu (red), *i*-C_5Xyl (orange), C_7Glu (grey), $C_{6,-2}Glu$ (yellow), $C_{8/10}Glyco$ (blue)

Then, the composition of the glycoside part was examined through two mass spectroscopy analyses:

- a FIA-HRMS (Flow Injection Analysis – High Resolution Mass Spectrometry) analysis was performed to detect all the compounds without separating them, using an ESI (Electron Spray Ionisation) source in negative mode.
- a LC-MS (Liquid Chromatography – Mass Spectrometry) analysis was also performed to separate molecules according to their polarities.

These analyses were only performed on one alkyl polypentoside (*i*-C_5Xyl), one alkyl polyglucoside (C_7Glu) and one alkyl polyglycoside, which is composed of some alkyl polyglucoside and some alkyl polypentoside ($C_{8/10}Glyco$).

The typical mass spectrum in negative ion mode of the commercial *i*-C_5Xyl is presented in **Figure III.2**. The molar mass of *iso*-amyl monoxyloside (*i*-C_5Xyl_1) is 220 g/mol. Therefore, the ion at *m/z* 265 corresponds to *i*-C_5Xyl_1 in its $[M+FA-H]^-$ form, with M the molecule analysed, FA, the mass of the formic acid (46 g/mol) and H the mass of the proton. Since the molar mass of *i*-C_5Xyl increases by 132 g/mol for each xylose unit added, the ions at *m/z* 397, 529 and 661 correspond to *iso*-amyl di-, tri- and tetra-xyloside respectively. The *i*-C_5Xyl_5 and *i*-C_5Xyl_6 are also part of the commercial mixture since their corresponding ions at *m/z* 793 and 925 are shown in the HRMS spectrum with low relative intensities (1.78 and 0.46 % respectively). Therefore, Appyclean 6505, the commercial form of *i*-C_5Xyl, is composed of molecules of *iso*-amyl polyxyloside with a degree of polymerisation (DP) ranging from 1 to 6.

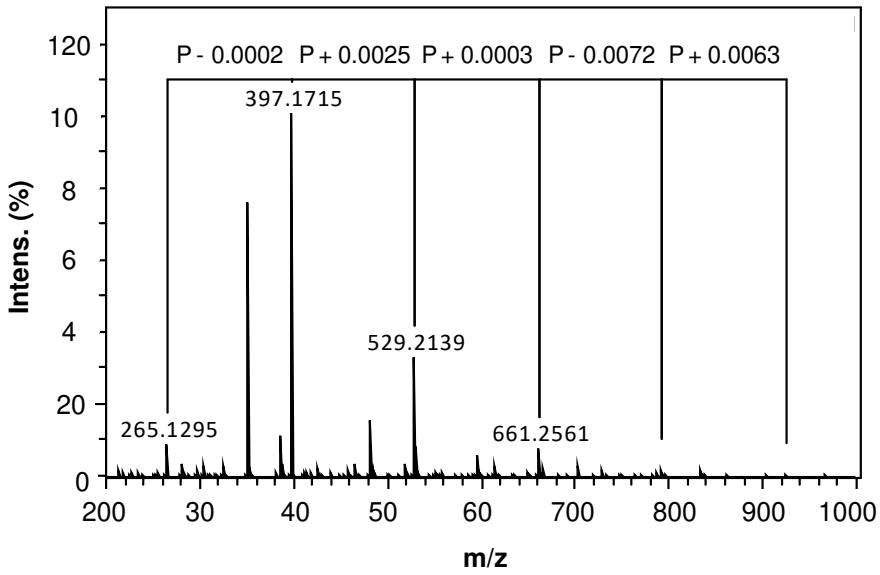

Figure III.2. High Resolution Mass Spectra of Appyclean 6505 (commercial *i*-C_5Xyl mixture) obtained by Flow Injection Analysis in negative ionization mode. The above annotation "P" corresponds to the addition of one pentose unit.

In addition, a liquid chromatography separated all the components of the commercial solutions. The MS-chromatograms of the ions at *m/z* 265.130 (*i*-C_5Xyl_1), 397.172 (*i*-C_5Xyl_2), 529.214 (*i*-C_5Xyl_3), 661.256 (*i*-C_5Xyl_4) and 793.294 (*i*-C_5Xyl_5) with an error of 0.005 are presented in **Figure III.3**. At least two different compounds can be identified as *i*-C_5Xyl_1 and four as *i*-C_5Xyl_2. Moreover, many isomers of *i*-C_5Xyl_3, *i*-C_5Xyl_4 and *i*-C_5Xyl_5 are observed without a sufficient separation to be counted. This is explained by the formation of different regioisomers while adding one xylose unit on another and by the fact that each *iso*-amyl mono or polyxyloside is a complex mixture of α/β-anomers and pyranoside/furanoside isomers,[130] inducing an inevitably increase of the variability with the number xylose units. Thanks to this variability, two isomers can have different lipophilicities, as confirmed by a different retention time in the LC column. Noteworthy, the response factors can vary from one molecule to another, so this analysis cannot be quantitative.

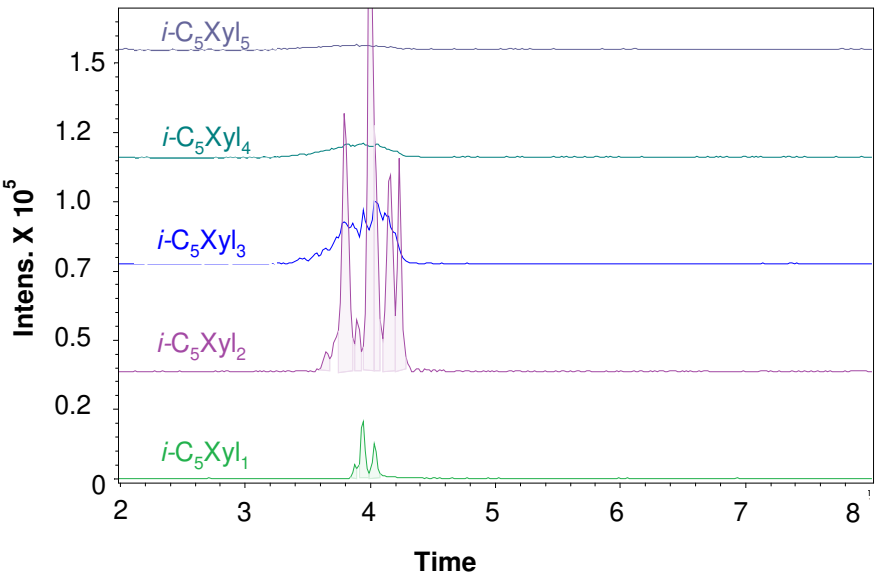

Figure III.3. LC-MS chromatogram of Appyclean 6505 (commercial *i*-C_5Xyl mixture) for the *m/z* 265.130 (*i*-C_5Xyl_1), 397.172 (*i*-C_5Xyl_2), 529.214 (*i*-C_5Xyl_3), 661.256 (*i*-C_5Xyl_4) and 793.298 (*i*-C_5Xyl_5).

Finally, to measure the average DP, a ^{1}H NMR analysis of the freeze-dried solution was performed in D_2O. In such solvent, the dissociation of the OH bonds and their exchange with D_2O is highly probable. Since the quantity of D_2O is in excess, the part of residual OH bonds compared to OD bonds is negligible (**Figure III.4**). From these affirmations, it is possible to compare the number of protons in the alkyl chain and in the xylose part on the ^{1}H NMR spectrum (**Figure III.5**).

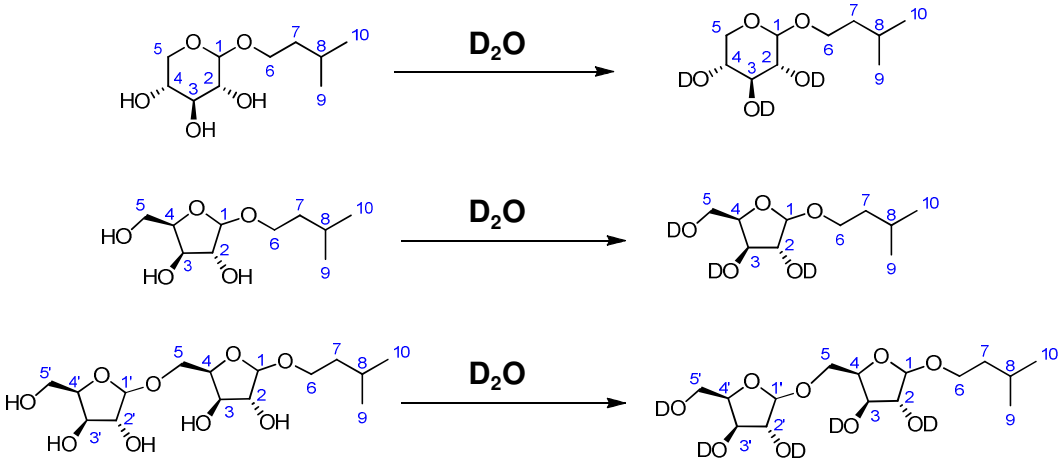

Figure III.4. Transformation of OH bonds in OD bonds of sugars in three examples of *i*-C_5Xyl molecules. From top to bottom, *iso*-amyl xylopyranoside, *iso*-amyl xylofuranoside, *iso*-amyl di-xylofuranoside, carbon numbers indicated in blue.

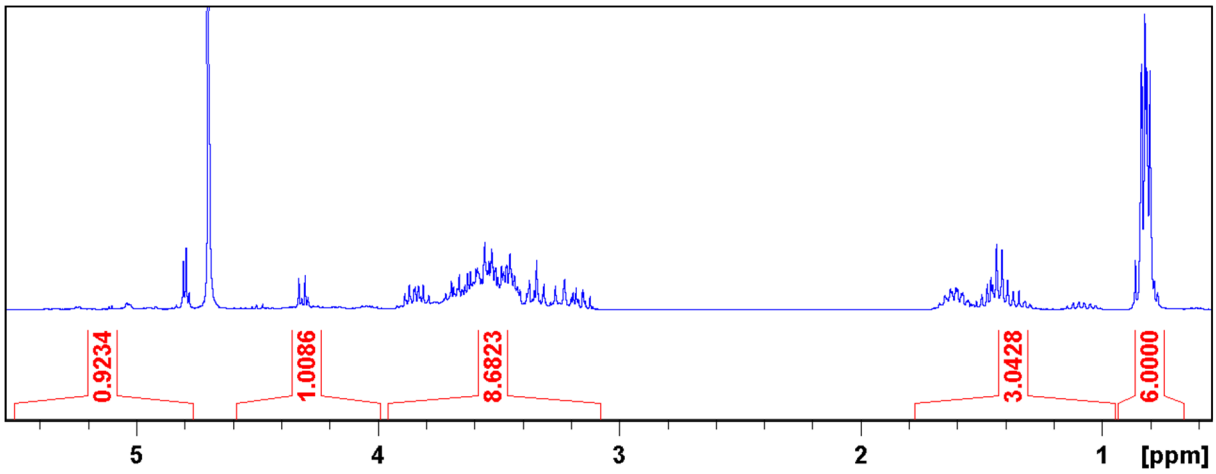

Figure III.5. ^{1}H NMR spectrum of Appyclean 6505 (commercial *i*-C_5Xyl mixture) in D_2O

Indeed, at 0.81 ppm, a signal corresponds to the CH_3 protons, accounting for six protons. Between 1 and 1.9 ppm, the signals correspond to protons on carbons 7 and 8 as confirmed by the integration for 3 protons. At 4.7 ppm, the signal corresponds to H_2O or HDO, which are formed from the exchange between OH and D_2O. Between 4.8 and 5.5 ppm, several small signals correspond to anomeric protons on carbons 1 and 1', depending on the anomer form and on the compound. However, they are confounded with the baseline, so they were not taken into account in the calculation of the average DP. Signals from 3 to 4.6 ppm correspond to the protons on carbons 2, 3, 4, 5 and 6, that is, 2 protons of the alkyl chain (carbon 6) and 5 protons for each xylose unit. In that case, there are 9.68 protons in this section. Thus, according to **Eq.III.1**, the average DP is 1.54.

$$DP = \frac{\text{protons from 3 to 4.6 ppm - 2}}{\text{protons in one xylose unit}} = \frac{1 + 8.68 - 2}{5} = 1.54 \qquad \text{(III.1)}$$

Concerning Sepiclear G7, the commercial form of C_7Glu, its DP ranges from 1 to 7 according to its spectrum in negative ion mode (**Figure III.6**). Indeed, the ions at *m/z* 323, 485, 647, 809, 971, 1133 $[M+FA-H]^-$, correspond to C_7Glu_1, C_7Glu_2, C_7Glu_3, C_7Glu_4, C_7Glu_5, C_7Glu_6 and C_7Glu_7 respectively (**Figure III.6**). According to the LC-MS, at least two isomers of C_7Glu_1 are detected but one seems to be highly predominant. At least five isomers of C_7Glu_2 and at least 13 isomers of C_7Glu_3 are detected. Again, the variability increases with the DP (**Figure III.7**).

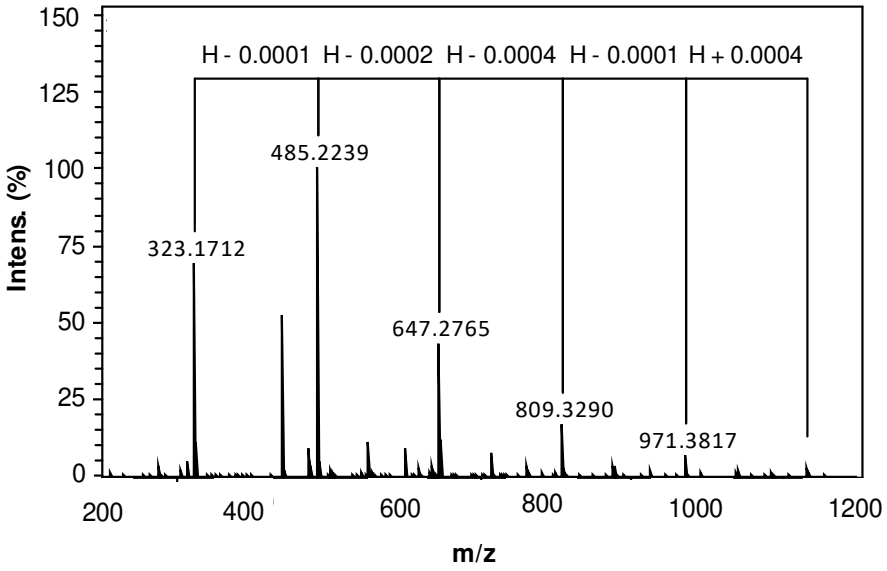

Figure III.6. High Resolution Mass Spectra of the Sepiclear G7 (commercial C_7Glu mixture) obtained by Flow Injection Analysis in negative ionization mode

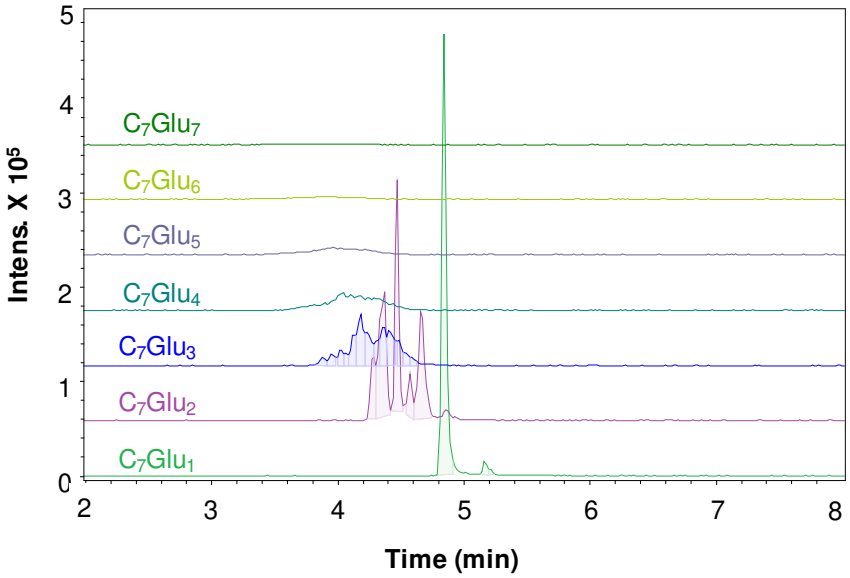

Figure III.7. LC-MS chromatogram of Sepiclear G7 (commercial C_7Glu mixture) for the *m/z* 323.171 (C_7Glu_1), 485.224 (C_7Glu_2), 647.279 (C_7Glu_3), 809.330 (C_7Glu_4), 971.382 (C_7Glu_5), 1133.435 (C_7Glu_6) and 1295.488 (C_7Glu_7), each m/z with an error of 0.005.

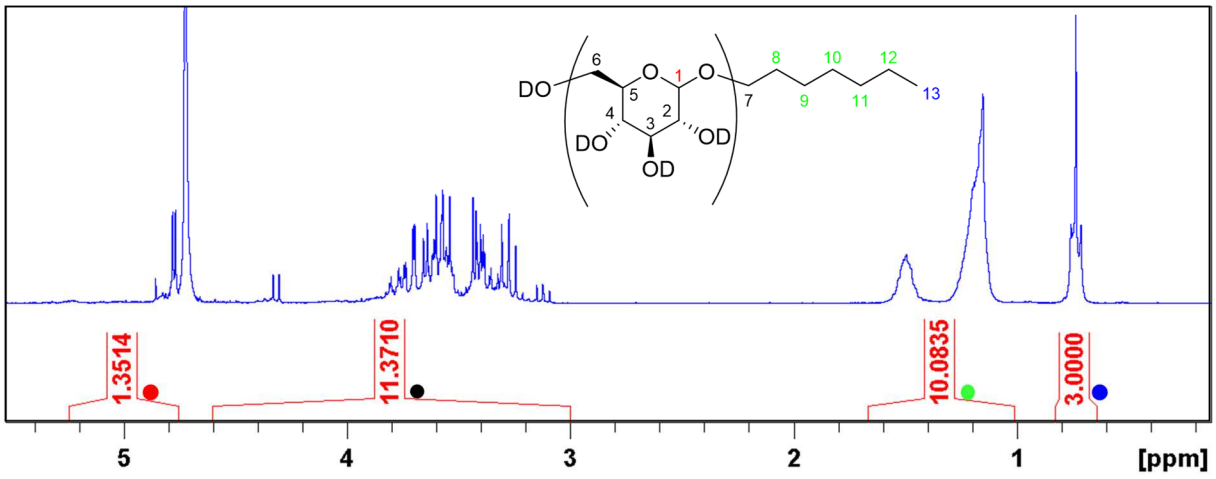

Figure III.8. ^{1}H NMR spectrum of Sepiclear G7 (commercial C_7Glu) in D_2O with integrals

As performed for *i*-C_5Xyl, the ^{1}H NMR analysis of the C_7Glu mixture in D_2O was performed to calculate its average DP (**Figure III.8**). Signals are attributed according to the colors:

- Blue / CH_3 protons on carbon 13 / 0.75 ppm
- Green / protons on carbons 8 to 12 / from 1 to 1.6 ppm
- Black / protons on carbons 2 to 6 (glucose) and carbon 7 (aliphatic part) / from 3 to 4.6 ppm
- Red / anomeric proton (carbon 1) / from 4.76 to 5.25 ppm

The average DP was found to be 1.56 according to **Eq.III.2**, which is similar to **Eq.III.1**. The same operation was performed for C_4Glu and $C_{6,-2}$Glu, leading to DP of 1.96 and 2.10 respectively (Spectra in **Appendixes 6 and 7**).

$$DP = \frac{\text{protons from 3 to 4.6 ppm - 2}}{\text{protons in one glucose unit}} \quad \text{(III.2)}$$

Finally, regarding $C_{8/10}$Glyco, the FIA-HRMS analysis shows as expected that the commercial solution is composed of a huge number of molecules (**Figure III.9**). Indeed, molecules can first be divided in two categories: octyl and decyl derivatives. Corresponding ions are indicated in the mass spectrum in blue and red respectively. Among the detected ions, the two lowest *m/z* 337 and 365 correspond to C_8Glu_1 and $C_{10}Glu_1$ $[M+FA-H]^-$ respectively. The other compounds are detected adding the mass of a pentose (noted P) such as xylose or arabinose or a hexose (noted H), corresponding here to a glucose. This way, a total of 16 compounds are indicated on the figure: C_8Glu_1, $C_8Glu_1Pent_1$, $C_8Glu_1Pent_2$, $C_8Glu_1Pent_3$, C_8Glu_2, $C_8Glu_2Pent_1$, C_8Glu_3, $C_8Glu_3Pent_1$ (in blue), $C_{10}Glu_1$, $C_{10}Glu_1Pent_1$, $C_{10}Glu_1Pent_2$, $C_{10}Glu_2$, $C_{10}Glu_2Pent_1$, $C_{10}Glu_3$, $C_{10}Glu_3Pent_1$, $C_{10}Glu_4$ (in red).

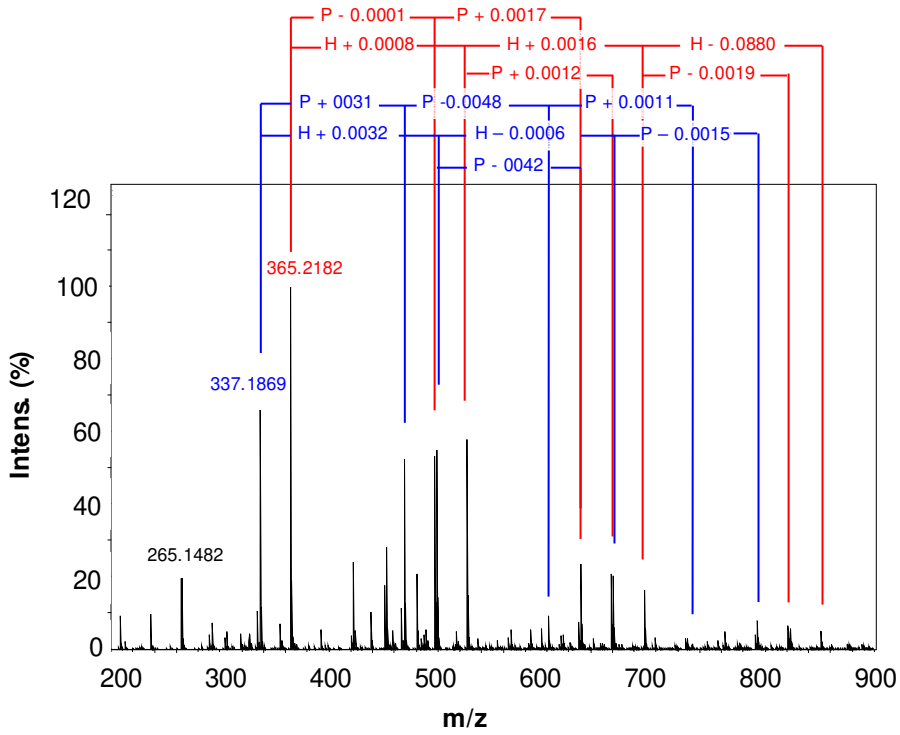

Figure III.9. High Resolution Mass Spectra of the Appyclean 6781 (commercial $C_{8/10}$Glyco mixture) obtained by Flow Injection Analysis in negative ionization mode

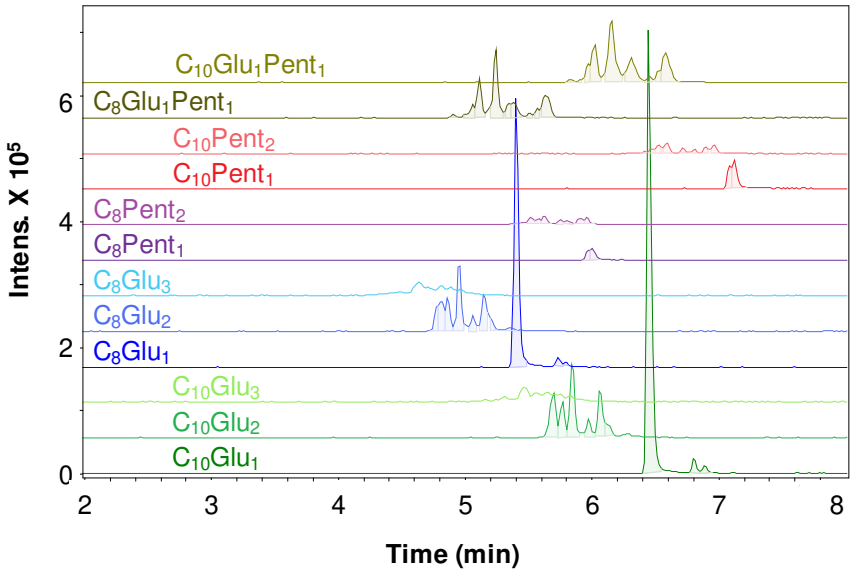

Figure III.10. LC-MS chromatogram of Appyclean 6781 (commercial $C_{8/10}$Glyco mixture) for the *m/z* (from top to bottom) 497.260 ($C_{10}Glu_1Pent_1$), 469.229 ($C_8Glu_1Pent_1$), 467.250 ($C_{10}Pent_2$), 335.208 ($C_{10}Pent_1$), 439.218 (C_8Pent_2), 307.176 (C_8Pent_1), 661.292 (C_8Glu_3), 499.240 (C_8Glu_2), 689.324 ($C_{10}Glu_3$), 527.270 ($C_{10}Glu_2$), 365.218 ($C_{10}Glu_1$),

The LC-MS confirms a huge variability of polarities and compounds (**Figure III.10**). This variability is higher than for Appyclean 6505 and Sepiclear G7 but the general conclusions are the same: the variability increases with the DP and for DP = 1, only two isomers are present, including one predominant. Noteworthy, C_8Glu_1 and $C_{10}Glu_1$ seem to be more concentrated than C_8Pent_1 and $C_{10}Pent_1$. If the response factor was the same for all the compounds, a ratio 70/30 of glucose/xylose could be calculated from the areas of the LC-MS chromatograms. However, this cannot be a precise quantification since the response factor generally depends on the molecule.

The ^{1}H NMR spectrum gives more information about the C_8/C_{10} ratio (**Figure III.11**). Indeed, when the signal at 0.8 ppm is calibrated for 3 protons, the signal at 1.11 ppm should be integrated for 10 protons in a C_8Glyco molecule and 12 protons in a C_{10}Glyco molecule. The experimental integration of the signal gives a value of 11.1 protons, indicating that 55 % of the molecules are decyl glycosides. Concerning the sugar polar head, the calculation is more complicated than previously, because the ratio hexose/pentose is not precisely quantified. If all the molecules were only composed of pentoses, the average DP would be 1.77 (using **Eq.III.1**), and on the contrary, if they were only composed of hexoses, the average DP would be of 1.47. Therefore, the average DP is obviously between 1.47 and 1.77 and depends on the hexose/pentose ratio. Even if the value is not precise, the ratio 70/30 calculated from LC-MS was used to estimate the average DP, resulting in a value of 1.55.

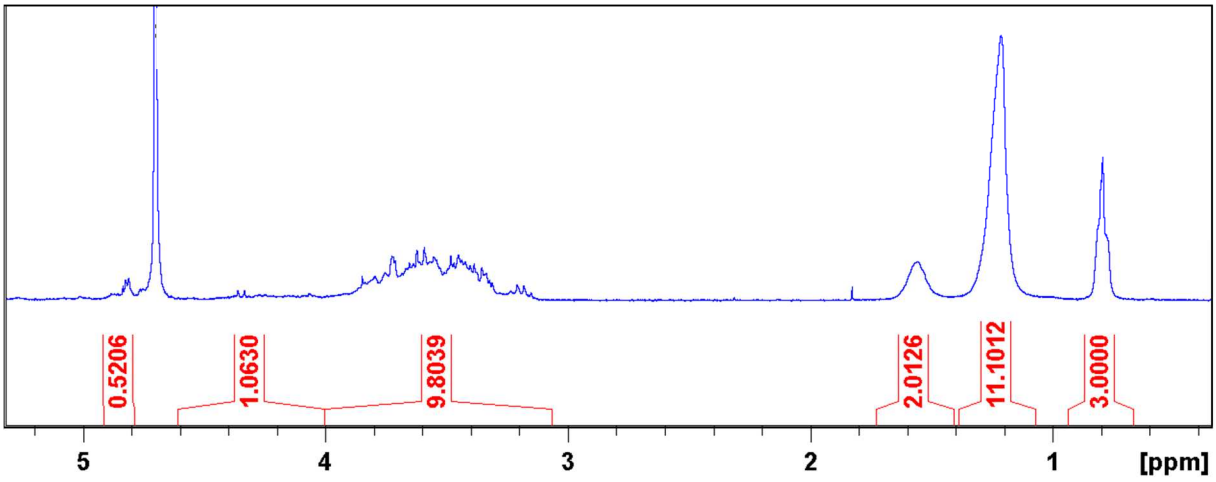

Figure III.11. ^{1}H NMR spectrum of Appyclean 6781 (commercial $C_{8/10}$Glyco mixture) in D_2O

Therefore, in the C_iGlyco series, *i*-C_5Xyl is the hydrotrope with the shortest alkyl chain, followed by $C_{8/10}$ Glyco, C_7Glu, C_4Glu and $C_{6,-2}$Glu. Indeed, during the process of C_iGlyco synthesis, the Fisher glycosylation of one sugar on another occurs more likely on a hexose than a pentose because of their conformation, according to Estrine et al.[130] Alkyl polypentosides such as *i*-C_5Xyl have thus generally a lower degree of polymerization (DP) than alkyl polyhexosides, leading to a lower molecular volume and hydrophilicity.[190,191]

b. Short-chain alkyl monoglycerols as pure synthetic bio-based hydrotropes

As far as alkyl glycerols are concerned, no large scale commercial source exists so far. Therefore, butyl, pentyl and *iso*-amyl monoglycerol ethers were synthesized in pure form at the laboratory scale. In the following document, they will be referred to as C_4, C_5, and *i*-C_5Gly.

Monoalkyl glycerol ethers C_iGly can be synthesized by a "green" approach in a one-step catalytic reductive alkylation of glycerol with an appropriate aldehyde (**Figure III.12**), carboxylic acid or ester, making them potentially bio-sourced molecules.[192,193]

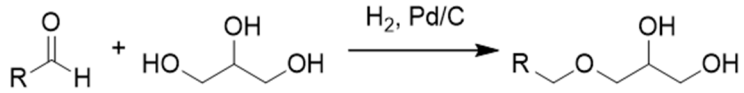

Figure III.12. Synthetic way of C_iGly through reductive alkylation (yield: 94 %, selectivity: 25/1)[192]

However, for the sake of convenience, alkyl glycerol ethers were synthesized by opening their corresponding epoxide with water under heating. Indeed, butyl glycidyl ether is commercially available, making the synthesis of C_4Gly very easy. For the other alkyl glycerol ether, their corresponding epoxide were synthesized in two steps from their corresponding alcohol and epichlorydrin, as previously reported.[94] The whole process of synthesis is reported in **Figure III.13**.

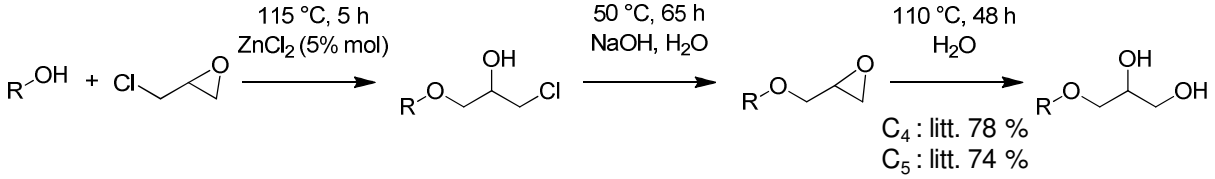

Figure III.13. Synthetic way of C_iGly through epoxide opening. Yields for C_4Gly and C_5Gly from ref[94]

c. Polarity, amphiphilicity and size of the molecules

Thanks to the knowledge of the precise structure of each alkyl glycoside and glycerol, their polarity, their amphiphilicity (HLB) and their molecular volume (V_m) can be predicted as previously for C_iE_j. HLB was calculated according to Griffin's equation[171] (**Eq.II.2**, section II.2.2) whereas log *P* and V_m were predicted with the COSMO-RS method. Since the DP of C_4Glu, *i*-C_5Xyl, and C_7Glu is comprised between 1 and 2, the values of log *P*, HLB and molecular volume (V_m) of the mixture were estimated as the weight average of the predicted values obtained for the corresponding alkyl mono- and di-glycoside. Similar prediction was performed for $C_{6,-2}$Glu using alkyl di- and tri-glucoside, and for $C_{8/10}$Glyco using C_8Glu_1 (14.2 %), C_8Glu_2 (17.3 %), $C_{10}Glu_1$ (17.3 %), $C_{10}Glu_2$ (21.2 %), C_8Xyl_1 (6.1 %), C_8Xyl_2 (7.4 %), $C_{10}Xyl_1$ (7.4 %), $C_{10}Xyl_2$ (9.1 %). This composition does not fully represent the one of the $C_{8/10}$Glyco mixture since no C_iGluPent neither C_iGlu_3 is found, but it gives a realistic average

DP, glucose/xylose ratio and C_8/C_{10} ratio, with a minimum set of molecules. The predicted values, as well as the molar mass are reported in **Appendixes 8 and 9** for each individual molecule, and the average values corresponding to the mixture are reported in **Table III.1**.

Noteworthy, in the glycoside series, log *P* increases, whereas HLB globally decreases with increasing the alkyl chain length '*i*'. It can be found an anomaly in the fact that the HLB of C_7Glu is lower than that of $C_{6,-2}$Glu (and log *P* C_7Glu > $C_{6,-2}$Glu). However, this can be explained by a higher DP of $C_{6,-2}$Glu, which thus becomes more hydrophilic. Moreover, the DP has a strong influence on M and V_m. Within the C_iGly series, only the log *P* differentiates the C_5Gly isomers. They seem to have a similar polarity compared to $C_{8/10}$Glyco, a higher lipophilicity compared to all alkyl glycosides (lower HLB), as well as lower M and V_m.

Table III.1. Predicted physicochemical descriptors of alkyl glycosides and alkyl glycerols

	DP[a]	M [b] (g/mol)	V_m [b, c] (Å^3)	log *P* [b, c]	HLB [b, d]
Alkyl glycosides					
C_4Glu	1.96	393	433	-1.54	17.0
i-C_5Xyl	1.54	292	335	-0.41	14.8
C_7Glu	1.56	370	430	0.46	14.3
$C_{6,-2}$Glu	2.10	472	539	0.24	15.1
$C_{8/10}$Glyco	1.55	384	457	1.73	13.0
Alkyl glycerols					
C_4Gly	1	148	196	1.23	12.3
C_5Gly	1	160	217	1.77	11.4
i-C_5Gly	1	160	218	1.67	11.4

[a] see section I.1.1.a and b; [b] Average values taking into account DP; [c] From Cosmo-*Quick*®, with a calculation based on the COSMO-RS method and refined with real values of similar molecules; [d] Calculated according to Griffin's relation

d. Surface activity and aggregation properties

The Critical Aggregation Concentration (CAC) is an important physicochemical property of amphiphiles, which can be experimentally measured by plotting the surface tension evolution against the amphiphile concentration. CAC and surface tension at the CAC (σ_{CAC}) have already been reported for C_4Gly, C_5Gly, *i*-C_5Gly[90], for the commercial form of C_4Glu[194], and have been measured here for the missing *i*-C_5Xyl, C_7Glu, $C_{6,-2}$Glu and $C_{8/10}$Glyco, as reported in **Figure III.14**. All the values are summarized in **Table III.2**.

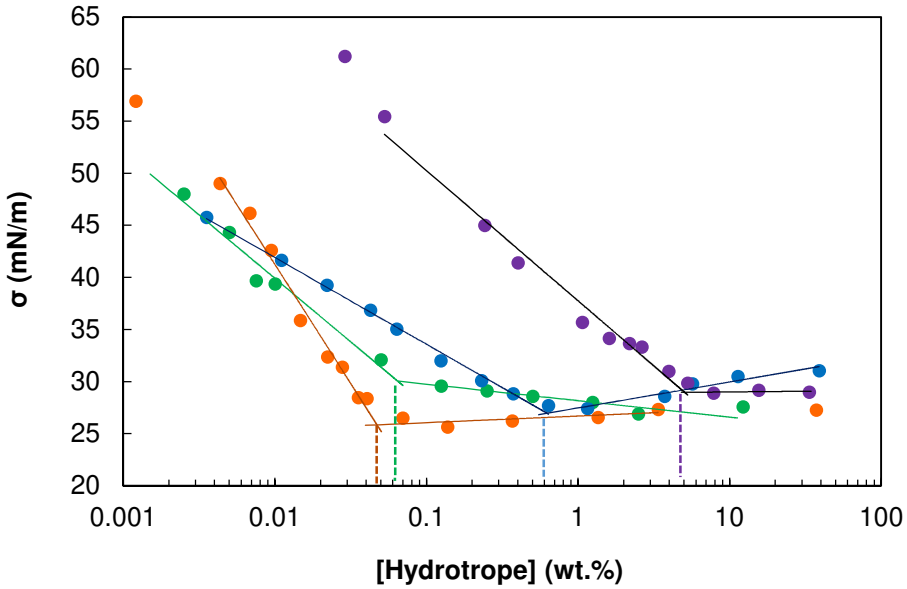

Figure III.14. Evolution of the surface tension (σ) with the amphiphile concentration for $C_{8/10}$Glyco (orange), $C_{6,-2}$Glu (green), C_7Glu (blue) and *i*-C_5Xyl (purple).

Table III.2. CAC and MHC of CiGlyco and CiGly measured by tensiometry and from the solubility curves of CA respectively. All experiments were performed at 25 °C, pH 2.

Abbreviation	CAC		σ_{CAC}	MHC
	wt.%	mol/L	(mN/m)	wt.%
Alkyl glycosides				
C_4Glu [194]	11.5	0.29	33	43*
i-C_5Xyl	5.5	0.19	28.9	9.0
C_7Glu	0.6	0.016	27.4	2.8
$C_{6,-2}$Glu	0.06	1.3×10^{-3}	26.9	1.7
$C_{8/10}$Glyco	0.05	1.3×10^{-3}	25.7	0.4
Alkyl glycerols				
C_4Gly	8.9	0.6 [90]	28.6 [90]	14
C_5Gly	2.4	0.15 [90]	25.3 [90]	4.8*[96]
i-C_5Gly	5.8	0.36 [90]	23.9 [90]	6.1*

* MHC obtained from the solubility curve of DR-13

The CAC are ranged in the following order: $C_{8/10}$Glyco < $C_{6,-2}$Glu < C_7Glu < C_5Gly < *i*-C_5Xyl ≈ *i*-C_5Gly < C_4Gly ≈ C_4Glu. Indeed, as already reported for linear ethoxylates with alkyl chains from 4 to 16 carbons,[195] alkyl erythritol and pentaerythritol with linear alkyl chains from 5 to

12 and 10 respectively,[96] the log(CAC) or log(CMC) linearly decreases with increasing *i* (**Figure III.15**). Furthermore and as expected, the minimal surface tensions decrease with increasing *i*, for both alkyl glycerols and glycosides. Finally, with an equivalent alkyl chain (C_4 and *i*-C_5), the alkyl glycerols seem more surface active than alkyl glycosides despite the fact that their polar head seem to have almost no effect on the CAC.

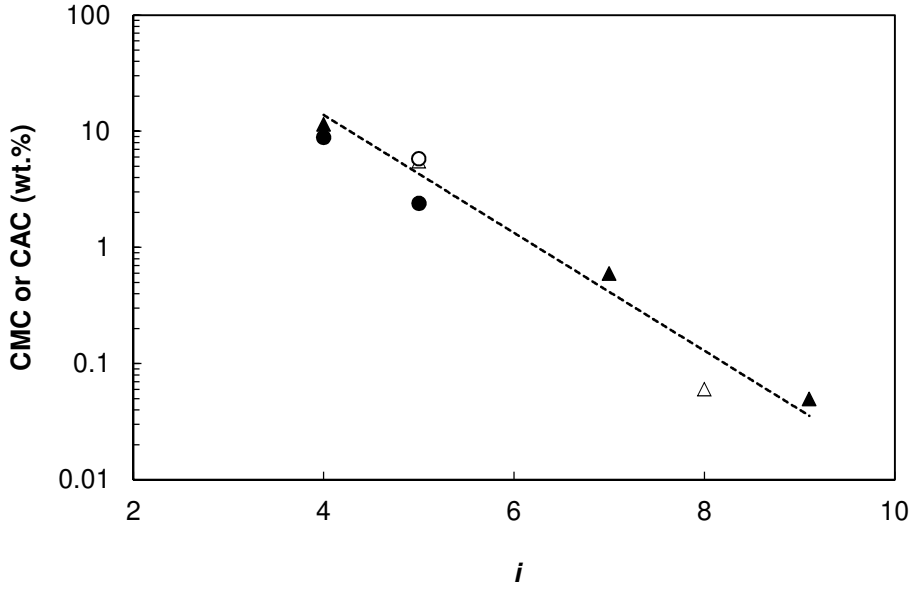

Figure III.15. Evolution of the CAC or CMC with the alkyl chain length (*i*). C_iGlyco (▲/△) and C_iGly (●/○), full symbols for linear alkyl chain (C_4, C_5, C_7, $C_{8/10}$) and empty symbols for branched alkyl chain by (*i*-C_5, $C_{6,-2}$)

III.1.2. Hydrotropic solubilization of phytochemicals

In view of extracting CA from rosemary, and because the intrinsic properties of amphiphiles do not provide any information on the phytochemical-amphiphile interactions, the solubility of CA in C_iGlyco and C_iGly solutions has been studied. In **Chapter II**, we have shown that an aqueous solution of C_4E_2 could solubilize more than 25 g/L of CA (above 30 wt.%), and that all the aqueous solutions of C_iE_j (30 wt.%) could solubilize at least 2.5 g/L of CA, the minimum concentration required to prevent the extraction from being limited by the solubility of CA. Interestingly, this solubilization induced a decrease in CP, and thus, in some cases, a phase separation. C_iE_j were also found to be more efficient than SXS, which solubilized less than 1 g/L at 30 wt.%, making the extraction limited by the solubility of CA. In this section, the solubilization power of C_iGlyco and C_iGly towards CA is reported, and the solubility of other phytochemicals is studied to evaluate the selectivity of the amphiphiles.

a. Determination of the Minimum Hydrotropic Concentration (MHC) and solubilization power of various amphiphiles

The MHC value (see section I.1.6) is a crucial parameter to set the required concentrations and volumes for the extraction. Therefore, the MHC of *i*-C_5Xyl, $C_{6,-2}$Glu, C_7Glu, $C_{8/10}$Glyco and C_4Gly were determined by solubilization of CA (**Figure III.16**), in the same conditions as previously reported for C_4E_2 in section II.2.1, which had a MHC of about 10 wt.%. The MHC of C_4Glu has already been reported from the solubility curves of Disperse Red-13 (DR-13), a hydrophobic dye, and was found to be 43 wt.%, a very important concentration which would certainly not be industrially interesting.[194] Concerning *i*-C_5Xyl, CA is solubilized above a MHC of 9 wt.% (**Figure III.16**), which is close to a reported value obtained with Sudan Red 7B (10 wt.%).[196]

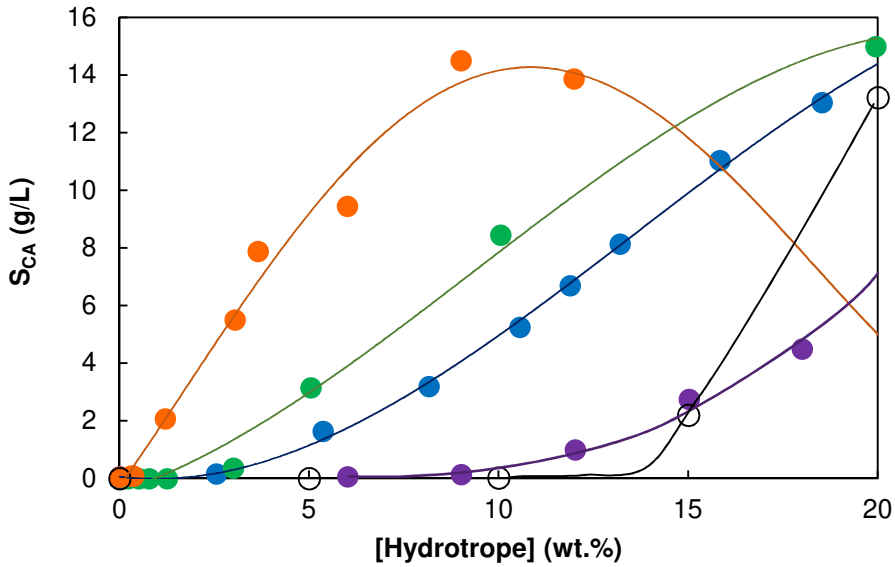

Figure III.16. CA solubility curves in $C_{8/10}$Glyco (orange), $C_{6,-2}$Glu (green), C_7Glu (blue) and *i*-C_5Xyl (purple), C_4Gly (empty black) aqueous solutions at pH 2, 25 °C

Table III.2 summarizes the CAC and MHC for each amphiphile and shows that the MHC are higher than the CAC, with a multiplying factor from 1.5 to 30, which suggests that these two properties have different physical chemical signification.[90,197] Indeed, the CAC reflects the concentration at which the hydrotrope starts self-assembling in water[86] whereas the MHC is more related to the formation of specific hydrotrope-solute complexes, which depends both on the hydrotrope and the solute properties.[85,198] For a long time, the self-assembly of hydrotropes in water was considered as a prerequisite for the solubilization of a hydrophobic solute and some molecular dynamics simulations confirmed it.[85,199] However, more recent studies based on thermodynamic considerations have suggested that the main driving force of solubilization is the hydrotrope accumulation around the drug, and that a competition between hydrotrope-hydrotrope and hydrotrope-solute association could occur, leading to decrease the solubilization in case of strong hydrotrope-hydrotrope association.[87]

In C_5Gly and *i*-C_5Gly, a phase separation occurred when CA was added before any saturation could be reached, as shown for C_5Gly in **Figure III.17**.[188] C_5Gly and *i*-C_5Gly in aqueous solution do not reach a CP below 100 °C, but a CP-phase separation has already been observed for both amphiphiles using the salting out property of Na_2SO_4.[90] Besides, an extrapolated CP was determined at 158 °C for C_5Gly using the Na_2SO_4, NaCl, and NaBr salting out effects.[90] From observations of the C_iE_j behavior in **chapter II** and this statement, it is likely that the CPs of C_5Gly and *i*-C_5Gly are decreased below room temperature due to the presence of CA.

At 5 wt.% C_5Gly, the solution was saturated in CA since a residual solid was observed. However, no CA was detected in the supernatant from the HPLC analysis. Therefore, this solution was certainly below the MHC, or at the MHC, considering that this latter has already been reported at 4.8 wt.% from DR-13 solubility curves. Above the MHC, no saturation was reached since the 10, 15 and 20 wt.% C_5Gly formed two phases: *(i)* an amphiphile-rich lower phase, which contain CA and *(ii)* a amphiphile-poor phase, which is enriched in water. Noteworthy, the amphiphile-rich phase is found at the bottom of the tube, contrary to C_iE_j aqueous solutions because of their densities (C_5Gly: 1.06[200] *vs* C_4E_1: 0.90[201]). Since the MHC of C_5Gly and *i*-C_5Gly cannot be measured for the solubilization of CA, they are indicated in **Table III.2** for the solubilization of DR-13 (and measured for *i*-C_5Gly for which the value was not found in the literature, curve in **Appendix 10**).

C_5Gly (wt.%)	**5**	**10**	**15**	**20**	**30**
Aspect					

Figure III.17. Pictures of C_5Gly solution after the addition of 20 g/L CA, at pH 2, 25°C. No residual solid is observed except in the 5 wt.% C_5Gly solution, below the MHC. CA is solubilized in the yellow amphiphile-rich lower phase.

In addition to MHC, it is important to know the CA solubility at the hydrotrope concentration used for the extraction. In view to compare extractions using C_iGlyco with the model established for C_iE_j, the CA solubility was measured at 30 wt.% concentration C_4Glu, *i*-C_5Xyl, C_7Glu, $C_{6,-2}Glu$, and $C_{8/10}Glyco$ at 25 °C and pH 2. The solubility of ursolic acid (UA) was also investigated under the same conditions to evaluate the selectivity of amphiphiles (**Figure III.18**).

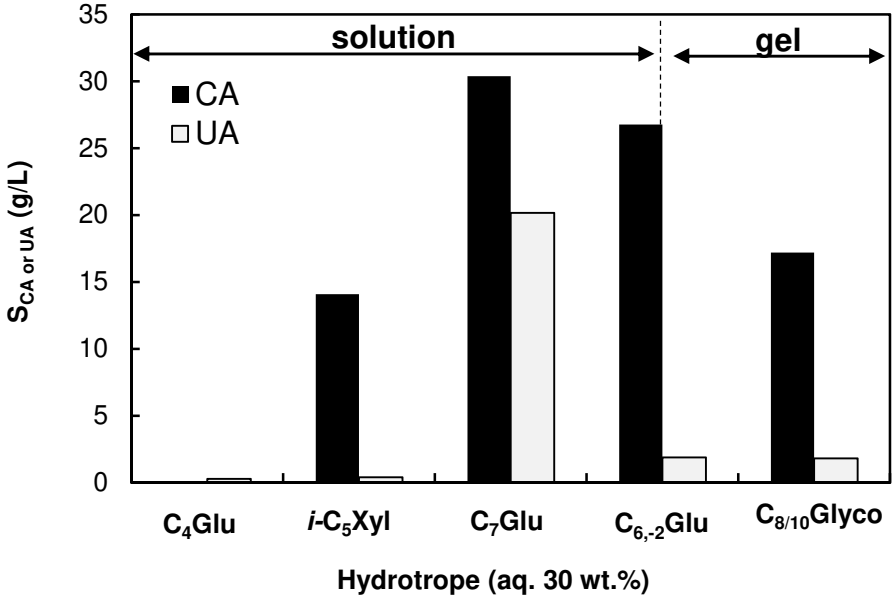

Figure III.18. Solubility of CA and UA in solutions of different C_iGlyco at 30 wt.% after stirring for 24 h at 25 °C, pH 2.

C_4Glu does not solubilize efficiently CA and only few amounts of UA at this concentration which is below the MHC following to the literature (2.0 mol/L,43 wt.%),[194] contrary to *i*-C_5Xyl, C_7Glu, $C_{6,-2}$Glu and $C_{8/10}$Glyco (**Table III.2**). C_7Glu solubilizes the highest amount of both CA (30.4 g/L) and UA (20.1 g/L), while *i*-C_5Xyl solubilizes the lowest amounts of CA (14.1 g/L) and UA (≈ 0.4 g/L). In between, $C_{6,-2}$Glu is also able to solubilize a high amount of CA (26.8 g/L). As mentioned previously, the main driving force of solubilization is the hydrotrope accumulation around the drug.[87] Therefore, the better efficiency of C_7Glu compared to *i*-C_5Xyl and $C_{6,-2}$Glu can be attributed to higher interactions between the hydrotrope and the solute, which may be related to the linear shape of its alkyl chain.[202]

Noteworthy, $C_{6,-2}$Glu forms a gel when UA is added, as well as $C_{8/10}$Glyco in presence of both CA and UA. Those gels are probably composed of LC, occurring with amphiphiles that have the longest alkyl chain of the series. Noteworthy, LC in binary systems water-$C_{8/10}$Glyco have been described above 70 wt.%, but the 30 wt.% solution is more viscous than the other C_iGlyco. The ability of UA to incorporate in cell membranes and stabilize them has been demonstrated in liposomes,[203] and suggests that UA forms strong interactions with $C_{6,-2}$Glu and $C_{8/10}$Glyco. After centrifugation of the gels, two phases stood out, a viscous lower one and a fluid supernatent, where concentrations of CA and UA were measured by HPLC. The values are reported in **Figure III.18**, but may underestimate the UA concentration in the gel before centrifugation. Thus, the highest ratio of CA/UA solubilities is found for *i*-C_5Xyl solution, making it the most attractive amphiphile for selective extractions.

b. Solute-dependence of the *iso*-amyl xyloside solubilization power

To further investigate the selective solubilization power of *i*-C_5Xyl towards CA and with the purpose of using *i*-C_5Xyl for the extraction of rosemary, the solubility curves of three phytochemicals of rosemary (CA, UA and rosmarinic acid, noted RA) measured at pH 2, 25 °C are presented in **Figure III.19**. In view to perform extractions at a plant/solvent ratio of 1:10 (w:v) and since CA is present at 2.72 wt.% in dried rosemary leaves, a minimal solubility of 2.72 g/L is required for a complete extraction of the available CA. According to its solubility curve in *i*-C_5Xyl, this minimal solubility is reached at 15 wt.% of *i*-C_5Xyl. The solubility of CA does not increase indefinitely along the hydrotrope concentration, the maximum of CA solubility (S_{max} = 14 g/L) being reached at C_{max} = 30 wt.% of *i*-C_5Xyl. CA extractions should thus be preferentially performed with hydrotropic solutions of *i*-C_5Xyl between 15 and 30 wt.%.

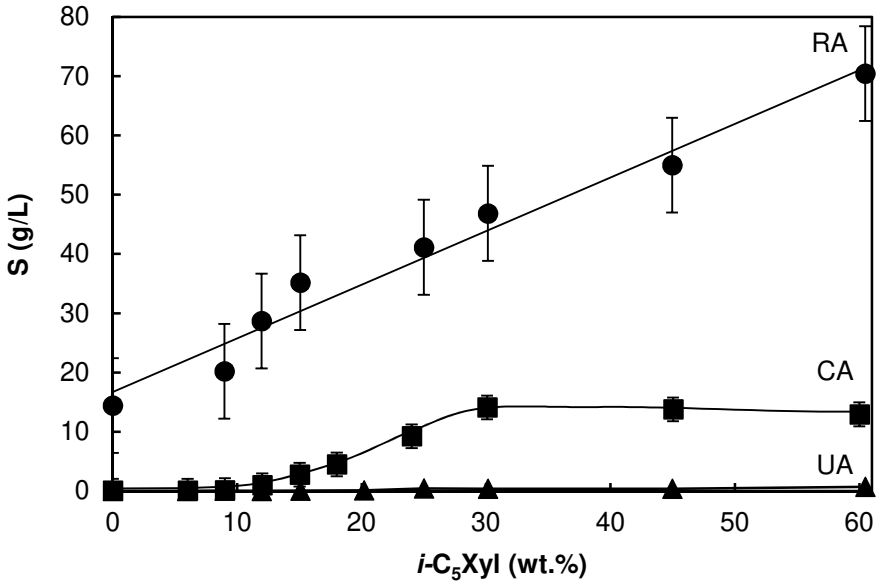

Figure III.19. Solubility curves of rosmarinic (RA), carnosic (CA) and ursolic (UA) acids in aqueous solutions of *i*-C_5Xyl at pH 2 and 25 °C, after 24 h of equilibration stirring.

Regarding RA, it is already soluble at 14 g/L in pure water, but its solubility can be increased up to 47 g/L in aqueous solutions of 30 wt.% *i*-C_5Xyl. On the opposite, *i*-C_5Xyl is not a good solubilizer for UA, a highly hydrophobic triterpenoid. Its solubility never exceeded 0.7 g/L and was only of 0.4 g/L in a 30 wt.% *i*-C_5Xyl solution. The differences between RA, CA and UA are in accordance with their log *P* which are respectively equal to 0.8, 5.4 and 8.7 (SciFinder® data). The ratio between the concentrations of solute solubilized at 0 and 30 wt.% of *i*-C_5Xyl (*i.e.* the solubility enhancement factor at 30 wt.%) is maximal for CA, which has an intermediate log *P* between those of RA and UA. A similar behavior has already been reported for the hydrotropic solubilization of drug molecules with hydrotropes such as urea, *N*,*N*-diethylnicotinamide (DENA) or *N*,*N*-dimethylbenzamide (DMBA). The solubilizations have

been reported to be maximal for hydrophobic drugs with polarities comprised in a specific range of log *P* depending on the hydrotrope (2-4.5 for urea and 4-10 for DENA and DMBA).[84,112]

To further investigate this interesting selectivity, the solubility of eight other solutes having different log *P* were compared in 0 to 60 wt.% *i*-C_5Xyl aqueous solutions. Two homologous series were chosen to minimize structural effects: four alkyl gallates with chain lengths of 3, 8, 12, 16 carbons atoms (abbreviated as C_iG), and three fatty acids with chain lengths of 14, 18, 22 carbons atoms (abbreviated as C_iFA). Camphor (C) was also studied as representative monoterpene, and because it was identified as component of rosemary.[204] For each solubility curve (**Figures III.20-22**), the slope of the pseudo-linear part, called the solubilization enhancement coefficient, was calculated, as well as the MHC. The precise measurement of the MHC can sometimes be difficult because of the detection limits. We thus chose to measure the MHC as the minimum hydrotrope concentration required to solubilize 0.1 g/L of solute, which is the threshold concentration to consider a solute as very slightly soluble in any solution, according to the World Health Organization.[205]

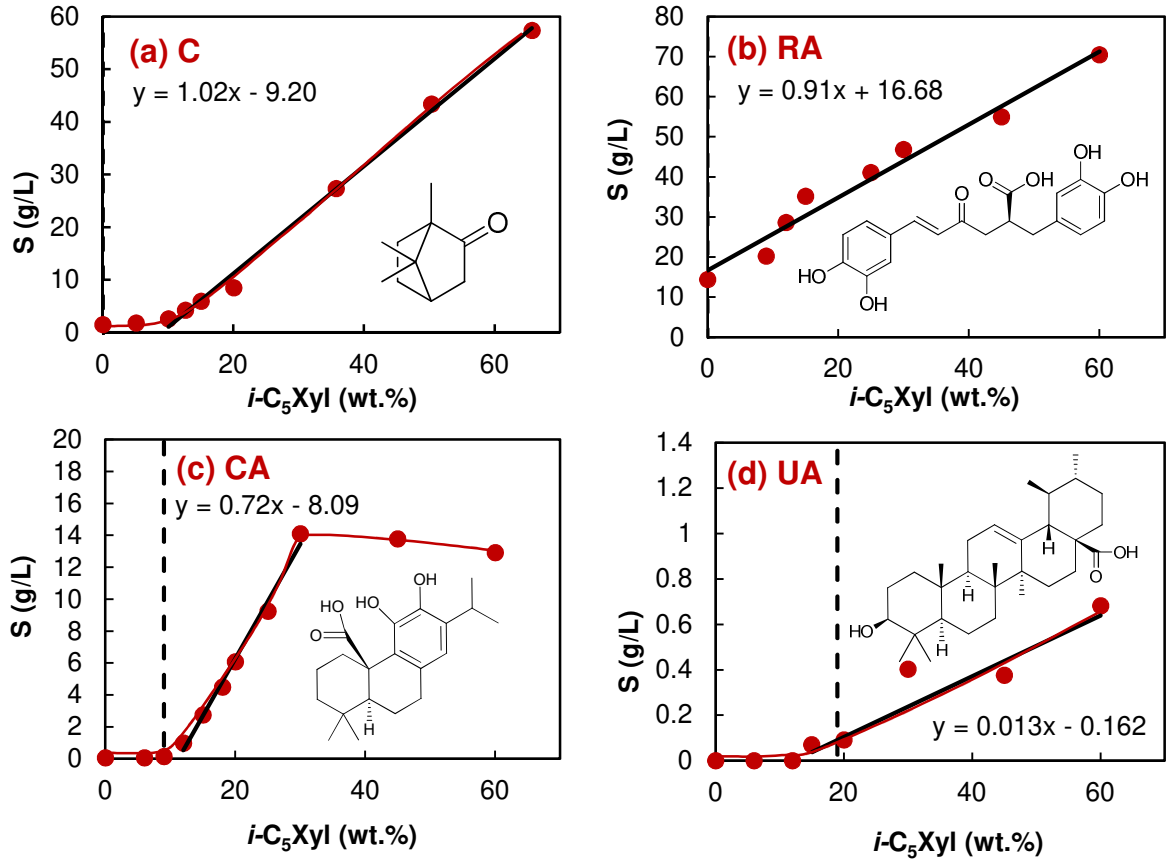

Figure III.20. Solubility curves of camphor (a), rosmarinic (b), carnosic (c) and ursolic (d) in solutions of *i*-C_5Xyl at pH 2 and 25 °C. MHC is represented in dotted line.

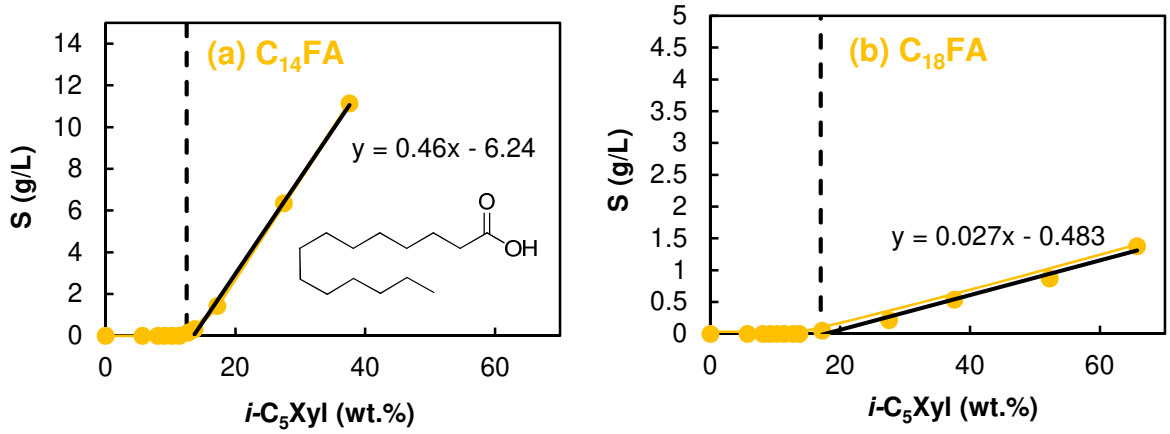

Figure III.21. Solubility curves of myristyl (a) and stearyl (b) acids as model molecules in solutions of *i*-C_5Xyl at pH 2 and 25 °C. MHC is represented in dotted line.

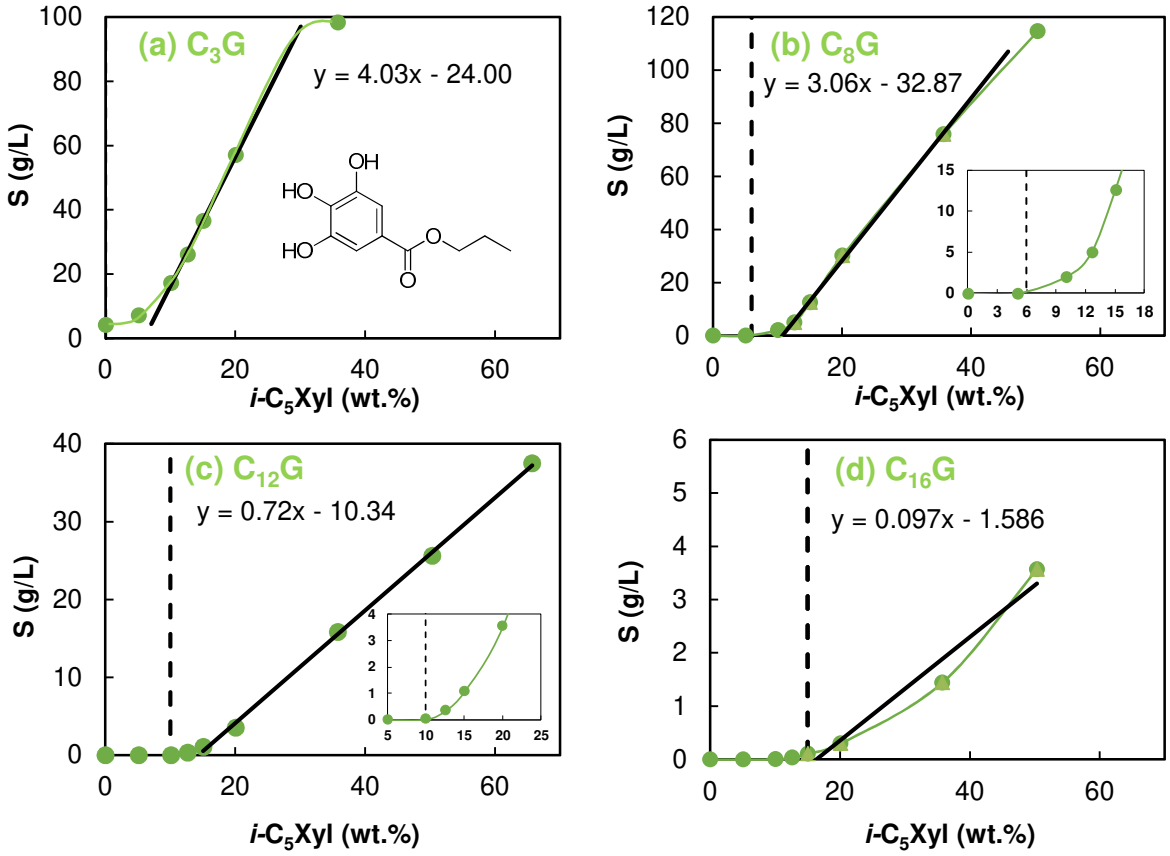

Figure III.22. Solubility curves of propyl (a), octyl (b), dodecyl (c) and hexadecyl (d) gallates as model molecules in solutions of *i*-C_5Xyl at 25 °C. MHC is represented in dotted line and a focus is made on the MHC region if necessary.

The solubilization enhancement coefficient and the solubility in water of each solute are plotted against their log *P* in **Figure III.23.** Noteworthy, all the molecules with a log *P* below 7 have

noticeable solubilization enhancement coefficients, between 0.5 and 3, meaning that they can be extracted with an adapted concentration of *i*-C5Xyl. Conversely, molecules with a log *P* above 7, such as UA, have a low solubilization enhancement coefficient, and C22FA is never solubilized (thus not reported). In addition, compounds with a log *P* < 3 have a significant water-solubility (above 1.5 g/L, the solubility of C), suggesting that they are unlikely to precipitate during hydrotropic dilution which will be done for the recovery step. Therefore, a distinction can be made between three groups: *(i)* below log *P* = 3, molecules such as RA will be extracted in *i*-C5Xyl aqueous solution but they will mostly not precipitate, *(ii)* from log *P* = 3 to 7.5, molecules such as CA will be extracted and could be recovered in the precipitate and *(iii)* above log *P* = 7.5, molecules such as UA are not likely to be extracted.

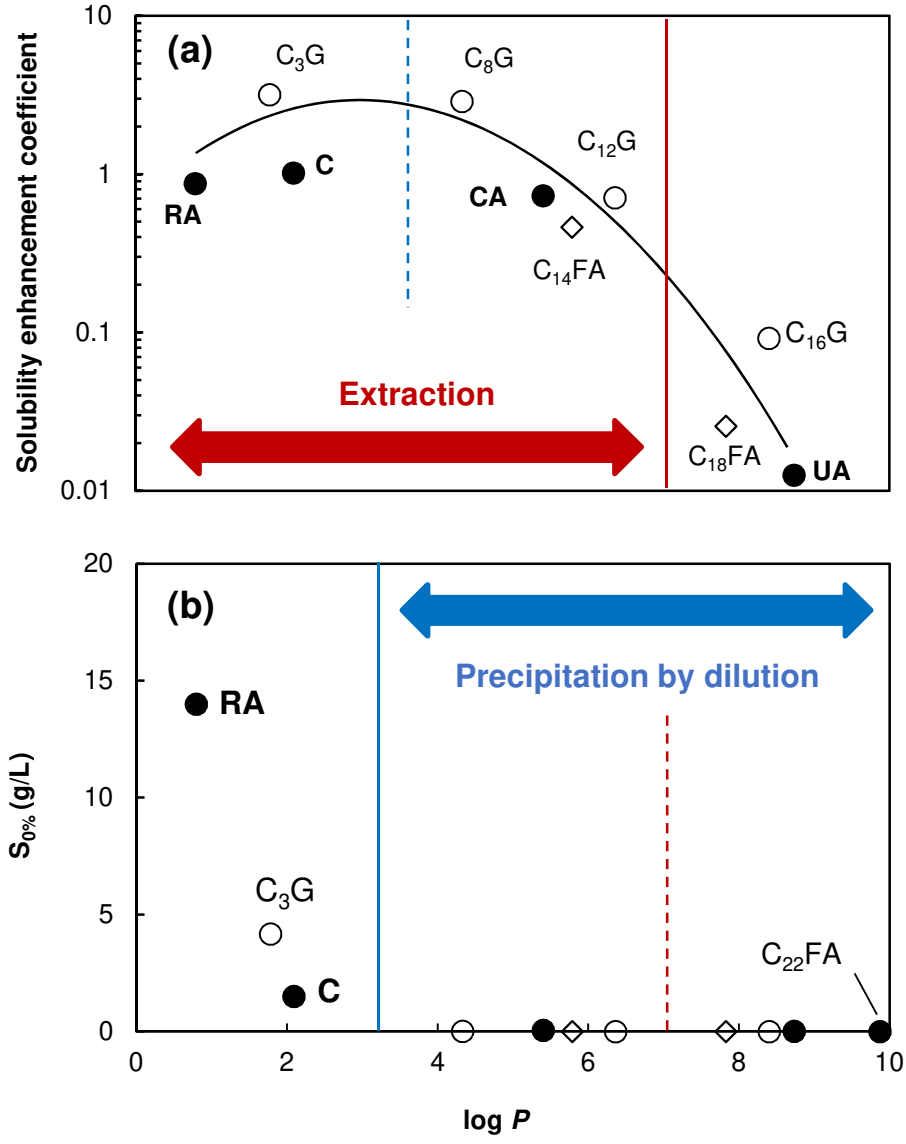

Figure III.23. (a) Solubilization enhancement factors and (b) water-solubility ($S_{0\%}$) of rosmarinic acid (RA), carnosic acid (CA), ursolic acid (UA), camphor (C), indicated in bold (black circles) and the model molecules alkyl gallates ($C_{3\text{-}16}G$, white circles) and fatty acids ($C_{14\text{-}22}FA$, white diamonds) as a function of their log *P* (SciFinder®, pH 2 for acids to ensure the predominance of the protonated form). The factors are calculated from the slope of the solubility curves at 25 °C (Figures III.20-22). The solubilities are measured by HPLC for CiG, CiFA, RA, CA and UA and GC-FID for C.

In addition, the MHC of *i*-C_5Xyl measured for each solute from **Figures III.20-22** were also plotted against their log *P* in **Figures III.24.** Interestingly, the MHC seems to linearly increase with log *P* from 0 to 9. This finding supports the theory that the MHC origin is the hydrotrope-solute interaction.[87,197] From a practical point of view, knowing the MHC is essential to perform an extraction since it gives indications on both the hydrotrope concentration required to solubilize the product and the dilution which must be applied to precipitate the extract. Thus, the fact that MHC depends on the solute should induce a possible selective extraction and/or precipitation. Indeed, a 15 wt.% *i*-C_5Xyl solution would be able to selectively solubilize molecules with log *P* below 7.5 such as CA rather than molecules with a log *P* above 7.5 such as UA.

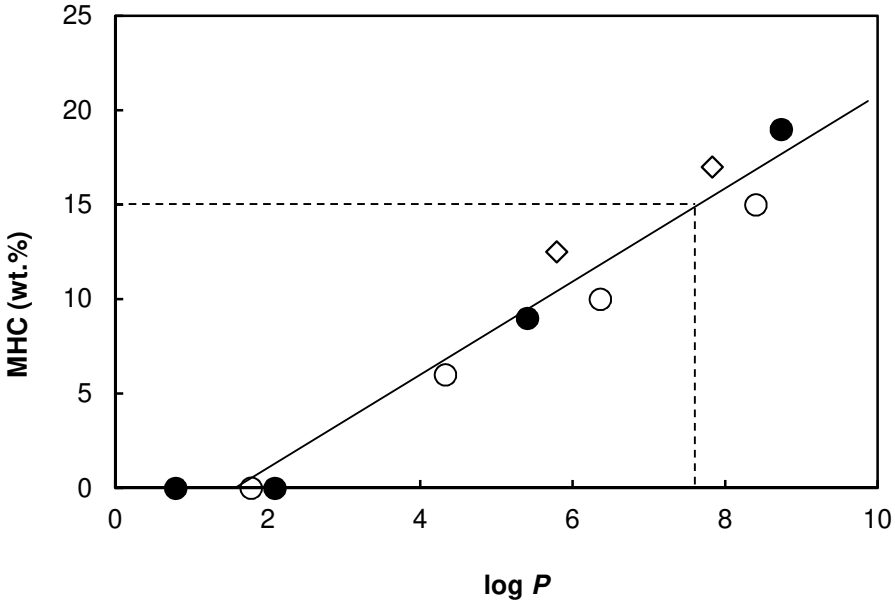

Figure III.24. MHC as a function of the log *P* of the solutes. Rosemary constituents are shown in black circles (●), alkyl gallates in white points (○) and fatty acids in white diamonds (◊).

III.2. Molecular model for the prediction of the extraction efficiency with sugar and glycerol-based hydrotropes

III.2.1. Validation of the model obtained with alkyl polyethylene glycol-based extractions

In **Chapter II**, the concentration of CA in the filtrate of extraction from whole rosemary leaves by aqueous solutions containing 30 wt.% C_iE_j (i = 4 to 12; j = 1 to 4) has been determined and discussed according to i and j.[188] The efficiency of short-chain C_iE_j (i < 8) to extract CA from whole leaves compared to longer ones (i > 8) was clearly demonstrated. Furthermore, based on the results and a systematic study on the C_iE_j series, the concentration of CA in the final filtrate could be quite well modeled with the molecular volume (V_m) and HLB or log P of the hydrotrope used for the extraction. Here, we tried to apply this model to the extractions using C_iGlyco and C_iGly under same conditions, *i.e.* with whole rosemary leaves for 48 h, at pH 2 and with 30 wt.% amphiphile. The kinetics of extractions was also studied from 1 to 8 h (kinetic study in **Appendixes 11-12**).

When the extraction is performed on whole rosemary leaves, amphiphiles must first cross the cell wall to be internalized and then, solubilize CA. C_iGlyco such as C_8Glu and $C_{12}Glu$ have been reported to make strong interactions with liposomes and cell membranes, leading to the breakdown of the lamellar structures and the formation of lipid-surfactant mixed micelles.[206] In the same study considering five linear C_iGlyco from C_8 to $C_{12}Glu$, the shorter the surfactant alkyl chain, the higher the permeability of bilayer structures. Same behavior might be expected with shorter hydrotropes.

As shown in **Figure III.25.a**, the maceration of rosemary in C_iGlyco solutions leads to the extraction of CA, except for C_4Glu for which the concentration used is below its MHC. Among C_iGlyco, *i*-C_5Xyl is the most efficient amphiphile and extracts 0.43 g/L of CA after 48 h. As reported for a series of C_iE_j hydrotropes, the most efficient ones have a short alkyl chain, a small molecular volume and are preferably lipophilic.[188] In the alkyl glycoside series, *i*-C_5Xyl is the hydrotrope with the shortest alkyl chain and also the smallest polar head group composed of pentose(s). Then, other C_iGlyco range in the following order: C_7Glu > $C_{8/10}Glyco$ > $C_{6,-2}Glu$ for the extraction at 48h. Noteworthy, $C_{6,-2}Glu$ is faster to extract CA than the other ones since all the CA is extracted in less than 24h (no increase of CA concentration between 24 and 48 h). This can also been found in the kinetics, since $C_{6,-2}Glu$ has the second highest k of the C_iGlyco, after *i*-C_5Xyl.

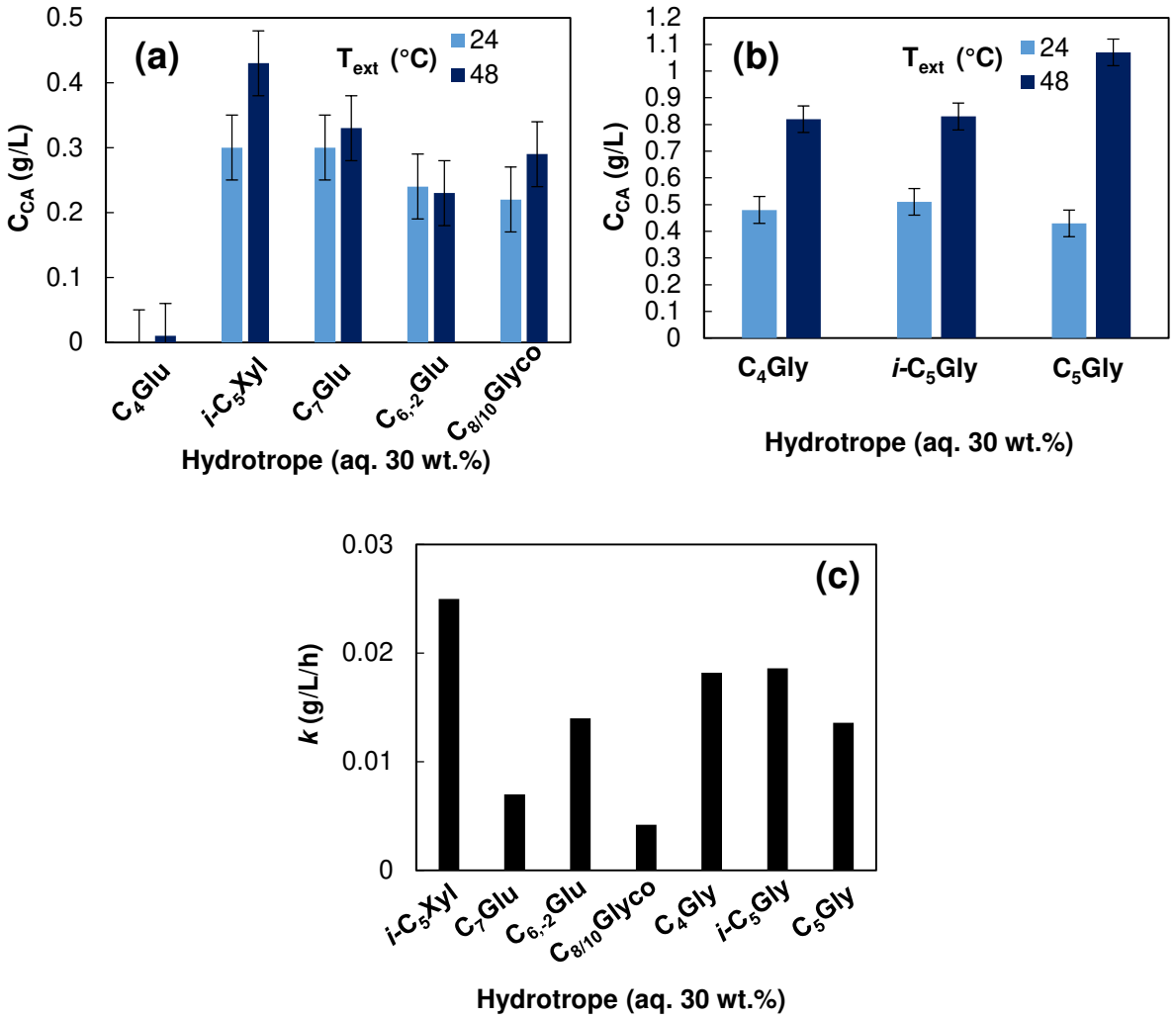

Figure III.25. Concentration in the filtrate of CA extracted from whole rosemary leaves after 24 and 48 h of stirring by 30 wt.% CiGlyco solutions (a) or 30 wt.% CiGly solution (b). Kinetic rate between 1 and 8 h of extraction (c).

With regard to CiGly, they are much more efficient than CiGlyco (between 0.8 and 1.1 g/L CA in the filtrate *vs* 0.43 g/L for *i*-C5Xyl), which can be attributed to their small polar head, leading to smaller molecular volumes. C4Gly and *i*-C5Gly seem to have the same efficiency because they have extracted the same concentration of CA after 24 and 48 h of maceration whereas C5Gly seems more efficient (**Figure III.25.b**). Indeed, with 1.07 g/L CA extracted after 48 h, C5Gly is competitive with the best CiEj (C5E2: 1.21, C4E1: 1.02 g/L CA). Interestingly, they are slower compared to *i*-C5Xyl (**Figure III.25.c).** To understand this phenomenon, alkyl polyglycosides and alkyl glycerols have been positioned with CiEj on the 2D-diagrams established for these latter showing the molecular volume (V_m) against log *P* or HLB on **Figures III.26 and 27**.

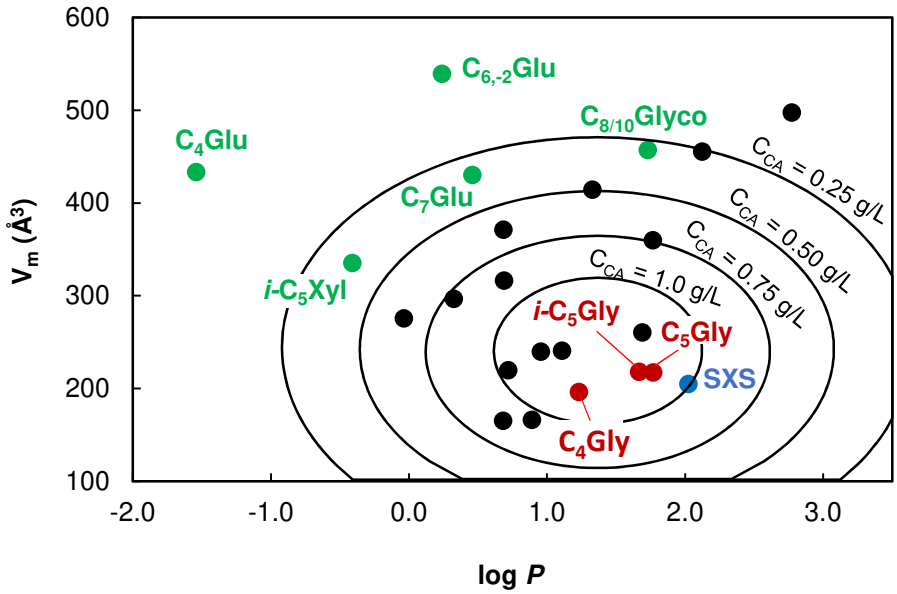

Figure III.26. Contour plot of the concentration of extracted CA from whole rosemary leaves after 48 h versus molecular volume and log *P* of the amphiphiles. Each contour line is calculated by Eq.II.4 and 5 and correspond to a concentration of CA extracted of 0.25, 0.5, 0.75 and 1 g/L as indicated. C_iGlyco are indicated in green, C_iGly in red, SXS in blue and C_iE_j in black.

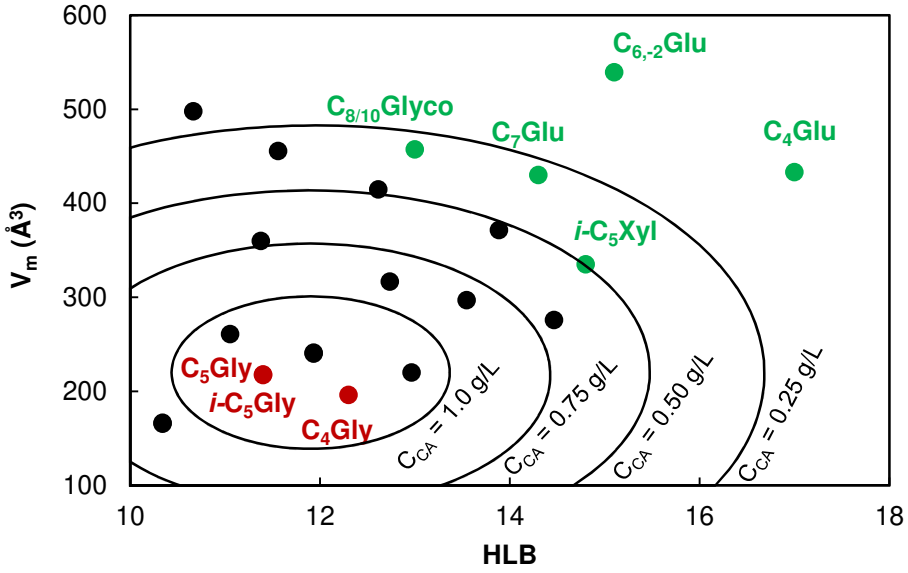

Figure III.27. Contour plot of the concentration of extracted CA from whole rosemary leaves after 48 h versus molecular volume and HLB of the amphiphiles. Each contour line is calculated by Eq.II.6 and 7 and correspond to a concentration of CA extracted of 0.25, 0.5, 0.75 and 1 g/L as indicated. C_iGlyco are indicated in green, C_iGly in red, and C_iE_j in black.

Considering the two models, C_4Glu and $C_{6,-2}Glu$ are further from the center than the contour line representing a concentration of CA of 0.25 g/L (**Figures III.26 and 27**), meaning that their extraction should result in a filtrate less concentrated than 0.25 g/L. As well, *i*-C_5Xyl, C_7Glu and $C_{8/10}Glyco$ should extract between 0.25 and 0.5 g/L of CA. All these assumptions are in accordance with the experimental values of 0.01 and 0.23 g/L for C_4Glu and $C_{6,-2}Glu$ and 0.43, 0.33 and 0.29 g/L for *i*-C_5Xyl, C_7Glu and $C_{8/10}Glyco$. Finally, in both figures, alkyl glycerols are located at the center of the circles, meaning that they are close to the maximum efficiency, and 1 g/L CA should be recovered in the filtrate after extraction. This is the case for C_5Gly, which extracts 1.07 g/L CA, but not for C_4Gly and *i*-C_5Gly which extract respectively 0.82 and 0.83 g/L CA.

The expected concentrations of CA in the filtrate of extraction were predicted more precisely according to Eq.II.4, II.5 and Eq.II.6 and II.7, and were plotted against the experimental values in **Figure III.28**. As previously concluded from the 2D-diagrams, the two models seem to be quite efficient to predict the efficiency of C_iGlyco, except for $C_{6,-2}Glu$. C_5Gly is also well predicted but *i*-C_5Gly and C_4Gly deviate from the model. Nevertheless, they are still predicted as efficient hydrotropes, and indeed, they are more efficient than most C_iE_j. Therefore, the model established for the concentration of CA extracted by aqueous solutions at 30 wt.% C_iE_j can be considered as valid for C_iGlyco and C_iGly.

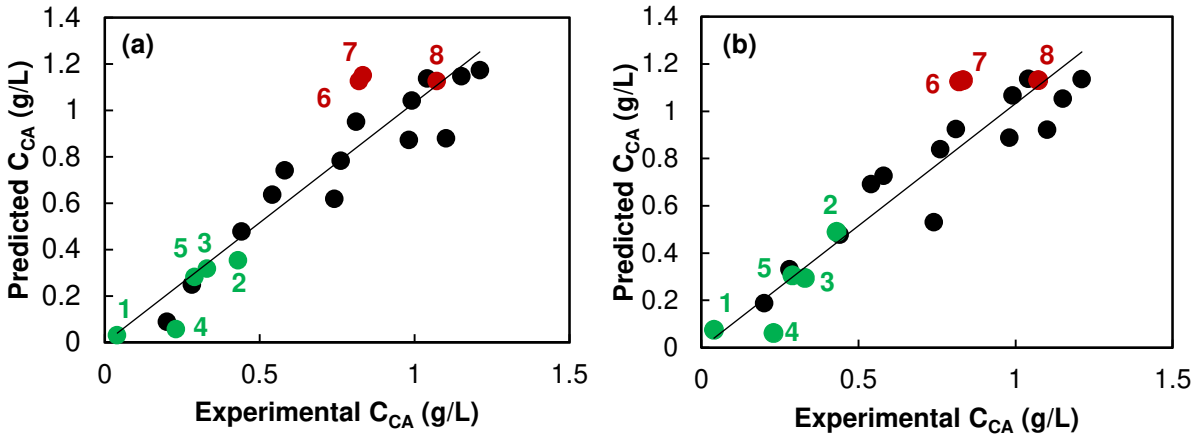

Figure III.28. Correlation between experimental and estimated concentration of CA extracted from whole rosemary leaves after 48 h. Estimation based on the prediction from V_m and log *P* (a) and V_m and HLB (b). C_iGlyco are indicated in green (1: C_4Glu, 2: *i*-C_5Xyl, 3: C_7Glu, 4: $C_{6,-2}Glu$, 5:$C_{8/10}Glyco$) and alkyl glycerols (6: C_4Gly, 7: *i*-C_5Gly, 8: C_5Gly) in red and C_iE_j in black.

III.2.2. Adaptation of the model to industrial purposes

In view to enlarge the accessibility of this model, we also attempted to establish one which could be used without requiring additional experiments nor having access to specific software such as COSMO-RS. For that purpose, we chose to keep HLB that can be calculated from the structure of the molecule and the molar mass instead of the molecular volume. Noteworthy, those descriptors are interesting for the short-chain amphiphiles that we use, but the HLB could be harder to get in the case of ionic compounds or amphiphiles that are not composed of a short alkyl chain and a polar head (*e.g.* nicotinamide). If the HLB cannot be calculated, it can still be experimentally determined, but these experiments are generally time-consuming.

Since the method of using C_iE_j seems to be efficient to predict the efficiency of all hydrotropes, this method was used herein, using only the linear C_iE_j because the difference of M and HLB cannot be made on isomers. As a result, the best M was found to be 146 g/mol, and the best HLB 12.1, close to the previous value obtained for the model with V_m (11.9). The model resulted in the following equations:

$$r^2 = \left(\frac{M - 146}{42.5}\right)^2 + (HLB - 12.1)^2 \quad \text{(III. 3)}$$

$$C_{CA} = 1.18 \times \exp\left(-0.065\ r^2\right) \quad \text{(III. 4)}$$

Noteworthy, the estimation of the concentration of CA in the filtrate after extraction was as effective with this model as with the previous ones for alkyl glycerols: the estimated value was close to the experimental one for C_5Gly (1.13 *vs* 1.07 g/L) and higher than the experimental one for C_4Gly and *i*-C_5Gly (1.18 and 1.13 *vs* 0.86 and 0.82 respectively, **Figure III.29**). For C_iGlyco, only the efficiencies of C_4Glu and *i*-C_5Xyl are well estimated, with a difference from experimental below 0.1 g/L, but the estimated values for C_7Glu and $C_{8/10}Glyco$ were further from the experimental ones than with the previous models using the molecular volume. This model gives an idea of the efficiency of C_iGly and C_iGlyco, however, it seems to be less effective than the previous ones such as the one established with log *P* and V_m. Indeed, although HLB can be a good indicator, its simple calculation does not fully relate of the intramolecular interactions which would influence an experimental HLB.

Furthermore, the HLB of propanol was estimated to 5.7 considering that the hydrophilic part was only composed of the alcohol function. Interestingly, the estimation of the efficiency of propanol did not effectively reflect reality (0.06 *vs* 0.93 g/L, **Figure III.29**). The estimation of the HLB was lower than that obtained by Alany et al. (7.48)[207], however, this value would lead to an estimated value of 0.23 g/L, far below the experimental value of 0.93 g/L. From this observation, the model can only be validated for molecules with a HLB above 10, and according to the method of calculation of HLB, for non-ionic amphiphiles for which a clear distinction can be made between the hydrophilic polar head and the lipophilic alkyl chain.

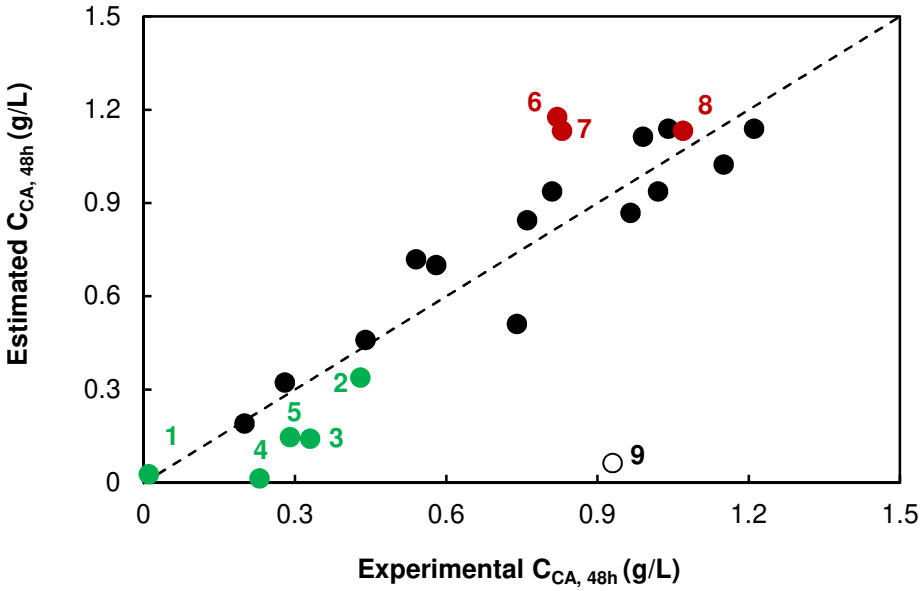

Figure III.29. Correlation between experimental and estimated concentration of CA extracted from whole rosemary leaves after 48 h, based on the model established for M and HLB. C_iGlyco are indicated in green (1: C_4Glu, 2: *i*-C_5Xyl, 3: C_7Glu, 4: $C_{6,-2}Glu$, 5:$C_{8/10}Glyco$) and C_iGly (6: C_4Gly, 7: *i*-C_5Gly, 8: C_5Gly) in red, propanol in empty point (9) and C_iE_j in black.

III.2.3. Influence of the leaf wettability

For both the previous models, and particularly for the models using M or HLB, it is difficult or even impossible to differentiate two isomers, such as C_5E_2 and *i*-C_5E_2 or C_5Gly and *i*-C_5Gly. However, the branching of the alkyl chain has clearly a negative effect on the efficiency of the hydrotrope. This has been previously attributed to a higher volume, but was not reflected by the estimation of the CA concentration in the filtrate. Indeed, all the models estimate almost the same efficiency for *i*-C_5Gly and its isomer C_5Gly while *i*-C_5Gly is about 20 % less efficient. To understand this phenomenon, contact angles of 2 µL droplets of water and hydrotropic solutions were measured on the upper side of rosemary leaves, as shown in **Figure III.30**. To limit the impact of the variability of the plant surface, which is inherent to the material, each contact angle was calculated from the mean value of ten measurements, resulting in standard values of about 5°, a common value for contact angle measurements on plant material.[208]

Contact angle (θ) reflects the wettability of the surface by the hydrotropic solution, and is connected with γ_{SG}, the surface free energy of rosemary, γ_{LG}, the interfacial tension between rosemary and the hydrotropic solution and γ_{SL}, the surface tension of the hydrotropic solution, also noted σ, by the Young equation (**Eq.III.5**):

$$\gamma_{SG} = \gamma_{SL} + \gamma_{LG} \cos\theta \qquad (III.5)$$

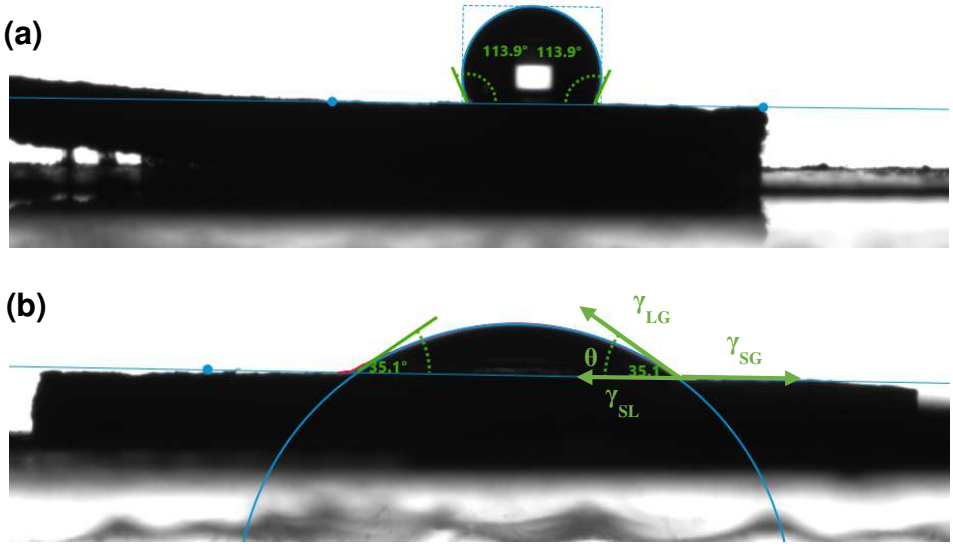

Figure III.30. Contact angle of water (a) and an aqueous solution of C_5Gly at 30 wt.% (b) on the upper side of rosemary leaves

Table III.3. summarizes the contact angles with rosemary and the surface tensions (σ) of water and the aqueous solutions containing 30 wt.% of hydrotropes, which have been measured at this concentration specifically for more precision. As expected, the presence of a hydrotrope decreases both θ and σ compared to neat water. Moreover, those two values evolve with the alkyl chain length in the following order: C_4 > C_5 > *i*-C_5 for both C_iE_2 and C_iGly series. Excluding the difference of glycoside nature, the same phenomenon occurs with C_4Glu > *i*-C_5Xyl. The polar head also influences both θ and σ in the same order: for the C_4 series, E_2 < Gly < sugar (Glu) and for the C_5 and *i*-C_5 series, Gly < E_2 < sugar (Xyl).

Table III.3. Contact angles observed between 2 µL droplets of aqueous hydrotropic solutions at 30 wt.% (or water) and the upper sides of rosemary leaves and surface tension of these solutions

		θ (°)	σ (mN/m)
	Water	106.4 ± 11.8	72.8
30 wt.% aq.	**C_4Gly**	58.9 ± 5.9	28.6
	C_5Gly	41.9 ± 7.1	26.8
	***i*-C_5Gly**	40.2 ± 5.3	25.3
	C_4E_2	56.8 ± 5.9	28.0
	C_5E_2	48.6 ± 6.2	30.0
	***i*-C_5E_2**	46.1 ± 4.3	28.5
	C_4Glu	79.1 ± 3.7	29.0
	***i*-C_5Xyl**	51.9 ± 6.2	37.0

Since γ_{SG} only depends on the plant surface, the value of $-\sigma.\cos\theta$ depends only on the interfacial tension γ_{SL} as shown by **Eq.III.6**. Those values were plotted against the concentration of CA extracted by the hydrotropic solutions in **Figure III.31**. Interestingly, two groups stand out, corresponding to the different alkyl chain lengths. Furthermore, for a similar alkyl chain length, the concentration of CA extracted seems to increase exponentially when γ_{SL} decreases, meaning that the concentration of extracted CA only depends on the interfacial tension and the alkyl chain length *i*. Indeed, when the interfacial tension decreases, interactions between the hydrotrope and the plant increases, which probably results in a higher adsorption of hydrotropes on the plant, hence an easier diffusion. However, this assumption should be verified for more amphiphiles.

$$-\sigma\cos\theta = \gamma_{SL} - \gamma_{SG} \qquad \text{(III. 6)}$$

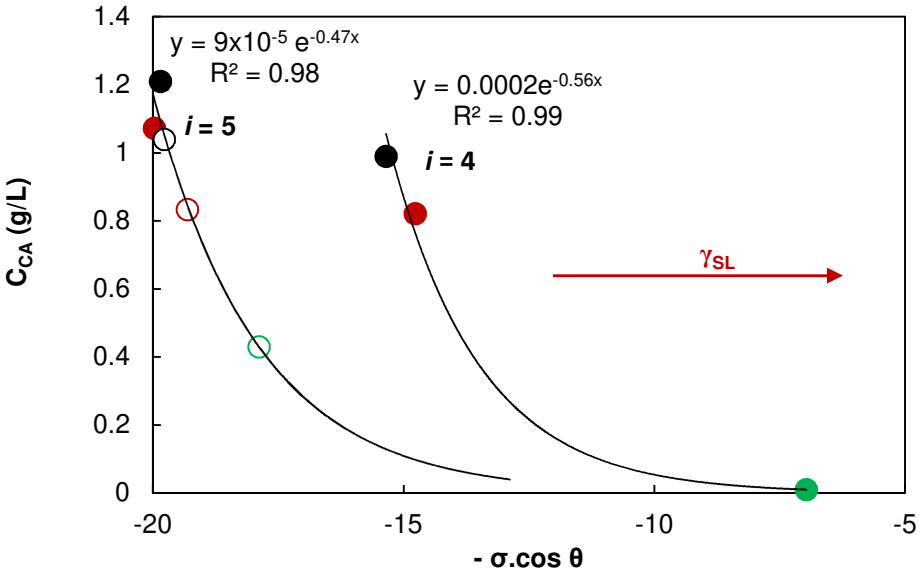

Figure III.31. Evolution of the concentration of CA extracted from whole rosemary leaves after 24 and 48 h of stirring by 30 wt.% C_iGlyco (green), C_iGly (red) and C_iE_2 (black) with $-\sigma\cos\theta$, *i.e.* with the interfacial tension γ_{SL}. Empty points represent branched alkyl chains.

III.2.4. Transposition of the model to ground rosemary and sage

The previous experiments highlighted C_5Gly and *i*-C_5Xyl as the best C_iGly and C_iGlyco respectively, thanks to their short alkyl chain, small polar heads compared to C_iGlyco for example and thus, small molecular volume. However, extractions of whole leaves of rosemary resulted in a concentration of CA in the filtrate of 1.07 and 0.43 g/L respectively, whereas 2.7 g/L could be expected if all the CA available was extracted. Considering that, in all the cases, about 20 % of the hydrotropic solution is not recovered because it is absorbed in dehydrated

rosemary leaves, the recovery rate at this time can be expected to be 32 and 13 %, which must obviously be increased.

To this aim, extractions with CiGly and *i*-C5Xyl were performed on ground rosemary in order to reduce the cell barriers and to release the phytochemicals of the cells. The results were compared with ground sage, which contained 1.85 wt.% CA for comparison (**Figure III.32**). Regarding extractions of rosemary, C5Gly was still the best hydrotrope and resulted in a concentration of CA in the filtrate of 2.53 g/L. Once again, *i*-C5Gly and C4Gly had an equivalent efficiency (2.37 g/L CA in the filtrate) and *i*-C5Xyl was less efficient than CiGly, with a CA concentration of 2.1 g/L. Therefore, the efficiency of hydrotropes was ranged in the same order than for the extraction of whole leaves. Regarding extractions of sage, those three latter hydrotropes had a similar efficiency and extracted around 1.3 g/L ± 0.04. C5Gly was found to be the best hydrotrope for this experiment too with 1.36 g/L CA extracted. However, the extraction of sage was less efficient than that with rosemary since the recovery rate of C5Gly can be estimated to 59 % for sage and 75 % for rosemary. Noteworthy, with *i*-C5Xyl the recovery rates can be estimated to 55 and 62 % for sage and rosemary respectively.

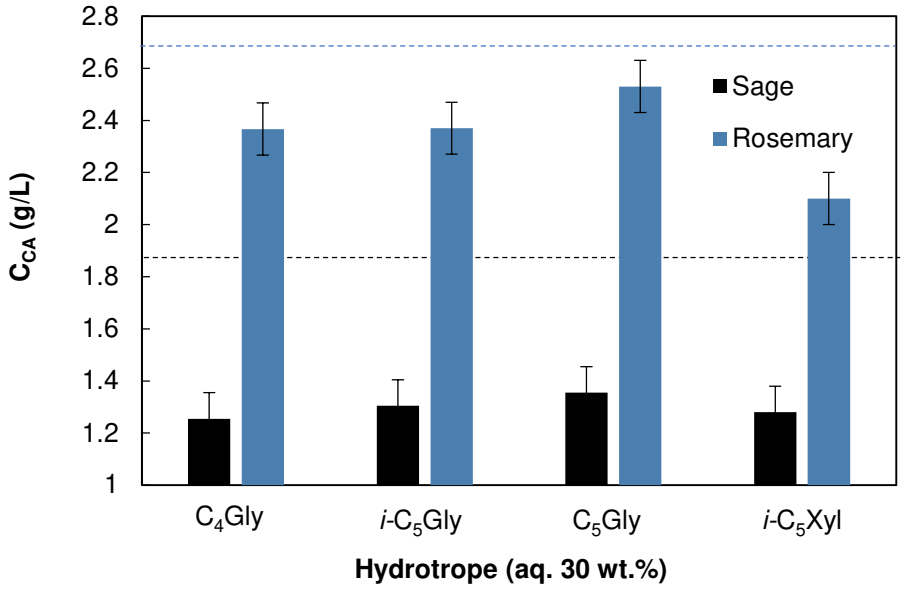

Figure III.32. Concentration in the filtrate of CA extracted from ground rosemary and sage leaves after 30 min of stirring by 30 wt.% CiGly solutions and *i*-C5Xyl. Dotted lines show the maximum concentration of CA which can be extracted from rosemary and sage leaves.

III.3. Optimisation of the hydrotropic extraction

In view to perform extractions at a larger scale, CiGlyco were found a better option compared to CiGly since they are commercially available and they seem to be more biodegradable.[132] Indeed, their high biodegradability has been demonstrated by the prescribed OECD 301 test for aerobic degradation in aqueous medium (28 days) and OECD 311 one for anaerobic biodegradability under sludge digester condition (60 days).[137,209–211] In addition, *iso*-amyl

polypentoside (*i*-C_5Xyl), heptyl polyglucoside (C_7Glu) and caprylyl/capryl polyglycosides ($C_{8/10}$Glyco) passed the OECD 301F test with results up to 86, 82 and 98% of biodegradation over 28 days.[134–136] Furthermore, no dermatologic irritation for decyl and octadecyl glucoside (C_{10}Glu, C_{18}Glu)[137] and moderate ocular irritations (for $C_{8/10}$Glyco or *i*-C_5Xyl according to the OECD 405 test)[130] have been found, along with low health toxicity (LD_{50} > 35 g/kg according to the OECD 401 test) for $C_{8/10}Glu_{1.6}$.[137] Eco-toxicity for aquatic organisms such as zooplankton and phytoplankton was found to be lower for C_iGlyco surfactants compared to C_iE_j and among the C_iGlyco, the branched ones are even less harmful than the linear ones.[212] In addition, C_iGlyco are easily prepared from bio-based resources, namely alcohols from fatty acids, and glucose or xylose from starch or hemicellulose.[130,213]

III.3.1. *Iso*-amyl xyloside, a very efficient sugar-based hydrotropic extractant

Extractions from ground rosemary were performed for 30 min at room temperature, with a plant/solution ratio of 10 g/100 mL, with *i*-C_5Xyl, C_7Glu and $C_{8/10}$Glyco, which were the most efficient C_iGlyco for the extraction of CA from whole rosemary leaves. According to the solubility curves, the hydrotropic concentrations were chosen so that each solution had a similar solubilization capacity for CA (6.5-8 g/L, **Figure III.16**). After filtration to separate the solution from the residual plant, CA concentration in the liquid extract was quantified by HPLC (**Table III.4**).

Table III.4. Mass yield and CA content in the liquid and solid extracts obtained from ground rosemary after 30 min of stirring in the hydrotropic solutions at room temperature.

Hydrotropes (conc. wt.%)	C_{CA}[a] (g/L)	Dilution factor	Dry extract	
			Mass yield (%)	CA content (wt.%)
***i*-C_5Xyl (22.5)**	2.05	2.5	5.3	12.6
C_7Glu (12)	1.9	4.2	2.2	7.9
$C_{8/10}$Glyco (4)	1.6	10	0.01	n.d.[b]

[a] CA content in the intermediate liquid extracts obtained after the extraction and the removal of plant residuals.
[b] Not enough recovered solid extract to be analyzed

i-C_5Xyl was the most effective extractant during the first step of extraction with 2.05 g/L of CA recovered in the filtrate. In order to recover CA, the hydrotropic solution was diluted just at the MHC with acidic water (pH 2) to precipitate insoluble materials forming the hydrotropic extract. The dilution factors (**Table III.4**) are the ratio between the concentration of the hydrotrope used for the extraction and of its MHC with CA (**Table III.2**). Then, the precipitate was recovered by Büchner filtration under vacuum and freeze-dried before HPLC

quantification of CA. The ratio between the mass obtained and the initial amount of rosemary is called the mass yield (**Eq. II.8**).

The extract with the highest mass yield and CA content (**Eq.II.9**) was obtained with *i*-C_5Xyl. Concerning $C_{8/10}$Glyco, the required dilution factor seems too high to precipitate CA. Indeed, the CA concentration decreased to 0.16 g/L, a value close to its solubility limit in pure water (0.08-0.1 g/L) (**Figure III.16**).

If *i*-C_5Xyl remains the best extractant on whole leaves, the extraction of CA is less efficient compared with ground leaves (1.92 g/L over 30 min vs 0.43 g/L over 48 h respectively). Even if C_iGlyco may pass through cell membranes, it is not sufficient to lead to equivalent mass transfer kinetics compared to the one induced by the grinding step. We thus optimized the process with *i*-C_5Xyl using ground leaves.

III.3.2. Identification of the key parameters for hydrotropic extraction with *iso*-amyl xyloside using a 2^4 fractional factorial design

a. Choice of the factors

Many factors can influence the final mass yield and recovery rate of the target molecules during the whole extraction process. The study of each factor and their interaction pairwise would require numerous experiments which can however be lowered thanks to an experimental design.[121,214–220] Though particle size plays an important role, it has been widely studied elsewhere and has thus been excluded from the optimization.[214,215,221] Anyway, an average size of 0.5 mm has been used herein as it is the most industrially accessible particle size due to the terpene content of rosemary leaves which make them become sticky during grinding. Four other factors were selected: time of extraction, hydrotrope concentration, stirring speed and temperature during maceration (**Figure III.33**). A two-level full factorial design was chosen since it is adapted to measure interactions between factors and identify the most significant ones. The plant/solution ratio was set at 5 g for 50 mL to minimize the use of hydrotropic solution while keeping a good dispersion of rosemary.

Two levels for each variable were defined as reported in **Table III.5**. They were chosen as extreme factors: weak (50 rpm) or vigorous (400 rpm) stirring, short (5 min) or long (30 min) extraction time and heating (60 °C) or room temperature (25 °C). For the hydrotrope concentration, the first level was defined at 15 wt.%, the concentration which solubilizes 2.7 g/L of CA, *i.e.* the expected concentration of CA if all the available CA in the 5 g of rosemary is extracted. The second level was chosen at the minimum concentration which is able to solubilize the highest concentration of CA, *i.e.* 30 wt.% (see **Figure III.19**).

Table III.5. Factors and levels of the experimental design.

Levels	X_1 Stirring (rpm)	X_2 Time (min)	X_3 [Hydrotrope] (wt.%)	X_4 Temperature (°C)
Low (- 1)	50	5	15	25
High (+ 1)	400	30	30	60

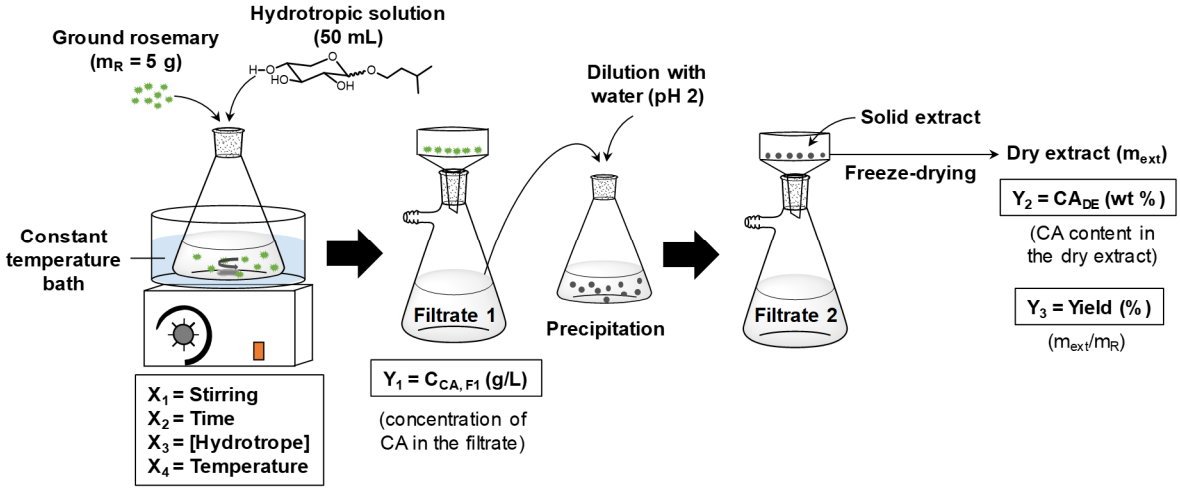

Figure III.33. Schematic representation of the different steps for the extraction of CA from ground rosemary with factors X_i and responses Y_i of the experimental design.

b. Calculation of the effects

A 2^4 factorial design was then constructed leading to 16 experiments (**Figure III.34**). The hydrotropic extraction process requires at least three steps (**Figure III.33**): *i)* maceration in the hydrotropic solution, *ii)* dilution below MHC and precipitation and *iii)* filtration of the precipitate to recover the solid extract. This wet solid extract is then freeze-dried. To evaluate the effect of the selected factors on the whole process, three responses were quantified: *i)* the CA concentration in the first filtrate after maceration ($Y_1 = C_{CA, F1}$ (g/L)), *ii)* the CA content in the dry extract ($Y_2 = CA_{DE}$ (wt.%)) and *iii)* the mass yield of the extraction (Y_3 = Mass yield (%)).

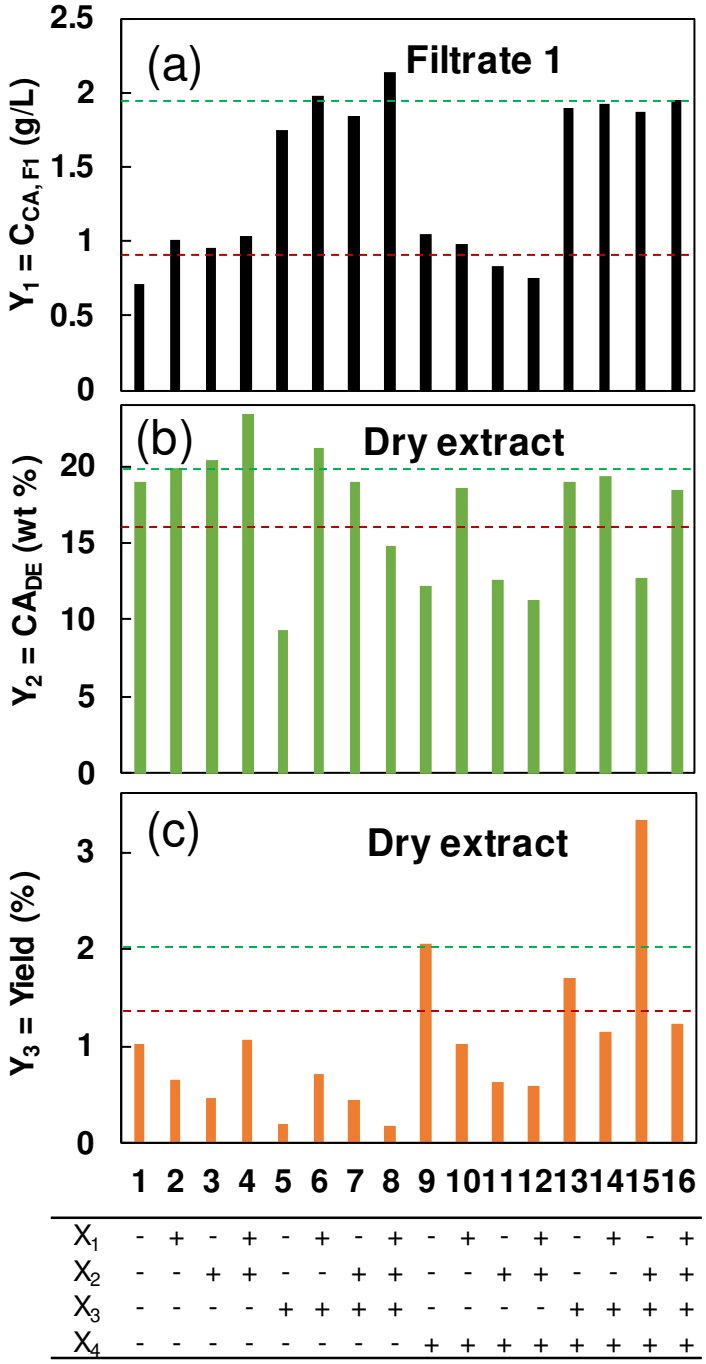

Figure III.34. 2^4 Factorial matrix of the 16 extractions of the experiment design performed with *i*-C_5Xyl and results on (a) the concentration of CA recovered in the filtrate after plant/solution extraction and separation, (b) the purity of CA in the dry extract and (c) the mass yield of the extraction.

The analysis of the results of the experimental design shown in **Figure III.34** leads to a mathematical expression (**Eq.III.7**) for each responses (Y) using the calculated coefficients b_i, referring to the effect of the factor i (i = 1 to 4), b_{ij} referring to the interaction between a factor i and a factor j, b_{ijk} and b_{ijkl}, referring to the interactions between the factors i, j and k or i, j, k, l respectively.

$$Y = b_0 + b_1 X_1 + b_2 X_2 + b_3 X_3 + b_4 X_4 + b_{12} X_1X_2 + b_{13} X_1X_3 + b_{14} X_1X_4 + b_{23} X_2X_3 + b_{24} X_2X_4 + b_{34} X_3X_4 + b_{123} X_1X_2X_3 + b_{124} X_1X_2X_4 + b_{134} X_1X_3X_4 + b_{234} X_2X_3X_4 + b_{1234} X_1X_2X_3X_4 \quad \text{(III.7)}$$

Table III.6 presents the calculated coefficients for the three responses. One experiment has been triplicated in order to get a standard deviation for each response (SD_Y) from which the standard deviation of the coefficients is calculated (SD_{bi}). Then, taking into account the Student coefficient (t) a significance threshold ($t.SD_{bi}$) can be calculated with a confidence level of 99 (***), 98 (**) and 95% (*) for each response. All the coefficients b_i, b_{ij}, b_{ijk} or b_{1234} below this threshold can be deleted from the mathematical expression. Significant coefficients are indicated in bold in **Table III.6**.

Table III.6. Estimated b coefficients of regression models using a 2^4 factorial design.

Coeff.	**Filtrate 1**	**Dry extract**	
	$C_{CA,\,F1}$ (g/L)	**CA_{DE} (wt.%)**	**Mass yield (%)**
b_0	**1.42*** **	**16.95*** **	**1.03*** **
b_1	0.05	**1.42***	- 0.21
b_2	0.01	- 0.37	- 0.04
b_3	**0.50*** **	- 0.21	0.09
b_4	- 0.01	**- 1.42***	**0.44****
b_{12}	- 0.01	**- 1.02***	- 0.02
b_{13}	0.03	0.31	- 0.10
b_{14}	- 0.06	- 0.02	**- 0.26**
b_{23}	0.03	- 0.12	0.21
b_{24}	- 0.06	**- 1.40***	0.02
b_{34}	0.00	**2.06****	**0.30***
b_{123}	0.02	- 0.32	- 0.27
b_{124}	0.01	0.72	- 0.05
b_{134}	0.01	- 0.17	- 0.10
b_{234}	0.03	0.08	0.23
b_{1234}	- 0.01	**1.94**	- 0.05
SD_Y	0.11	0.89	0.24
SD_{bi}	0.03	0.22	0.06
$t.SD_{bi}$(95%)	0.2	1.0	0.3

* Significant with a confidence level of 0.95, ** Significant with a confidence level of 0.98, *** Significant with a confidence level of 0.99.

c. Increase in the concentration of carnosic acid extracted from rosemary (Y_1)

Regarding the CA concentration in the filtrate after maceration (**Table III.6**), b_3 is the only significant coefficient ($p < 0.01$). Thus, the concentration of hydrotrope (X_3) is the only factor which has a significant influence on the maceration and the mathematical expression is greatly simplified (**Eq.III.8**).

$$C_{CA,\,F1} = 1.42 + 0.50\,X_3 \qquad \text{(III. 8)}$$

The stirring (X_1), the time (X_2) and the temperature of extraction (X_4) can be fixed to the level -1 or +1 with nearly no influence on this step. This constitutes a great difference compared to DES extraction of CA from rosemary, which highly depend on time and temperature.[63] This is well perceptible in the results. Indeed, two distinctive groups stand out (**Figure III.34.a**): experiments 1 to 4 and 9 to 12 were performed with 15 wt.% *i*-C_5Xyl and clearly give less efficient results ($Y_1 \approx 0.9$ g/L) than those for which $X_3 = 1$, which used 30 wt.% of hydrotrope ($Y_1 \approx 1.9$ g/L, exp 5 to 8 and 13 to 16). To better visualize the effect of the hydrotrope concentration, **Figure III.35** represents the factor X_3 on the horizontal axis, and the factors X_1, X_2 and X_4 on the vertical axis. The mean value of the response for $X_3 = +1$ ($Y_1 = 1.9$) and for $X_3 = -1$ ($Y_1 = 0.9$) are indicated and marked with a red or green rectangle.

(a) $b_3 = 0.5$

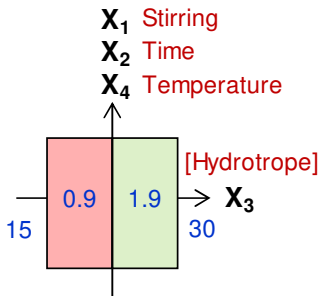

Figure III.35. Representation using NemrodW® of the significant principal effect b_3 for Y_1 ($C_{CA,\,F1}$) of the experimental design of rosemary extraction by *i*-C_5Xyl.

d. Increase of the carnosic acid content (Y_2)

With regards to the CA content in the dry extract, the mathematical model can be expressed as followed (**Eq.III.9**):

$$Y_2 = 16.9 + 1.4\,X_1 - 1.4\,X_4 - 1.0\,X_{12} - 1.4\,X_{24} + 2.1\,X_{34} \qquad \text{(III. 9)}$$

The coefficient b_{1234} is not taken into account since it is generally neglected in regard to other interaction coefficients. Its value is probably due to a small lack of fit of the expression of the mathematical model, but this should not interfere with the interpretation of the effect of the X_i factors on CA_{DE}. Since the mathematical model includes the coefficients b_{12}, b_{24} and b_{34} which are significant, the corresponding interactions are represented in **Figures III.36** and ranked by

decreasing importance. Inside each square is indicated the value corresponding to the average of the responses. Green zones correspond to favorable conditions for increasing CA_{DE}. It can be seen that for each of the three interactions studied separately, a CA content greater than 19.4 wt.% is obtained. On the opposite, red areas are operating conditions that should be avoided, otherwise CA contents will drop below 15 wt.%. These CA content levels (19.4 and 15 wt.%) have been materialized with two horizontal dashed lines in **Figure III.34.b**.

The study of the interactions reveals non-simultaneous favorable conditions for all the factors. However, there are several possible operating conditions to obtain a CA content in the dry extract greater than 19.5 wt.% (**Figure III.36**). That for, two factors must be set in accordance with one or two of the three favorable cases ($X_1 = 1$, $X_2 = -1$) or ($X_2 = 1$ and $X_4 = -1$) or ($X_3 = X_4 = -1$) but at the same time, no unfavorable conditions must be realized ($X_1 = X_2 = -1$) or ($X_2 = X_4 = 1$) or ($X_3 = -1$, $X_4 = 1$).

According to the study of the X_3X_4 interaction (**Figure III.36.a**) which is the most important ($b_{34} = 2.06$), the best conditions are a low hydrotrope concentration (15 wt.%) and a low temperature (25 ° C). This effectively corresponds to experiments 1 to 4 for which the response Y_2 (CA_{DE}) is greater than 19 wt.%. On the other hand, if the extraction is performed at high temperature (60 °C) and with a low hydrotrope concentration (15 wt.%), the conditions are very unfavorable and the CA content will be very low ($Y_2 = CA_{DE} < 13$ wt.%, Exp 9, 11 and 12 in **Figure III.34**). Heating the solution can promote the degradation of CA, or the extraction of undesired components from rosemary (hereafter referred to as "by-products") and therefore decrease the selectivity of the extraction.

Another way to reach 19 wt.% content (**Figure III.36.b**) is to keep the temperature low ($X_4 = -1$) and work with a high stirring speed ($X_2 = +1$), corresponding to experiments 3, 4 and 7 in **Figure III.34.b**. This confirms the deleterious effect of the temperature on CA content despite it has no effect on the concentration of CA in the filtrate, and highlights the influence of the stirring. All unfavorable conditions excluded, **Figure III.36.c** shows that a high CA content ($CA_{DE} > 19$ wt.%) can alternatively be obtained with a high stirring speed and short maceration time, as depicted by the responses of experiments 2, 6 and 14 of **Figure III.34.b**. This suggests that the extraction of by-products is avoided by stopping the extraction after 5 min, without affecting the CA recovery. In other words, the extraction of CA seems faster than the by-products one.

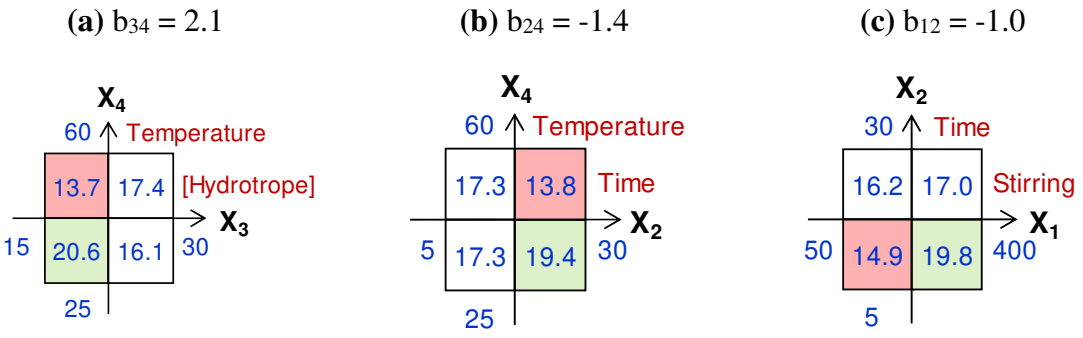

Figure III.36. Representation using NemrodW® of the significant principal interactions X_iX_j for Y_2 (CA_{DE}) responses of the experimental design of rosemary extraction by *i*-C_5Xyl.

e. Increase of the mass yield (Y_3)

Considering only the interactions of first order (neglecting the 2nd order interaction b_{123} which again might come from a faulty fit of the model), **Eq.III.10** expresses the overall mass yield Y_3 as a function of factors X_i.

$$Y_3 = 1.0 + 0.4\,X_4 - 0.3\,X_{14} + 0.3\,X_{34} + 0.2\,X_{23} \qquad \text{(III. 10)}$$

Temperature (X_4) is a very important factor since it constitutes the most important effect (b_4) and is involved in the two most important interactions (b_{34} and b_{14}). **Figures III.37 a** and **b** show that the most favorable conditions for the most important interactions (X_3-X_4 and X_1-X_4 respectively) are a high hydrotrope concentration, a high temperature and a low agitation. Indeed, experiments 13 and 15 meet all those conditions and their mass yields are higher than 1.7% (**Figure III.37.c**), whereas the medium mass yield is 1.0%. The highest mass yield (3.3%) is reached for the experiment 15 which meet all the favorable conditions. On the opposite, when an unfavorable condition of the 2 main interactions is achieved (Exp 1, 3, 5-8), the mass yields drop to less than 1% (**Figure III.34.c**). Therefore, the most important condition to maximize the mass yield is to perform the extraction at 60 ° C.

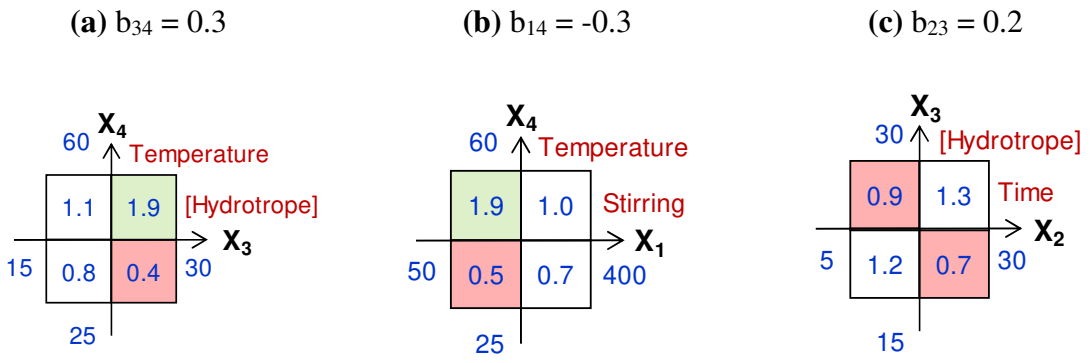

Figure III.37. Representation using NemrodW® of the significant principal interactions X_iX_j for Y_3 (Mass yield) responses of the experimental design of rosemary extraction by *i*-C_5Xyl.

f. Best compromise between Y_1, Y_2 and Y_3

Among the four studied variable factors, the higher the hydrotrope concentration, the higher the CA concentration in the filtrate (Y_1), while temperature, stirring and time have no significant effect on $C_{CA,\,F1}$ after the first step of extraction. The two responses Y_2 and Y_3 are mainly governed by the X_3X_4 interaction ([hydrotrope]/temperature) but **Figures III.36.a and III.37.a** show that the most favorable areas for Y_2 and Y_3 are opposite. Thus it is not possible to maximize Y_2 (CA content in the dry extract) and Y_3 (mass yield) at the same time. With a high temperature and with a high hydrotrope concentration, an important concentration of both CA and by-products are extracted and thus recovered in the dry extract, which is characterized by a low CA content (low Y_2), but in return by a high mass of extract (high Y_3). It follows that

high temperature and hydrotrope concentration cause the extraction of by-products from rosemary while CA extraction would not be favored by this combination.

III.3.3. Optimization of the hydrotropic extraction with *iso*-amyl xyloside

a. Optimal hydrotrope concentration

To adjust the hydrotrope concentration more precisely, extractions of ground rosemary leaves were performed at room temperature for 30 min under intermediate stirring (250 rpm). The concentration of CA was analyzed in the filtrate, as shown on **Figure III.38**. Noteworthy, the efficiency of the hydrotropic solution increases from the MHC to a plateau at 18 wt.%, at which the concentration of CA extracted remains stable between 2 – 2.1 g/L. Indeed, a solution with a medium *i*-C_5Xyl concentration of 18 or 22.5 wt.% has the same efficiency as the hydrotropic solution at 30 wt.%. This is of particular interest for a future industrial process since it allows to limit *i)* the cost related to hydrotrope and *ii)* the dilution factor required to pass below the MHC.

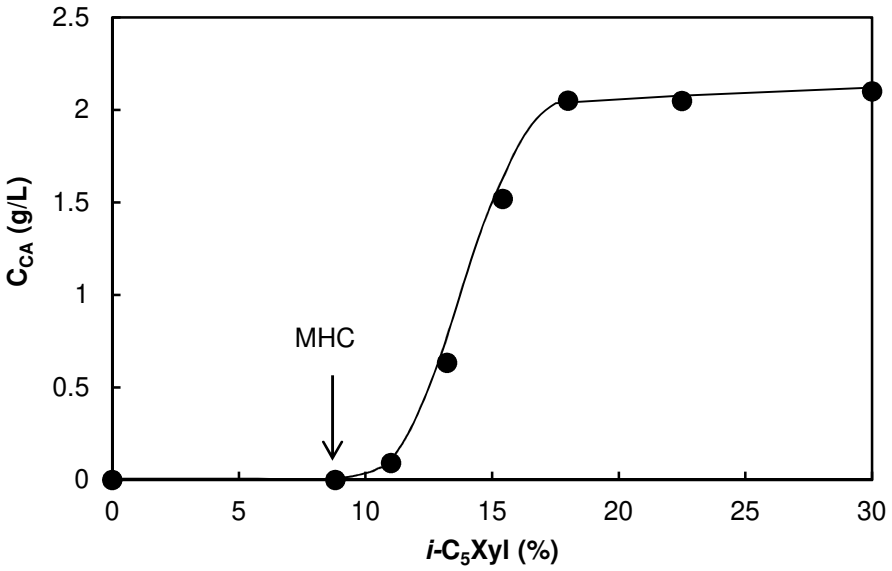

Figure III.38. Influence of the *i*-C_5Xyl concentration on the concentration of CA recovered in the filtrate after 30 min of extraction at 25 °C, pH 2.

b. Optimal time

Finally, to complete the experiments of the factorial design, which showed no effect of increasing the time from 5 to 30 min, we studied the kinetics of the extraction from 5 to 60 min. This kinetic study, showed in **Figure III.39**, confirmed that the concentration of CA in the filtrate reached a plateau after only 5 min of extraction (the first sampling) and slightly decreased when the time increased to 1 h. This can be attributed to the degradation of CA. However, at a large scale, it should be difficult to operate an extraction of less than 30 min, so

this time was kept as the optimal one for the following study. After 30 min of extraction with 22.5 wt.% *i*-C_5Xyl at room temperature, 57 % of the available CA were recovered in the filtrate.

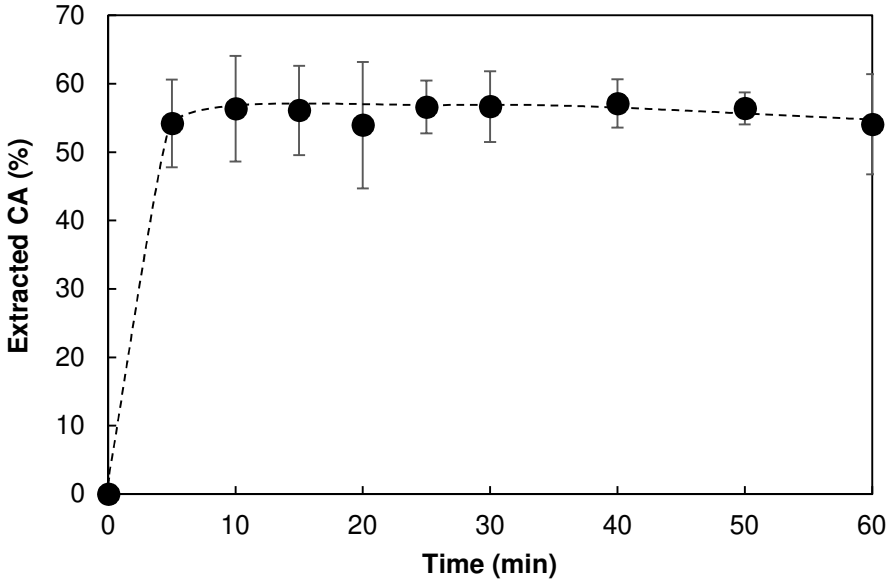

Figure III.39. Kinetic study of the estimated amount of extracted CA in the hydrotropic solution, considering that 20 % of the hydrotropic solution is absorbed by the plant. Extractions performed with aqueous solutions at 22.5 wt.% *i*-C_5Xyl, at 25 °C, pH 2.

III.4. Experimental part

III.4.1. Composition of the alkyl polyglycosides C_iGlyco

a. Thermogravimetric analysis (TGA) and proton nuclear magnetic resonance (^{1}H NMR)

TGA: 10 mg of the commercial mixtures were heated under nitrogen 10 °C/min from 30 to 500 °C on a TA Instruments TGA Q/50 apparatus.

^{1}H NMR: All alkyl polyglycosides were freeze-dried until constant mass, dissolved in D_2O and analyzed with a Brücker apparatus (300 MHz).

b. Mass spectroscopy analysis.

Appyclean 6505, Sepiclear G7 and Appyclean 6781 (commercial forms of *i*-C_5Xyl, C_7Glu and $C_{8/10}$Glyco) were freeze-dried over 24 h and then analyzed by FIA-HRMS and a LC-MS method on a Q-TOF mass sprectrometer maXis (Brüker). The nebulizer gas was set at 0.6 bar and 2.0 bar respectively, the dry gas flow at 7.0 L/min and 9.0 L/min respectively and for both analyses,

the capillary voltage was set at 4000 V. The mass spectrometer was equipped with a C_{18} column from Waters (UPLC HSS T3 – 2.1 x 100 mm – 1.7 µm) maintained at 40 °C. The mobile phase was composed of (A) 0.1% formic acid/water and (B) 0.08% formic acid/acetonitrile. The multi-step linear solvent gradient used was: 0-0.2 min, 3 %B; 0.2-6 min, 3-60% B, 6-6.5 min, 60-90% B, 6.5-7.5 min, 90% B 7.5-7.6 min, 90-3% B and 7.6-8.6 min, 3% B; flow rate 500 µL/min; injection volume 2.5 µL.

III.4.2. Physicochemical properties and descriptors of alkyl polyglycosides C_iGlyco and alkyl monoglycerols C_iGly

a. COSMO-RS calculations of the log *P* and V_m values

See section II.6.4

b. Critical Aggregation Concentration (CAC) determination by tensiometry

See section II.6.3.

III.4.3. Solubility curves of rosemary contituents, fatty acids and alkyl gallates in hydrotropic aqueous solutions.

Solubility curves of CA in C_iGlyco and C_4Gly were performed following the procedure of section II.6.2. For other solutes, same procedure was followed with adapted solute. The amount of solubilized solute was determined by HPLC quantification (for RA, UA, alkyl gallates and fatty acids) or GC quantification (camphor).

a. Quantification of camphor by GC-FID

Hydrotropic solutions (500 µL) were extracted with 500 µL of ethyl acetate and then, diluted by a factor 10 or 100 depending on the concentration of camphor. Analyses were performed using an Agilent GC Trace apparatus equipped with a PTV injector and a FID detector 6890N/G1530N. The PTV injector (injection = 2 µL) was held at 80 °C for 2 min, then heated at 20 °C/min to 260 °C and maintained at this temperature for 6 min. Separation was achieved on a 30 HP-1 methyl siloxane column with 320 µm internal diameter and 0.25 µm film thickness (Agilent J&W). The column was held at 80 °C for 3 min, then heated at 10 °C/min to 300 °C and maintained at this temperature for 10 min. Carrier gas (N_2) flow rate was set at 1 mL/min. The detector temperature was set at 300 °C.

b. Quantification of UA, RA, alkyl gallates and fatty acids by HPLC

Hydrotropic solutions were diluted by a factor 5 (or 100 in the case of RA) in MeOH (0.1 % TFA). Analyses were performed using an HPLC apparatus LC 20AD from Shimadzu equipped with an autosampler (injection = 10 or 20 µL), a Uptisphere C_{18} column (Interchim, 5 µm particle, 4.6 x 250 mm) maintained at 30 °C, a UV detector (SPD 20A) set at 210 nm for UA, 330 nm for RA, 275 nm for C_8, C_{12} an C_{16}G and 300 nm for C_3G or a ELSD LT-II Shimadzu detector maintained at 40 °C for fatty acids. The mobile phase was a mixture of MeOH (0.1% TFA)/water, in a 70:30 ratio for RA, 80:20 for C_3G and C_8G, 90:10 for UA, C_{12}G and C_{16}G and 100:0 for fatty acids in isocratic mode, with a flow rate set at 1 mL/min.

III.4.4. Contact angle measurements

Homogeneous solutions were prepared with 30 wt.% hydrotrope in water. Leaves were chosen as straight as possible and stuck by a double-sided adhesive tape on a microscopic lamella which was locked to the base. Thanks to a syringe, a droplet of 2 µL of hydrotropic solution was deposited on the leaf surface. Contact angles were captured with a Drop Shape Analyser (DSA – 100, Krüss) equipped with a camera. The angle between the drop and the surface of the leaves was measured by the software of the apparatus (Advance).

III.4.5. Hydrotropic extractions

a. With whole rosemary leaves

See section II.6.5.a

b. Typical extractions with ground rosemary leaves

Hydrotropic solutions were prepared at the specify hydrotrope concentrations and acidified at pH 2 with 1% (v/v) phosphoric acid. Extractions were performed by macerating ground rosemary in the hydrotropic solution with a solid:liquid ratio 1:10 w:v under magnetic stirring (250 rpm) at room termperature (25 °C) during 30 min, unless for the kinetic study (several samplings between 0 and 60 min). The volume of solution, the hydrotropes, plants and the hydrotrope concentration are precised in **Table III.7**. Then, plants were separated by Büchner filtration (cellulose filter, Φ = 8 µm) and the concentration of CA in the filtrate was quantified by HPLC.

Table III.7. Different experimental conditions for typical extractions.

section	Hydrotropic or surfactant solution			Plant	
	Amphiphile	Concentration (wt.%)	Volume (mL)	Type	Mass (g)
III.2.4	C_iGly, *i*-C_5Xyl	30	10	Rosemary Sage	1
III.3.1	*i*-C_5Xyl, C_7Glu, $C_{8/10}$Glyco	22.5 12 4	100	Rosemary	10
III.3.3.a	*i*-C_5Xyl	0 - 30	100	Rosemary	10
III.3.3.b	*i*-C_5Xyl	22.5	1000	Rosemary	100

c. Experimental design

Extractions were performed by macerating 5 g of rosemary in 50 mL of a hydrotropic solution (solid:liquid ratio 1:10 w:v) under magnetic stirring in the specific modalities defined by the experimental design (time, stirring speed, hydrotrope concentration and temperature). Plants were then separated by Büchner filtration (cellulose filter, Φ = 8 µm).

d. Typical precipitation method

The filtrates (section III.3.1 and III.3.2. Experimental design) were precipitated by sudden dilution with acidic water (H_3PO_4, 1% v/v, pH 2) to reach the MHC and thus, induce the precipitation of the extracts. Then, the solution was stirred at 350 rpm for 30 min and settled for 30 min. The precipitate was recovered by filtration under vacuum, using the specified filters (cellulose, Φ = 3 µm). Finally, they were diluted in MeOH (0.1 % TFA) to quantify their CA content by HPLC.

e. Experimental design statistics

The coefficients of effects, noted b, were calculated using Microsoft Excel. The experiment 13 was repeated three times to perform a "repeated measures Student t-test": the standard deviations $\sigma(Y)$ and $\sigma(b_i)$ of the response and the effects were calculated and the significance threshold with a 95, 98 or 99% confidence level were determined using the Student t-distribution table (two-tailed), with the corresponding *p*-value (< 0.05, 0.02 or 0.01) and a degree of freedom of 2 (3 repeated experiments -1). The determination of the significant X_iX_j interactions was performed with NemrodW®.

III.5. Conclusions of Chapter III

Agro-resources are increasingly attractive to replace petro-based organic solvents in common processes due to their generally higher biocompatibility. Therefore, **Chapter III** was dedicated to the investigation of the efficiency of CA extraction with aqueous solutions of commercial alkyl polyglycosides (C_iGlyco) with *i* ranging from 4 to 8 and synthetic alkyl monoglycerols (C_iGly), with $i = 4$ or 5. In addition, one C_iGlyco surfactant ($C_{8/10}Glyco$) was compared with hydrotropes. First, we have characterized the average structure of the C_iGlyco mixtures, which are very complex with a degree of polymerisation (DP) between 1 and 7, and found an average DP between 1.5 and 2.1, depending on the amphiphile. Thanks to this characterization, physicochemical properties such as MHC, CAC, surface tension were measured and descriptors such as HLB, log *P*, molecular volume, and molar mass were estimated for C_iGlyco, as well as for C_iGly and were used to validate the relationship between those descrptors and the efficiency of hydrotropes established in **Chapter II** for C_iE_j.

This way, we have also shown how agro-based C_iGlyco and C_iGly hydrotropes can extract more or less efficiently CA from rosemary. C_iGly and especially pentyl glycerol C_5Gly was very efficient regarding the extraction of whole and ground leaves of rosemary (1.07 g/L and 2.53 g/L CA recovered in the filtrate respectively, in comparison with a maximum concentration expected of 2.72 g/L). C_iGlyco were less efficient than C_iGly to extract CA but *iso*-amyl polyxyloside (*i*-C_5Xyl) has been highlighted as the most suitable C_iGlyco to extract CA from both ground and whole leaves compared to caprylyl/capryl polyglycosides ($C_{8/10}Glyco$) and heptyl polyglucosides (C_7Glu). This can be related with the fact that *i*-C_5Xyl has the lowest DP of the C_iGlyco series, and a short alkyl chain, and thus, a small molecular volume. In addition, the efficiency of *i*-C_5Xyl to solubilize more or less efficiently some products, depending on their partition coefficient was shown with homologous series of alkyl gallates and fatty acids, and phytochemicals of rosemary. This partition coefficient - solubilities relationship presage finer selectivity during the extractions compared to the use of solvents, for which the solubility depends more on the polarity than the amphiphilicity.

The optimization of the extraction parameters with *i*-C_5Xyl by a 2^4 factorial design showed that in a first step, it is important to extract CA with a relatively high hydrotrope content, *i.e.* 30 wt.% rather than 15 wt.%. Then, we have shown that this concentration can be lowered to 18 wt.% without affecting the efficiency of the extraction. Moreover, the temperature during extraction (step 1) also plays a key role for the precipitation (step 2) of the insoluble material. At high temperature (60 °C rather than 25 °C), extracts with a high mass yield but a low purity in CA are produced, suggesting the extraction of a higher fraction of by-products at high temperature. Inversely, the maximum purity of 23.3% was obtained after extractions performed at low temperatures but in detriment to the mass yield. The stirring speed, the concentration of hydrotrope and the time have less impact but interactions with temperature were found.

Chapter IV. Optimization of the rosemary extract recovery and purification

The recovery of a solid extract in the context of a solvent extraction can be a simple and efficient step performed by evaporation. In order to ensure the competitiveness of a hydrotropic extraction compared to a solvent extraction, a simple and energy saving technique must be designed and optimized to recover all the extracted target molecules.

As mentioned in the literature review (**Chapter I**), three main methods are described to ensure the precipitation or crystallization of the extracts: *(i)* evaporating or distilling the solvent, which are convenient methods given their low boiling point, *(ii)* cooling the solution when the solubility of the solute depends on the temperature *(iii)* adding an anti-solvent. Moreover, the Hydrotropic Cloud Point Extraction (HCPE) using C_4E_1 as the hydrotrope failed to efficiently recover CA due to its high thermodegradability (**Chapter II**). Therefore, this chapter focuses on **optimizing the recovery of a hydrotropic extract of rosemary either by cooling or dilution.** Considering the results of **Chapter III**, extractions were performed with alkyl polyglycosides (C_iGlyco), in particular with *i*-C_5Xyl, which was determined to be the optimal hydrotrope in regards to its efficiency, commercial availability and biodegradability.

IV.1. Precipitation of the extract by cooling

Among the reported hydrotropic extractions in the literature, only a few use a cooling process for the recovery of a solid extract. This has been described for the extraction of piperine from NaCS solution, concentrated at 1 M (MHC = 0.1 M). Gaulkar and Gaikar concluded that this technique was “a better option compared with the precipitation by dilution” because it avoids the use of large volumes of water and the hydrotropic solution can directly be reused.[119] In addition, a high purity precipitate (95 %) could be obtained by cooling from 80 to 30 °C a hydrotropic solution of sodium cumene sulfonate (NaCS) used to extract diosgenin, a phytosteroidal saponin, from dioscorea rhizomes. However, the amount of diosgenin in the precipitate was small, and the authors found it more efficient to combine cooling and dilution with water, giving a precipitate with higher mass yield but lower purity, and then washing the precipitate to remove undesirable products.[222] Out of these two examples, to our knowledge, the precipitation or crystallization of a hydrotropic extract only by cooling has never been reported again.

Thus, based on the understanding of the physicochemical phenomena induced by cooling and involving crystallization, which are first reviewed in this section, and after studying crystallization in model solutions containing pure CA, the precipitation of CA from hydrotropic extracts of rosemary has been attempted by this way.

IV.1.1. Influence of the temperature on physicochemical phenomena involved in the solubilization process

a. Relationship between temperature, solubility and crystallization in solvents

In solvents, the solubility of an organic compound results of a competition between solute-solvent, solute-solute, and solvent-solvent interactions, which can be hydrogen bonds, Van der Waals interactions, or "hydrophobic interactions". For example, in a polar solvent like water, strong hydrogen bonds organize the molecules between them, the system must therefore spend energy to insert different molecule between those of the solvent since it will destructure the network.[223] To decrease the energy of the system, solute-solvent interactions are created provided that they have similar polarities: this is the 'like dissolves like' theory.

A temperature increase induces the breakdown of hydrogen bonds and less optimal polar interactions. The effect can occur on both the solute-solvent and the solvent-solvent interactions. However, in the case of organic compounds (or salts), an increased solubility is generally observed during heating, and can be explained by a reduction in the structuring of the solvent, inducing less energy required to solubilize a molecule. This effect can be represented by the Apelblat model (**Eq.IV.1**), with S, the solubility of the solute, S_0 = 1 mol/kg, the constants A, B and C constants relative to the solvent-solute system, and T (K) the temperature.[224]

$$\ln\left(\frac{S}{S_0}\right) = A + \frac{B}{T} + C \ln(T) \qquad (IV.1)$$

Moreover, remarking that the water-solubilities of 47 solutes including for example amino acids or sugars exponentially increase with temperature, an empirical model (**Eq.IV.2**) has also been proposed with "*a*", the solubility at 0 °C and "*b*" a constant depending on the solvent-solute system.[225] Thanks to this model, the temperature gap required to double the solubility can be calculated, and is comprised between 10 and 70 °C, depending on the solute, with an average value of 20 °C. In other words, increasing the temperature of 20 °C causes the solubility to double.

$$S = a\, e^{b\,T} \qquad (IV.2)$$

The same behavior has been observed for the solubility in organic solvents, for example, the dissolution of *p*-nitrophenylacetonitrile was measured in sixteen organic solvents between 5 and 60 °C. The Apelblat model was found to be effective in modelling solubility curves, and by analyzing data from the literature, the empirical model also fits the curve, as shown for the solubilization of *p*-nitrophenylacetonitrile in ethanol in **Figure IV.1**.[226] Thanks to the temperature dependence of solubility, supersaturation can be achieved by cooling. However, the particles do not crystallize as soon as the saturation curve is reached: there is a metastable zone, as shown in **Figure IV.2**. Nucleation, which is the first part of the crystallization process, occurs spontaneously when the metastable zone limit is reached. Then, the particles grow

bigger, so less and less material is solubilized, and the effective supersaturation decreases. The metastable zone width can be increased by rapid cooling for example, but it is hardly predictable.[227,228]

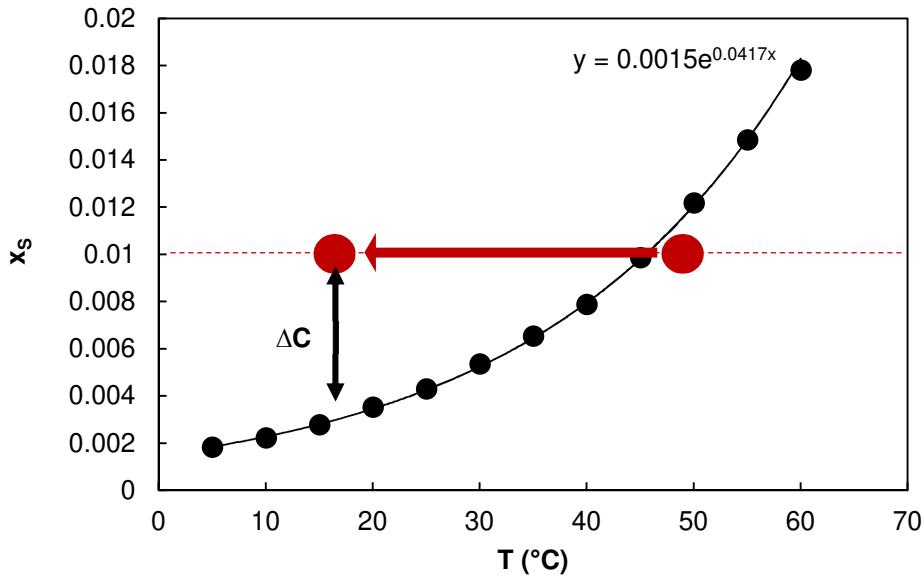

Figure IV.1. Evolution of the *p*-nitrophenylacetonitrile molar fraction (x_S) in ethanol with temperature from ref[226] and representation of the supersaturation (ΔC) obtained by cooling.

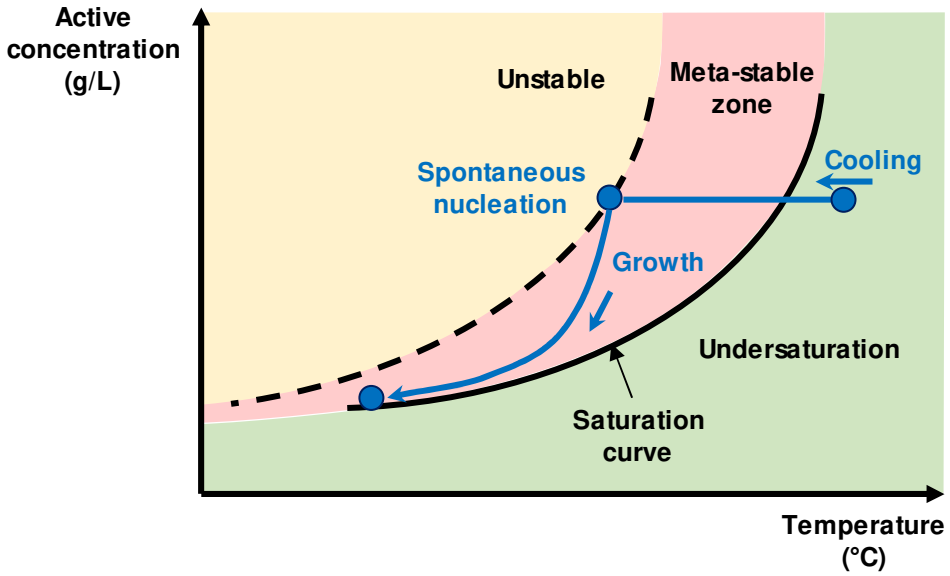

Figure IV.2. Solubility (saturation) curve and typical de-supersaturation profile during crystallization induced by cooling, adapted from Billot et al.[229]

In comparison, an aqueous solution of an organic compound solubilized in aggregates of surfactants or hydrotropes is a more complex system since the interactions between the three

components (water, amphiphile, solute) must be considered in addition to the solute-solute, amphiphile-amphiphile and water-water interactions.

b. Aggregation and solubilization in aggregates

Temperature dependence of the Critical Aggregation and Micellar Concentrations (CAC and CMC)

Surfactants and hydrotropes aggregate above their CMC and CAC respectively, and this aggregation is enabled by amphiphile-amphiphile, amphiphile-water and water-water interactions. For many types of surfactants, a decrease in temperature induces an increase in CMC as measured for $C_{12}E_8$, sodium dodecylbenzene sulfonate (LAS), sodium dioxyethylene glycol monododecyl sulfate (SLES) and rhamnolipids (mono-rhamnose, $C_{10}C_{10}R_1$ and di-rhamnose $C_{10}C_{10}R_2$) at 25 and 10 °C.[230] This effect suggests that surfactants are more hydrophobic while increasing temperature (lower CMC indicates higher hydrophobicity) and may be explained by the breaking of hydrogen bonds between amphiphiles and water due to molecular agitation, the same well-known effect that explains the cloud point phase separation. On the opposite, at a lower temperature, amphiphiles make more interactions in water, so they seem more hydrophilic, and CMC occurs at higher concentration.

A comprehensive analysis of the evolution of CMC with the temperature for ionic surfactants[231] such as SDS or dodecyl trimethyl ammonium bromide showed that CMC first decreases when the temperature increases from 10 to 25 °C, then increases above 25 °C. This indicates a competition between a higher hydrophobicity given by the breaking of solute-solvent hydrogen bonds and higher hydrophilicity due to lower hydrophobic effect. Indeed, the water disorder at high temperature makes the presence of a surfactant molecule in water less expensive in energy, therefore the hydrophobic effect is weakened and the surfactant becomes apparently more hydrophilic (indicated by the CMC increase). This behavior has also been observed for non-ionic surfactants such as dodecyl polyethylene glycol ethers ($C_{12}E_j$, with j = 4, 6 or 8)[232] and decyl glucoside (β-C_{10}Glu)[233], which have a minimum CMC at 50 °C and 35 °C respectively.

Regarding hydrotropes, the evolution of the CAC with temperature remains uncertain but it is likely that same behaviors occur for surfactants and hydrotropes since they are of similar structure. Moreover, if aggregation is considered to be a prerequisite for solubilization, a CAC change should induce a change in solubilization behavior.

Influence of the temperature on the solubility

The solubility curves of many organic compounds such as piperine[119], andrographolide[107] or alizarin[234] were measured in hydrotropic solutions of NaCS (piperine), NaBMGS (andrographolide), NaPTS, citric acid or nicotinamide (alizarin) at different temperatures (from 25 to 80 °C for piperine and andrographolide, at 50 and 60 °C for alizarin). In all cases, the solubility increased with temperature, and interestingly, the MHC and the C_{max} did not

change.[234] Noteworthy, the increase in solubility of piperine with temperature in NaCS solution has been adequately correlated with an exponential function, in the form of equation (Eq.IV.2), which had been established for solvents.

The particularities of the physicochemical phenomena involved in the increase in solubility due to heating in hydrotropic solutions have been investigated. A molecular dynamics simulation of the NaCS-water system showed that aggregates are more likely to form at high temperatures (tested between 25 and 85 °C), due to a higher apparent hydrophobicity.[235] This easier formation of aggregates could explain the higher solubility of organic solutes. However, a calculation of the complexation constants of another study that investigated the solubility of two drugs (estrone and griseofulvin) in nicotinamide solutions at 20 and 40 °C revealed that the solute-amphiphile interaction would decrease with increasing temperature. The authors attribute the increase in solubility due to heating of these two drugs to their higher intrinsic water-solubility.[236]

Regarding short amphiphiles such as *i*-C_5Xyl, the evolution of their solubilization and aggregation with temperature has not yet been studied, their use as hydrotropes being quite recent.

IV.1.2. Measurements of the crystallization temperature

a. Turbidity as a crystallization indicator

The crystallization phenomenon involves nucleation and growth, which are complex and still poorly understood phenomena.[237] During nucleation, new particles are created, whereas during growth, the existing particles grow and the number of large particles increases. Noteworthy, in an industrial process, a maximum crystal growth is required to ensure efficient and easy recovery of the crystals by filtration.

When the crystals size reaches several micrometers, the solution becomes turbid, and the particle obscuration can be measured by light reflection.[237] Indeed, the turbidity probe (immersed into the solvent) emits light in the direction of a mirror, which reflects it back to the detector (**Figure IV.3**). In the presence of suspended crystals, the light is scattered in all directions and the intensity of the light beam is reduced. Then, an increase in turbidity indicates crystals growth.[237]

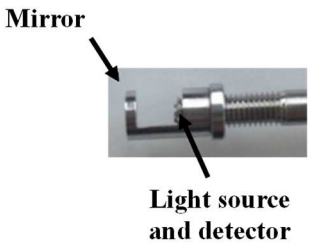

Figure IV.3. The turbidity probe emits a light beam in the solution to the mirror, which reflects it back to the detector.

Since turbidity can be measured only above a certain size of particles, its measure does not provide any information on the nucleation rate. However, from a practical point of view, such measurements are best suited to understand crystallization for the purpose of recovering an extract. For example, turbidity measurements were performed at several pH (between 2 and 12) to find the best one to precipitate the proteins extracted from canola meal. The maximum turbidity was found in the range of pH 4-6, indicating the precipitation of the proteins.[238]

In this study, the system of interest is basically composed of water, *i*-C_5Xyl and rosemary extract. However, since the extraction of rosemary leads to a crude extract composed of many molecules, the system was first simplified to three components: water, *i*-C_5Xyl, CA. Noteworthy, the pH was adjusted to 2 using 1 % (v/v) of H_3PO_4 to ensure that CA is not soluble in water, and to limit its degradation.[91] All measurements were performed at the University of Avignon using the Crystal Eyes (HEL) technology, which includes electronics, turbidity and temperature probes, PC and software (**Figure IV.4**). The solution was magnetically stirred and thermoregulated by the cooling circulator following the predetermined cooling and heating rates. However, the temperature was measured more precisely into the solution by the temperature probe because there is always a small difference between the controlled temperature in the water bath and in the solution due to heat loss or due to a delay caused by heat transfer through the double-walled (thermostated) beaker glass.

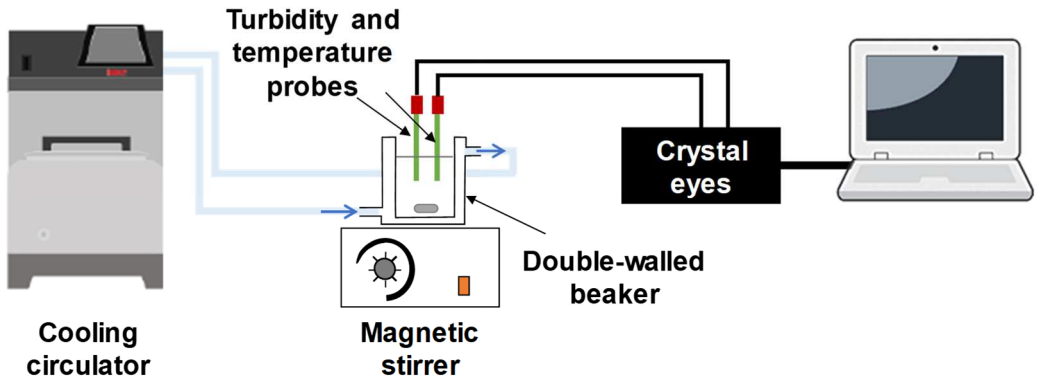

Figure IV.4. Crystal growth monitoring using Crystal Eyes® apparatus. The solution is magnetically stirred in a double-walled thermoregulated beaker. The temperature is controlled in the water bath of the cooling/heating circulator and checked in the vessel by the temperature probe. Finally, the turbidity probe send data to the computer.

At the beginning of the experiment, the solution must be completely limpid. Indeed, the turbidity (arbitrary unit) measures the sample obscuration, *i.e.* the amount of reflected light by the mirror. This measure is converted to a voltage signal and recorded by the WinISO software. Temperature was set above 70 °C at the beginning of each experiment to make sure that the solution was clear (a temperature of 75 °C set to the cooling circulator leaded to a temperature in the beaker of 72 – 73 °C). Then, two successive cooling cycles from 72 °C to 15 °C were

performed at a cooling rate of 2 °C/min, separated by a heating cycle (2 °C/min). The turbidity was automatically measured every 20 seconds.

Figure IV.5 plots the turbidity and the temperature *versus* time for two crystallization cycles using 9 wt.% *i*-C_5Xyl solution, corresponding to the MHC. The first observation is the confirmation of the increase in solubility while heating: at 70 °C, at least 0.3 g/L are solubilized whereas only 0.15 g/L are soluble at ambient temperature (section III.1.2). Moreover, during the first time of cooling (red curve) the turbidity stays almost constant below 0.5. A significant increase is then observed above 33 min, when the temperature drops below 36 °C, meaning that particles of several microns are generated and grow. Turbidity increases up to about 40 min (23 °C) and then, two phenomena are observed: *(i)* an overall decrease in turbidity, which generally relates to a reduction in crystals size, and *(ii)* several peaks, which are artefacts due to the deposit of large particles on the turbidity probe, between the mirror and the detector. Those peaks reflect the presence of sticky particles, which adhere to the probe and the glass walls of the beaker. They are removed from the probe after a few seconds thanks to the vigorous stirring. However, a pasty precipitate remains on the magnetic bar and at the bottom of the beaker. If the larger particles are sticky, they are likely to agglomerate each other and grow until they settle or get stuck on the walls. This could explain the reduction in turbidity.

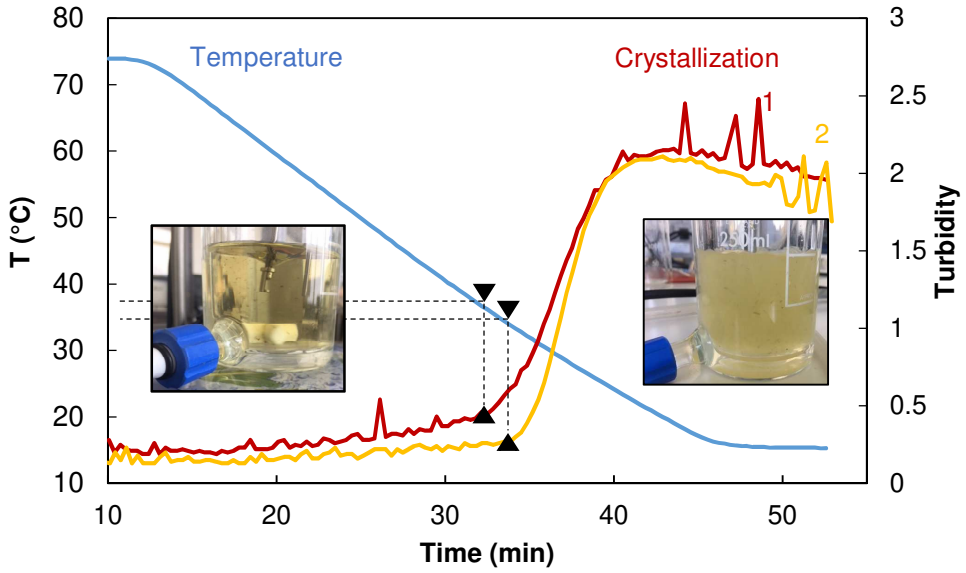

Figure IV.5. Evolution of the temperature (blue) and the turbidity during two cycles of crystallization of pure CA (0.3 g/L) in a 9 wt.% *i*-C_5Xyl solution at pH 2 in a double walled beaker. The turbidity during the first and second cycles are represented in red and yellow respectively.

After the first crystallization, the solution is heated to 75 °C, so that it becomes clear again. The evolution of turbidity during the second crystallization cycle is similar to that of the first, with a stable part, a sharp increase and then, and a slight decrease with peaks showing the presence of large sticky particles. However, the crystallization point is reached at lower temperature (34

°C). The thermodegradation of CA at high temperature could be responsible for the delayed crystallization by lowering the amount of CA that has to be solubilized, but this is not the best hypothesis since the degradation products of CA (*e.g.* carnosol) are not water-soluble either.[63] Moreover, the same surprising phenomenon has already been reported for the crystallization of L,D-malic acid in water.[237] Therefore, this effect must be related to a higher metastable zone width. For the next experiments, only the temperatures of the first crystallizations will be measured since they are more comparable to a simple cooling process. Also, a 5-points smoothing will be applied on the turbidity curves to facilitate their analysis.

b. The dependency of the crystallization temperature following to the hydrotrope concentration

In order to select the hydrotrope concentration for the extraction and CA crystallization tests, solutions of *i*-C_5Xyl at 9, 11 and 13 wt.% were compared. The composition of each system was adapted so that the CA concentration is the one of its saturation at room temperature, *i.e.* 0.15, 0.5 and 1.6 g/L respectively (**Figure IV.6b**). The turbidity and temperatures curves during the first crystallization and the dissolution steps are presented for each experiment.

At 9 wt.% (green curve, **Figure IV.6c**) and at 11 wt.% (red curve, **Figure IV.6d**), the turbidity increases as soon as the solution is cooled. Moreover, a sharp increase occurs when the temperature drops below 26 °C in case of the solution at 11 wt.%, whereas for the one at 9 wt.%, the transition is more progressive and earlier (28 min - 43 °C). The maximum of turbidity, is obtained for the solution at 11 wt.%, however, after having reached a maximum, the turbidity immediately reduces, meaning that agglomeration takes place (**Figure IV.6d**).

At 13 wt.%, the turbidity slightly increases from about 30 °C (**Figure IV.6e**). The turbidity does not increase above 1, so only few and small particles should have been generated. This latter point is problematic for the extraction because if 1.6 g/L cannot be crystallized efficiently, it is likely that a rosemary extract cannot be efficiently recovered by cooling either. However, CA is not the only molecule extracted from rosemary, and the presence of other molecules could allow the precipitation of the extract. One may even imagine that the impurities may be first precipitated, followed by CA in order to purified the extract.

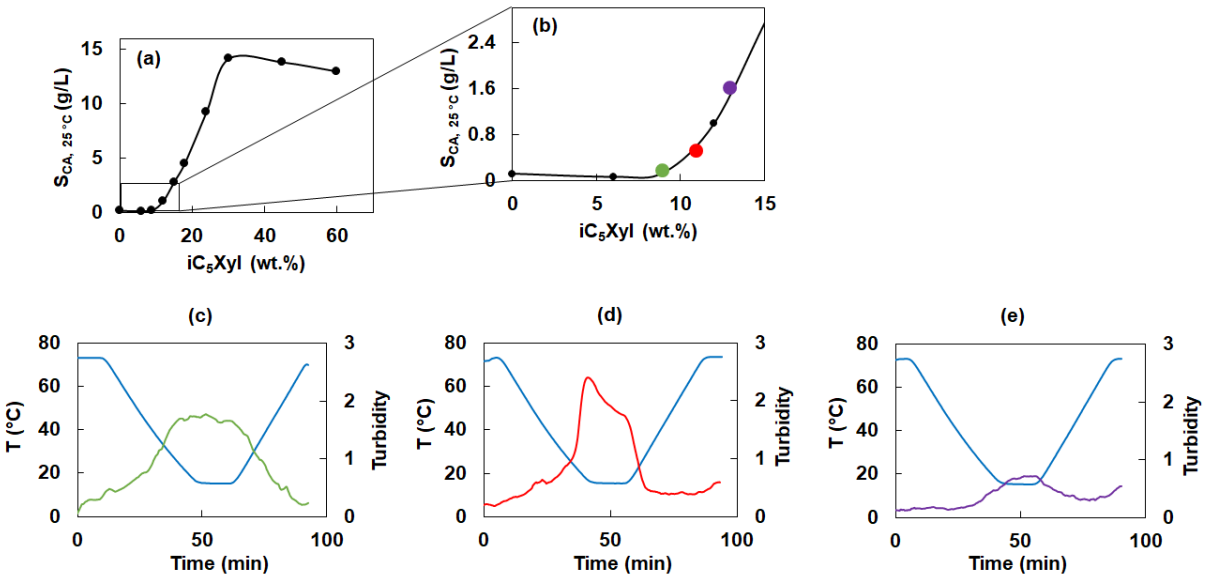

Figure IV.6. Entire solubility curve of CA at room temperature (25 °C) in *i*-C_5Xyl solutions (a), same solubility curve zoomed on the MHC (b). The green, red and purple dots represent CA concentrations used at 9, 11 and 13 wt.% of *i*-C_5Xyl for crystallization experiments (c, d, e). Turbidity (green, red or purple depending on CA- *i*-C_5Xyl concentrations) and temperature (blue) curves during first cooling and first heating cycles are presented. All experiments were performed at pH 2 to avoid CA deprotonation.

c. Influence of the extract concentration on the crystallization

To compare pure CA and a rosemary extract, the same turbidity experiments were performed with an extract enriched in CA (62.7 wt.%) obtained from an ethanolic extraction of rosemary. Using the 13 wt.% *i*-C_5Xyl solution, two concentrations of extract were tested and compared to pure CA (1.6 g/L): the same concentration of extract (1.5 g/L) and the same effective concentration of CA (2.5 g/L of extract). The results are presented in **Figure IV.7.**

The turbidity curves of the solutions containing 1.6 g/L of CA and 1.5 g/L of extract are very similar, but the precipitation of the extract gives higher turbidity, meaning that larger or more numerous particles are certainly formed. The same behavior is observed for the experiment performed with 2.5 g/L of extract, which showed a sharper increase in turbidity. Therefore, a rosemary extract containing 1.6 g/L of CA could be precipitated thanks to the presence of co-extracted products. Noteworthy, maximum concentrations of CA of 2 - 2.5 g/L can be expected from hydrotropic extractions with *i*-C_5Xyl according to our previous results in **chapter III.** Therefore, CA solubility at low temperature must be below 0.2 g/L to recover at least 90 % of the extract.

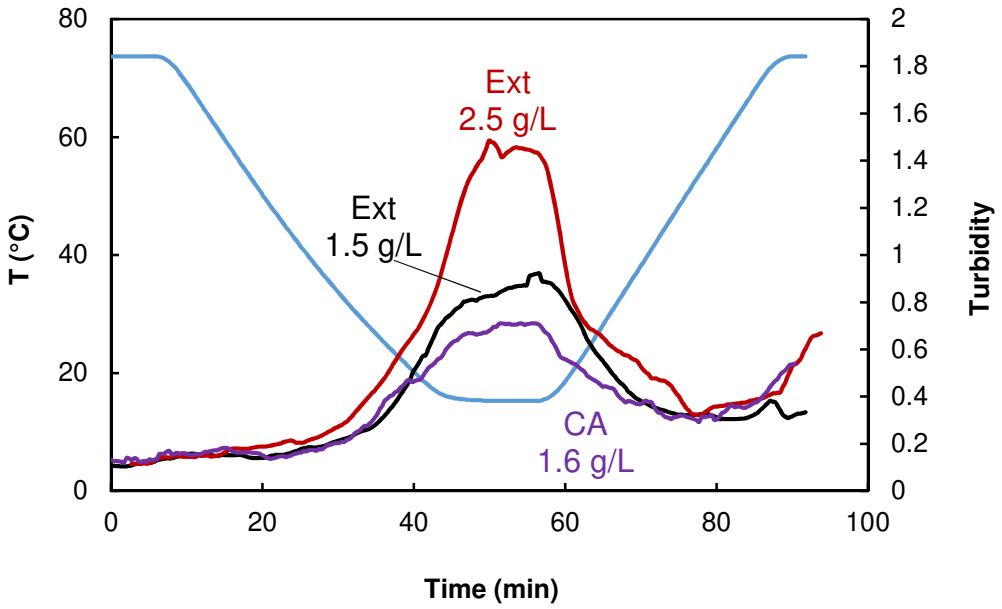

Figure IV.7. Temperature (blue curve) during a cooling and heating cycle and turbidity of solutions of *i*-C_5Xyl at 13 wt.%, pH 2 with 1.6 g/L of pure CA (purple), 1.5 g/L (black) and 2.5 g/L (red) of a rosemary extract (62.7 wt.% CA) loaded.

To check the compliance with this requirement, the turbidity of five 9 wt.% *i*-C_5Xyl solutions containing 0, 0.1, 0.25, 0.5 and 1 g/L of extract (62.7 wt.% of CA) was measured during a cooling and heating cycle (**Figure IV.8**). Solutions containing 0.25, 0.5 and 1 g/L seem to have similar behaviors: a sharp increase in turbidity is observed during the cooling step until reaching a value between 2 and 2.5, with a slight increase of the crystallization temperatures which occurs at 55, 56 and 60 °C respectively.

The temperature at the inflexion of the turbidity curves during the heating step can be considered as the dissolution temperature, and it was found to be between 45 and 50 °C when the extract concentration is comprised between 0.25 and 1 g/L. The differences between the crystallization and dissolution temperature comes from the metastable zone, which corresponds to about 10 °C in these cases. Regarding the solution containing 0.1 g/L of extract, its turbidity does not increase above 1, meaning that this precipitate may be harder to recover by filtration, and may thus constitute the concentration loss by a cooling process.

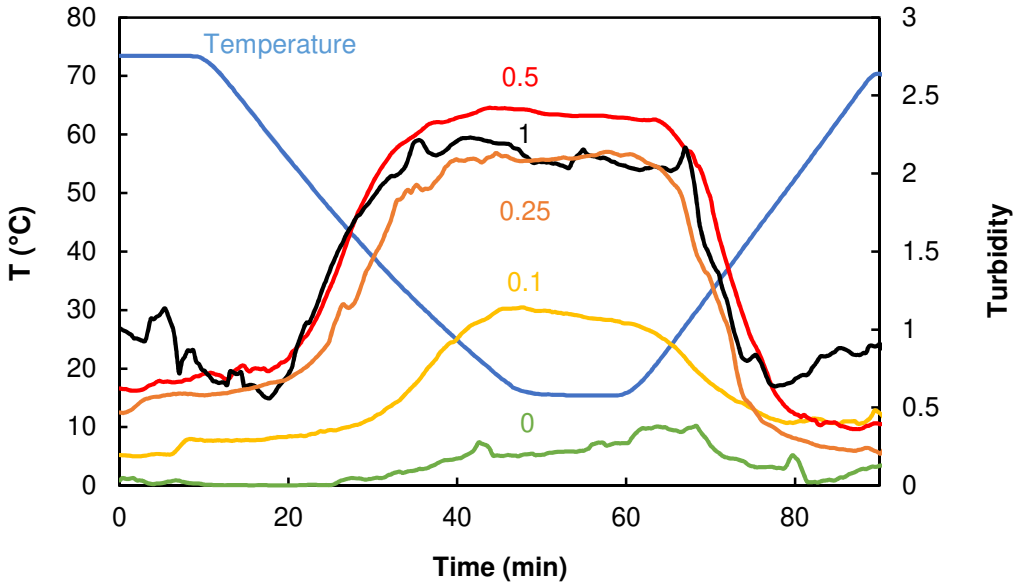

Figure IV.8. Temperature (blue curve) during a cooling and heating cycle and turbidity of solutions of *i*-C_5Xyl at 9 wt.%, pH 2 with 0, 0.1, 0.25, 0.5 and 1 g/L of a rosemary extract (62.7 wt.% CA) loaded, represented by the green, yellow, orange, red and black respectively.

IV.1.3. Precipitation of the rosemary extract by cooling

Solutions of *i*-C_5Xyl at 9 wt.% could be of interest for the extraction process followed by cooling because 0.25 to 1 g/L of extract can be solubilized above 50 °C but precipitate at low temperatures. Solutions at 13 wt.% seem less suitable despite the higher solubility of CA because precipitation could occur only if many co-products are extracted.

To verify those assumptions, extractions of ground rosemary were performed with 9, 11, 13 and 15 wt.% *i*-C_5Xyl solutions at 55 °C for 30 min. Then, the mixtures were filtered under vacuum to separate the solutions from the plants using preheated vessels and the filtrates were cooled down to 10 °C while magnetic stirred to induce homogeneous precipitation. Finally, the solutions were filtered through 1 µm glass microfiber filters and the concentration of CA was quantified in the filtrates by HPLC. In most cases, no precipitate was observed on the filters, so the recovered CA could not be quantified from it. The fraction of precipitated CA was thus calculated by the difference between the concentration of CA remained in the filtrate and the one previously quantified in the crude extract.

With a 9 wt.% solution, only 23 % of extracted CA is recovered in the filtrate, so 73 % may be recovered by precipitation using more efficient filtration systems. The hypothesis formulated following to the previous turbidity experiments is verified: it is possible to extract CA at 55 °C and to recover it by cooling. However, only 0.05 g/L are extracted (**Table IV.1**), and the extraction efficiency can be increased by a factor 100 or 200 by using a 13 or 15 wt.% solution respectively. Indeed, the extractions performed at a higher hydrotrope level result in

concentrated crude extracts, but they could not be precipitated at 10 °C since the concentration of CA in the filtrate did not change. This is in agreement with the results of the previous section showing that the precipitation of 1.6 g/L of CA (or 1.5 g/L of extract including 0.9 g/L of CA) was not efficient, and that only 0.7 g/L of CA could be extracted at 55 °C (**Table IV.1**).

Table IV.1 Concentration of CA extracted at 55 °C

***i*-C_5Xyl (%)**		**9**	**11**	**13**	**15**
Extraction 55 °C	$C_{CA, ext}$ (g/L)	0.047	0.32	0.66	1.02
Crystallization 10 °C, filtration (1 µm)	Recovered (%)	73	25	0	0
	Lost in the filtrate (%)	27	75	100	100

Therefore, from a practical point of view, a simple process of extraction and precipitation by cooling is not possible with *i*-C_5Xyl despite turbidity measurements have shown crystal growth while lowering the temperature in many cases. This procedure should however not be ruled out for other hydrotropic systems keeping in mind that, based on turbidity data, crystal density and growth depend at least on the two following factors:

- the extract concentration (its increase results in more numerous and larger crystals)
- the hydrotrope concentration (no linear relationship, optimal has to be found).

IV.2. Precipitation of the extracts by hydrotropic dilution

Precipitation by dilution with water is the conventional process to recover the hydrotropic extract. For example, it has already been performed to recover boswellic acids from NaNBBS solutions,[239] or curcuminoids from NaCS solutions.[117] The main disadvantage of such process is the high amount of water required to dilute the hydrotropic solution below the MHC. Indeed, for each of these experiments, extractions have been performed at 2 M and MHC occurs at 0.1 M, so the solutions must be diluted by 20 (19 L of water for 1 L of hydrotropic solution). However, the dilution factor can be reduced by changing the hydrotrope and optimizing the process, as shown for the recovery of piperine from NaBMGS extract which was also used at 2 M, but has a MHC of only 0.8 M: a dilution by a factor 2.5 was sufficient to precipitate the extract. Moreover, the precipitation has not always been easy: the expected precipitation of limonin by dilution with water occurred in the case of the extraction with NaCS, but not in NaS solution.[219] Therefore, precipitation is solute-hydrotrope dependant. It was shown in **chapter III** that a rosemary extract could be precipitated from *i*-C_5Xyl solutions, and the following study focuses on optimizing this step and understanding the mechanisms involved in the precipitation.

IV.2.1. Relative importance of eight precipitation conditions

a. Selection of the factors and their levels for the experimental design

The precipitation process depend on many factors that can influence the size and shape of the recovered amorphous solid or crystals, the recovery rate of the target molecule(s), and the purity of the extract.[117,139,240] Noteworthy, the formation of large particles is preferred to easily recover the extract by filtration. Too small particles can cause a slower filtration because of the clogging of the pores, or lower mass yield if the filter porosity is larger than the particles. The study of numerous factors in parallel can represent a tedious work, but an experimental design can help to reduce the number of experiments and identify which ones are the most impacting. First, the number of factors and their levels must be listed.

In all precipitation processes, particles are formed from a supersaturated solution by nucleation and growth. A high initial supersaturation leads to the spontaneous formation of numerous nuclei and hence, to small particles.[241] Furthermore, the initial supersaturation is basically the difference between the effective solute concentration $[S]_{eff}$ and its solubility S, which depends on the hydrotrope concentration (**Eq.IV.3**). $[S]_{eff}$ depends on both the initial solute concentration $[S]_i$ and the dilution, which is proportional to the initial hydrotrope concentration $C_{H,i}$ (**Eq.IV.4**) and can be increased by a higher volume of water added.

$$\Delta C = [S]_{eff} - S = \frac{[S]_i}{\text{dilution}} - S \qquad \text{(IV.3)}$$

$$\text{Minimal dilution} = \frac{C_{H,i}}{MHC} \qquad \text{(IV.4)}$$

In this study, the effect of different conditions on the precipitation of a rosemary extract is investigated. For this purpose, 100 g of ground rosemary were extracted in 1000 mL of hydrotropic solutions under the conditions optimized from the experimental design in **Chapter III**, and the 800 mL of the recovered filtrate were splitted in several samples of 42 mL (equivalent to a volume recovered from a 50 mL extraction with 5 g of rosemary). Therefore, the initial concentrations of *i*-C_5Xyl $C_{H,i}$ were of 30 wt.% and, as a result of the extraction, the concentration (HPLC) of CA were of 2.25 g/L (**Figure IV.9**). The dilution can thus be adjusted by changing the volume of added water for each sample. This factor is noted X_1 in the experimental design (**Table IV.2**).

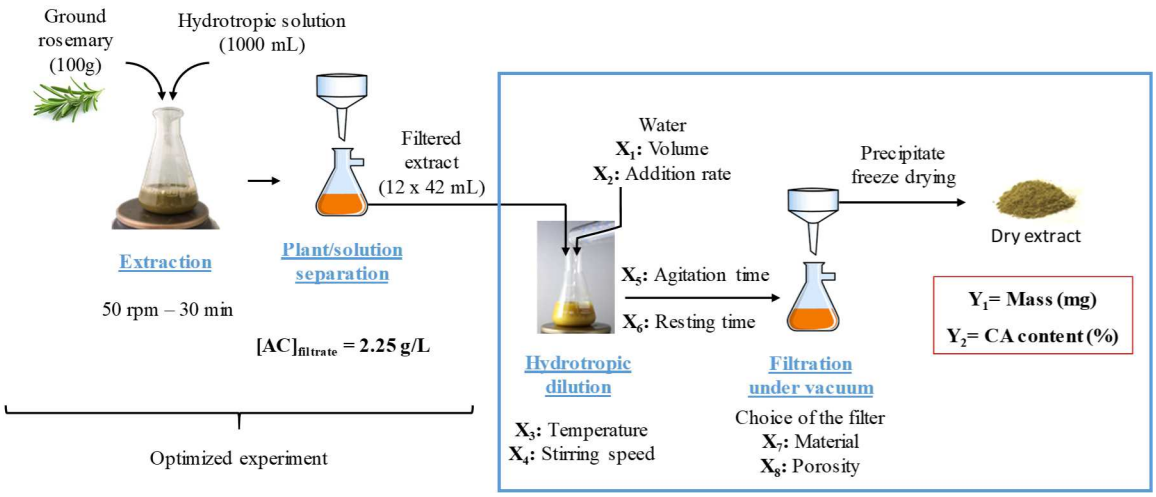

Figure IV.9. Extraction and precipitation process, factors (X_i) and responses (Y_i) of the experimental design

For choosing X_1 levels, the supersaturation and the maximum amount of CA that can be recovered were plotted against the dilution (**Figure IV.10b**) after being calculated from the differences observed in **Figure IV.10a** between the effective concentration of CA (red curve) and the CA solubility (blue curve) which evolve with the dilution. The 4-fold dilution (resulting in a 7.5 wt.% *i*-C_5Xyl solution) was chosen since it should lead to almost the highest yield (**Figure IV.10b**). However, this is also the point of the highest supersaturation (black curve), so it may lead to small crystals. The second level was chosen at a resulting hydrotrope concentration of 11.5 wt.%, since it is the point where the effective concentration of CA theoretically equals the saturation (**Figure IV.10a**). Therefore, the supersaturation must be low and particles should be large.

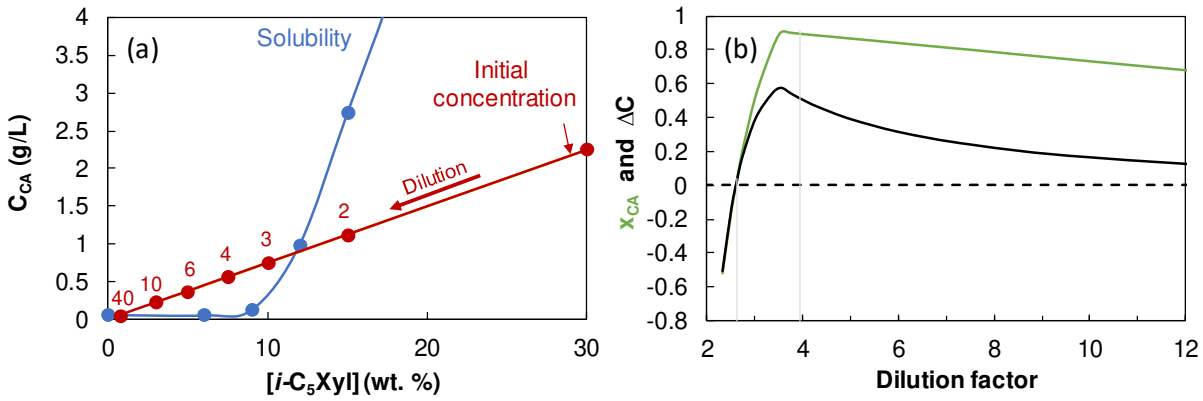

Figure IV.10. (a) Solubility curve of CA in *i*-C_5Xyl (blue), initial concentration in the rosemary extract performed with the optimized parameter, and effective concentrations reached with different dilution factors, specified above the red points (red). (b) Initial supersaturation (ΔC (g/L), black) and maximum fraction of CA recovered (x_{CA}, green) plotted *versus* the dilution factor, calculated from curves of (a).

The water addition rate, the temperature, and the stirring speed have already been reported as factors inducing larger or smaller crystals.[117,222] Indeed, large particles of 2-naphtol from NaCS solutions were obtained at high temperature (55 > 35 > 25 °C) and low water addition rate (0.033 > 0.054 > 0.095 g/min). Besides, a high stirrer speed resulted in higher nucleation rates (small crystals) by disrupting the formed agglomerates.[240] Those factors were reported as X_2, X_3 and X_4 in the experimental design (**Table IV.2**, **Figure IV.9**). Their levels have been chosen to be extreme:

- the water addition rate between 10 mL/sec, corresponding to a sudden one-portion addition, and 0.05 mL/sec, corresponding to one drop per second.
- the temperature was compared between 10 (low) and 40 °C (high). It should be pointed out that the water added for the dilution was not thermostated for practical reasons. This may minimize the responses for experiments with one portion additions, especially for high dilutions, both levels trending toward room temperature, but would not impact the other ones.
- the stirring speed levels were chosen as slow (50 rpm) and fast (500 rpm)

To increase the particles size, their agglomeration can be favored by the increased time of agitation, called residence time.[242] Indeed, when stirring continues during a certain time after the addition of the anti-solvent is completed, it has been shown that particles generally continue to grow. A residence time without stirring (settling period) was also added as a factor of the experimental design (X_6). The factors agitation and settling were noted X_5 and X_6 with the levels 0 (this step is not performed) or 1 h. Finally, the nature (X_7) and the porosity (X_8) of the filters were integrated in the experimental design (**Table IV.2**, **Figure IV.9**). Low porosities were chosen (1 and 3 µm) to evaluate if the 3 µm filters are sufficiently effective in recovering the extracts. Both types of filters existed in cellulose nitrate and glass microfibers so the material of the filters was added to check if it could have an effect on the efficiency of the process.

Table IV.2. Factors and levels of the experimental design

	Factor	-1	+1
X_1	*i*-C_5Xyl (wt.%) after dilution [Dilution]	7.5 [4]	11.5 [2.6]
X_2	Water addition rate (mL/min)	0.05	10
X_3	Temperature (°C)	10	40
X_4	Stirring speed (rpm)	50	500
X_5	Stirring time (h)	0	1
X_6	Settling time (h)	0	1
X_7	Nature of the filter	Cellulose nitrate	Glass microfiber
X_8	Filter porosity (µm)	1	3

b. Results of the factorial design

Studying each factor would require numerous experiments. To lower this number, we performed an experimental design using a Hadamard matrix, which provides an efficient screening of the factors: all eight factors can be screened in only twelve experiments (**Table IV.3**).[243] At the end of the process, sticky precipitates were recovered, even after freeze drying, as shown in **Table IV.3**. Their darkness changed following to the experiments but a lighter precipitate did not seem to be correlated with a higher CA content (see section II.5.1, **Eq.II.9**). The effect of the eight factors summarized in **Table IV.2** were observed on the extract mass (Y_1) after freeze-drying (over about 6 h, until reaching a constant mass) and the CA content (Y_2) quantified by HPLC, as shown in **Figure IV.9**.

The analysis of the results of the experimental design presented in **Table IV.3** leads to a mathematical expression (**Eq.IV.5**) for each responses (Y) using the calculated coefficients b_i, referring to the effect of the factor i (i = 1 to 8).

$$Y = b_0 + \sum_{i=1}^{8} b_i X_i \qquad \text{(IV.5)}$$

In addition to the twelve experiments, the sixth experiment, the one giving the best results, was performed two more times to calculate the standard deviation of each response (SD_Y), the subsequent standard deviation of the effects (SD_{bi}) and significance levels of the factors, according to the *t*-Student with a confidence level of 95 % ($p < 0.05$). The significant coefficients b_i are represented in blue in **Figure IV.11** whereas the non-significant ones are represented in grey. The non-significant coefficients can be supressed from **Eq.IV.5**. According to the calculated significant level, only X_2 and X_8 have a significant influence on the mass of the extract (**Figure IV.11a**), which can thus be calculated with the following equation (**Eq.IV.6**):

$$Y_1 = 308 - 37\,X_2 - 27\,X_8 \qquad \text{(IV. 6)}$$

Therefore, to increase the recovered mass of the extract, X_2 and X_8 must be at their – 1 levels, corresponding to a low addition rate and a filter porosity of 1 µm instead of 3 µm. Indeed, the slow addition of antisolvent has often be used to get large particles, which can be related to the lower effective supersaturation, resulting in lower nucleation rates, and higher growth rates.[117,240] The fact that the filter porosity is a significant factor shows that some particles that are smaller than 3 µm can be recovered by 1 µm-filters, leading to higher average mass of the precipitate of 27 mg (increase in mass yield of 0.5 %, considering that the solution corresponds to an extraction of 5 g rosemary).

Table IV.3. Algebraic signs of the experimental conditions and main results

	X_0	X_1	X_2	X_3	X_4	X_5	X_6	X_7	X_8	Y_1 $m_{extract}$ (mg)	Y_2 CA content (wt.%)	Filter
1	+	+	+	-	+	+	+	-	-	263	9.7	
2	+	-	+	+	-	+	+	+	-	234	13.0	
3	+	+	-	+	+	-	+	+	+	333	8.7	
4	+	-	+	-	+	+	-	+	+	276	12.4	
5	+	-	-	+	-	+	+	-	+	264	12.2	
6	+	-	-	-	+	-	+	+	-	381	17.4	
7	+	+	-	-	-	+	-	+	+	359	9.9	
8	+	+	+	-	-	-	+	-	+	247	8.6	
9	+	+	+	+	-	-	-	+	-	394	8.7	
10	+	-	+	+	+	-	-	-	+	210	10.9	
11	+	+	-	+	+	+	-	-	-	362	6.1	
12	+	-	-	-	-	-	-	-	-	373	3.2	
SD_Y										21	0.3	
SD_{bi}										36	0.1	
tSD_{bi}										26	0.4	

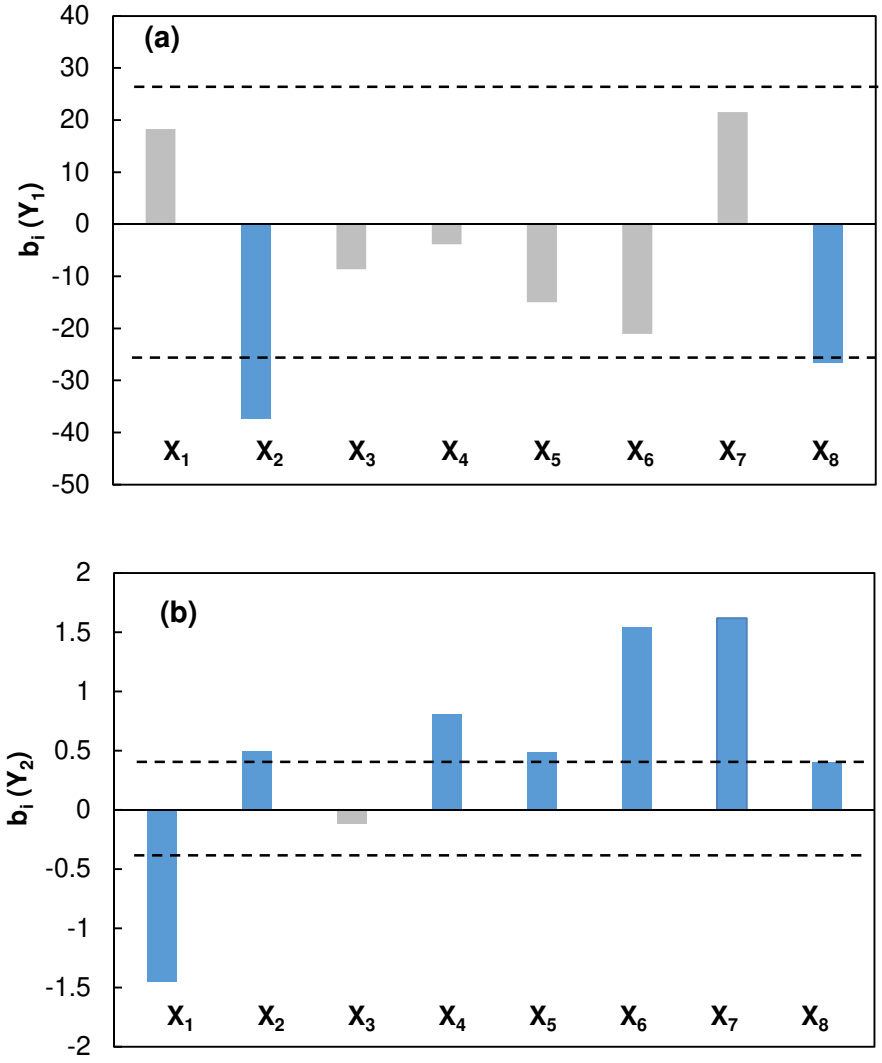

Figure IV.11. Graphical representation of the b_i coefficients estimated by linear regression from a Hadamard design for eight variables for the mass of the extract Y_1 (a) and for the CA content Y_2 (b). The dotted line represents the significance limit with a 95 % confidence level. The significant b_i are highlighted in blue.

Regarding the CA content, seven factors seem to have a significant influence on the response. Surprisingly, only the temperature (X_3) seems to have no influence both on the CA content and on the extract mass, with a confidence level of 95 % (**Figure IV.11b**). CA content (wt.%) can thus be calculated with the following equation (**Eq. IV.7**).

$$Y_2 = 10.1 - 1.5\ X_1 + 0.5\ X_2 + 0.8\ X_4 + 0.5\ X_5 + 1.5\ X_6 + 1.5\ X_7 + 0.4\ X_8 \qquad (IV.7)$$

Among those factors, three are particularly important, with an effect above 1 ($p < 0.01$):

(i) The dilution by 4 ($X_1 = -1$) is preferred over a dilution by 2.6 (level +1). This may be related to an effect similar to washing: at 7.5 wt.% of *i*-C_5Xyl (dilution by 4), the hydrotrope is less likely to be found in the precipitate since it is less concentrated, resulting in higher CA content.

(ii) Interestingly, the settling step ($X_6 = +1$) seems to increase the CA content. This factor is not significant for Y_1, but is close to the significant level ($p < 0.05$), and has an antagonist effect on Y_1 and Y_2. During the experiments, it has been observed in many cases a sticky deposit in the vessel, which could not be removed during the filtration. This sticky aspect should come from the presence of the hydrotrope since the same behavior has been observed in the turbidity experiments (section IV.1) for systems containing only CA, *i*-C_5Xyl and water. Thus, if hydrotrope-charged particles deposit at the bottom of the vessel during the settling step, then only the hydrotrope-free particles are filtered, leading to a lower recovered mass but a more concentrated extract.

(iii) The nature of the filter, which should be in glass microfiber ($X_7 = +1$) rather than in cellulose nitrate. Noteworthy, despite this factor is not significant for Y_1 it is the only factor which is positive for both Y_1 and Y_2, meaning that cellulose nitrate filters are completely unsuitable to this application. This may be due to different hydrophobicity of the filters and thus, different retention levels of CA, co-extracted compounds and/or hydrotrope, leading to different CA contents.

The factors X_5 and X_8 have a weak influence on Y_2 but anyway, they should be rather at their + 1 level. X_8 is the porosity of the filter, so the use of large pores seems to induce higher CA content, meaning that large particles are likely to be more concentrated in CA than small ones. The fact that b_5 is positive would suggest an enrichment in CA of the particles along with the time, but in fact, as explained above, due to the deposit of some materials on the walls and the loss in mass yield, it rather reflects less hydrotrope-charged particles. This means that hydrotropes would have more time to disperse in water.

The factors X_2 and X_4 should also be set at their +1 level (rapid water addition rate and high stirring speed). This effect cannot be attributed to the particles size since a rapid water addition and a high stirring speed should lead to small particles, so it should be attributed to the composition of the particles. It is likely that the incorporation of hydrotropes in precipitates is avoided by a high nucleation rate and aggregate disruption induced by the rapid water addition or by a high stirring speed respectively. In other words, smaller aggregates will contain less

hydrotropes due to a lower volumic fraction and exhibit higher specific surfaces to get them out.

IV.2.2. Purification of the rosemary hydrotropic extracts

a. Composition of the extract

The maximum CA content obtained with the experimental design is 17.1 wt.%. For industrial applications, this content should be improved. To find out which molecules can be removed, a hydrotropic extraction of ground rosemary was performed with medium conditions (*i*-C_5Xyl: 22.5 wt.%, 20°C, 300 rpm), followed by precipitation with medium conditions (dilution factor: 2.5 to reach 9 wt.%, 250 rpm, 30 mi agitation, 30 min settling) and filtration under vacuum through glass microfiber 1µm-filter. The precipitate was finally freeze-dried until reaching a constant mass. As reported above, a dark and pasty precipitate was recovered on the filter. The composition was analyzed by the analytical department of Naturex.

Unfortunately, only 47 wt.% of the extract could be identified (**Figure IV.12**). Despite freeze-drying until no mass evolution, a high amount of residual water is expected in the other part, but has not been quantified. CA and its derivatives such as carnosol (CAR) or 12-*o*-methyl carnosic acid (MCA) compose the major part of the analyzed extract (total: 23.5 wt.%), but interestingly, the CA content (17 wt.%) is similar to that of the experiment number 6 from the above experimental design (17.4 ± 0.3 wt.%). The other identified phytochemicals (*e.g.* fatty acids, flavonoids) amount to 4.2 wt.%, *i.e.* 4 times less concentrated than CA. Nevertheless, there is more *i*-C_5Xyl (19.2 wt.%) than CA recovered in the extract. Finally, as expected from the *i*-C_5Xyl selectivity, the CA content of the extract is 40, 10 and 7 times the content of RA, triterpenes and volatiles respectively, whereas their concentrations *in planta* are supposed to be in the same order of magnitude. Thus, CA seems to have been concentrated in the extract.

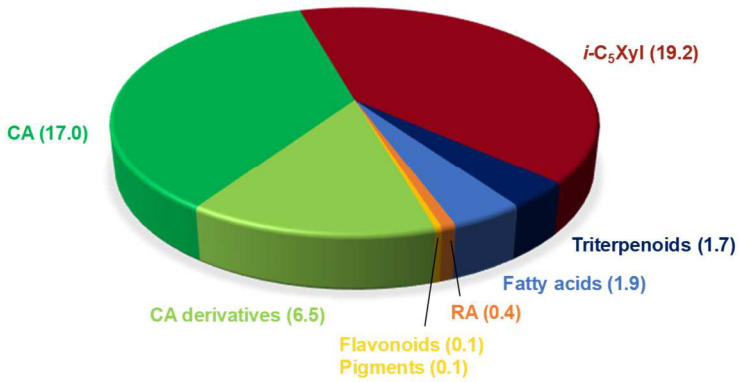

Figure IV.12. Composition of a rosemary hydrotropic extract performed with 22.5 wt.% *i*-C_5Xyl at pH 2, 20 °C, and diluted to 9 wt.% with acidic water, stirred and settled for both 30 min, filtered under vacuum through a 1 µm glass microfiber filter, and freeze-dried.

b. Purification of the extracts

Since an important part of the precipitate is composed of the hydrotrope, its removal through additional washing with water has been investigated. Acidic water (pH 2) was used to avoid CA deprotonation so that it remains insoluble.

Extractions of ground rosemary were performed with 22.5 wt.% *i*-C_5Xyl, at room temperature (25 °C) during 30 min under stirring (250 rpm). The plant was separated from the hydrotropic solution by filtration under vacuum (8 µm cellulose filter). To simplify the process, the washings were first investigated on extracts recovered by centrifugation. Therefore, the filtrate of the extraction was equally separated in seven conical centrifuge tubes (10 mL each) and diluted by a factor 2.5, by adding 15 mL of acidic water to the filtrate (**Figure IV.13**). The solution became cloudy and was centrifuged for 5 min (5000 rpm). The supernatant was removed from all the centrifuge tubes and one of the precipitates was freeze-dried and analyzed by HPLC. It contained 13 wt.% of CA and 26 wt.% of *i*-C_5Xyl, corresponding to 17.2 and 35.2 mg of CA and *i*-C_5Xyl respectively. In all the remaining centrifuge tubes, 10 mL of acidic water were added to the precipitate, and the mixture was manually agitated for 5 min, sonicated for 5 min more and manually agitated again until the precipitate was completely dispersed (5 – 10 min). Then, they were centrifuged again (5000 rpm, 5 min) and two of them were freeze-dried before HPLC analysis. This procedure was repeated again so that two precipitates were washed once, two others were washed twice and the last two were washed three times (**Figure IV.13**). Noteworthy, green powders were obtained after washings instead of the initial pasty dark precipitate, as shown in **Figure IV.13.**

The hydrotrope *i*-C_5Xyl, CA and its derivatives (CAR and MCA) were quantified in the precipitates by HPLC, and their recovered mass was calculated thanks to global precipitate weight (**Figure IV.14a**). The amount of *i*-C_5Xyl was reduced to 10.6 wt.% after a single washing and was totally removed after the third one. Its removal can be related to the fact that the precipitate becomes more powdered. Despite between 1 and 2.5 mg of CA were lost at each washing step, resulting in a final mass of 11.6 mg in the precipitate, the CA content in the precipitate reached from 13 to 22.1 wt.% thanks to the decrease of the global mass.

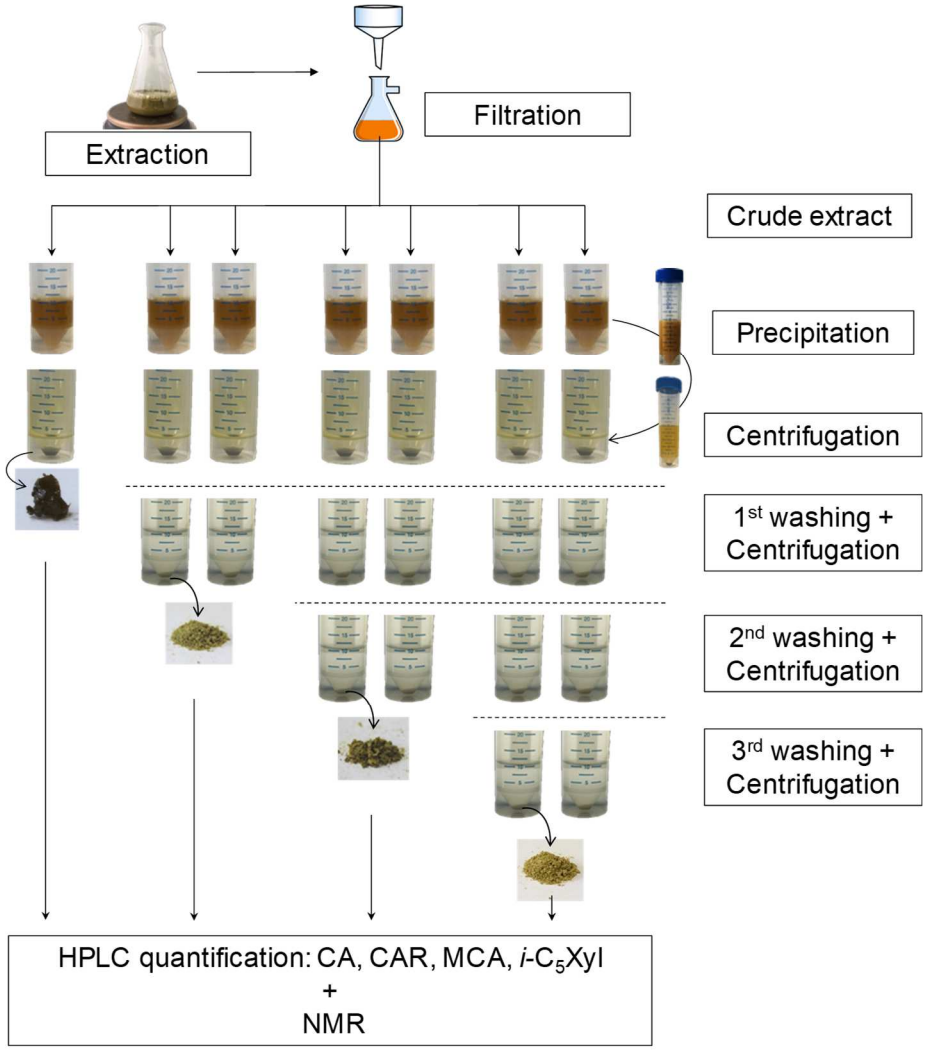

Figure IV.13 Experimental procedure to evaluate the effect of washings on the residual quantity of carnosic acid (CA), carnosol (CAR), methyl carnosic acid (MCA) and hydrotrope *i*-C_5Xyl in the precipitate recovered by centrifugation

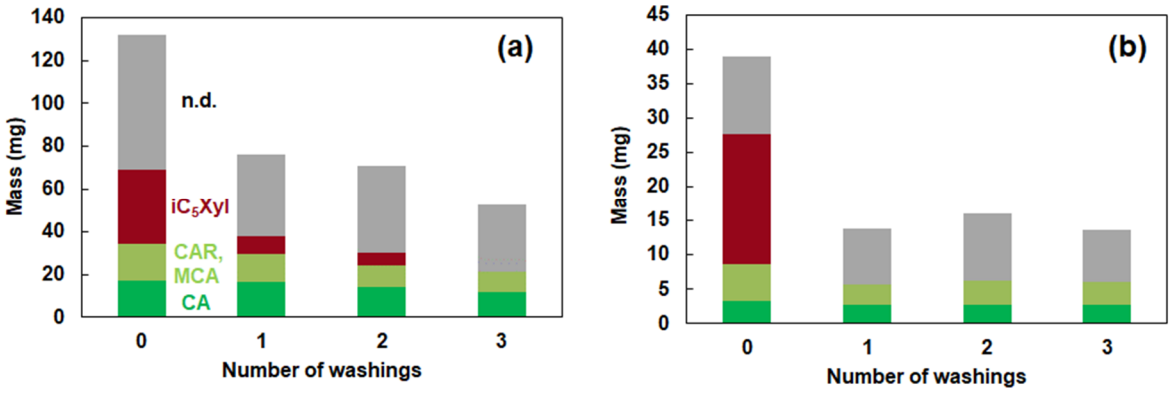

Figure IV.14. Effect of the washing steps on the composition of the precipitates recovered by centrifugation after extraction with 22.5 wt.% *i*-C_5Xyl at 25 °C during 30 min, separation plant/solution by filtration under vacuum, dilution of the crude extract by a factor 2.5 (a) or 4 (b), separation of the precipitate by centrifugation. The contents of CA: carnosic acid, CAR: carnosol, MCA: methyl carnosic acid, *i*-C_5Xyl: *iso*-amyl xyloside are determined by HPLC and other compounds determined from the total yield

HPLC analysis allow to quantify precisely the hydrotrope in the precipitates using an ELSD detector, but this can also be shown by ^{1}H NMR. Indeed, the spectrum of the precipitate that had been washed 3 times is very similar to the one of CA (**Figure IV.15**, spectra e and f). The numerous peaks in the region between 2.8 and 4 ppm in the *i*-C_5Xyl spectrum, which are characteristic of the carbohydrate protons, are present in the spectrum of the precipitate before washing, but not after washing. The peak at 6.33 ppm is characteristic of the aromatic ^{1}H in CA and interestingly, a second peak appears at 6.4 ppm in the extract. Their ratios are in both dilution cases about 7:3, suggesting that the minor compound is MCA, in accordance with the HPLC results. Moreover, the characteristic peak of CAR is present at 6.7 ppm and the ratio CA:CAR is found to be 5:1. Since it does not increase with the number of washings, CA is not degraded during the process. Finally, the comparison between the precipitates and pure CA (between 0.6 and 1.8 ppm) confirms that the extract is not completely pure. However, no characteristic compounds could be identified.

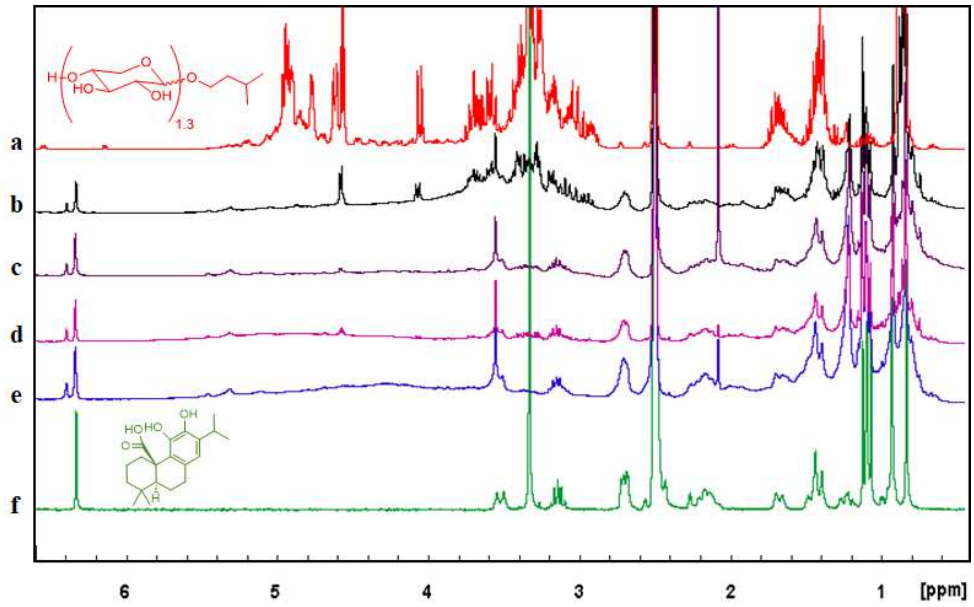

Figure IV.15. ^{1}H NMR spectra of *i*-C_5Xyl (a), precipitates obtained by 2.5-fold dilution without washing (b), after one (c), two (d) and three (e) washing steps, compared to pure CA (f) in DMSO-d_6.

Exactly the same procedure (**Figure IV.13**) was performed on the crude extract obtained by a 4-fold dilution, *i.e.* by adding 30 mL of acidic water. Compared to the dilution by 2.5, a lower mass of *i*-C_5Xyl is recovered (19 mg), but it represents a larger proportion in the precipitate (49 wt.%). As far as CA is concerned, its recovered mass has been reduced compared to the first experiment by a factor 5. It can be partially explained by its intrinsic water solubility. Indeed, if the volume used for dilution is doubled, the CA mass which remain in water is also doubled, but alone, it should not explain the difference observed between the 2.5-fold and the 4-fold dilutions. Interestingly, only one washing was sufficient to remove all the 19 mg of *i*-C_5Xyl (**Figure IV.14b**)

c. Comparison with the different processes

Interestingly, after the same extraction with 22.5 wt.% *i*-C_5Xyl, the CA content was lower in the precipitates recovered by centrifugation compared that recovered by filtration with 1 µm-filter (13 wt.% *vs* 17 wt.%), whereas the *i*-C_5Xyl content was higher (26 wt.% *vs* 19 wt.%). Noteworthy, the CA recovery rate by centrifugation, which represents the proportion of CA recovered compared to CA available in the plant (see section II.5.1, **Eq.II.10**), was higher by centrifugation than filtration with 1 µm-filter (50 *vs* 40 %), as shown in **Table IV.5.** It means that *(i)* all the CA is not recovered by filtration and *(ii)* some particles with a high *i*-C_5Xyl content are recovered by centrifugation, but not by filtration through 1 µm filters.

Whether the precipitate was recovered by filtration (3 µm) or centrifugation, three washing steps increased the CA content (from 12.6 to 26.5, or from 13.1 to 22.1 wt.% respectively) but reduced the global mass yield by a factor 2. In the case of centrifugation, the recovery rate was reduced from 50 to 34 wt.%, but when the precipitate was recovered on a cellulose filter (3 µm), the recovery rate did not seem to be impacted. Noteworthy, this step seems to be efficient only if the precipitate is well dispersed in water. However, because of its pasty aspect, it is generally stuck to the filter. A magnetic bar was thus placed over the filter and stirred (400 rpm) during the washing (20 mL) so that the precipitate was mechanically unstuck from the filter and dispersed in water. Then, the same filter was used for the filtration under vacuum, and the procedure was repeated two more times. A green powder was obtained with a 2.6 % yield and 26.5 wt.% CA.

Finally, the results of the extraction performed with the optimized conditions of the experimental designs for both the extraction step (**chapter III**) and the precipitation step (section IV.2.1) were compared to the other experiments. The optimized conditions are summarized in **Table IV.4**. The temperature of 10 °C was selected rather than 40 °C because its coefficient b_3 is negative for both Y_1 and Y_2. However, it should not have a strong effect on the result since b_3 it is not significant. The plant/solvent ratio was kept at 1/10 and two experiments were performed: the first on a volume of 50 mL, was recovered by filtration, and the second on a volume of 100 mL was recovered by centrifugation and washed, to compare the two processes.

Table IV.4. Optimized conditions for the extraction and precipitation process

Extraction	Optimization	Precipitation	Optimization
[Hydrotrope] (%)	30	**% *i*-C_5Xyl after dilution [Dilution]**	7.5 [4]
		Water addition rate (mL/min)	0.05
Time (min)	30	**Temperature (°C)**	10
		Stirring speed (rpm)	500
Temperature (°C)	25	**Stirring time (h)**	1
		Settling time (h)	1
Stirring speed (rpm)	50	**Nature of the filter**	Glass microfiber
		Filter porosity (µm)	1

A concentration of 2.21 g/L was obtained in the crude extract, *i.e.* the filtrate obtained from the plant/solution filtration. After the precipitation, a mass yield of 7.2 % and a recovery rate of CA of 55 % were reached, so this procedure can be considered as the most efficient hydrotropic extraction to recover the maximum amount of CA. After the filtration, the final extract contained 20.5 % of CA. It could be increased only to 24.6 % by the washing procedure described above. Indeed, the dispersion of the precipitate in water was not very efficient because the precipitate was more stuck on the glass microfiber filter than on the cellulose one. Therefore, this process was complicated to perform, leading to the reduction of the recovery rate of CA from 55 to 40 %. This drawback is due to the filter material, because when performed with the cellulose (3 µm) filters, no CA was lost.

Table IV.5. Comparison of the extracts obtained by optimized filtration or centrifugation and washing with water. In each case, ground rosemary is extracted for 30 min.

Extraction technique	**Conventional**	**Not optimized**					**Optimized**	
Solvent	Acetone			*i*-C_5Xyl 22.5 wt.%			*i*-C_5Xyl 30 wt.%	
Recovery technique(1)	E	F (3 µm)		C		F (1 µm)	F (1 µm)	
Precipitate washings	No	No	3	No	3	No	No	3
Mass yield (%)	12.7	5.2	2.63	10.5	4.2	6.5	7.2	4.5
CA content (%)	20.0	12.6	26.5	13.1	22.1	17.0	20.5	24.6
Recovery rate (%)	92	24	25	50	34	40	55	40

(1) The extract was recovered either by evaporation (E), filtration under vacuum (F) or centrifugation (C) and then, freeze-dried.

An extraction with acetone was performed in comparison with common conditions (30 min of stirring, room temperature, extract recovered by evaporation). Interestingly, the same CA content was reached with the optimized procedure, but the acetone extract had a higher recovery rate.

Finally, to validate the antioxidant properties of the extracts, the autoxidation of fatty acid methyl esters (FAMEs) in their presence was investigated using RapidOxy apparatus. The antioxidant properties are determined mainly by the ability to delay the beginning of the oxidation generally performed under high oxygen overpressure (300 kPa) and at high temperature (110 °C). This induction period reflects the antioxidant power. For example, an induction time of 5.6 h was measured for CA from the curve presented below. All the oxidative times were measured three times, and the error was found to be 0.1 h (**Figure IV.16**). The longer the induction period, the stronger the antioxidant power.[14]

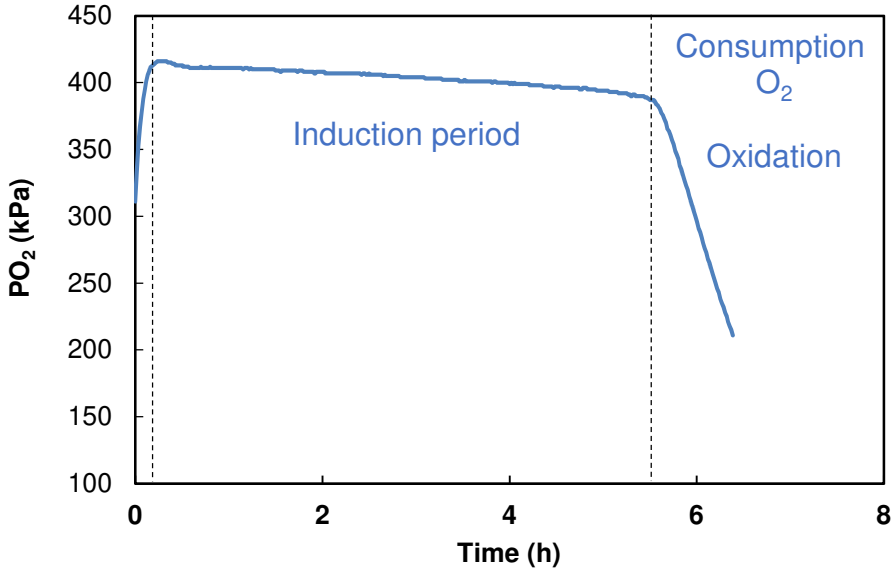

Figure IV.16. Evolution of the oxygen pressure (PO_2) with the time during the oxidation of sunflower FAMEs in the presence of 0.1 % CA (20 mg in 2 mL using Rapidoxy® apparatus.

Extracts with the lowest and the highest CA contents (12.6 and 26.5 wt.%) were compared to pure CA and to the acetone extract (20 wt.%) at a same amount (0.1 wt.% of extracts in 2 mL) of FAMEs). Noteworthy, the induction time is not proportional with the CA content, as already observed for pure antioxidants such as BHT (**Figure IV.17**).[244] However, the better efficiency than expected can be also attributed to CA derivatives, or other polyphenols such as rosmarinic acid which also have an antioxidant effect, or may provide additional antioxidant capacity.[245]

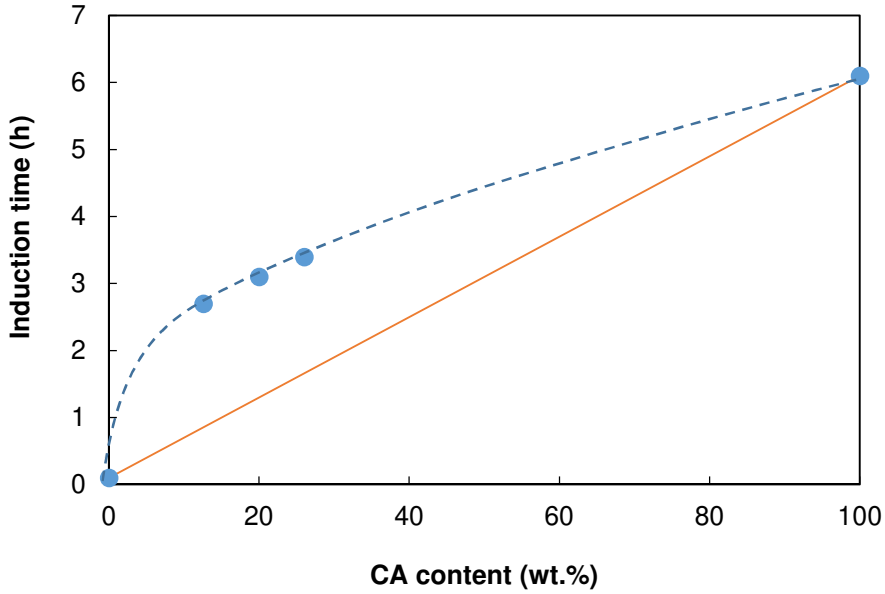

Figure IV.17. Oxidative induction time of several rosemary extracts measured on the autoxidation of sunflower FAMEs (0.1 wt.% for 2 mL, 400 kPa O_2, 110°C), as a function of their CA concentration

IV.2.3. Microscopic observation of the particles formed by hydrotropic dilution

The conclusions from the experimental design give some insights on the precipitation mechanism but some conditions still need adjustments. For example, it showed that extractions should be performed at 30 wt.% rather than 15 wt.% *i*-C_5Xyl. However, another experiment has shown that the amount of extracted CA did not increase above 18 wt.%. The reduction of the hydrotrope concentration from 30 wt.% to 18 wt.% would also reduce the quantity of water required for dilution factor from 3.3 to 2 to reach a final concentration of 9 wt.%, which is suitable for industrial application. Moreover, it has been demonstrated that agitation and settling times were important to increase the CA content, but it would be interesting for industrial application to reduce them to the minimum. Thus, the precipitation kinetics has been studied to optimize those three conditions, to confirm the assumptions from the experimental design and to provide a deeper understanding of the precipitation mechanism.

a. Hydrotropic precipitation of pure carnosic acid solutions

To facilitate the understanding of the crystallization mechanism, the experiments were first performed on a model system composed of CA, *i*-C_5Xyl and acidic water (1 % v/v H_3PO_4). Three solutions with different initial *i*-C_5Xyl concentrations were prepared ($C_{H,i}$ = 18, 22.5 or 30 wt.%) with 2.5 g/L of CA solubilized (100 mg in 40 mL) and diluted at room temperature with water (dropwise addition) under stirring (500 rpm). The final hydrotrope concentration was selected to 9 wt.% rather than 7.5 wt.% because this study focuses on the growth of the crystals, whereas reaching a concentration of 7.5 wt.% increases the CA content. It corresponds to a dilution with 1, 1.5, 2.3 volumes of water depending on the $C_{H,i}$.

When the dilution was completed, the solution was stirred for one hour more and settled for another hour. About 10 µm of the bulk solution were collected when it was possible every 5 or 10 min at the beginning of the experiment and every 15 or 20 min during the settling step. The collected solution was observed under numeric microscope. The experiments were performed twice and for each microscopic observation, several images of the solution were taken, and the size of the particles were measured with the microscope software (Keyence).

For each experiment, the generated crystals evolve similarly. Before or just after crystallization, small black particles (1 - 2 µm) are observed. Then, at the beginning of crystallization, needle-like crystals of 10 µm long and 1 µm wide appear, this is the nucleation stage (**Figure IV.18**). The same primary crystals are recovered immersed in amorphous, transparent and spherical particles which seem to grow with time (from about 20 to 500 µm diameter). Moreover, the concentration of needle-like particles seems to increase around and into the particles with increasing time. Then, the particles can evolve in two ways: *(i)* the consolidation of the large particles or *(ii)* their breaking causing the release of needle-like particles or small agglomerates. In this first case, the amorphous phase seems to have disappeared, and the particles shape

become irregular (**Figure IV.18**). The needle-like particles are supposed to be composed of CA, so the amorphous phase must be composed of *i*-C_5Xyl, or a mixture of *i*-C_5Xyl -water.

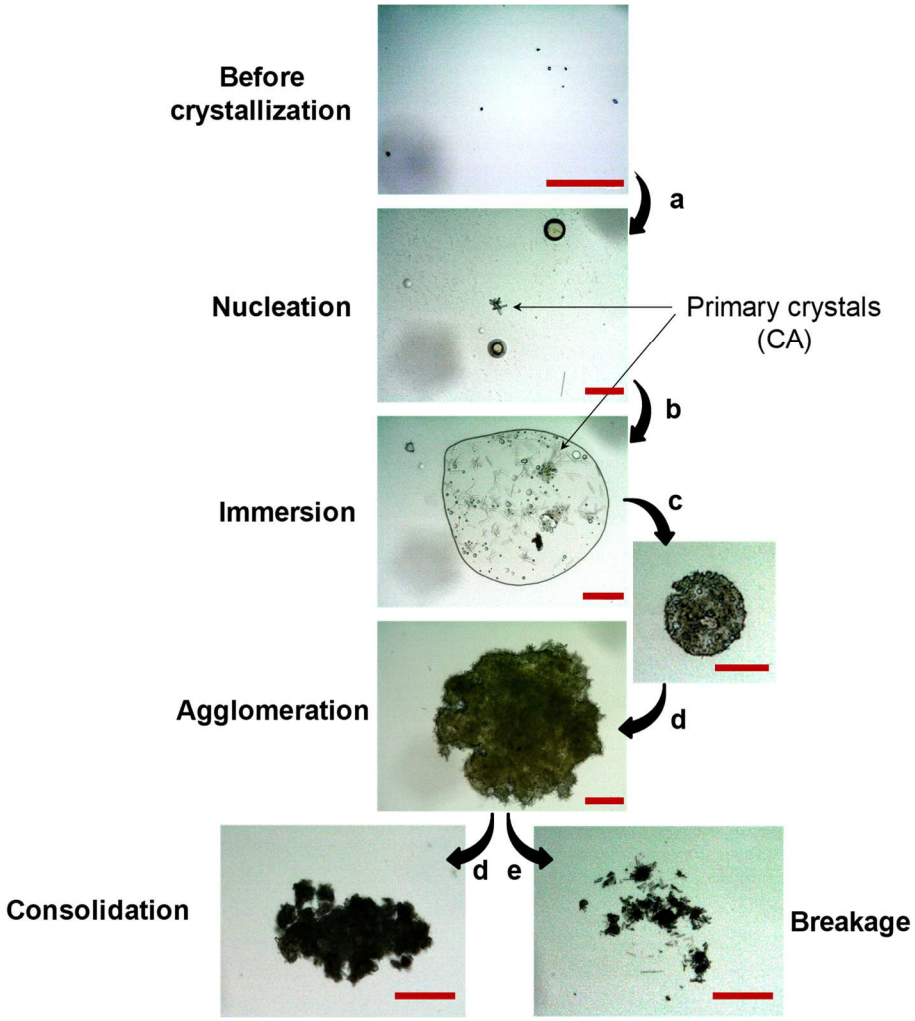

Figure IV.18. Typical evolution of the CA crystals shape formed by dilution of a *i*-C_5Xyl solution. Scale bars = 50 µm.

The microscopic images presented in **Figure IV.18** typically describe the mechanism involved in the aggregation with a bridging liquid, where the bridging liquid would be the hydrotrope.[242] In such process, the generation of primary crystals is induced either by cooling or anti-solvent addition. Then, it consists of their agglomeration thanks to the addition of a third liquid, the so-called bridging liquid, which must be immiscible with the anti-solvent to form droplets (in which particles agglomerate by getting immersed if the droplets are larger than the crystals), and exhibit a good wettability towards the crystals.[242] For example, aqueous solutions of salicylic acid can be crystallized using ethanol and agglomerated in chloroform droplets.[246] The agglomerates are subsequently consolidated and then, a growth or a breakage is observed. This process is generally called spherical agglomeration.

Therefore, the evolution of our system is clearly similar to this process although *i*-C_5Xyl is fully miscible with water. Indeed, it surprisingly forms large droplets in which CA particles aggregate. Noteworthy, this phenomenon has not been observed when hydrotropic dilution was performed in absence of CA. The formation of *i*-C_5Xyl droplets is thus induced by the presence of CA. It can be rationalized by the fact that the previous assemblies of hydrotropes and CA in aggregates in the hydrotropic solution (C > MHC) are disaggregated while the solution is diluted (step "a"), inducing the release of some hydrotrope molecules in the solution and thus, making the aggregates more concentrated in CA (hence their precipitation). However, it is likely that CA and *i*-C_5Xyl still have a strong affinity so that some hydrotrope molecules remain around it while CA precipitates, leading to small droplets, which coalesce (step "b"). Then, the system evolves by the CA crystallization, *i.e.* solute-solute interactions is stronger than solute-hydrotrope ones, releasing hydrotropes molecules in water (step "c"). Therefore, irregular particles are created, and can further consolidate by surface and internal crystallization (step "d"). If the needle-like crystals did not have the time to consolidate, it leads to the breakage of the particles (step "e"), as shown in **Figure IV.18**.

Noteworthy, increasing the stirring speed breaks the aggregates, making them smaller and less porous, and thus favors the consolidation of particles.[247] This would explain the higher CA content observed in the experimental design with a high stirring speed: particles are more consolidated and less porous, so *i*-C_5Xyl has less space inside the particles to stay, and CA is thus more concentrated.

Overall, the particles morphology did not change with the $C_{H,i}$, however, the size of particles, the evolution of crystals with the time, the appearance of the precipitate recovered by filtration did. The initial CA concentration was the same (2.5 g/L) but since the experiments with 18, 22.5 and 30 wt.% required a different dilution by 2, 2.5 and 3.3 respectively, the final CA concentration and thus, the solute/hydrotrope concentration differed. In spherical agglomeration process, the bridging liquid to solute ratio (BSR) is considered as the most critical parameter. Indeed, at low BSR there is insufficient bridging liquid to promote complete agglomeration whereas at high BSR large, very porous, and irregularly shaped agglomerates are formed (**Figure IV.19**).[242,248]

Figure IV.19. Evolution of the particles with the BSR in spherical agglomeration process, from ref[248]

During each crystallization (performed twice), images were taken at regular intervals and the diameters of 5 – 15 particles were recorded to provide a representative overview of the growth of the particles. **Figure IV.20** presents the particles sizes plotted *versus* time, with t = 0 the end of dilution, and the aspect of the solution during the process. For each experiment, the particles grow at the beginning of the crystallization, reach a maximum and then, smaller particles are observed in solution. As expected, the particles size reduces during the settling stage, because the larger and heavier particles deposit at the bottom of the Erlenmeyer by gravity. When the $C_{H,i}$ is 22.5 or 30 wt.%, the maximum size was reached before the settling step, about 15 min after the dilution was completed. Moreover, the initially most concentrated solution generated very large particles. In the graphic, the maximum size is 580 µm diameter, but some particles were larger and could not be measured with the microscope since they could not be entirely seen with the lens (**Figure IV.21**). It is likely that this solution provides particles larger than 1 mm. The generation of large particles can induce their recovery on the vessel walls by sticking effect, which could explain the reduction of the particles diameter 45 min before the settling step.

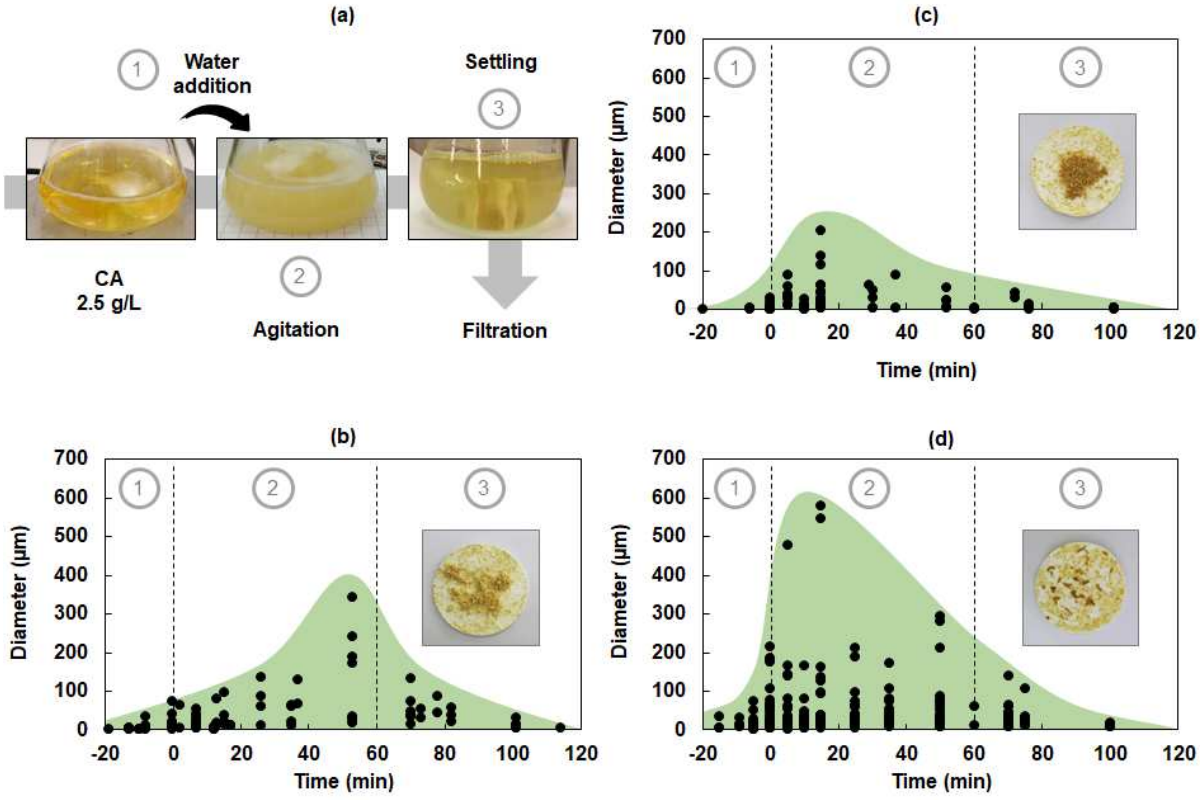

Figure IV.20. (a) General aspect of the solution before and after dilution, during agitation and settling steps. (b, c, d) Representative particles diameter *versus* time observed by numeric microscope during hydrotropic precipitation at pH 2, 25 °C and images of the glass microfiber filters (Φ =1 µm) obtained after Büchner filtration of solutions initially containing (b) 18, (c) 22.5, (d) 30 wt.% of *i*-C_5Xyl and 2.5 g/L of CA and diluted to 9 wt.%.

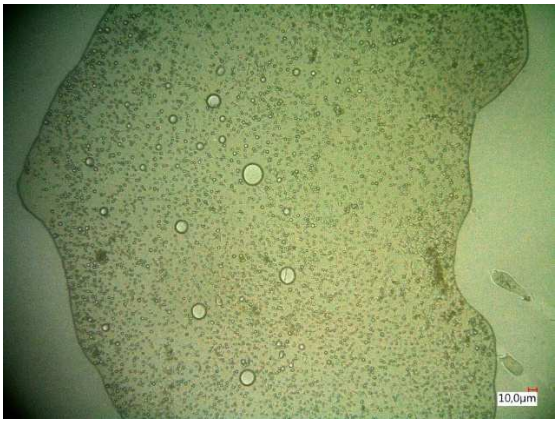

Figure IV.21. Microscopic image of a particle generated by the dilution of the 30 wt.% *i*-C_5Xyl solution to 9 wt.% in presence of CA (2.5 g/L), taken after 15 min of residence time. Aggregate width = 547 µm.

Finally, it should be noted that the growth of the particles and the morphologic changes are not correlated. Indeed, for the solution at $C_{H,i}$ = 30 wt.%, particles with a visible transparent amorphous phase where CA is immersed (aspect shown in **Figure IV.18** and **Figure IV.21**) are observed until t = 70 min, whereas no amorphous phase are visible at the beginning of the settling step in the two other experiments. This can be the reason why the recovered precipitate on the filter is sticky for the solution at $C_{H,i}$ = 30 wt.% and it is a powder for the solutions at $C_{H,i}$ = 18 and 22.5 wt.%. Both assumptions suggest that a high amount of *i*-C_5Xyl is recovered in the precipitate with CA for the solution at $C_{H,i}$ = 30 wt.%, but not for the solutions at $C_{H,i}$ = 18 and 22.5 wt.%. Once again, this is a similar effect compared to the one occurring in spherical aggregation since the solution at $C_{H,i}$ = 30 wt.% is the solution with the most important hydrotrope/solute ratio (see **Figure IV.19**).[242,246]

b. Precipitation of a hydrotropic rosemary extract

As reported in section IV.2.2, a rosemary extract is not pure in CA because by-products are extracted in the same time. Thus, the behavior of hydrotropic extracts during precipitation was compared to the precipitation of CA, to point out the similarities and differences. Extractions of 5 g of rosemary were performed with 50 mL of solutions containing 18, 22.5 and 30 wt.% *i*-C_5Xyl. After the plant/hydrotropic solution separation by filtration, the liquid extracts were diluted with acidic water (pH 2) to 9 wt.%, stirred for 1 h and settled for 1 h. As for pure CA, solutions were observed through numeric microscopy.

Numerous spherical particles from 1 to 3 µm were observed when the hydrotropic extract was precipitated whereas needle-like particles had been formed from pure CA precipitation. Other large particles (**Figure IV.22c, d**) are observed and **Figure IV.22a** and **b** suggest that they are formed by agglomeration of the particles **(a)** followed by coalescence **(b)**. It is likely that the resulting particles are first irregular **(c)** and then, homogenise to become quite spherical **(d)**.

Some small solid particles from the plant which passed through the filter (parts of trichomes from example) are also observed and initiate aggregation around them (**Figure IV.23**).

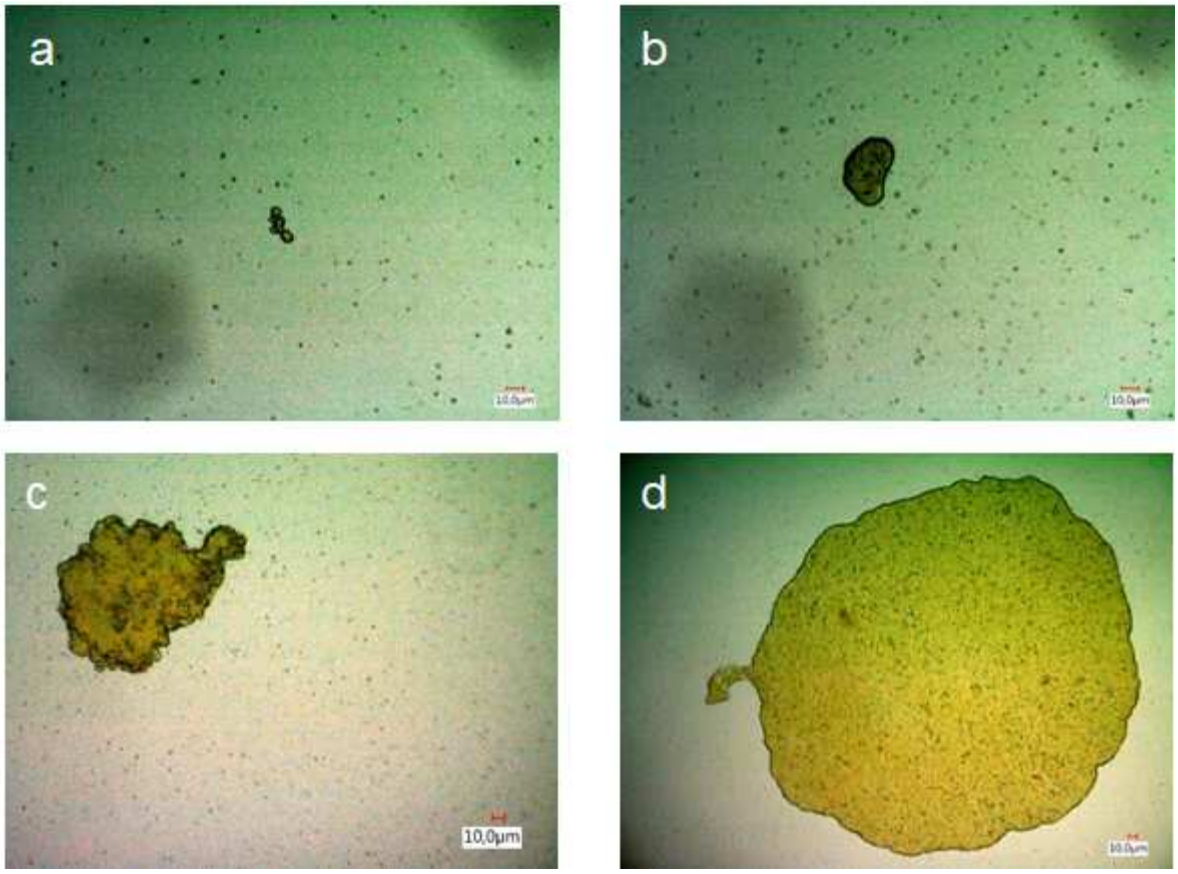

Figure IV.22. Microscopic images of particles at different stages of the agglomeration/coalescence process of the crude extract performed at $C_{H,i}$ = 30 wt.% and diluted to 9 wt.%. Images were taken during the settling step. (a) Flocculation, (b) Coalesced particle, (c) Agglomerate with irregular shape, (d) Large spherical agglomerate

Figure IV.23. Microscopic images of an agglomerate during the precipitation of the crude extract performed at $C_{H,i}$ = 18 wt.% and diluted to 9 wt.%. Trichomes that must have been removed from rosemary during the hydrotropic extraction are visible at the center of the agglomerate

Noteworthy, at the end of the settling steps, numerous small black particles (1 -3 µm) remain in suspension, as shown in **Figure IV.22**. This phenomenon should be related to the results of the experimental design, showing that the use of a 1µm-filter rather than a 3µm-filter resulted

in a higher yield, but lower CA content. The fact that the porosity is a significant factor for the yield is obviously explained by the presence of those small particles at the end of the process, which can pass through the 3 µm-filters. However, their recovery seems to lower the CA content, so they should be composed of a higher hydrotrope fraction compared to large particles, or of other extracted components. Due to higher surface specific areas, it is likely that they adsorb more hydrotropes on their surface that the bigger particles. Since small particles are still in suspension during the settling step and regarding that their aggregation needs agitation to facilitate their encounter, it is likely that the agitation step has not been long enough and that small particles would continue to aggregate if the residence time is longer.

IV.3. Experimental part

IV.3.1. Carnosic acid quantification by HPLC

The major part of CA quantifications were performed with procedure presented in general experimental part, section B, but two other HPLC procedures are decribed for this chapter, depending on the application.

a. Preparation of the samples.

For each HPLC procedure, the samples were previously diluted by 10 in methanol (HPLC grade) containing 0.1 % (v/v) of TFA and filtered with 0.2 µm PTFE syringe filters.

b. Procedure 1 (Naturex).

The mobile phase was an isocratic solution containing 65 % of acetonitrile and 35 % of acidic water (0.5 % H_3PO_4). The flow rate was set to 1.5 mL/min. A C_{18} 5 µm (250 x 4.5 mm) column was used at 25 °C. CA and CAR were detected at 230 nm.

c. Procedure 2 (Lille)

Analyses were performed using an HPLC apparatus LC 20AD from Shimadzu equipped with an autosampler (injection = 10 µL), a C_{18} column (Interchim, 5 µm particle, 3.0 x 150 mm), and a UV detector (SPD 20A) set at 210 and 230 nm and an ELSD detector (LT-II from Shimadzu) The temperature was maintained at 30 °C in the oven and in both detectors. The mobile phase was a mixture of methanol (0.1 % (v/v) TFA) (A) and water (B). The gradient elution started at 60% of solvent A for 20 min, was increased to 80% for 5 min, and stabilized

at 80 % for 30 min. The flow rate was 0.25 mL/min from 0 to 25 min and was increased to 0.5 mL/min after 30 min of analysis. The hydrotrope *i*-C_5Xyl was detected by ELSD at 7.5 min and CA was detected both by ELSD and UV at 38 min of retention time.

IV.3.2. Measurement of the turbidity through Crystal Eyes system.

The hydrotropic solution of *i*-C_5Xyl (100 mL) was prepared in a thermostated double walled beaker and adjusted to pH 2 with 1 % (v/v) of phosphoric acid (85 %). The required mass of CA or extract was added to the solution. The temperature ramps were provided by a programmable water-bath in a cooling circulator (Huber). It was first adjusted to 70 °C before starting the experiment, and the powder of CA or extract was dispersed with an Ultra Turrax T 25 (IKA) at 15000 rpm to ensure its complete dissolution. Then, the thermo-controlled circulator was programmed with two cycles from 70 to 15 °C, with heating ramps set at 2 °C/min and temperature stabilization at the extrema for 20 min.

All the measurements presented herein were obtained using a HEL E1450S turbidity probe and a temperature probe operated by Crystal Eyes software and immersed in the hydrotropic solution. The solutions were stirred at 250 rpm using a magnetic bar.

IV.3.3. Extraction and precipitation methods

a. Extraction followed by precipitation by cooling.

The hydrotropic solution of *i*-C_5Xyl (100 mL) was prepared in a double walled beaker at the required concentration and acidified to pH 2 with 1 % (v/v) of phosphoric acid (85 %). Rosemary leaves (10 g) were grounded to 0.5 mm by a IKA® MF10 grinder and added to the hydrotropic solution. The mixture was stirred for 30 min at 250 rpm at 55 °C (temperature controlled by the cooling circulator). Then, the plant was separated from the solution by a Büchner filtration under vacuum using a 5-15 µm filter which had previously been heated to 55 °C to avoid the precipitation of the extract in the filter. The vessel used for the filtration was also preheated at 55 °C in an oven. Then, the filtrate was cooled to 10 °C to induce the precipitation. It was then filtered through 1 µm glass microfiber filter. Since no precipitate was observed in most cases, the filtrate was analysed by HPLC to determine the amount of CA retained on the filter (procedure 1).

b. Experimental design.

An extraction was performed using 100 g of ground rosemary and 1000 mL of hydrotropic solution containing 30 wt.% of *i*-C_5Xyl, at pH 2 (1 % (v/v) H_3PO_4 85 %). For the grinding, 20 g of rosemary was milled in a blender (Philips HR2056/90) for 1 min providing a powder with

an average particle size of about 0.5 mm. The mixture was magnetically stirred at 50 rpm for 30 min at 25 °C. Then, the plant material was separated from the solution by a Büchner filtration under vacuum using a cellulose filter (8 µm) to recover 700 mL of enriched solution of CA (2.25 g/L according to the HPLC analysis). The filtrate was separated in 15 samples of 42 mL each, which were diluted with acidic water (pH 2, 1 % (v/v) H_3PO_4 85 %) with the conditions specified in the experimental design. The temperature was controlled using a thermostated water bath. The precipitate was filtered using the specified filters and freeze-dried over about 6 hours until the mass remained stable (- 50 °C, 0.2 mbar). The resulting extracts were weighted, diluted in 50 mL of methanol and analysed by HPLC (experimental part, section B).

c. Experimental design statistics

The coefficients of effects, noted b, were calculated using Microsoft Excel. The experiment 6 was repeated three times to perform a "repeated measures Student t-test": the standard deviations SD(Y) and SD(b_i) of the response and the effects were calculated and the significance threshold with a 95 % confidence level was determined using the Student t-distribution table (two-tailed), with the corresponding *p*-value (< 0.05) and a degree of freedom of 2 (3 repeated experiments -1).

d. Conventional extractions.

In section IV.2, the hydrotropic extracts were prepared from 10 or 100 g of ground rosemary, following the procedure described in section III.4.5.b.

e. Conventional precipitation.

The crude hydrotropic extract was precipitated by sudden dilution with a factor 2.5 with acidic water (pH 2). The *i*-C_5Xyl concentration decreased to 9 wt.%, which induced the precipitation of the extract. The next steps are already described in section III.4.5.d.

f. Recovery of the precipitate by centrifugation and washing procedure.

After a conventional extraction with 100 mL of hydrotropic solution, the crude extract solution (78 mL recovered) was split in 7 equal samples of 10 mL, as presented in **Figure IV.13**, and the sudden dilution by 2.5 or 4 with acidic water was directly performed in the 50 mL Falcon® centrifuge tubes. Then, the precipitate was separated from the supernatant by centrifugation (5 min, 5000 rpm) with a Sigma 2 -16 PK centrifuge. All the precipitates were dark and pasty before washing. Then, 10 mL of acidic water (pH 2) were added to six of the seven tubes to wash the extract, which were manually agitated for 5 min, sonicated for 5 min and manually

agitated again for 5 to 10 min until complete dispersion of the extract. The six tubes were centrifuged (5 min, 5000 rpm) and this procedure was repeated once on four tubes and twice on two tubes. The final precipitates were freeze-dried (- 50 °C, 0.2 mbar), weighted, diluted in methanol (1 % v/v TFA) and analyzed by HPLC to quantify both *i*-C_5Xyl and CA. Then, methanol was removed by evaporation under vacuum, and the extracts were dissolved in DMSO-d_6 to be analyzed by ^{1}H NMR. NMR spectra were recorded on a Bruker 300 apparatus and calibrated relative to residual solvent peaks (H_2O: 3.33 ppm; DMSO-d_6: 2.54 ppm).

g. Recovery of the precipitate by filtration and washing procedure

After a conventional extraction with 100 mL of hydrotropic solution, and a conventional precipitation, the precipitate was recovered on a 2 – 3 µm cellulose filter. Then, the precipitate was washed by taking off the filter, and put it in a glass recipient with a magnetic bar (400 rpm) to unstick it from the filter as explained in the text. Thanks to the mechanical action of the magnetic bar, the precipitate could be unstuck from the filter and dispersed in acidic water. Then, the filter was taken back and used to filtrate the washing solution. After three washing steps, the precipitate was freeze-dried (- 50 °C, 0.2 mbar), weighted, diluted in methanol (1 % v/v TFA) to be analyzed by HPLC (procedure 3).

IV.3.4. Measurement of the oxidative induction time.

FAMEs were synthesized from sunflower oil and sodium methanolate in methanol at room temperature (25 °C) for 12 hours, then extracted with petroleum ether three times and purified through neutral aluminium oxide column, using petroleum ether as eluent. The purity of FAMEs was assessed by NMR ^{1}H, and they were stored at - 20 °C.

Then, 2 mL of sunflower FAMEs were placed in a teflon container in the RapidOxy apparatus (Anton Paar). The oxygen overpressure was set to 300 kPa and the temperature to 110 °C. Antioxidant was added at 0.1 wt.%, using a presolubilized solution in ethyl acetate 20 g/L. The overpressure was measured by the software OxyLogger.

IV.3.5. Microscopic observation of the crystals.

Hydrotropic solutions of *i*-C_5Xyl (50 mL) at 18, 22.5 and 30 wt.% containing 2.5 g/L of CA were prepared. To ensure CA solubilization, the solutions were set to 40 °C until they became completely limpid, then cooled down to room temperature. The solutions were diluted with acidic water (1 % (v/v) H_3PO_4 85 %, pH 2) to the MHC (9 wt.% of *i*-C_5Xyl). The water addition

rate was kept to 0.05 mL/sec using dropping funnel. After all the required water was added, the solutions were stirred for 1 h at 500 rpm and then, settled without stirring for 1 h. During all this process, samples (10 µL) were collected and observed by a numeric microscope to determine the crystal sizes and shapes. This procedure was performed two times for each *i*-C_5Xyl concentration.

The same procedure was performed after extractions using the conventional procedure described above, with 50 mL of hydrotropic solutions at 18, 22.5 and 30 wt.% *i*-C_5Xyl for 5 g of rosemary.

IV.4. Conclusions of chapter IV

This chapter was an opportunity to compare the different techniques to recover a rosemary hydrotropic extract and to understand the mechanism of hydrotropic precipitation. Hydrotropic dilution with acidic water was found much more efficient compared to cooling to recover the hydrotropic crude extract. Indeed, thanks to a Hadamard experimental design, and to the use of appropriate filters, the recovery rate of CA could be increased by a factor 2 and the CA content in a dry extract without washing could reach up to 20.5 wt.%, the same content that can be obtained with acetone. We showed that washing the extract with water could enhance the CA rate by about 25 %. However, the recovery rate reached with acetone could not be equalled with *i*-C_5Xyl. The precipitation process still needs to be improved in accordance with the conclusions on the crystallization mechanism hereunder.

From the conclusions of the Hadamard experimental design and microscopic observations, a mechanism of rosemary extract crystallization by *i*-C_5Xyl can be proposed in accordance to the literature. It is basically composed of three steps, presented in **Figure IV.24**:

- **Nucleation:** The hydrotropic solution is diluted to a concentration at which rosemary extract is saturated. Thus, the rosemary extract precipitates in spherical particles. This shape is due to the presence of by-products since pure CA forms needle-like crystals. With slow dilution, only few particles are generated first, then grow.

- **Growth:** Thanks to strong solute-hydrotrope interactions, the particles of rosemary extract are immersed in larger hydrotrope-rich particles. Then, thanks to stirring, these particles meet, aggregate and finally coalesce. When they become too large and too heavy, they settle down and fix on the vessel glass walls. A low hydrotrope concentration or a too vigorous stirring limit their growth and thus their fixation on the vessel walls. On the contrary, the longer the residence (agitation) time, the larger the aggregates. During this step, *i*-C_5Xyl acts as a bridging liquid.

- **Concentration:** During the residence time, extract particles get closer, bond and consolidate. In the same time, probably due to stirring and further crystallization, hydrotropes are removed from the particles and solubilized in the solution.

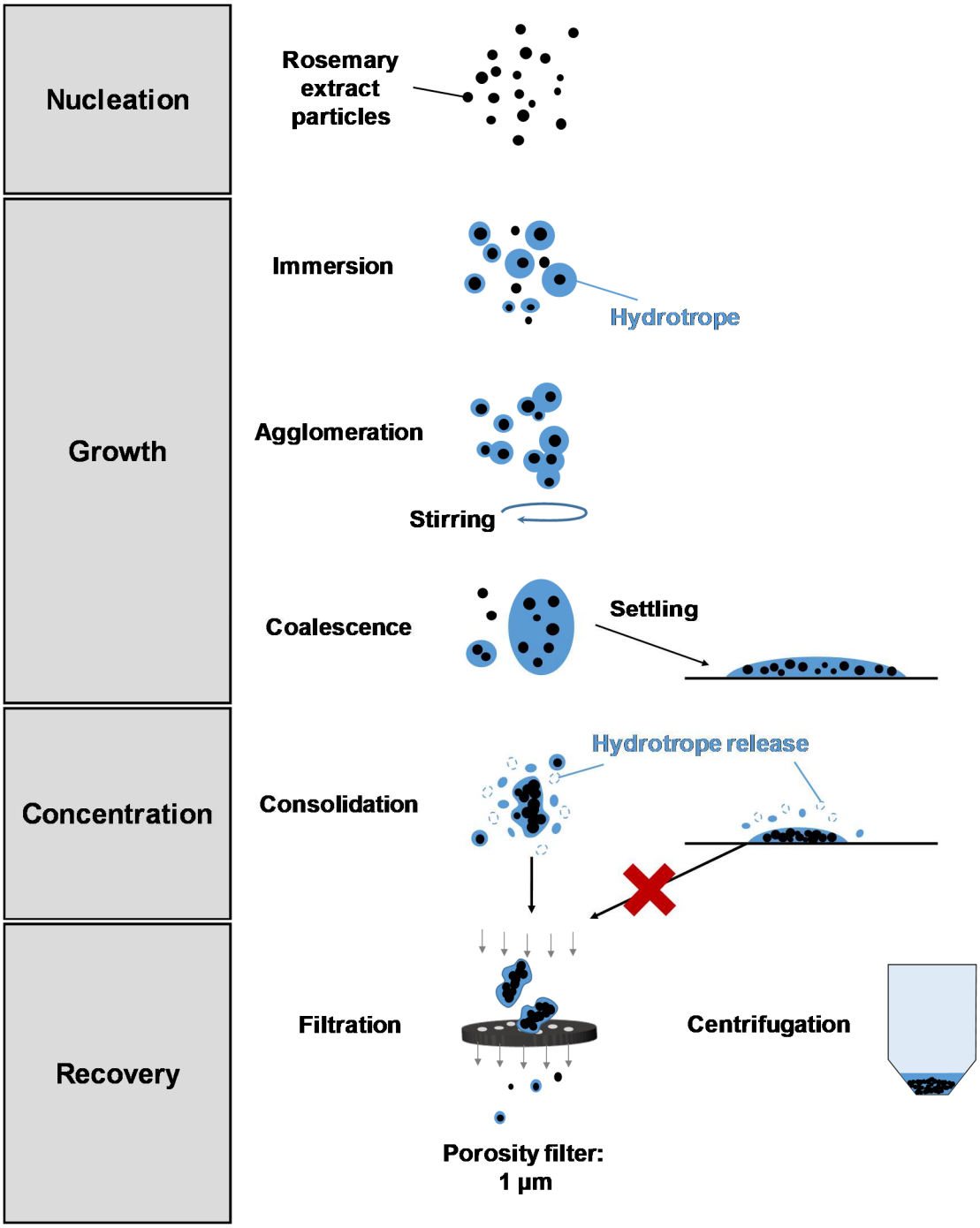

Figure IV.24. Mechanism of hydrotropic precipitation of a rosemary extract by dilution with water.

Finally, the extract particles are recovered by either filtration or centrifugation. Filtration separate the large extract particles from the small ones which were either removed from the particles during the consolidation step, or did not have the time to agglomerate. They are composed of other extracted compounds or enriched in hydrotropes (more adsorption on more surface specific area). On the contrary, centrifugation recovers all particles, resulting in a lower CA content but a higher mass yield. Noteworthy, the consolidation of the extract particles continues during filtration and centrifugation. According to HPLC measurements, the residual

hydrotrope can be totally removed thanks to washing, providing rosemary extract as a non-sticky powder.

Therefore, to increase the recovery rate, three interesting options could be investigated: *(i)* reduce the water addition rate, *(ii)* increase the residence time during which the solution is stirred *(iii)* centrifuge the solution after the optimized process.

General conclusion

Carnosic acid (CA) is a phenolic diterpene which naturally occurs in rosemary and sage. It has received a special attention in recent years due to its strong antioxidant power. Indeed, the high antioxidant capacity induced by its catechol group (**Figure V.1**) and its ability to regenerate the corresponding phenolic hydroxyls from the *o*-quinone formed by oxidation makes CA suitable for replacing controversial synthetic ingredients such as BHA or BHT in cosmetic or food preparations.

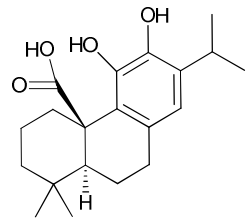

Figure V.1. Chemical structure of carnosic acid

Nowadays, ethanol and other solvents such as acetone or hexane are commonly used to extract CA from rosemary and sage. However, in a responsible, environmental and sustainable approach, their use should be avoided in order to limit the release of VOC, as well as the risks related to health of operator and to high flammability. This thesis aimed to investigate the potential of aqueous solution of nonionic hydrotropes as alternatives to organic solvents in the process of CA extraction. Indeed, hydrotropes are small amphiphilic molecules generally composed of a polar head which provides interactions with water and an apolar alkyl chain bearing a number of carbon atoms which does not exceed 8, otherwise the amphiphile is called surfactant. Such a structure confers them the ability to form aggregates or clusters in water, thus enhancing the solubilization of hydrophobic compounds such as CA.

Thereby, three families of hydrotropes, namely **alkyl polyethylene glycol ethers C_iE_j** (**chapter II**), **alkyl polyglycosides C_iGlyco** and **monoalkyl glycerols C_iGly** (**chapter III**) bearing alkyl chain lengths from 4 to 8 have been investigated in details. There were chosen for their several reasons: *i*) their accessibility as commercial materials in the case of some C_iE_j and C_iGlyco, *ii*) the availability of a large range notably for the C_iE_j (*i* from 4 to 8 and *j* from 1 to 4), *iii*) their bio-based origin. Our approach has consisted in performing first a systematic study on the petro-sourced C_iE_j to gain a better understanding of the mode of action of hydrotropes and then secondly to extent the scope to the bio-based ones with the aim of developing a suitable system for a potential industrial production. Thus, we were also interested in the process of extraction, which we studied and optimized with the most promising amphiphile.

In the first part of the thesis, we focused on the mechanism and the relationships between the chemical and physicochemical features of the hydrotropes and their efficiency as extractants. Extractions were performed from whole leaves of rosemary so that the mass transfer of extracted molecules resulted only from the action of the hydrotropes. The comparison of the content of CA recovered in the fourteen aqueous solutions of **alkyl polyethylene glycol ethers** (C_iE_j with the alkyl chain length i = 4 - 12 and the number of ethylene oxide units j = 1-4) after extraction at room temperature highlighted **C_5E_2** and **C_4E_1** as the most efficient hydrotropes able to extract **1.21 g/L in 24 h and 1.02 g/L CA in 8 h** respectively. For comparison, aqueous solutions of propanol at the same concentration (30 wt.%) extracted 0.93 g/L in 48 h, and ethanol at 96 wt.% reached 1.24 g/L CA in 24 h (CA not soluble in 30 wt.% ethanol). Thanks to a systematic study carried out on the range of C_iE_j, some key features could be identified: a

molecular volume V_m close to 240 or 218 (depending on the model), a **partitioning coefficient log *P*** equal to 1.37 and a **hydrophilic lipophilic balance HLB** of 12, thanks to the following equations modelling the CA concentration as a function of these three descriptors:

$$C_{CA} = 1.2 \times \exp\left(-0.3 \times \left(\frac{V_m - 240}{100}\right)^2 + (\log P - 1.37)^2\right)$$

$$C_{CA} = 1.15 \times \exp\left(-0.066 \times \left(\frac{V_m - 218}{55}\right)^2 + (HLB - 12)^2\right)$$

In addition, microscopic observations allowed to show the different modes of action between the hydrotropic solutions and solvents such as ethanol. Indeed, the combined actions of water and C_iE_j favors the destruction of the leaves, resulting in the **release of the phytochemicals** in the solution and easier access of the aqueous hydrotrope to the cells while ethanol only enhances the **mass transfer of actives**, without affecting the structure of the plant (**Figure V.2**).

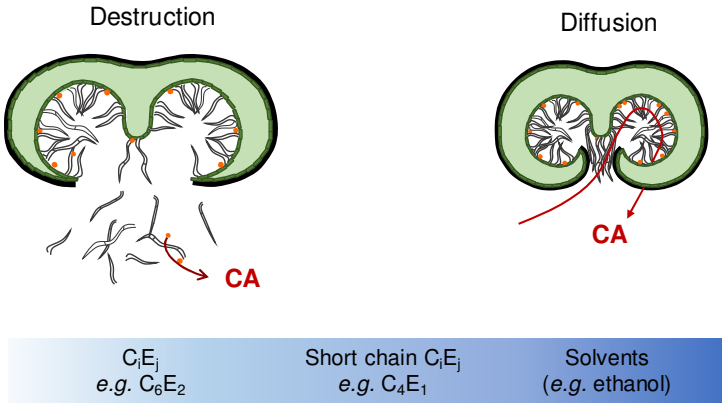

Figure V.2. Scheme of two different modes of action of solvents and aqueous solutions of C_iE_j for the extraction of CA from rosemary leaves (presented in cross sections)

However, though efficient, C_iE_j cannot be industrially used because of their petro-sourced origin, their low biodegradability and their potential toxicity (*e.g.* C_4E_1 is classified as VOC and toxic or hazardous air contaminant). Accordingly, in order to develop a process with bio-based hydrotropes, the efficiency of three synthetic **monoalkyl glycerols** (C_iGly with i = 4 - 5) has then been assessed. **Pentyl glycerol (C_5Gly)** was found to be more efficient than butyl glycerol **(C_4Gly)** and than its isomer *iso*-amyl glycerol **(*i*-C_5Gly)** with 1.07 g/L of CA recovered in the hydrotropic solution after 48 h of extraction. By grinding the plant, a concentration of 2.53 g/L CA could be reached in the filtrate of extraction after only 30 min, close to the maximum value expected of 2.7 g/L. From this observation, despite the fact that the grinding step is not straightforward to implement at the large scale, it is an important process parameter of extraction since the efficiency is increased by a factor 2.5, while the time is considerably reduced from 48 h to 30 min.

Alkyl polyglycosides constitute the second family of bio-based hydrotropes which was investigated. ***Iso*-amyl polyxyloside** was the most efficient hydrotrope of this family, and could

extract 0.43 g/L CA from whole leaves, with a maximum concentration expected of 2.7 g/L. This concentration could be increased to 2.1 g/L by grinding the plant. Noteworthy, its higher efficiency compared to other alkyl polyglycosides, as well as its lower efficiency compared to C_iE_j, was attributed to its structure, in accordance with the key features pointed out with the systematic study of C_iE_j. Indeed, *iso*-amyl polyxyloside has the smallest polar head of the alkyl polyglycosides since it is only composed of pentoses and has the lowest degree of polymerisation, but also a larger polar head than most of C_iE_j, conferring it a higher polarity, hydrophilicity and volume than C_iE_j, and the lowest of the alkyl polyglycosides.

The influence of the volume and polarity or hydrophilicity of hydrotropes were attributed to their ability to **diffuse through cell barriers**, but contact angle measurements of hydrotropic solutions with $i = 4$ and 5 on rosemary leaves showed the influence of the hydrotrope structure on interfacial tension, and therefore, on their **adsorption** on the plant surface. Indeed, it was shown that *(i)* the interfacial tension is lower for a linear chain than a branched one, and for a hydrophobic polar head rather than a hydrophilic one: $C_iE_2 < C_iGly < G_iGlyco$ and *(ii)* for a same alkyl chain length, the concentration of CA in the hydrotropic solution exponentially increases when the interfacial tension decreases.

Despite alkyl polyglycosides were less efficient than monoalkyl glycerols, their commercial availability and their higher biodegradability made them hydrotropes of particular interest, and ***iso*-amyl polyxyloside** was found a good compromise to adapt hydrotropic extraction on ground rosemary at a larger scale. The advantages and drawbacks of using hydrotropes (i = 3-7) and solvents are summarized in **Figure V.3**, as well as the concentration of CA recovered in the filtrate after extractions of whole rosemary leaves for 48 h.

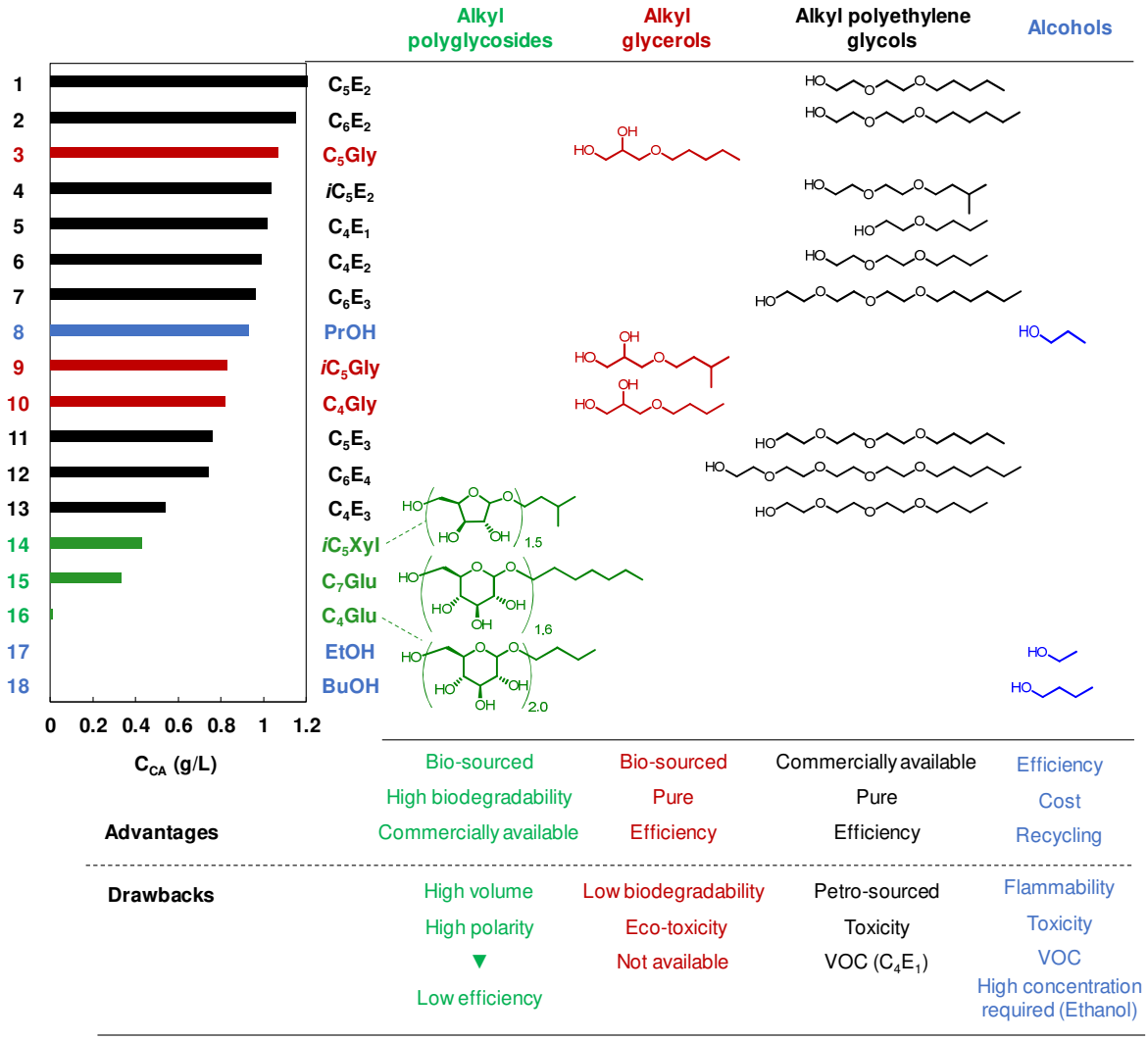

Figure V.3. Concentration of CA in the aqueous solution at 30 wt.% hydrotrope or solvent (with *i* = 3-7) after 48 h of maceration of whole rosemary leaves under stirring at pH 2, chemical structures of hydrotropes ranged by order of efficiency, advantages and drawbacks relative to their use.

As mentioned previously, grinding the plant appears as a mandatory step to recover a maximum amount of CA. Indeed, by grinding the plant, cell barriers are broken and thus, cells automatically release phytochemicals in the hydrotropic solution. However, many co-products could also be easily extracted in addition to CA, hence a less selective extraction. To overcome this drawback, the **selectivity** of solubilization of several alkyl polyglycosides was studied in **chapter III**. ***Iso*-amyl polyxyloside** was found to be the most selective hydrotrope with its small alkyl chain length, limiting the solubility of the apolar ursolic acid, and allowing solubilization of CA. With a too small alkyl chain length, butyl polyglucoside could not solubilize enough CA, resulting in an inefficient extraction that was limited by the solubility of CA rather than by the diffusion of the amphiphile. On the contrary, a too long alkyl chain (*i* > 8) was also found to be inefficient due to very high viscosity attributed to the formation of liquid crystals typically encountered with surfactants.

The alkyl chain length has also an important influence on the **recovery** of CA. Indeed, the most efficient recovery method was found to be the dilution under the Minimum Hydrotropic Concentration (MHC) to precipitate the extract. However, increasing the alkyl chain length resulted in reducing the MHC, thus increasing the dilution factor required to precipitate the extract. Therefore, considering that the dilution factor was applied to both the amphiphile and the solute, the CA concentration could be reduced to its solubility limit, so that CA did not precipitate. This consideration promotes once again the use of hydrotropes rather than surfactants. **Figure V.4** summarizes the relationship between structure, physicochemical properties and role of hydrotropes in the entire extraction process.

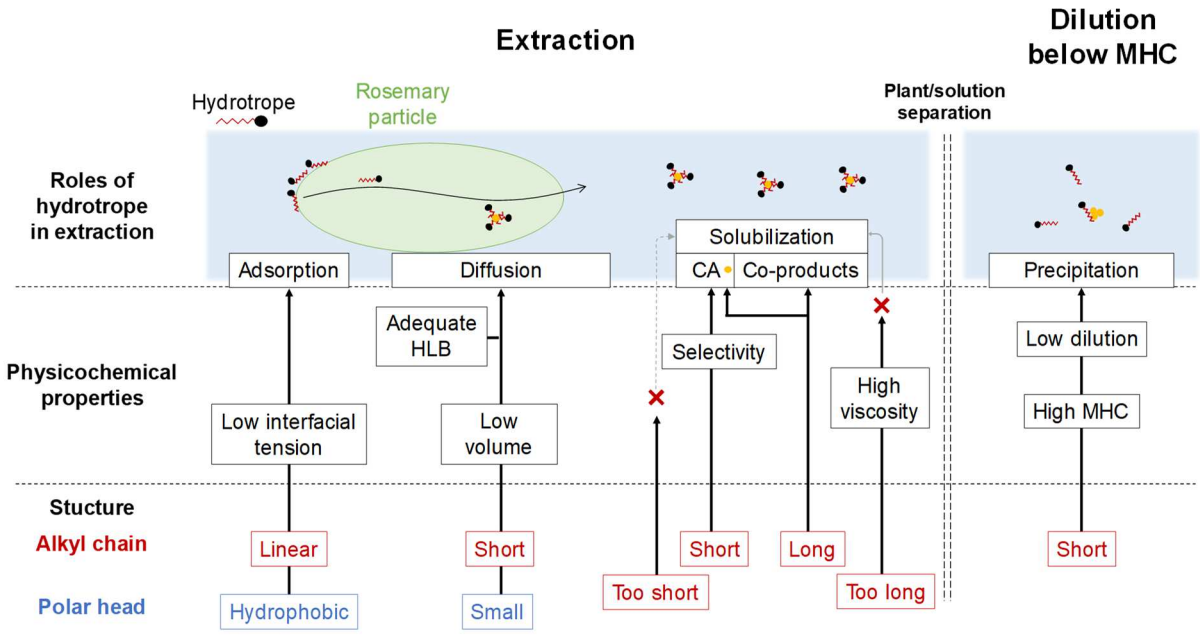

Figure V.4. Roles of hydrotropes in the extraction mechanism and influence of their structure one their physicochemical properties and on their role during extraction.

A second part of the thesis was devoted to **optimizing** the entire extraction process using *iso*-amyl polyxyloside, namely the conditions for both the extraction of CA from rosemary and its recovery in solid form (**chapter III and IV** respectively). A first experimental design using a 2^4 fractional matrix on the **extraction** conditions showed that *(i)* the most important condition to extract a high CA concentration is the **hydrotrope concentration**, *(ii)* increasing the temperature and the time of extraction has a great influence on the final solid extract, but not on the extract mass of CA recovered, meaning that CA is more accessible than co-products of extraction. However, although 2.1 g/L of CA could be recovered in the first filtrate with the best experiment (62 % of the available CA), the major part of CA was lost during the precipitation. This step was thus optimized in **chapter IV** in order to increase the recovery of CA from the hydrotropic solution.

The **hydrotropic precipitation** step was first optimized using a Hadamard factorial design, which analyzed the relative importance and the influence of eight factors of the precipitation (dilution rate, hydrotrope concentration after dilution, temperature, stirring, time of stirring,

time of settling, nature and porosity of the filter) on the mass yield and the CA content in the extract. A low **dilution rate** and a low **porosity of the filters** (1 µm) were found to be determinant conditions to increase the mass yield. By combining the best conditions of precipitation, the recovery rate could be increased from 24 to 55 %, thus only 6 % of CA was lost in the filtrate. The resulting extract contained 20.5 wt.% CA, the same content as that obtained from a conventional extraction with acetone (**Table V.1**). However, the recovered extracts were pasty, which should be avoided for industrial applications in order to facilitate its recovery.

To explain this aspect, the **mechanism of hydrotropic precipitation** was investigated thanks to microscopic observations. Indeed, it seems that the hydrotropes act as a "bridging liquid", *i.e.* particles of precipitated extract are immersed in droplets of hydrotrope, which size seems to increase with the hydrotrope concentration. Those particles are highly concentrated in both CA and hydrotrope and certainly grow by a phenomenon of agglomeration. An adequate agitation allows particles to meet and thus, to agglomerate while preventing the particles to form smaller ones, which would pass through the filters. Finally, to avoid having a pasty extract, the hydrotrope can be removed by washing with water. However, this step has so far resulted in an additional loss of 15 % CA (**Table V.1**).

Table V.1. Comparison of different extraction techniques (30 min maceration under stirring) of CA from ground rosemary leaves.

Extraction technique	**Conventional**	**Not optimized**		**Optimized**	
Solvent	Acetone	*i*-C_5Xyl (wt.%) 22.5		30	
Recovery technique	Evaporation	Filtration (3 µm)		Filtration (1 µm)	
Precipitate washing	0	0	3	0	3
Yield (%)	12.7	5.2	2.63	7.2	4.5
CA content (%)	20.0	12.6	26.5	20.5	24.6
Recovery rate (%)	92	24	25	55	40

The objectives of this thesis work were at different levels: *i*) finding an efficient and safe aqueous solution of nonionic hydrotropes as an alternative to organic solvents for the extraction of CA from rosemary, *ii)* understanding the physicochemical mechanism and the roles of hydrotropes during the extraction process, and finally *iii)* optimizing the entire process. Despite monoalkyl glycerols were found to be more efficient than *iso*-amyl polyxyloside in extracting CA from whole and ground leaves of rosemary, *i*-C_5Xyl was chosen as the best compromise owing to its higher biodegradability and its commercial-availability. By performing the extraction on ground leaves with 30 wt.% *iso*-amyl polyxyloside without no intensification nor heating, and with optimum filters, dilution and dilution rate, an extract with a CA content of 20 wt.% could be obtained. It contained 55 % of the available CA and 6 % of CA were lost during the precipitation. However, considering that at least 20 % of the available CA are lost in the plant due to high absorption of aqueous solution by the dehydrated leaves, it should be interesting to extract again the leaves to recover the remaining part of CA. Finally, alcohols are

still more easily recyclable than hydrotropic solutions thanks to their low boiling points, but in a "green" approach, the dilute solution, which still contains hydrotrope, could further be heated to evaporate the amount of water that has been added during the dilution step, and could this was be recycled. **Figure V.5** summarizes the roles of hydrotropes and other conditions during extraction and proposes suggestions for future research.

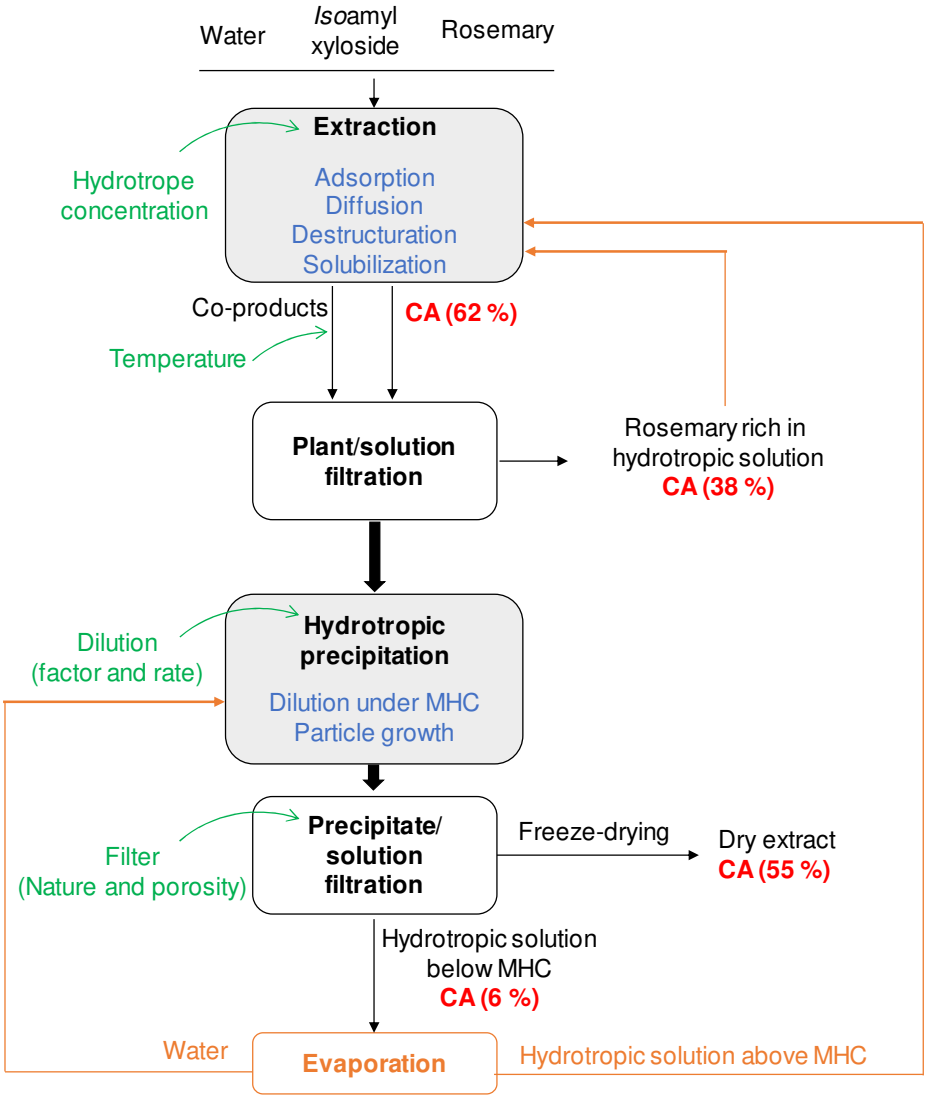

Figure V.5. Schematic diagram of the CA extraction, most important factors (green), roles of hydrotrope (blue), location of CA (red) and perspective of research for better optimization and recycling (orange)

References

(1) Brewer, M. S. Natural Antioxidants: Sources, Compounds, Mechanisms of Action, and Potential Applications. *Compr. Rev. Food Sci. Food Saf.* **2011**, *10* (4), 221–247. DOI: 10.1111/j.1541-4337.2011.00156.x.

(2) Domínguez, R.; Pateiro, M.; Gagaoua, M.; Barba, F. J.; Zhang, W.; Lorenzo, J. M. A Comprehensive Review on Lipid Oxidation in Meat and Meat Products. *Antioxidants* **2019**, *8* (10), 429. DOI: 10.3390/antiox8100429.

(3) Farhoosh, R.; Johnny, S.; Asnaashari, M.; Molaahmadibahraseman, N.; Sharif, A. Structure–Antioxidant Activity Relationships of o-Hydroxyl, o-Methoxy, and Alkyl Ester Derivatives of p-Hydroxybenzoic Acid. *Food Chem.* **2016**, *194*, 128–134. DOI: 10.1016/j.foodchem.2015.08.003.

(4) Barlow, S. M. Toxicological Aspects of Antioxidants Used as Food Additives. In *Food Antioxidants*; Hudson, B. J. F., Ed.; Elsevier Applied Food Science Series; Springer Netherlands: Dordrecht, **1990**; pp 253–307. DOI: 10.1007/978-94-009-0753-9_7.

(5) Lourenço, S. C.; Moldão-Martins, M.; Alves, V. D. Antioxidants of Natural Plant Origins: From Sources to Food Industry Applications. *Molecules* **2019**, *24* (22), 4132. DOI: 10.3390/molecules24224132.

(6) Ribeiro-Santos, R.; Carvalho-Costa, D.; Cavaleiro, C.; Costa, H. S.; Albuquerque, T. G.; Castilho, M. C.; Ramos, F.; Melo, N. R.; Sanches-Silva, A. A Novel Insight on an Ancient Aromatic Plant: The Rosemary (*Rosmarinus Officinalis* L.). *Trends Food Sci. Technol.* **2015**, *45* (2), 355–368. DOI: 10.1016/j.tifs.2015.07.015.

(7) Chipault, J. H.; Mizuno, G. R.; Hawkins, J. M.; Lundberg, W. O. The Antioxidant Properties of Natural Spices. *J. Food Sci.* **1952**, *17* (1–6), 46–55. DOI: 10.1111/j.1365-2621.1952.tb16737.x.

(8) Birtić, S.; Dussort, P.; Pierre, F.-X.; Bily, A. C.; Roller, M. Carnosic Acid. *Phytochemistry* **2015**, *115*, 9–19. DOI: 10.1016/j.phytochem.2014.12.026.

(9) Sebranek, J. G.; Sewalt, V. J. H.; Robbins, K. L.; Houser, T. A. Comparison of a Natural Rosemary Extract and BHA/BHT for Relative Antioxidant Effectiveness in Pork Sausage. *Meat Sci.* **2005**, *69* (2), 289–296. DOI: 10.1016/j.meatsci.2004.07.010.

(10) Richheimer, S. L.; Bernart, M. W.; King, G. A.; Kent, M. C.; Beiley, D. T. Antioxidant Activity of Lipid-Soluble Phenolic Diterpenes from Rosemary. *J. Am. Oil Chem. Soc.* **1996**, *73* (4), 507–514. DOI: 10.1007/BF02523927.

(11) Linde, H. Ein neues Diterpen aus *Salvia officinalis* L. und eine Notiz zur Konstitution von Pikrosalvin. *Helv. Chim. Acta* **1964**, *47* (5), 1234–1239. DOI: 10.1002/hlca.19640470517.

(12) Wenkert, E.; Fuchs, A.; McChesney, J. D. Chemical Artifacts from the Family Labiatae. *J. Org. Chem.* **1965**, *30* (9), 2931–2934. DOI: 10.1021/jo01020a012.

(13) Aruoma, O. I.; Halliwell, B.; Aeschbach, R.; Löligers, J. Antioxidant and Pro-Oxidant Properties of Active Rosemary Constituents: Carnosol and Carnosic Acid. *Xenobiotica* **1992**, *22* (2), 257–268. DOI: 10.3109/00498259209046624.

(14) Guitard, R.; Paul, J.-F.; Nardello-Rataj, V.; Aubry, J.-M. Myricetin, Rosmarinic and Carnosic Acids as Superior Natural Antioxidant Alternatives to α-Tocopherol for the Preservation of Omega-3 Oils. *Food Chem.* **2016**, *213*, 284–295. DOI: 10.1016/j.foodchem.2016.06.038.

(15) Munne-Bosch, S. Subcellular Compartmentation of the Diterpene Carnosic Acid and Its Derivatives in the Leaves of Rosemary. *Plant Physiol.* **2001**, *125* (2), 1094–1102. DOI: 10.1104/pp.125.2.1094.

(16) del Baño, M. J.; Lorente, J.; Castillo, J.; Benavente-García, O.; del Río, J. A.; Ortuño, A.; Quirin, K.-W.; Gerard, D. Phenolic Diterpenes, Flavones, and Rosmarinic Acid Distribution during the Development of Leaves, Flowers, Stems, and Roots of *Rosmarinus Officinalis*. Antioxidant Activity. *J. Agric. Food Chem.* **2003**, *51* (15), 4247–4253. DOI: 10.1021/jf0300745.

(17) Munné-Bosch, S.; Alegre, L. Changes in Carotenoids, Tocopherols and Diterpenes during Drought and Recovery, and the Biological Significance of Chlorophyll Loss in *Rosmarinus Officinalis* Plants. *Planta* **2000**, *210* (6), 925–931. DOI: 10.1007/s004250050699.

(18) Brückner, K.; Božić, D.; Manzano, D.; Papaefthimiou, D.; Pateraki, I.; Scheler, U.; Ferrer, A.; de Vos, R. C. H.; Kanellis, A. K.; Tissier, A. Characterization of Two Genes for the Biosynthesis of Abietane-Type Diterpenes in Rosemary (*Rosmarinus Officinalis*) Glandular Trichomes. *Phytochemistry* **2014**, *101*, 52–64. DOI: 10.1016/j.phytochem.2014.01.021.

(19) Werker, E. Function of Essential Oil-Secreting Glandular Hairs in Aromatic Plans of Lamiacea — a Review. *Flavour Fragr. J.* **1993**, *8* (5), 249–255. DOI: 10.1002/ffj.2730080503.

(20) Pintore, G.; Usai, M.; Bradesi, P.; Juliano, C.; Boatto, G.; Tomi, F.; Chessa, M.; Cerri, R.; Casanova, J. Chemical Composition and Antimicrobial Activity of *Rosmarinus Officinalis* L. Oils from Sardinia and Corsica. *Flavour Fragr. J.* **2002**, *17* (1), 15–19. DOI: 10.1002/ffj.1022.

(21) Conde-Hernández, L. A.; Espinosa-Victoria, J. R.; Trejo, A.; Guerrero-Beltrán, J. Á. CO2-Supercritical Extraction, Hydrodistillation and Steam Distillation of Essential Oil of Rosemary (*Rosmarinus Officinalis*). *J. Food Eng.* **2017**, *200*, 81–86. DOI: 10.1016/j.jfoodeng.2016.12.022.

(22) Carvalho, R. N.; Moura, L. S.; Rosa, P. T. V.; Meireles, M. A. A. Supercritical Fluid Extraction from Rosemary (*Rosmarinus Officinalis*): Kinetic Data, Extract's Global Yield, Composition, and Antioxidant Activity. *J. Supercrit. Fluids* **2005**, *35* (3), 197–204. DOI: 10.1016/j.supflu.2005.01.009.

(23) Allaf, T.; Tomao, V.; Ruiz, K.; Bachari, K.; ElMaataoui, M.; Chemat, F. Deodorization by Instant Controlled Pressure Drop Autovaporization of Rosemary Leaves Prior to Solvent Extraction of Antioxidants. *LWT - Food Sci. Technol.* **2013**, *51* (1), 111–119. DOI: 10.1016/j.lwt.2012.11.007.

(24) White, A. I.; Jenkins, G. L. *Salvia Carnosa* (Dougl.). I—A Phytochemical Study**Abstracted from a Part of the Thesis Presented to the Graduate Faculty of the University of Minnesota by Allen I. White in Partial Fulfilment of the Requirements for the Degree of Doctor of Philosophy. *J. Am. Pharm. Assoc. Sci. Ed* **1942**, *31* (2), 33–37. DOI: 10.1002/jps.3030310201.

(25) Mena, P.; Cirlini, M.; Tassotti, M.; Herrlinger, K.; Dall'Asta, C.; Del Rio, D. Phytochemical Profiling of Flavonoids, Phenolic Acids, Terpenoids, and Volatile Fraction of a Rosemary (*Rosmarinus Officinalis* L.) Extract. *Molecules* **2016**, *21* (11), 1576. DOI: 10.3390/molecules21111576.

(26) Borrás-Linares, I.; Stojanović, Z.; Quirantes-Piné, R.; Arráez-Román, D.; Švarc-Gajić, J.; Fernández-Gutiérrez, A.; Segura-Carretero, A. *Rosmarinus Officinalis* Leaves as a Natural Source of Bioactive Compounds. *Int. J. Mol. Sci.* **2014**, *15* (11), 20585–20606. DOI: 10.3390/ijms151120585.

(27) Mulinacci, N.; Innocenti, M.; Bellumori, M.; Giaccherini, C.; Martini, V.; Michelozzi, M. Storage Method, Drying Processes and Extraction Procedures Strongly Affect the Phenolic Fraction of Rosemary Leaves: An HPLC/DAD/MS Study. *Talanta* **2011**, *85* (1), 167–176. DOI: 10.1016/j.talanta.2011.03.050.

(28) Kontogianni, V. G.; Tomic, G.; Nikolic, I.; Nerantzaki, A. A.; Sayyad, N.; Stosic-Grujicic, S.; Stojanovic, I.; Gerothanassis, I. P.; Tzakos, A. G. Phytochemical Profile of *Rosmarinus Officinalis* and *Salvia Officinalis* Extracts and Correlation to Their Antioxidant and Anti-Proliferative Activity. *Food Chem.* **2013**, *136* (1), 120–129. DOI: 10.1016/j.foodchem.2012.07.091.

(29) Bellumori, M.; Innocenti, M.; Binello, A.; Boffa, L.; Mulinacci, N.; Cravotto, G. Selective Recovery of Rosmarinic and Carnosic Acids from Rosemary Leaves under Ultrasound- and Microwave-Assisted Extraction Procedures. *Comptes Rendus Chim.* **2016**, *19* (6), 699–706. DOI: 10.1016/j.crci.2015.12.013.

(30) Olmos, E.; Sánchez-Blanco, M. J.; Ferrández, T.; Alarcón, J. J. Subcellular Effects of Drought Stress in *Rosmarinus Officinalis*. *Plant Biol.* **2007**, *9* (1), 77–84. DOI: 10.1055/s-2006-924488.

(31) Maffei, M. Discriminant Analysis of Leaf Wax Alkanes in the Lamiaceae and Four Other Plant Families. *Biochem. Syst. Ecol.* **1994**, *22* (7), 711–728. DOI: 10.1016/0305-1978(94)90057-4.

(32) Maffei, M.; Mucciarelli, M.; Scannerini, S. Environmental Factors Affecting the Lipid Metabolism in *Rosmarinus Officinalis* L. *Biochem. Syst. Ecol.* **1993**, *21* (8), 765–784. DOI: 10.1016/0305-1978(93)90089-A.

(33) Dumbrava, D.-G.; Moldovan, C.; Raba, D.-N.; Popa, M.-Viorica. Vitamin C, Chlorophylls, Carotenoids and Xanthophylls Content in Some Basil (*Ocimum Basilicum* L.) and Rosemary (*Rosmarinus Officinalis* L.) Leaves Extracts. *J. Agroaliment. Process. Technol.* **2012**, *18*, 253–258, 6.

(34) Oliveira, G. de A. R.; de Oliveira, A. E.; da Conceição, E. C.; Leles, M. I. G. Multiresponse Optimization of an Extraction Procedure of Carnosol and Rosmarinic and Carnosic Acids from Rosemary. *Food Chem.* **2016**, *211*, 465–473. DOI: 10.1016/j.foodchem.2016.05.042.

(35) Jacotet-Navarro, M.; Rombaut, N.; Fabiano-Tixier, A.-S.; Danguien, M.; Bily, A.; Chemat, F. Ultrasound versus Microwave as Green Processes for Extraction of Rosmarinic, Carnosic and Ursolic Acids from Rosemary. *Ultrason. Sonochem.* **2015**, *27*, 102–109. DOI: 10.1016/j.ultsonch.2015.05.006.

(36) Aeschbach, R.; Philippossian, G. Procédé d'obtention d'acide Carnosique et Son Utilisation Pour Ses Propriétés Anticarcinogènes et Antivirales., April 15, **1992**.

(37) Chemat, F.; Strube, J. *Green Extraction of Natural Products*; Wiley-VCH Verlag GmbH & Co. KGaA, **2015**.

(38) Rostagno, M. A. *Natural Product Extraction: Principles and Applications*; RSC green chemistry; Royal Soc. of Chemistry: Cambridge, **2013**.

(39) Bart, H.-J. *Industrial Scale Natural Products Extraction*; Pilz, S., Bart, H.-J., Eds.; Wiley-VCH: Weinheim, Germany, **2011**.

(40) Díaz Reinoso, B.; González Muñoz, M. J.; Domínguez González, H. Chapter 1 - Introduction. In *Water Extraction of Bioactive Compounds*; Dominguez González, H., González Muñoz, M. J., Eds.; Elsevier, **2017**; pp 1–50. DOI: 10.1016/B978-0-12-809380-1.00001-2.

(41) Soquetta, M. B.; Terra, L. de M.; Bastos, C. P. Green Technologies for the Extraction of Bioactive Compounds in Fruits and Vegetables. *CyTA - J. Food* **2018**, *16* (1), 400–412. DOI: 10.1080/19476337.2017.1411978.

(42) Sixt, M.; Koudous, I.; Strube, J. Process Design for Integration of Extraction, Purification and Formulation with Alternative Solvent Concepts. *Comptes Rendus Chim.* **2016**, *19* (6), 733–748. DOI: 10.1016/j.crci.2015.12.016.

(43) Bailey, D. T.; Richheimer, S. L.; Bank, V. R.; King, B. High Purity Carnosic Acid from Rosemary and Sage Extracts by Ph-Controlled Precipitation. WO1996034534A1, November 7, **1996**.
(44) Cravotto, G.; Boffa, L.; Mantegna, S.; Perego, P.; Avogadro, M.; Cintas, P. Improved Extraction of Vegetable Oils under High-Intensity Ultrasound and/or Microwaves. *Ultrason. Sonochem.* **2008**, *15* (5), 898–902. DOI: 10.1016/j.ultsonch.2007.10.009.
(45) Chemat, F.; Abert Vian, M.; Fabiano-Tixier, A.-S.; Nutrizio, M.; Režek Jambrak, A.; Munekata, P. E. S.; Lorenzo, J. M.; Barba, F. J.; Binello, A.; Cravotto, G. A Review of Sustainable and Intensified Techniques for Extraction of Food and Natural Products. *Green Chem.* **2020**, *22* (8), 2325–2353. DOI: 10.1039/C9GC03878G.
(46) Allaf, T.; Allaf, K. Fundamentals of Process-Intensification Strategy for Green Extraction Operations. In *Green Extraction of Natural Products*; Chemat, F., Strube, J., Eds.; Wiley-VCH Verlag GmbH & Co. KGaA: Weinheim, Germany, **2015**; pp 145–172. DOI: 10.1002/9783527676828.ch5.
(47) Belwal, T.; Ezzat, S. M.; Rastrelli, L.; Bhatt, I. D.; Daglia, M.; Baldi, A.; Devkota, H. P.; Orhan, I. E.; Patra, J. K.; Das, G.; Anandharamakrishnan, C.; Gomez-Gomez, L.; Nabavi, S. F.; Nabavi, S. M.; Atanasov, A. G. A Critical Analysis of Extraction Techniques Used for Botanicals: Trends, Priorities, Industrial Uses and Optimization Strategies. *TrAC Trends Anal. Chem.* **2018**, *100*, 82–102. DOI: 10.1016/j.trac.2017.12.018.
(48) Rodríguez-Rojo, S.; Visentin, A.; Maestri, D.; Cocero, M. J. Assisted Extraction of Rosemary Antioxidants with Green Solvents. *J. Food Eng.* **2012**, *109* (1), 98–103. DOI: 10.1016/j.jfoodeng.2011.09.029.
(49) Petigny, L.; Özel, M. Z.; Périno, S.; Wajsman, J.; Chemat, F. Water as Green Solvent for Extraction of Natural Products. In *Green Extraction of Natural Products*; Chemat, F., Strube, J., Eds.; Wiley-VCH Verlag GmbH & Co. KGaA: Weinheim, Germany, **2015**; pp 237–264. DOI: 10.1002/9783527676828.ch7.
(50) Hosni, K.; Hassen, I.; Chaâbane, H.; Jemli, M.; Dallali, S.; Sebei, H.; Casabianca, H. Enzyme-Assisted Extraction of Essential Oils from Thyme (*Thymus Capitatus* L.) and Rosemary (*Rosmarinus Officinalis* L.): Impact on Yield, Chemical Composition and Antimicrobial Activity. *Ind. Crops Prod.* **2013**, *47*, 291–299. DOI: 10.1016/j.indcrop.2013.03.023.
(51) Filly, A.; Fernandez, X.; Minuti, M.; Visinoni, F.; Cravotto, G.; Chemat, F. Solvent-Free Microwave Extraction of Essential Oil from Aromatic Herbs: From Laboratory to Pilot and Industrial Scale. *Food Chem.* **2014**, *150*, 193–198. DOI: 10.1016/j.foodchem.2013.10.139.
(52) Sicaire, A.-G.; Vian, M.; Fine, F.; Joffre, F.; Carré, P.; Tostain, S.; Chemat, F. Alternative Bio-Based Solvents for Extraction of Fat and Oils: Solubility Prediction, Global Yield, Extraction Kinetics, Chemical Composition and Cost of Manufacturing. *Int. J. Mol. Sci.* **2015**, *16* (12), 8430–8453. DOI: 10.3390/ijms16048430.
(53) Chemat, F.; Vian, M. A.; Cravotto, G. Green Extraction of Natural Products: Concept and Principles. *Int. J. Mol. Sci.* **2012**, *13* (7), 8615–8627. DOI: 10.3390/ijms13078615.
(54) King, J. W. Modern Supercritical Fluid Technology for Food Applications. *Annu. Rev. Food Sci. Technol.* **2014**, *5* (1), 215–238. DOI: 10.1146/annurev-food-030713-092447.
(55) Sahena, F.; Zaidul, I. S. M.; Jinap, S.; Karim, A. A.; Abbas, K. A.; Norulaini, N. A. N.; Omar, A. K. M. Application of Supercritical CO2 in Lipid Extraction – A Review. *J. Food Eng.* **2009**, *95* (2), 240–253. DOI: 10.1016/j.jfoodeng.2009.06.026.
(56) Herrero, M.; Plaza, M.; Cifuentes, A.; Ibáñez, E. Green Processes for the Extraction of Bioactives from Rosemary: Chemical and Functional Characterization via Ultra-Performance Liquid Chromatography-Tandem Mass Spectrometry and in-Vitro Assays. *J. Chromatogr. A* **2010**, *1217* (16), 2512–2520. DOI: 10.1016/j.chroma.2009.11.032.

(57) Sánchez-Camargo, A. del P.; Valdés, A.; Sullini, G.; García-Cañas, V.; Cifuentes, A.; Ibáñez, E.; Herrero, M. Two-Step Sequential Supercritical Fluid Extracts from Rosemary with Enhanced Anti-Proliferative Activity. *J. Funct. Foods* **2014**, *11*, 293–303. DOI: 10.1016/j.jff.2014.10.014.

(58) Ali, A.; Chua, B. L.; Chow, Y. H. An Insight into the Extraction and Fractionation Technologies of the Essential Oils and Bioactive Compounds in *Rosmarinus Officinalis* L.: Past, Present and Future. *TrAC Trends Anal. Chem.* **2019**, *118*, 338–351. DOI: 10.1016/j.trac.2019.05.040.

(59) Knez, Ž.; Hrnčič, M. K.; Čolnik, M.; Škerget, M. Chemicals and Value Added Compounds from Biomass Using Sub- and Supercritical Water. *J. Supercrit. Fluids* **2018**, *133*, 591–602. DOI: 10.1016/j.supflu.2017.08.011.

(60) Ibañez, E.; Kubátová, A.; Señoráns, F. J.; Cavero, S.; Reglero, G.; Hawthorne, S. B. Subcritical Water Extraction of Antioxidant Compounds from Rosemary Plants. *J. Agric. Food Chem.* **2003**, *51* (2), 375–382. DOI: 10.1021/jf025878j.

(61) Giacometti, J.; Bursać Kovačević, D.; Putnik, P.; Gabrić, D.; Bilušić, T.; Krešić, G.; Stulić, V.; Barba, F. J.; Chemat, F.; Barbosa-Cánovas, G.; Režek Jambrak, A. Extraction of Bioactive Compounds and Essential Oils from Mediterranean Herbs by Conventional and Green Innovative Techniques: A Review. *Food Res. Int.* **2018**, *113*, 245–262. DOI: 10.1016/j.foodres.2018.06.036.

(62) Zu, G.; Zhang, R.; Yang, L.; Ma, C.; Zu, Y.; Wang, W.; Zhao, C. Ultrasound-Assisted Extraction of Carnosic Acid and Rosmarinic Acid Using Ionic Liquid Solution from *Rosmarinus Officinalis*. *Int. J. Mol. Sci.* **2012**, *13* (9), 11027–11043. DOI: 10.3390/ijms130911027.

(63) Wojeicchowski, J. P.; Ferreira, A. M.; Abranches, D. O.; Mafra, M. R.; Coutinho, J. A. P. Using COSMO-RS in the Design of Deep Eutectic Solvents for the Extraction of Antioxidants from Rosemary. *ACS Sustain. Chem. Eng.* **2020**, *8* (32), 12132–12141. DOI: 10.1021/acssuschemeng.0c03553.

(64) Cláudio, A. F. M.; Ferreira, A. M.; Freire, M. G.; Coutinho, J. A. P. Enhanced Extraction of Caffeine from Guaraná Seeds Using Aqueous Solutions of Ionic Liquids. *Green Chem.* **2013**, *15* (7), 2002. DOI: 10.1039/c3gc40437d.

(65) Bogdanov, M. G. Ionic Liquids as Alternative Solvents for Extraction of Natural Products. In *Alternative Solvents for Natural Products Extraction*; Chemat, F., Vian, M. A., Eds.; Springer Berlin Heidelberg: Berlin, Heidelberg, **2014**; pp 127–166. DOI: 10.1007/978-3-662-43628-8_7.

(66) Kunz, W.; Häckl, K. The Hype with Ionic Liquids as Solvents. *Chem. Phys. Lett.* **2016**, *661*, 6–12. DOI: 10.1016/j.cplett.2016.07.044.

(67) Hulsbosch, J.; De Vos, D. E.; Binnemans, K.; Ameloot, R. Biobased Ionic Liquids: Solvents for a Green Processing Industry? *ACS Sustain. Chem. Eng.* **2016**, *4* (6), 2917–2931. DOI: 10.1021/acssuschemeng.6b00553.

(68) Lavaud, A.; Laguerre, M.; Birtić, S.; Fabiano-Tixier, A. S.; Roller, M.; Chemat, F.; Bily, A. C. Eutectic Extraction Solvents, Extraction Methods by Eutectigenesis Using Said Solvents, and Extracts Derived from Said Extraction Methods. WO2016162703A1, October 13, **2016**.

(69) Katsoyannos, E.; Gortzi, O.; Chatzilazarou, A.; Athanasiadis, V.; Tsaknis, J.; Lalas, S. Evaluation of the Suitability of Low Hazard Surfactants for the Separation of Phenols and Carotenoids from Red-Flesh Orange Juice and Olive Mill Wastewater Using Cloud Point Extraction: Other Techniques. *J. Sep. Sci.* **2012**, *35* (19), 2665–2670. DOI: 10.1002/jssc.201200356.

(70) Bi, W.; Tian, M.; Row, K. H. Extraction and Concentration of Tanshinones in *Salvia Miltiorrhiza* Bunge by Task-Specific Non-Ionic Surfactant Assistance. *Food Chem.* **2011**, *126* (4), 1985–1990. DOI: 10.1016/j.foodchem.2010.12.059.
(71) Kiathevest, K.; Goto, M.; Sasaki, M.; Pavasant, P.; Shotipruk, A. Extraction and Concentration of Anthraquinones from Roots of *Morinda Citrifolia* by Non-Ionic Surfactant Solution. *Sep. Purif. Technol.* **2009**, *66* (1), 111–117. DOI: 10.1016/j.seppur.2008.11.017.
(72) Leite, A. C.; Ferreira, A. M.; Morais, E. S.; Khan, I.; Freire, M. G.; Coutinho, J. A. P. Cloud Point Extraction of Chlorophylls from Spinach Leaves Using Aqueous Solutions of Nonionic Surfactants. *ACS Sustain. Chem. Eng.* **2018**, *6* (1), 590–599. DOI: 10.1021/acssuschemeng.7b02931.
(73) Yazdi, A. S. Surfactant-Based Extraction Methods. *TrAC Trends Anal. Chem.* **2011**, *30* (6), 918–929. DOI: 10.1016/j.trac.2011.02.010.
(74) Zhou, J.; Sun, J. B.; Xu, X. Y.; Cheng, Z. H.; Zeng, P.; Wang, F. Q.; Zhang, Q. Application of Mixed Cloud Point Extraction for the Analysis of Six Flavonoids in Apocynum Venetum Leaf Samples by High Performance Liquid Chromatography. *J. Pharm. Biomed. Anal.* **2015**, *107*, 273–279. DOI: 10.1016/j.jpba.2015.01.003.
(75) Shi, Z.; Zhu, X.; Zhang, H. Micelle-Mediated Extraction and Cloud Point Preconcentration for the Analysis of Aesculin and Aesculetin in *Cortex Fraxini* by HPLC. *J. Pharm. Biomed. Anal.* **2007**, *44* (4), 867–873. DOI: 10.1016/j.jpba.2007.03.035.
(76) Schneider, P.; Bischoff, F.; Müller, U.; Bart, H.-J.; Schlitter, K.; Jordan, V. Plant Extraction with Aqueous Two-Phase Systems. *Chem. Eng. Technol.* **2011**, *34* (3), 452–458. DOI: 10.1002/ceat.201000420.
(77) Spir, L. G.; Ataide, J. A.; De Lencastre Novaes, L. C.; De Borba Gurpilhares, D.; Moriel, P.; Silveira, E.; Pessoa, A.; Tambourgi, E. B.; Mazzola, P. G. Application of an Aqueous Two-Phase Micellar System to Extract Bromelain from Pineapple (*Ananas Comosus*) Peel Waste and Analysis of Bromelain Stability in Cosmetic Formulations. *Biotechnol. Prog.* **2015**, *31* (4), 937–945. DOI: 10.1002/btpr.2098.
(78) Padalkar, K.; Gaikar, V. Extraction of Piperine from *Piper Nigrum* (Black Pepper) by Aqueous Solutions of Surfactant and Surfactant + Hydrotrope Mixtures. *Sep. Sci. Technol.* **2008**, *43*, 3097–3118. DOI: 10.1080/01496390802063887.
(79) Tani, H.; Kamidate, T.; Watanabe, H. Micelle-Mediated Extraction. *J. Chromatogr. A* **1997**, *780* (1–2), 229–241. DOI: 10.1016/S0021-9673(97)00345-2.
(80) Melnyk, A.; Namieśnik, J.; Wolska, L. Theory and Recent Applications of Coacervate-Based Extraction Techniques. *TrAC Trends Anal. Chem.* **2015**, *71*, 282–292. DOI: 10.1016/j.trac.2015.03.013.
(81) Neuberg, Carl. Hydrotropic Phenomena. I. *Biochem. Z.* **1916**, *76*, 107–176.
(82) Bauduin, P.; Testard, F.; Zemb, Th. Solubilization in Alkanes by Alcohols as Reverse Hydrotropes or "Lipotropes." *J. Phys. Chem. B* **2008**, *112* (39), 12354–12360. DOI: 10.1021/jp804668n.
(83) Subbarao, C. V.; Chakravarthy, I. P. K.; Sai Bharadwaj, A. V. S. L.; Prasad, K. M. M. Functions of Hydrotropes in Solutions. *Chem. Eng. Technol.* **2012**, *35* (2), 225–237. DOI: 10.1002/ceat.201100484.
(84) Kim, J. Y.; Kim, S.; Papp, M.; Park, K.; Pinal, R. Hydrotropic Solubilization of Poorly Water-Soluble Drugs. *J. Pharm. Sci.* **2010**, *99* (9), 3953–3965. DOI: 10.1002/jps.22241.
(85) Cui, Y.; Xing, C.; Ran, Y. Molecular Dynamics Simulations of Hydrotropic Solubilization and Self-Aggregation of Nicotinamide. *J. Pharm. Sci.* **2010**, *99* (7), 3048–3059. DOI: 10.1002/jps.22077.

(86) Balasubramanian, D.; Srinivas, V.; Gaikar, V. G.; Sharma, M. M. Aggregation Behavior of Hydrotropic Compounds in Aqueous Solution. *J. Phys. Chem.* **1989**, *93* (9), 3865–3870. DOI: 10.1021/j100346a098.
(87) Shimizu, S.; Matubayasi, N. The Origin of Cooperative Solubilisation by Hydrotropes. *Phys. Chem. Chem. Phys.* **2016**, *18* (36), 25621–25628. DOI: 10.1039/C6CP04823D.
(88) Kunz, W.; Holmberg, K.; Zemb, T. Hydrotropes. *Curr. Opin. Colloid Interface Sci.* **2016**, *22*, 99–107. DOI: 10.1016/j.cocis.2016.03.005.
(89) Bauduin, P.; Renoncourt, A.; Kopf, A.; Touraud, D.; Kunz, W. Unified Concept of Solubilization in Water by Hydrotropes and Cosolvents. *Langmuir* **2005**, *21* (15), 6769–6775. DOI: 10.1021/la050554l.
(90) Queste, S.; Bauduin, P.; Touraud, D.; Kunz, W.; Aubry, J.-M. Short Chain Glycerol 1-Monoethers — a New Class of Green Solvo-Surfactants. *Green Chem* **2006**, *8* (9), 822–830. DOI: 10.1039/B603973A.
(91) Honda, S.; Ishida, R.; Hidaka, K.; Masuda, T. Stability of Polyphenols under Alkaline Conditions and the Formation of a Xanthine Oxidase Inhibitor from Gallic Acid in a Solution at pH 7.4. *Food Sci. Technol. Res.* **2019**, *25* (1), 123–129. DOI: 10.3136/fstr.25.123.
(92) Maier, G. P.; Bernt, C. M.; Butler, A. Catechol Oxidation: Considerations in the Design of Wet Adhesive Materials. *Biomater. Sci.* **2018**, *6* (2), 332–339. DOI: 10.1039/C7BM00884H.
(93) Guo, R.; Compo, M. E.; Friberg, S. E.; Morris, K. The Coupling Action of a Hydrotrope and Structure Transition from Lamellar Liquid Crystal. *J. Dispers. Sci. Technol.* **1996**, *17* (5), 493–507. DOI: 10.1080/01932699608943519.
(94) Lebeuf, R.; Illous, E.; Dussenne, C.; Molinier, V.; Silva, E. D.; Lemaire, M.; Aubry, J.-M. Solvo-Surfactant Properties of Dialkyl Glycerol Ethers: Application as Eco-Friendly Extractants of Plant Material through a Novel Hydrotropic Cloud Point Extraction (HCPE) Process. *ACS Sustain. Chem. Eng.* **2016**, *4* (9), 4815–4823. DOI: 10.1021/acssuschemeng.6b01101.
(95) Zhu, Y.; Durand, M.; Molinier, V.; Aubry, J.-M. Isosorbide as a Novel Polar Head Derived from Renewable Resources. Application to the Design of Short-Chain Amphiphiles with Hydrotropic Properties. *Green Chem.* **2008**, *10* (5), 532–540. DOI: 10.1039/B717203F.
(96) Herbinski, A.; Métay, E.; Da Silva, E.; Illous, E.; Aubry, J.-M.; Lemaire, M. An Eco-Compatible Pathway to New Hydrotropes from Tetraols. *Green Chem.* **2018**, *20* (6), 1250–1261. DOI: 10.1039/C7GC02990J.
(97) Tye, Y. Y.; Lee, K. T.; Wan Abdullah, W. N.; Leh, C. P. The World Availability of Non-Wood Lignocellulosic Biomass for the Production of Cellulosic Ethanol and Potential Pretreatments for the Enhancement of Enzymatic Saccharification. *Renew. Sustain. Energy Rev.* **2016**, *60*, 155–172. DOI: 10.1016/j.rser.2016.01.072.
(98) Ji, H.; Lv, P. Mechanistic Insights into the Lignin Dissolution Behaviors of a Recyclable Acid Hydrotrope, Deep Eutectic Solvent (DES), and Ionic Liquid (IL). *Green Chem* **2020**, *22* (4), 1378–1387. DOI: 10.1039/C9GC02760B.
(99) Wu, X.; Zhang, T.; Liu, N.; Zhao, Y.; Tian, G.; Wang, Z. Sequential Extraction of Hemicelluloses and Lignin for Wood Fractionation Using Acid Hydrotrope at Mild Conditions. *Ind. Crops Prod.* **2020**, *145*, 112086. DOI: 10.1016/j.indcrop.2020.112086.
(100) McKee, R. H. Recovery of Cellulose and Lignin from Wood. US2308564, **1938**.
(101) Chen, L.; Dou, J.; Ma, Q.; Li, N.; Wu, R.; Bian, H.; Yelle, D. J.; Vuorinen, T.; Fu, S.; Pan, X.; Zhu, J. (J. Y.). Rapid and Near-Complete Dissolution of Wood Lignin at ≤80°C by a Recyclable Acid Hydrotrope. *Sci. Adv.* **2017**, *3* (9). DOI: 10.1126/sciadv.1701735.

(102) Novy, V.; Nielsen, F.; Olsson, J.; Aïssa, K.; Saddler, J. N.; Wallberg, O.; Galbe, M. Elucidation of Changes in Cellulose Ultrastructure and Accessibility in Hardwood Fractionation Processes with Carbohydrate Binding Modules. *ACS Sustain. Chem. Eng.* **2020**, *8* (17), 6767–6776. DOI: 10.1021/acssuschemeng.9b07589.
(103) Raman, G.; Gaikar, V. G. Extraction of Piperine from *Piper Nigrum* (Black Pepper) by Hydrotropic Solubilization. *Ind. Eng. Chem. Res.* **2002**, *41* (12), 2966–2976. DOI: 10.1021/ie0107845.
(104) Dandekar, D. V.; Gaikar, V. G. Hydrotropic Extraction of Curcuminoids from Turmeric. *Sep. Sci. Technol.* **2003**, *38* (5), 1185–1215. DOI: 10.1081/SS-120018130.
(105) Latha, C. Selective Extraction of Embelin from Embelia Ribes by Hydrotropes. *Sep. Sci. Technol.* **2006**, *41* (16), 3721–3729. DOI: 10.1080/01496390600957207.
(106) Mishra, S. P.; Gaikar, V. G. Hydrotropic Extraction Process for Recovery of Forskolin from *Coleus Forskohlii* Roots. *Ind. Eng. Chem. Res.* **2009**, *48* (17), 8083–8090. DOI: 10.1021/ie801728d.
(107) Mishra, S. P.; Gaikar, V. G. Aqueous Hydrotropic Solution as an Efficient Solubilizing Agent for Andrographolide from *Andrographis Paniculata* Leaves. *Sep. Sci. Technol.* **2006**, *41* (6), 1115–1134. DOI: 10.1080/01496390600633675.
(108) Jenamayjayan, D.; Jayakumar, C.; Gandhi, N. N. Separation of a Phenol/*o*-Chlorophenol Mixture through Hydrotropy. *J. Chem. Eng. Data* **2009**, *54* (6), 1923–1926. DOI: 10.1021/je800421y.
(109) Gaikar, V. G.; Phatak, P. V. Selective Solubilization of Isomers in Hydrotrope Solutions: *o-/p* chlorobenzoic Acids and *o-/p* nitroanilines. *Sep. Sci. Technol.* **1999**, *34* (3), 439–459. DOI: 10.1081/SS-100100660.
(110) Kumar, S. T.; Prakash, D. G.; Nagendra Gandhi, N. Effect of Hydrotropes on Solubility and Mass Transfer Coefficient of Lauric Acid. *Korean J. Chem. Eng.* **2009**, *26* (5), 1328–1333. DOI: 10.1007/s11814-009-0219-2.
(111) Prakash, D. G.; Kumar, S. T.; Gandhi, N. N. Enhancement of Solubility and Mass Transfer Coefficient of Benzoic Acid Through Hydrotropy. *Pol. J. Chem. Technol.* **2013**, *15* (1), 46–50. DOI: 10.2478/pjct-2013-0009.
(112) Herbig, M. E.; Evers, D.-H. Correlation of Hydrotropic Solubilization by Urea with LogD of Drug Molecules and Utilization of This Effect for Topical Formulations. *Eur. J. Pharm. Biopharm.* **2013**, *85* (1), 158–160. DOI: 10.1016/j.ejpb.2013.06.022.
(113) Balachandran, S.; Prakash, D. G.; Anantharaj, R.; Paul, M. R. D. J. Enhancement of Aqueous Solubility and Extraction of Lauric Acid Using Hydrotropes and Its Interaction Studies by COSMO-RS Model. *J. Dispers. Sci. Technol.* **2020**, *0* (0), 1–10. DOI: 10.1080/01932691.2020.1789471.
(114) Martín, Á.; Rodríguez-Rojo, S.; Navarrete, A.; de Paz, E.; Queiroz, J.; José Cocero, M. CHAPTER 8. Post-extraction Processes: Improvement of Functional Characteristics of Extracts. In *Natural Product Extraction: Principles and Applications*; Rostagno, M. A., Prado, J. M., Eds.; Royal Society of Chemistry: Cambridge, **2013**; pp 285–313. DOI: 10.1039/9781849737579-00285.
(115) Florence, A. J.; Shankland, N.; Johnston, A. Crystallization in Final Stages of Purification. In *Natural Products Isolation*; Sarker, S. D., Latif, Z., Gray, A. I., Eds.; Humana Press: Totowa, NJ, **2005**; pp 275–295. DOI: 10.1385/1-59259-955-9:275.
(116) Xiao, W.; Lei, F.; Hengqiang, Z.; Xiaojing, L. CHAPTER 9. Isolation and Purification of Natural Products. In *Natural Product Extraction: Principles and Applications*; Rostagno, M. A., Prado, J. M., Eds.; Royal Society of Chemistry: Cambridge, **2013**; pp 314–362. DOI: 10.1039/9781849737579-00314.

(117) Dandekar, D. V.; Gaikar, V. G. Precipitation of Curcuminoids from Hydrotrope Solution: Crystal Nucleation and Growth Kinetics from Batch Experiments. *Sep. Sci. Technol.* **2003**, *38* (15), 3625–3644. DOI: 10.1081/SS-120024221.
(118) Lunkenheimer, K.; Schrödle, S.; Kunz, W. Dowanol DPnB in Water as an Example of a Solvo-Surfactant System: Adsorption and Foam Properties. In *Trends in Colloid and Interface Science XVII*; Springer Berlin Heidelberg: Berlin, Heidelberg, **2004**; pp 14–20. DOI: 10.1007/b93970.
(119) Gaulkar, S. U.; Gaikar, V. G. Precipitation of Piperine from Hydrotropic Solutions: Study of Crystal Nucleation and Growth Kinetics from Batch Experiments. *Sep. Sci. Technol.* **2004**, *39* (14), 3431–3452. DOI: 10.1081/SS-200034344.
(120) Gandhi, N. Extraction of Vanillin Through Hydrotropy. *Asian J. Chem.* **2012**.
(121) Desai, M. A.; Parikh, J. Hydrotropic Extraction of Citral from *Cymbopogon Flexuosus* (Steud.) Wats. *Ind. Eng. Chem. Res.* **2012**, *51* (9), 3750–3757. DOI: 10.1021/ie202025b.
(122) Thakker, M. R.; Parikh, J. K.; Desai, M. A. Ultrasound Assisted Hydrotropic Extraction: A Greener Approach for the Isolation of Geraniol from the Leaves of *Cymbopogon Martinii*. *ACS Sustain. Chem. Eng.* **2018**, *6* (3), 3215–3224. DOI: 10.1021/acssuschemeng.7b03374.
(123) Solanki, K. P.; Desai, M. A.; Parikh, J. K. Improved Hydrodistillation Process Using Amphiphilic Compounds for Extraction of Essential Oil from Java Citronella Grass. *Chem. Pap.* **2020**, *74* (1), 145–156. DOI: 10.1007/s11696-019-00861-3.
(124) Hartati, I.; Kurniasari, L.; Anas, Y.; Aniq, N. The Application of Hydrotropes as Medium in the Extraction of Andrographolide. *Indones. J. Pharm.* **2014**, *25* (4), 265. DOI: 10.14499/indonesianjpharm25iss4pp265.
(125) Devendra, L. P.; Gaikar, V. G. Is Sodium Cinnamate a Photoswitchable Hydrotrope? *J. Mol. Liq.* **2012**, *165*, 71–77. DOI: 10.1016/j.molliq.2011.10.010.
(126) Lee, J.; Lee, S. C.; Acharya, G.; Chang, C.; Park, K. Hydrotropic Solubilization of Paclitaxel: Analysis of Chemical Structures for Hydrotropic Property. *Pharm. Res.* **2003**, *20* (7), 1022–1030. DOI: 10.1023/A:1024458206032.
(127) Patel, A.; Malinovska, L.; Saha, S.; Wang, J.; Alberti, S.; Krishnan, Y.; Hyman, A. A. ATP as a Biological Hydrotrope. *Science* **2017**, *356* (6339), 753–756. DOI: 10.1126/science.aaf6846.
(128) Molinier, V.; Aubry, J.-M. Chapter 4. Sugar-Based Hydrotropes: Preparation, Properties and Applications. In *Carbohydrate Chemistry*; Pilar Rauter, A., Lindhorst, T., Queneau, Y., Eds.; Royal Society of Chemistry: Cambridge, **2014**; Vol. 40, pp 51–72. DOI: 10.1039/9781849739986-00051.
(129) Durand, M.; Zhu, Y.; Molinier, V.; Féron, T.; Aubry, J.-M. Solubilizing and Hydrotropic Properties of Isosorbide Monoalkyl- and Dimethyl-Ethers. *J. Surfactants Deterg.* **2009**, *12* (4), 371–378. DOI: 10.1007/s11743-009-1128-4.
(130) Estrine, B.; Marinkovic, S.; Jérome, F. Synthesis of Alkyl Polyglycosides From Glucose and Xylose for Biobased Surfactants: Synthesis, Properties, and Applications. In *Biobased Surfactants*; Elsevier, **2019**; pp 365–385. DOI: 10.1016/B978-0-12-812705-6.00011-3.
(131) Moon, H.-J.; Jeya, M.; Kim, I.-W.; Lee, J.-K. Biotechnological Production of Erythritol and Its Applications. *Appl. Microbiol. Biotechnol.* **2010**, *86* (4), 1017–1025. DOI: 10.1007/s00253-010-2496-4.
(132) Queste, S.; Michina, Y.; Dewilde, A.; Neueder, R.; Kunz, W.; Aubry, J.-Marie. Thermophysical and Bionotox Properties of Solvo-Surfactants Based on Ethylene Oxide, Propylene Oxide and Glycerol. *Green Chem.* **2007**, *9*, 491–499. DOI: 10.1039/b617852a.
(133) Matsumura, S.; Imai, K.; Yoshikawa, S.; Kawada, K.; Uchibor, T. Surface Activities, Biodegradability and Antimicrobial Properties of *n*-Alkyl Glucosides, Mannosides and

Galactosides. *J. Am. Oil Chem. Soc.* **1990**, *67* (12), 996–1001. DOI: 10.1007/BF02541865.
(134) Wheatoleo. Safety Data Sheet - Appyclean 6505. **2012**.
(135) Wheatoleo. Safety Data Sheet - Appyclean 6781. **2012.**
(136) SEPPIC. Safety Data Sheet - Sepiclear SL 7 G. **2017**.
(137) Geetha, D.; Tyagi, R. Alkyl Poly Glucosides (APGs) Surfactants and Their Properties: A Review. *Tenside Surfactants Deterg.* **2012**, *49* (5), 417–427. DOI: 10.3139/113.110212.
(138) Riera, S. F.; Cohen, R. A. Alkyl Polyglucoside Compound Influences Freshwater Plankton Community Structure in Floating Field Mesocosms. *Ecotoxicology* **2016**, *25* (8), 1458–1467. DOI: 10.1007/s10646-016-1697-8.
(139) Soares, B. P.; Abranches, D. O.; Sintra, T. E.; Leal-Duaso, A.; García, J. I.; Pires, E.; Shimizu, S.; Pinho, S. P.; Coutinho, J. A. P. Glycerol Ethers as Hydrotropes and Their Use to Enhance the Solubility of Phenolic Acids in Water. *ACS Sustain. Chem. Eng.* **2020**, *8* (14), acssuschemeng.0c01032. DOI: 10.1021/acssuschemeng.0c01032.
(140) Milow, C. A.; Bailly, L.; Judd, C.; Richter, N. Jeannine. Improved Methods for Botanical and/or Algae Extraction., **2013**.
(141) Mandeau, A.; Leti, M. Method for Producing an Extract of a Matrix of Vegetable Origin by Extrusion with a Hydrotrope Solution. WO2016146838, **2015**.
(142) Gibson, T. Phase-Transfer Synthesis of Monoalkyl Ethers of Oligoethylene Glycols. *J. Org. Chem.* **1980**, *45* (6), 1095–1098. DOI: 10.1021/jo01294a034.
(143) Queste, S.; Salager, J. L.; Strey, R.; Aubry, J. M. The EACN Scale for Oil Classification Revisited Thanks to Fish Diagrams. *J. Colloid Interface Sci.* **2007**, *312*, 98–107. DOI: 10.1016/j.jcis.2006.07.004.
(144) Ontiveros, J. F.; Pierlot, C.; Catte, M.; Molinier, V.; Pizzino, A.; Salager, J.-L.; Aubry, J.-M. Classification of Ester Oils According to Their Equivalent Alkane Carbon Number (EACN) and Asymmetry of Fish Diagrams of C10E4/Ester Oil/Water Systems. *J. Colloid Interface Sci.* **2013**, *403*, 67–76. DOI: 10.1016/j.jcis.2013.03.071.
(145) Miyajima, T.; Uno, Mitsuru. Process for Producing Glyceryl Ether., July 27, **2000**.
(146) Garcia-Lisbona, M. N.; Galindo, A.; Jackson, G.; Burgess, A. N. An Examination of the Cloud Curves of Liquid-Liquid Immiscibility of Aqueous Solutions of Alkyl Polyoxyethylene Surfactants Using the SAFT-HS Approach with Transferable Parameters. *J. Am. Chem. Soc.* **1998**, *120*, 4191–4199. DOI: 10.1021/JA9736525.
(147) Ontiveros, J. F.; Pierlot, C.; Catte, M.; Molinier, V.; Salager, J.-L.; Aubry, J.-Marie. A Simple Method to Assess the Hydrophilic Lipophilic Balance of Food and Cosmetic Surfactants Using the Phase Inversion Temperature of $C_{10}E_4$/*n*-Octane/Water Emulsions. *Colloids Surf. Physicochem. Eng. Asp.* **2014**, *458*, 32–39. DOI: 10.1016/j.colsurfa.2014.02.058.
(148) Salimon, J.; Salih, N.; Yousif, E. Industrial Development and Applications of Plant Oils and Their Biobased Oleochemicals. *Arab. J. Chem.* **2012**, *5* (2), 135–145. DOI: 10.1016/j.arabjc.2010.08.007.
(149) Abd El-Ghaffar, M. A.; Sherif, M. H.; Taher El-Habab, A. Synthesis, Characterization, and Evaluation of Ethoxylated Lauryl-Myrisityl Alcohol Nonionic Surfactants as Wetting Agents, Anti-Foamers, and Minimum Film Forming Temperature Reducers in Emulsion Polymer Lattices. *J. Surfactants Deterg.* **2017**, *20* (1), 117–128. DOI: 10.1007/s11743-016-1898-4.
(150) Höfer, R.; Bigorra, J. Green Chemistry—a Sustainable Solution for Industrial Specialties Applications. *Green Chem* **2007**, *9* (3), 203–212. DOI: 10.1039/B606377B.
(151) Posada, J. A.; Patel, A. D.; Roes, A.; Blok, K.; Faaij, A. P. C.; Patel, M. K. Potential of Bioethanol as a Chemical Building Block for Biorefineries: Preliminary Sustainability

Assessment of 12 Bioethanol-Based Products. *Bioresour. Technol.* **2013**, *135*, 490–499. DOI: 10.1016/j.biortech.2012.09.058.

(152) Schowanek, D.; Borsboom-Patel, T.; Bouvy, A.; Colling, J.; de Ferrer, J. A.; Eggers, D.; Groenke, K.; Gruenenwald, T.; Martinsson, J.; Mckeown, P.; Miller, B.; Moons, S.; Niedermann, K.; Pérez, M.; Schneider, C.; Viot, J.-F. New and Updated Life Cycle Inventories for Surfactants Used in European Detergents: Summary of the ERASM Surfactant Life Cycle and Ecofootprinting Project. *Int. J. Life Cycle Assess.* **2018**, *23* (4), 867–886. DOI: 10.1007/s11367-017-1384-x.

(153) D'Angelo, M.; Onori, G.; Santucci, A. Study of Aggregation of N-Butoxyethanol in Water by Compressibility and Surface Tension Measurements. *Chem. Phys. Lett.* **1994**, *220*, 59–63. DOI: 10.1016/0009-2614(94)00128-6.

(154) Loschen, C.; Klamt, A. COSMO *Quick* : A Novel Interface for Fast σ-Profile Composition and Its Application to COSMO-RS Solvent Screening Using Multiple Reference Solvents. *Ind. Eng. Chem. Res.* **2012**, *51* (43), 14303–14308. DOI: 10.1021/ie3023675.

(155) Jacotet-Navarro, M.; Laguerre, M.; Fabiano-Tixier, A.-S.; Tenon, M.; Feuillère, N.; Bily, A.; Chemat, F. What Is the Best Ethanol-Water Ratio for the Extraction of Antioxidants from Rosemary? Impact of the Solvent on Yield, Composition, and Activity of the Extracts. *Electrophoresis* **2018**, *39* (15), 1946–1956. DOI: 10.1002/elps.201700397.

(156) Schick, M. J. *Nonionic Surfactants: Physical Chemistry*; Surfactant science series; M. Dekker: New York, **1987**.

(157) Kahlweit, M.; Strey, R.; Busse, G. Weakly to Strongly Structured Mixtures. *Phys. Rev. E* **1993**, *47* (6), 4197–4209. DOI: 10.1103/PhysRevE.47.4197.

(158) Christensen, S. P.; Donate, F. A.; Frank, T. C.; LaTulip, R. J.; Wilson, L. C. Mutual Solubility and Lower Critical Solution Temperature for Water + Glycol Ether Systems. *J. Chem. Eng. Data* **2005**, *50*, 869–877. DOI: 10.1021/je049635u.

(159) Zhang, Y.; Smuts, J. P.; Dodbiba, E.; Rangarajan, R.; Lang, J. C.; Armstrong, D. W. Degradation Study of Carnosic Acid, Carnosol, Rosmarinic Acid, and Rosemary Extract (*Rosmarinus Officinalis* L.) Assessed Using HPLC. *J. Agric. Food Chem.* **2012**, *60* (36), 9305–9314. DOI: 10.1021/jf302179c.

(160) Ashizawa, R.; Noguchi, T. Effects of Hydrogen Bonding Interactions on the Redox Potential and Molecular Vibrations of Plastoquinone as Studied Using Density Functional Theory Calculations. *Phys. Chem. Chem. Phys.* **2014**, *16* (24), 11864–11876. DOI: 10.1039/C3CP54742F.

(161) Lindman, B.; Medronho, B.; Karlström, G. Clouding of Nonionic Surfactants. *Curr. Opin. Colloid Interface Sci.* **2016**, *22*, 23–29. DOI: 10.1016/j.cocis.2016.01.005.

(162) Grundl, G.; Müller, M.; Touraud, D.; Kunz, W. Salting-out and Salting-in Effects of Organic Compounds and Applications of the Salting-out Effect of Pentasodium Phytate in Different Extraction Processes. *J. Mol. Liq.* **2017**, *236*, 368–375. DOI: 10.1016/j.molliq.2017.03.091.

(163) Mukherjee, P.; Padhan, S. K.; Dash, S.; Patel, S.; Mishra, B. K. Clouding Behaviour in Surfactant Systems. *Adv. Colloid Interface Sci.* **2011**, *162* (1–2), 59–79. DOI: 10.1016/j.cis.2010.12.005.

(164) Patel, U.; Dharaiya, N.; Bahadur, P. Preservative Solubilization Induces Microstructural Change of Triton X-100 Micelles. *J. Mol. Liq.* **2016**, *216*, 156–163. DOI: 10.1016/j.molliq.2015.12.079.

(165) Goto, A.; Nihei, M.; Endo, F. Solubilization of Methylparaben in Nonionic Surfactant Micelles in Aqueous Solution. *J. Phys. Chem.* **1980**, *84* (18), 2268–2272. DOI: 10.1021/j100455a011.

(166) Rosen, M. J. *Surfactants and Interfacial Phenomena*, 3rd ed.; Wiley-Interscience: Hoboken, N.J, **2004**.
(167) Matsubara, H.; Takumi, H.; Takamatsu, T.; Takiue, T.; Aratono, Makoto. Surface Adsorption and Micelle Formation of Aqueous Solutions of Polyethyleneglycol and Sugar Surfactants. *Colloid Polym. Sci.* **2009**, *287*, 1077–1082. DOI: 10.1007/s00396-009-2066-4.
(168) Lukowicz, T. Synergistic Solubilisation of Fragrances in Binary Surfactant Systems and Prediction of their EACN Value with COSMO-RS, **2015**.
(169) Rojas, O. J.; Stubenrauch, C.; Schulze-Schlarmann, J.; Claesson, P. M. Interactions between Nonpolar Surfaces Coated with the Nonionic Surfactant N-Dodecyl-β-d-Maltoside. *Langmuir* **2005**, *21* (25), 11836–11843. DOI: 10.1021/la051938e.
(170) Bergfeld, W. F.; Belsito, D. V.; Klaassen, C. D.; Hill, R.; Liebler, D.; Marks, J. G.; Shank, R. C.; Slaga, T. J.; Snyder, P. W.; Andersen, F. A. Safety Assessment of Xylene Sulfonic Acid, Toluene Sulfonic Acid, and Alkyl Aryl Sulfonate Hydrotropes as Used in Cosmetics. *Int. J. Toxicol.* **2011**, *30* (6_suppl), 270S-283S. DOI: 10.1177/1091581811429085.
(171) Griffin, W. C. Classification of Surface-Active Agents by "HLB." *J. Soc. Cosmet. Chem. 1 1949 311* **1949**, *1*, 311–326.
(172) Limberg, S.; Belkoura, L.; Woermann, D. Static and Dynamic Light Scattering Experiments with an Iso-Butoxyethanol/Water Mixture of Critical Composition. *J. Mol. Liq.* **1997**, *73,74*, 223–237. DOI: 10.1016/S0167-7322(97)00069-X.
(173) Schubert, K. V.; Strey, R.; Kahlweit, M. A New Purification Technique for Alkyl Polyglycol Ethers and Miscibility Gaps for Water-CiEj. *J. Colloid Interface Sci.* **1991**, *141*, 21–29. DOI: 10.1016/0021-9797(91)90298-M.
(174) Smith, S.; Wiseman, P.; Boudreau, L.; Marangoni, G.; Palepu, R. Effect of Microheterogeneity on Bulk and Surface Properties of Binary Mixtures of Polyoxyethene Glycol Monobutyl Ethers with Water. *J. Solut. Chem.* **1994**, *23*, 207–222. DOI: 10.1007/BF00973547.
(175) Mitchell, D. J.; Tiddy, G. J. T.; Waring, L.; Bostock, T.; McDonald, M. P. Phase Behaviour of Polyoxyethylene Surfactants with Water. Mesophase Structures and Partial Miscibility (Cloud Points). *J. Chem. Soc. Faraday Trans. 1 Phys. Chem. Condens. Phases* **1983**, *79* (4), 975–1000. DOI: 10.1039/F19837900975.
(176) Miyake, M.; Yamashita, Y. Chapter 24 - Molecular Structure and Phase Behavior of Surfactants. In *Cosmetic Science and Technology*; Sakamoto, K., Lochhead, R. Y., Maibach, H. I., Yamashita, Y., Eds.; Elsevier: Amsterdam, **2017**; pp 389–414. DOI: 10.1016/B978-0-12-802005-0.00024-0.
(177) Lang, J. C.; Morgan, R. D. Nonionic Surfactant Mixtures. I. Phase Equilibria in $C_{10}E_4$–H_2O and Closed-loop Coexistence. *J. Chem. Phys.* **1980**, *73* (11), 5849–5861. DOI: 10.1063/1.440028.
(178) Burghardt, M.; Friedmann, A.; Schreiber, L.; Riederer, M. Modelling the Effects of Alcohol Ethoxylates on Diffusion of Pesticides in the Cuticular Wax of *Chenopodium Album* Leaves. *Pest Manag. Sci.* **2006**, *62* (2), 137–147. DOI: 10.1002/ps.1139.
(179) Burghardt, M.; Schreiber, L.; Riederer, Markus. Enhancement of the Diffusion of Active Ingredients in Barley Leaf Cuticular Wax by Monodisperse Alcohol Ethoxylates. *J. Agric. Food Chem.* **1998**, *46*, 1593–1602. DOI: 10.1021/JF970737G.
(180) Riederer, M.; Burghardt, M.; Mayer, S.; Obermeier, H.; Schoenherr, Joerg. Sorption of Monodisperse Alcohol Ethoxylates and Their Effects on the Mobility of 2,4-D in Isolated Plant Cuticles. *J. Agric. Food Chem.* **1995**, *43*, 1067–1075. DOI: 10.1021/jf00052a041.
(181) Satchivi, N. M. Modeling Xenobiotic Uptake and Movement: A Review. In *Retention, Uptake, and Translocation of Agrochemicals in Plants*; ACS Symposium Series;

American Chemical Society, **2014**; Vol. 1171, pp 41–74. DOI: 10.1021/bk-2014-1171.ch003.

(182) Bemporad, D.; Essex, J. W.; Luttmann, C. Permeation of Small Molecules through a Lipid Bilayer: A Computer Simulation Study. *J. Phys. Chem. B* **2004**, *108* (15), 4875–4884. DOI: 10.1021/jp035260s.

(183) Ghaemi, Z.; Minozzi, M.; Carloni, P.; Laio, A. A Novel Approach to the Investigation of Passive Molecular Permeation through Lipid Bilayers from Atomistic Simulations. *J. Phys. Chem. B* **2012**, *116* (29), 8714–8721. DOI: 10.1021/jp301083h.

(184) Lodish, H. F. *Molecular Cell Biology*, Eighth edition.; W.H. Freeman-Macmillan Learning: New York, **2016**.

(185) Dharaiya, N.; Bahadur, P. Phenol Induced Growth in Triton X-100 Micelles: Effect of PH and Phenols' Hydrophobicity. *Colloids Surf. Physicochem. Eng. Asp.* **2012**, *410*, 81–90. DOI: 10.1016/j.colsurfa.2012.06.021.

(186) Pinelo, M.; Zornoza, B.; Meyer, A. S. Selective Release of Phenols from Apple Skin: Mass Transfer Kinetics during Solvent and Enzyme-Assisted Extraction. *Sep. Purif. Technol.* **2008**, *63* (3), 620–627. DOI: 10.1016/j.seppur.2008.07.007.

(187) Krakowska, A.; Rafińska, K.; Walczak, J.; Kowalkowski, T.; Buszewski, B. Comparison of Various Extraction Techniques of *Medicago Sativa*: Yield, Antioxidant Activity, and Content of Phytochemical Constituents. *J. AOAC Int.* **2017**, *100* (6), 1681–1693. DOI: 10.5740/jaoacint.17-0234.

(188) Mazaud, A.; Lebeuf, R.; Laguerre, M.; Nardello-Rataj, V. Hydrotropic Extraction of Carnosic Acid from Rosemary with Short Chain Alkyl Polyethylene Glycol Ethers. *ACS Sustain. Chem. Eng.* **2020**, *8* (40), 15268–15277. DOI: 10.1021/acssuschemeng.0c05078.

(189) Thakker, M. R.; Desai, M. A.; Parikh, J. K. Extraction of Phytochemicals Using Neoteric Solvents. *J. Agroecol. Nat. Resour. Manag.* **2014**, *1* (3), 153–158.

(190) Martel, F.; Estrine, B.; Plantier-Royon, R.; Hoffmann, N.; Portella, C. Development of Agriculture Left-Overs: Fine Organic Chemicals from Wheat Hemicellulose-Derived Pentoses. In *Carbohydrates in Sustainable Development I*; Rauter, A. P., Vogel, P., Queneau, Y., Eds.; Springer Berlin Heidelberg: Berlin, Heidelberg, 2010; Vol. 294, pp 79–115. DOI: 10.1007/128_2010_54.

(191) Brusa, C.; Muzard, M.; Rémond, C.; Plantier-Royon, R. β-Xylopyranosides: Synthesis and Applications. *RSC Adv.* **2015**, *5* (110), 91026–91055. DOI: 10.1039/C5RA14023D.

(192) Shi, Y.; Dayoub, W.; Chen, G.-R.; Lemaire, M. Selective Synthesis of 1-O-Alkyl Glycerol and Diglycerol Ethers by Reductive Alkylation of Alcohols. *Green Chem.* **2010**, *12* (12), 2189. DOI: 10.1039/c0gc00202j.

(193) Sutter, M.; Dayoub, W.; Métay, E.; Raoul, Y.; Lemaire, M. 1-*o*-Alkyl (Di)Glycerol Ethers Synthesis from Methyl Esters and Triglycerides by Two Pathways: Catalytic Reductive Alkylation and Transesterification/Reduction. *Green Chem.* **2013**, *15* (3), 786–797. DOI: 10.1039/C3GC36907B.

(194) Ranoux, A.; Lemiegre, L.; Benvegnu, T. Synthesis and Evaluation of *C*-Glycosides as Hydrotropes and Solubilizing Agents. *Sci. China Chem.* **2010**, *53* (9), 1957–1962. DOI: 10.1007/s11426-010-4055-3.

(195) Mattei, M.; Kontogeorgis, G. M.; Gani, R. Modeling of the Critical Micelle Concentration (CMC) of Nonionic Surfactants with an Extended Group-Contribution Method. *Ind. Eng. Chem. Res.* **2013**, *52* (34), 12236–12246. DOI: 10.1021/ie4016232.

(196) Chemat, F. *Eco-extraction du végétal: procédés innovants et solvants alternatifs*; Dunod: Paris, 2014.

(197) Shimizu, S.; Matubayasi, N. Hydrotropy: Monomer–Micelle Equilibrium and Minimum Hydrotrope Concentration. *J. Phys. Chem. B* **2014**, *118* (35), 10515–10524. DOI: 10.1021/jp505869m.
(198) Booth, J. J.; Abbott, S.; Shimizu, S. Mechanism of Hydrophobic Drug Solubilization by Small Molecule Hydrotropes. *J. Phys. Chem. B* **2012**, *116* (51), 14915–14921. DOI: 10.1021/jp309819r.
(199) Coffman, R. E.; Kildsig, D. O. Hydrotropic Solubilization — Mechanistic Studies. *Pharm. Res.* **1996**, *13* (10), 1460–1463. DOI: 10.1023/A:1016011125302.
(200) Malinovskii, M. S.; Vvedenskii, V. M. Alkyl Ethers of Glycerol. *Zhurnal Obshchei Khimii* **1953**, *23*, 219–220.
(201) Douheret, G.; Davis, M. I.; Reis, J. C. R.; Fjellanger, I. J.; Vaage, M. B.; Hoiland, Harald. Aggregative Processes in Aqueous Solutions of Isomeric 2-Butoxyethanols at 298.15 K. *Phys. Chem. Chem. Phys.* **2002**, *4*, 6034–6042. DOI: 10.1039/B208598D.
(202) Von Rybinski, W. Alkyl Glycosides and Polyglycosides. *Curr. Opin. Colloid Interface Sci.* **1996**, *1* (5), 587–597. DOI: 10.1016/S1359-0294(96)80096-3.
(203) Han, S. K.; Ko, Y. I.; Park, S. J.; Jin, I. J.; Kim, Y. M. Oleanolic Acid and Ursolic Acid Stabilize Liposomal Membranes. *Lipids* **1997**, *32* (7), 769–773. DOI: 10.1007/s11745-997-0098-9.
(204) Liu, T.; Sui, X.; Zhang, R.; Yang, L.; Zu, Y.; Zhang, L.; Zhang, Y.; Zhang, Z. Application of Ionic Liquids Based Microwave-Assisted Simultaneous Extraction of Carnosic Acid, Rosmarinic Acid and Essential Oil from *Rosmarinus Officinalis*. *J. Chromatogr. A* **2011**, *1218* (47), 8480–8489. DOI: 10.1016/j.chroma.2011.09.073.
(205) World Health Organization. *The International Pharmacopoeia*; World Health Organization, **2006**.
(206) López, O.; Cócera, M.; Coderch, L.; Barbosa-Barros, L.; Parra, J. L.; de la Maza, A. Applications of Alkyl Glucosides in the Solubilization of Liposomes and Cell Membranes. In *Sugar-Based Surfactants*; Carnero Ruiz, C., Ed.; CRC Press, **2008**; Vol. 20086234. DOI: 10.1201/9781420051674.ch15.
(207) Alany, R. G.; Rades, T.; Agatonovic-Kustrin, S.; Davies, N. M.; Tucker, I. G. Effects of Alcohols and Diols on the Phase Behaviour of Quaternary Systems. *Int. J. Pharm.* **2000**, *196* (2), 141–145. DOI: 10.1016/S0378-5173(99)00408-1.
(208) Fernández, V.; Khayet, M. Evaluation of the Surface Free Energy of Plant Surfaces: Toward Standardizing the Procedure. *Front. Plant Sci.* **2015**, *6*. DOI: 10.3389/fpls.2015.00510.
(209) Pantelic, I.; Cuckovic, B. Alkyl Polyglucosides: An Emerging Class of Sugar Surfactants. In *Alkyl Polyglucosides*; Elsevier, **2014**; pp 1–19. DOI: 10.1533/9781908818775.1.
(210) OECD. *Test No. 311: Anaerobic Biodegradability of Organic Compounds in Digested Sludge: By Measurement of Gas Production*; OECD Guidelines for the Testing of Chemicals, Section 3; OECD, **2006**. DOI: 10.1787/9789264016842-en.
(211) OECD. *Test No. 301: Ready Biodegradability*; OECD Guidelines for the Testing of Chemicals, Section 3; OECD, **1992**. DOI: 10.1787/9789264070349-en.
(212) Madsen, T.; Petersen, G.; Seierø, C.; Tørsløv, J. Biodegradability and Aquatic Toxicity of Glycoside Surfactants and a Nonionic Alcohol Ethoxylate. *J. Am. Oil Chem. Soc.* **1996**, *73* (7), 929–933. DOI: 10.1007/BF02517997.
(213) Atsumi, S.; Hanai, T.; Liao, J. C. Non-Fermentative Pathways for Synthesis of Branched-Chain Higher Alcohols as Biofuels. *Nature* **2008**, *451* (7174), 86–89. DOI: 10.1038/nature06450.

(214) Brusotti, G.; Ngueyem, T. A.; Biesuz, R.; Caccialanza, G. Optimum Extraction Process of Polyphenols from Bridelia Grandis Stem Bark Using Experimental Design. *J. Sep. Sci.* **2010**, *33* (11), 1692–1697. DOI: 10.1002/jssc.200900717.
(215) Ćujić, N.; Šavikin, K.; Janković, T.; Pljevljakušić, D.; Zdunić, G.; Ibrić, S. Optimization of Polyphenols Extraction from Dried Chokeberry Using Maceration as Traditional Technique. *Food Chem.* **2016**, *194*, 135–142. DOI: 10.1016/j.foodchem.2015.08.008.
(216) Achat, S.; Tomao, V.; Madani, K.; Chibane, M.; Elmaataoui, M.; Dangles, O.; Chemat, F. Direct Enrichment of Olive Oil in Oleuropein by Ultrasound-Assisted Maceration at Laboratory and Pilot Plant Scale. *Ultrason. Sonochem.* **2012**, *19* (4), 777–786. DOI: 10.1016/j.ultsonch.2011.12.006.
(217) Mané, C.; Souquet, J. M.; Ollé, D.; Verriés, C.; Véran, F.; Mazerolles, G.; Cheynier, V.; Fulcrand, H. Optimization of Simultaneous Flavanol, Phenolic Acid, and Anthocyanin Extraction from Grapes Using an Experimental Design: Application to the Characterization of Champagne Grape Varieties. *J. Agric. Food Chem.* **2007**, *55* (18), 7224–7233. DOI: 10.1021/jf071301w.
(218) Costa-Machado, A. R. M.; Bastos, J. K.; de Freitas, L. A. P. Dynamic Maceration of *Copaifera Langsdorffi* Leaves: A Technological Study Using Fractional Factorial Design. *Rev. Bras. Farmacogn.* **2013**, *23* (1), 79–85. DOI: 10.1590/S0102-695X2012005000116.
(219) Dandekar, D. V.; Jayaprakasha, G. K.; Patil, B. S. Hydrotropic Extraction of Bioactive Limonin from Sour Orange (*Citrus Aurantium* L.) Seeds. *Food Chem.* **2008**, *109* (3), 515–520. DOI: 10.1016/j.foodchem.2007.12.071.
(220) Brereton, R. G. *Chemometrics: Data Analysis for the Laboratory and Chemical Plant*; Wiley: Chichester, West Sussex, England; Hoboken, NJ, **2003**.
(221) Khan, M. K.; Abert-Vian, M.; Fabiano-Tixier, A.-S.; Dangles, O.; Chemat, F. Ultrasound-Assisted Extraction of Polyphenols (Flavanone Glycosides) from Orange (*Citrus Sinensis* L.) Peel. *Food Chem.* **2010**, *119* (2), 851–858. DOI: 10.1016/j.foodchem.2009.08.046.
(222) Mishra, S. P.; Gaikar, V. G. Recovery of Diosgenin from *Dioscorea* Rhizomes Using Aqueous Hydrotropic Solutions of Sodium Cumene Sulfonate. *Ind. Eng. Chem. Res.* **2004**, *43* (17), 5339–5346. DOI: 10.1021/ie034091v.
(223) Louwerse, M. J.; Maldonado, A.; Rousseau, S.; Moreau-Masselon, C.; Roux, B.; Rothenberg, G. Revisiting Hansen Solubility Parameters by Including Thermodynamics. *Chemphyschem* **2017**, *18* (21), 2999–3006. DOI: 10.1002/cphc.201700408.
(224) Apelblat, A.; Manzurola, E.; Abo Balal, N. The Solubilities of Benzene Polycarboxylic Acids in Water. *J. Chem. Thermodyn.* **2006**, *38* (5), 565–571. DOI: 10.1016/j.jct.2005.07.007.
(225) Black, S.; Muller, F. On the Effect of Temperature on Aqueous Solubility of Organic Solids. *Org. Process Res. Dev.* **2010**, *14* (3), 661–665. DOI: 10.1021/op100006y.
(226) Chen, G.; Liang, J.; Han, J.; Zhao, H. Solubility Modeling, Solute–Solvent Interactions, and Thermodynamic Dissolution Properties of *p*-Nitrophenylacetonitrile in Sixteen Monosolvents at Temperatures Ranging from 278.15 to 333.15 K. *J. Chem. Eng. Data* **2019**, *64* (1), 315–323. DOI: 10.1021/acs.jced.8b00811.
(227) Harner, R. S.; Ressler, R. J.; Briggs, R. L.; Hitt, J. E.; Larsen, P. A.; Frank, T. C. Use of a Fiber-Optic Turbidity Probe to Monitor and Control Commercial-Scale Unseeded Batch Crystallizations. *Org. Process Res. Dev.* **2009**, *13* (1), 114–124. DOI: 10.1021/op8001504.
(228) Yang, H.; Florence, A. J. Relating Induction Time and Metastable Zone Width. *CrystEngComm* **2017**, *19* (28), 3966–3978. DOI: 10.1039/C7CE00770A.

(229) Billot, P.; Couty, M.; Hosek, P. Application of ATR-UV Spectroscopy for Monitoring the Crystallisation of UV Absorbing and Nonabsorbing Molecules. *Org. Process Res. Dev.* **2010**, *14* (3), 511–523. DOI: 10.1021/op900281m.
(230) Liley, J. R.; Penfold, J.; Thomas, R. K.; Tucker, I.; Petkov, J.; Stevenson, P.; Banat, I. M.; Marchant, R.; Rudden, M.; Webster, J. The Performance of Surfactant Mixtures at Low Temperatures. *J. Colloid Interface Sci.* **2019**, *534*, 64–71. DOI: 10.1016/j.jcis.2018.08.099.
(231) Schick, M. J. Effect of the Temperature on the Critical Micelle Concentration of Nonionic Detergents. Thermodynamics of Micelle Formation. *J. Phys. Chem.* **1963**, *67* (9), 1796–1799. DOI: 10.1021/j100803a013.
(232) Chen, L.-J.; Lin, S.-Y.; Huang, C.-C.; Chen, E.-M. Temperature Dependence of Critical Micelle Concentration of Polyoxyethylenated Non-Ionic Surfactants. *Colloids Surf. Physicochem. Eng. Asp.* **1998**, *135* (1–3), 175–181. DOI: 10.1016/S0927-7757(97)00238-0.
(233) Castro, G.; Garrido, P. F.; Amigo, A.; Brocos, P. Boosting the Use of Thermoacoustimetry in Micellization Thermodynamics Studies by Easing an Objective Determination of the Cmc. *Fluid Phase Equilibria* **2018**, *478*, 1–13. DOI: 10.1016/j.fluid.2018.08.011.
(234) Prakash, D. G.; Kumar, S. T.; Gandhi, N. N. Enhencement of Solubility and Mass-Transfert Coefficient of 1,2-Dihydroxy-9,10-Anthraquinone (Alizarin) through Hydrotropy. *Chem. Eng. Commun.* **2009**, *197* (4), 423–433. DOI: 10.1080/00986440903155998.
(235) Das, S.; Paul, S. Exploring Molecular Insights into Aggregation of Hydrotrope Sodium Cumene Sulfonate in Aqueous Solution: A Molecular Dynamics Simulation Study. *J. Phys. Chem. B* **2015**, *119* (7), 3142–3154. DOI: 10.1021/jp512282x.
(236) Sanghvi, R.; Evans, D.; Yalkowsky, S. H. Stacking Complexation by Nicotinamide: A Useful Way of Enhancing Drug Solubility. *Int. J. Pharm.* **2007**, *336* (1), 35–41. DOI: 10.1016/j.ijpharm.2006.11.025.
(237) Coles, S. J.; Threlfall, T. L. A Practical Guide to the Measurement of Turbidity Curves of Cooling Crystallisations from Solution. *CrystEngComm* **2020**, *22* (10), 1865–1874. DOI: 10.1039/C9CE01622H.
(238) Gerzhova, A.; Mondor, M.; Benali, M.; Aider, M. Study of Total Dry Matter and Protein Extraction from Canola Meal as Affected by the PH, Salt Addition and Use of Zeta-Potential/Turbidimetry Analysis to Optimize the Extraction Conditions. *Food Chem.* **2016**, *201*, 243–252. DOI: 10.1016/j.foodchem.2016.01.074.
(239) Raman, G.; Gaikar, V. G. Hydrotropic Solubilization of Boswellic Acids from Boswellia Serrata Resin. *Langmuir* **2003**, *19* (19), 8026–8032. DOI: 10.1021/la034611r.
(240) Raynaud-Lacroze, P. O.; Tavare, N. S. Separation of 2-Naphthol: Hydrotropy and Precipitation. *Ind. Eng. Chem. Res.* **1993**, *32* (4), 685–691. DOI: 10.1021/ie00016a015.
(241) Thorat, A. A.; Dalvi, S. V. Liquid Antisolvent Precipitation and Stabilization of Nanoparticles of Poorly Water Soluble Drugs in Aqueous Suspensions: Recent Developments and Future Perspective. *Chem. Eng. J.* **2012**, *181–182*, 1–34. DOI: 10.1016/j.cej.2011.12.044.
(242) Pitt, K.; Peña, R.; Tew, J. D.; Pal, K.; Smith, R.; Nagy, Z. K.; Litster, J. D. Particle Design via Spherical Agglomeration: A Critical Review of Controlling Parameters, Rate Processes and Modelling. *Powder Technol.* **2018**, *326*, 327–343. DOI: 10.1016/j.powtec.2017.11.052.
(243) *Screening: Methods for Experimentation in Industry, Drug Discovery, and Genetics*; Dean, A., Lewis, S., Eds.; Springer: New York, NY, **2006**.

(244) Tohma, H.; Gülçin, İ.; Bursal, E.; Gören, A. C.; Alwasel, S. H.; Köksal, E. Antioxidant Activity and Phenolic Compounds of Ginger (*Zingiber Officinale* Rosc.) Determined by HPLC-MS/MS. *J. Food Meas. Charact.* **2017**, *11* (2), 556–566. DOI: 10.1007/s11694-016-9423-z.

(245) Erkan, N.; Ayranci, G.; Ayranci, E. Antioxidant Activities of Rosemary (*Rosmarinus Officinalis* L.) Extract, Blackseed (*Nigella Sativa* L.) Essential Oil, Carnosic Acid, Rosmarinic Acid and Sesamol. *Food Chem.* **2008**, *110* (1), 76–82. DOI: 10.1016/j.foodchem.2008.01.058.

(246) Kawashima, Y.; Okumura, M.; Takenaka, H.; Kojima, A. Direct Preparation of Spherically Agglomerated Salicylic Acid Crystals During Crystallization. *J. Pharm. Sci.* **1984**, *73* (11), 1535–1538. DOI: 10.1002/jps.2600731110.

(247) Blandin, A. F.; Mangin, D.; Rivoire, A.; Klein, J. P.; Bossoutrot, J. M. Agglomeration in Suspension of Salicylic Acid Fine Particles: Influence of Some Process Parameters on Kinetics and Agglomerate Final Size. *Powder Technol.* **2003**, *130* (1), 316–323. DOI: 10.1016/S0032-5910(02)00210-3.

(248) Peña, R.; Nagy, Z. K. Process Intensification through Continuous Spherical Crystallization Using a Two-Stage Mixed Suspension Mixed Product Removal (MSMPR) System. *Cryst. Growth Des.* **2015**, *15* (9), 4225–4236. DOI: 10.1021/acs.cgd.5b00479.

Appendixes

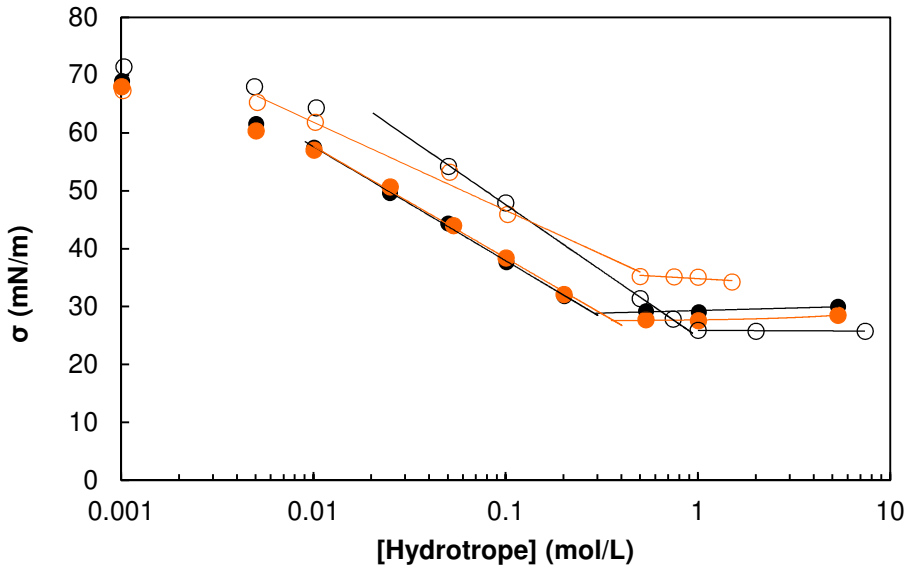

Appendix 1 Surface tension curves of *i*-C_5E_2 (•), C_5E_2 (•), *i*-C_4E_1 (○) and C_4E_3 (○) as a function of their concentration

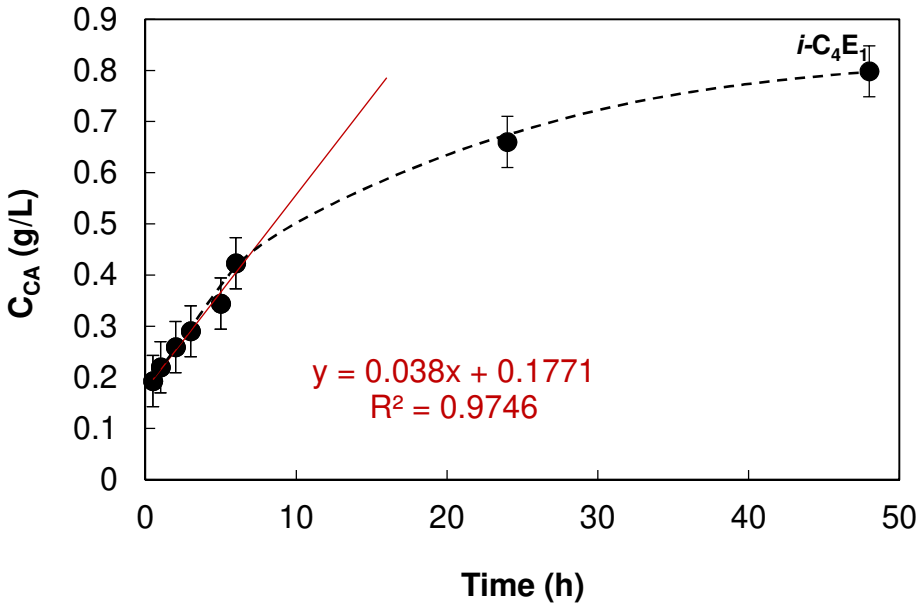

Appendix 2. Kinetics of the extractions performed with aqueous solutions containing 30 wt.% *i*-C_4E_1 at 25 °C, pH 2 between 0 and 48 h

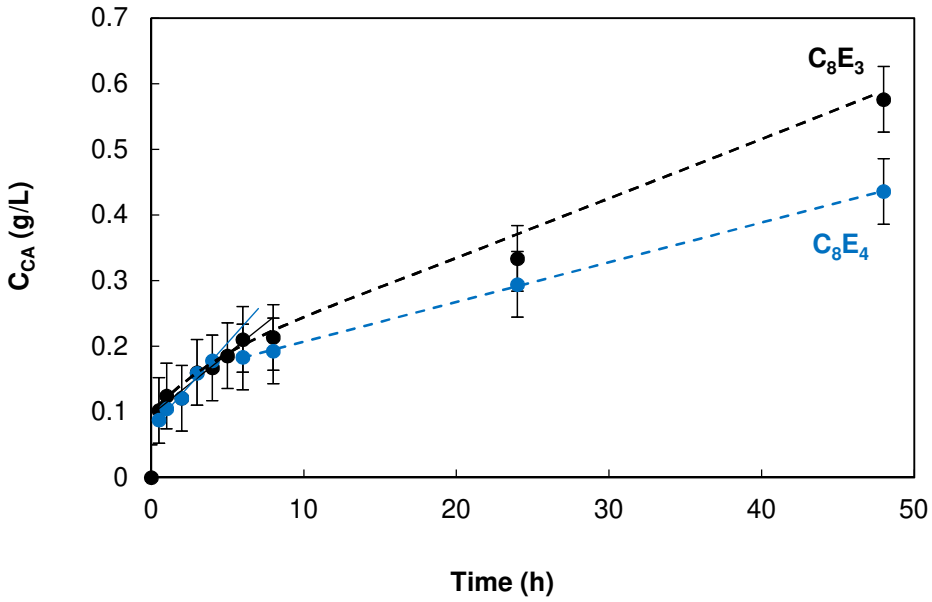

Appendix 3. Kinetics of the extractions performed with aqueous solutions containing 30 wt.% C_8E_3 (black) and C_8E_4 (blue) at 25 °C, pH 2 between 0 and 48 h

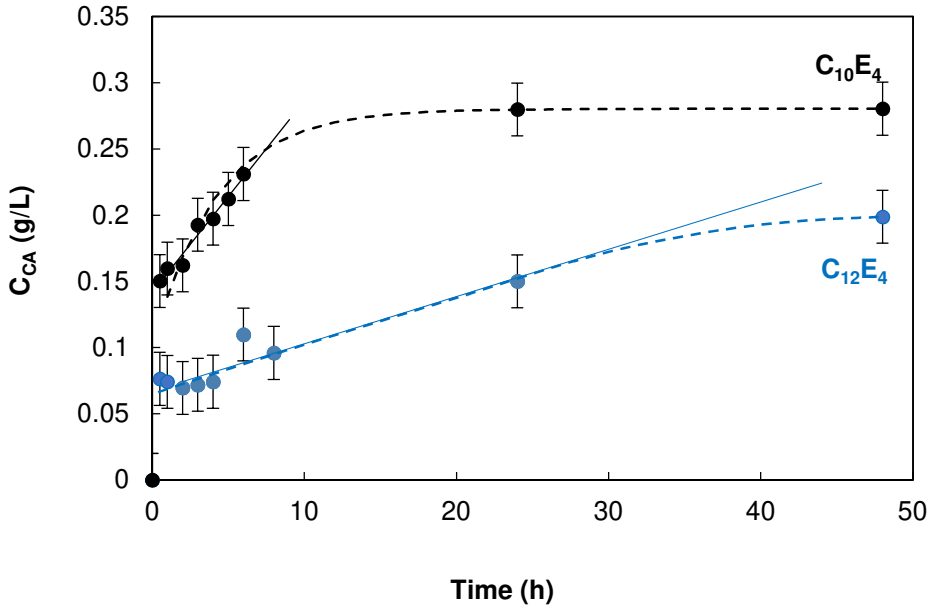

Appendix 4. Kinetics of the extractions performed with aqueous solutions containing 30 wt.% $C_{10}E_4$ (black) and $C_{12}E_4$ (blue) at 25 °C, pH 2 between 0 and 48 h

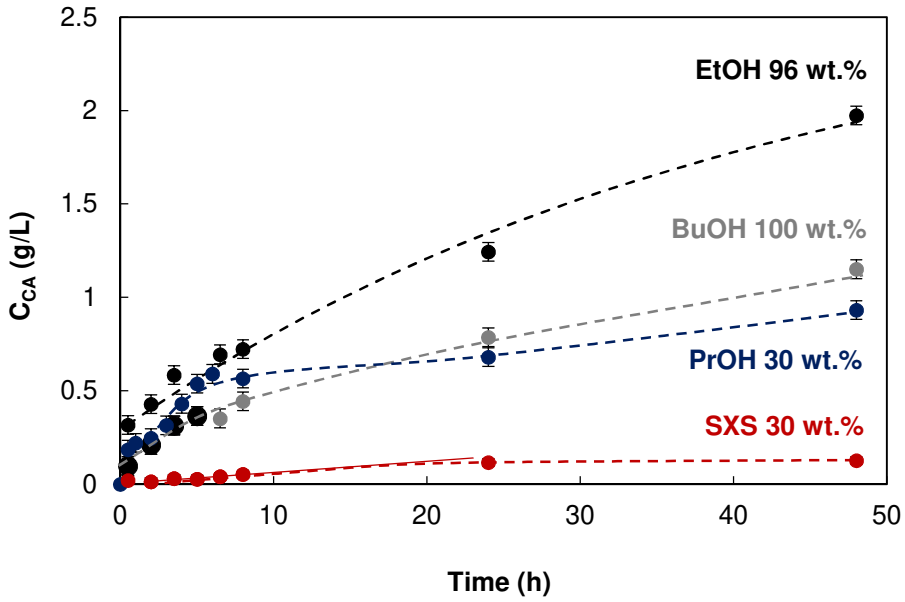

Appendix 5. Kinetics of the extractions performed with aqueous solutions containing 30 wt.% propanol (blue) and sodium xylene sulfonate (red), 96 wt.% ethanol and 100 % butanol at 25 °C, pH 2 between 0 and 48 h

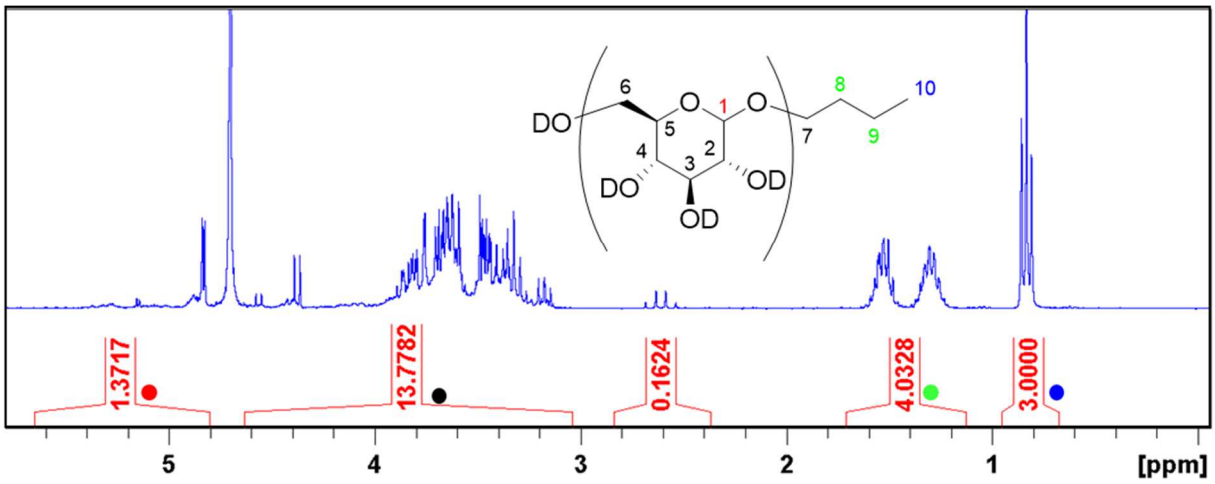

Appendix 6. ^{1}H NMR spectrum of C_4Glu in D_2O with integrals

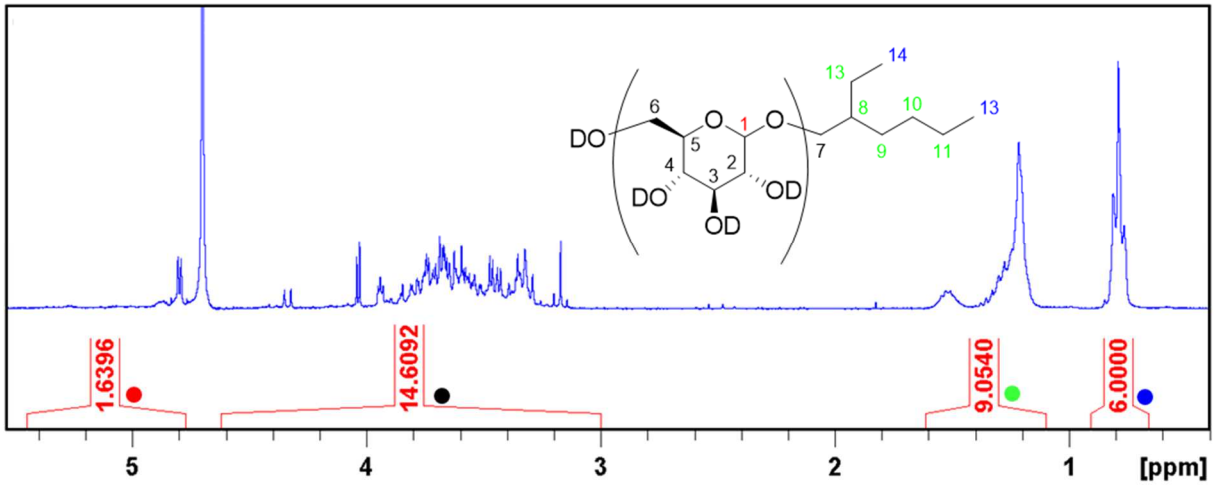

Appendix 7. ^{1}H NMR spectrum of $C_{6,-2}$Glu in D_2O with integrals

Appendix 8. Predicted physicochemical properties of single C_4Glu, *i*-C_5Xyl, C_7Glu and $C_{6,-2}$Glu of various DP

Amphiphile	DP	M (g/mol)	Vm (Å^3)	log *P*	HLB	%
C_4Glu	1	236	276	-0.91	15.2	4
	2	400	440	-1.56	17.1	96
***i*-C_5Xyl**	1	220	264	0.01	13.6	46
	2	354	396	-0.76	15.9	54
C_7Glu	1	278	339	0.83	12.9	44
	2	442	502	0.18	15.4	56
$C_{6,-2}$Glu	1	292	359	0.96	12.3	0
	2	456	523	0.31	15.0	90
	3	620	687	-0.34	16.2	10

Appendix 9. Predicted physicochemical properties of single molecules in the $C_{8/10}$Glyco mixture

nC	Polar head	DP	M (g/mol)	Vm (Å3)	log *P*	HLB	%
8	Xyl	1	262	326	1.75	11.4	6.1
		2	396	458	0.98	14.2	7.4
	Glu	1	292	359	1.40	12.3	14.2
		2	456	523	0.75	15.0	17.3
10	Xyl	1	290	367	2.74	10.3	7.4
		2	424	499	1.97	13.3	9.1
	Glu	1	320	401	2.54	11.2	17.3
		2	484	565	1.89	14.1	21.2

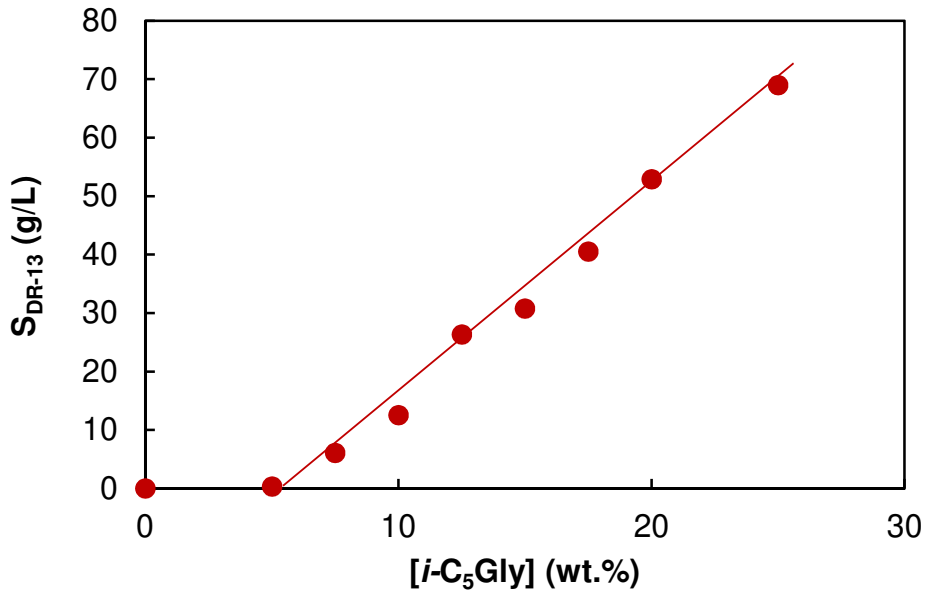

Appendix 10. Solubility curve of DR-13 in *i*-C_5Gly aqueous solutions, at pH 2 and 25 °C.

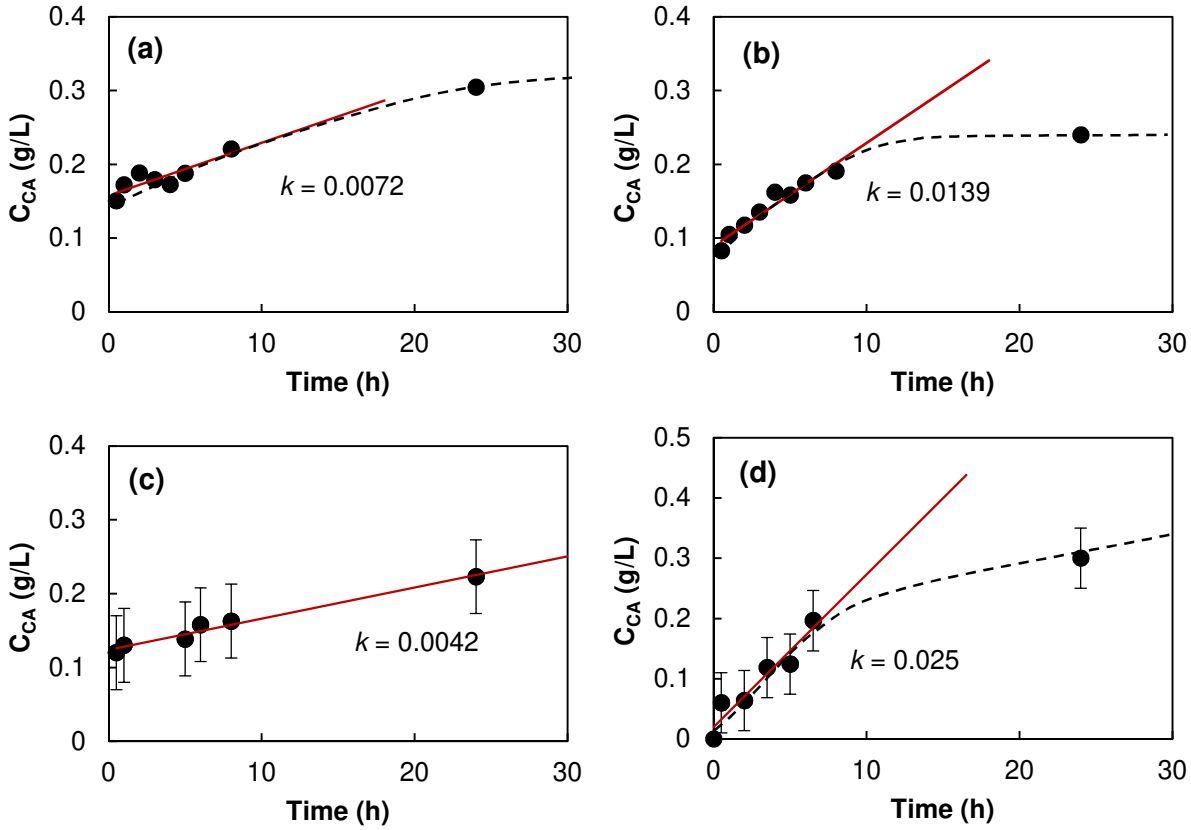

Appendix 11. Linear evolution of the concentration of extracted CA during the diffusion step for alkyl glycosides: *i*-C_5Xyl (a), C_7Glu (b), $C_{6,-2}$Glu (c), $C_{8/10}$Glyco (d).

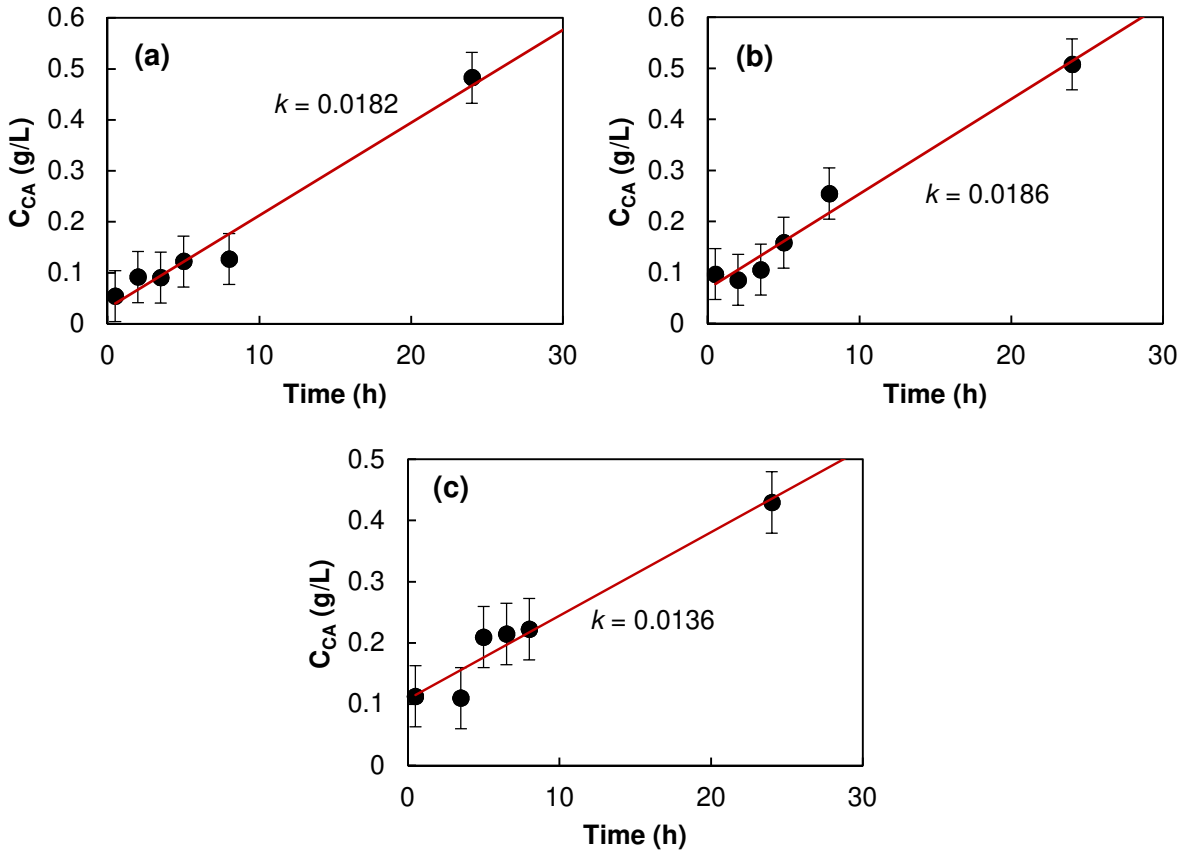

Appendix 12. Linear evolution of the concentration of extracted CA during the diffusion step for alkyl glycerols: C_4Gly (a), *i*-C_5Gly (b), C_5Gly (c).

Résumé

Les préoccupations grandissantes concernant la santé et l'environnement rendent la demande en ingrédients naturels toujours plus forte. Parallèlement, les fournisseurs d'ingrédients naturels tentent de rendre les procédés d'extraction plus performants, plus sûrs, moins consommateurs en énergie et en ressources non-renouvelables. Les hydrotropes, capables de solubiliser des composés hydrophobes dans l'eau, constituent une alternative prometteuse aux solvants organiques, souvent dérivés du pétrole, potentiellement explosifs et émetteurs de composés organiques volatiles. Afin de développer un nouveau procédé d'extraction hydrotropique efficace à base d'amphiphiles biosourcés, nous nous sommes intéressés à la compréhension des cinétiques et des phénomènes physico-chimiques impliqués dans l'extraction de l'acide carnosique (AC), un puissant antioxydant phénolique présent dans le romarin et la sauge officinale. L'extraction de l'AC par des hydrotropes modèles de type éthers de polyéthylène glycol a permis de démontrer l'efficacité et la compétitivité de l'extraction hydrotropique par rapport à une extraction conventionnelle utilisant un solvant. Des relations structure/propriétés physico-chimiques/efficacité ont été établies, puis généralisées aux hydrotropes biosourcés à base de glycérol (éthers de butyle, pentyle, et isopentyle) ou de sucres comme le xyloside d'amyle qui a été sélectionné par la suite pour son efficacité, sa biodégradabilité et sa disponibilité. L'optimisation des conditions d'extraction à l'aide de plans d'expériences a permis de doubler la quantité d'AC récupéré dans l'extrait sec. Pour finir, différentes techniques de précipitation de l'AC contenu dans des solutions hydrotropiques ont été comparées afin de faciliter sa récupération. Parmi elles, l'addition d'eau comme anti-solvant s'est révélée la plus efficace pour précipiter l'AC extrait du romarin. Sur la base de la composition et de l'aspect du précipité obtenu selon différentes conditions de précipitation, nous avons finalement pu établir un mécanisme visant à expliquer les différentes étapes de la précipitation hydrotropique.

Mots-clés : Extraction, Romarin, Hydrotrope, Acide carnosique, Physicochimie, Xyloside d'amyle

Abstract:

The growing concerns for health and environment makes the demand for natural ingredients ever higher. At the same time, natural ingredients manufacturers are trying to design effective, safer and less energy-costly extraction processes while avoiding the use of non-renewable resources. Hydrotropes are able to solubilize hydrophobic compounds in water, and constitute a promising alternative to organic solvents, which are often derived from petroleum, potentially explosives and producers of volatile organic compounds. To design a new effective hydrotropic extraction process using biobased amphiphiles, we investigated the physical chemical and kinetic phenomena governing the extraction of carnosic acid (CA), a powerful phenolic antioxidant that occurs in rosemary and sage. The CA extraction using alkyl polyethylene glycols ethers as model hydrotropes demonstrated the efficiency and the competitiveness of hydrotropic extractions compared to conventional solvent extractions. Quantitative Structure/properties relationship (QSPR) studies were established and generalized to biobased hydrotropes including butyl or pentyl glycerol ethers, and sugar-based hydrotropes such as amyl xyloside, which was further selected for its efficiency, biodegradability and commercial availability. The optimization of the extraction conditions led to double the CA recovered in the dry extract. Finally, different techniques have been investigated to precipitate CA from a hydrotropic solution. Among them, the addition of water as an anti-solvent appears as the more effective for precipitating CA from rosemary extract. Finally, the comparison of the precipitate composition and aspect obtained using various precipitation conditions led us to establish a mechanism explaining the different steps of the hydrotropic precipitation.

Key words: Extraction, Rosemary, Hydrotrope, Carnosic acid, Physicochemistry, Amyl xyloside